Origin and genesis of dissolved organic matter: A study by Py-GC/MS-IRMS

Dissertation

zur Erlangung des akademischen Grades

doctor rerum naturalium (Dr. rer. nat.)

vorgelegt in englischer Sprache dem Rat

der Chemisch-Geowissenschaftlichen Fakultät

der Friedrich-Schiller-Universität, Jena

von

Dipl. Geol. Oliver Kracht

geboren am 08.05.1967, Frankfurt/Main

Gutachter:

1. Prof. Dr. G. Büchel (Friedrich-Schiller-Universität Jena)
2. Prof. Dr. Dr. F. H. Frimmel (Universität Karlsruhe)
3. Dr. G. Gleixner (MPI für Biogeochemie, Jena)

Tag der öffentlichen Verteidigung: 11. Juli, 2001

E R R A T U M

Figure 4.4 on page 19 was supposed to show a correlation of O-alkyl-C with tar (Figure C). The diagram suggests "that the tar fraction results from ... and not from O-alkyl-C rich polymers such as cellulose."

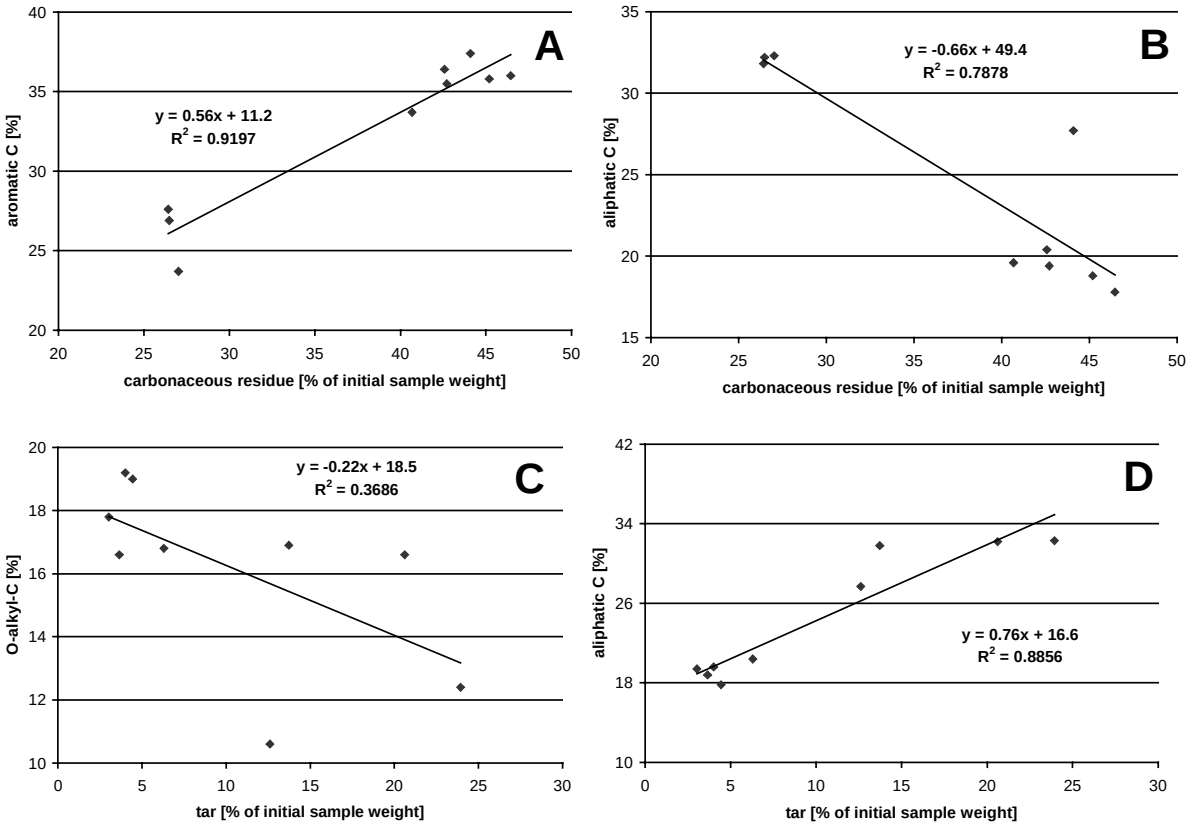

Figure 4.4: Correlation diagrams between structural NMR-data and residues of pyrolysis reactions. Data points are based on results obtained from pyrolysis of all fulvic acids of the ROSIG samples: A and B) carbonaceous residue in the pyrolysis tube, C and D) tar precipitated on the walls of the glass liner. NMR-data from Lankes and Lüdemann (2001) and listed in Appendix I.

Summary

Dissolved organic matter (DOM) is a ubiquitous and dynamic component of lakes, rivers, and oceans. The composition of DOM is influenced by both local biological sources such as plants and dominant microbial, geochemical, and physical processes occurring in the aquatic and surrounding environments. This diversity of potential sources and processes results in a heterogeneous mixture with a characteristic organic chemical signature for individual aquatic ecosystems. Samples from natural systems such as a bog lake, groundwater and soil percolate but also from anthropogenically influenced systems like a brown coal processing waste water reservoir and a waste water treatment plant were taken to provide reference material in a special research program on refractory organic substances in the environment (ROSE, German: ROSIG). The objective of the program was to identify common characteristics and differences with respect to the origin and genesis of the DOM.

The variation of stable isotope ratios can be used to interpret the formation of organic matter and to determine the source of a compound as the natural isotope abundance in organic compounds depends on physical and chemical processes occurring during (bio)synthesis. This study elaborated Curie-point pyrolysis (773 K) coupled to a gas chromatograph to volatilize and separate the complex and heterogeneous mixture of organic DOM into structural subunits. Stable carbon isotopes ($^{13}C/^{12}C$ ratios) of the pyrolysis products were subsequently analyzed by isotope ratio-mass spectrometry and identification was achieved by mass spectrometry.

Pyrolysis of isolated fulvic acids from the five aquatic ecosystems yielded primarily products of carbohydrates and lignin. The $\delta^{13}C$ values of the pyrolysis products derived from these plant biopolymers exhibited differences which are characteristic for their natural precursor material. Several carbohydrate derived substances, however, indicated an enrichment of ^{13}C suggesting secondary microbial synthesis. Microbial activity was particularly indicated in the fulvic acids of the waste water treatment plant by acetamide, a compound produced upon pyrolysis of microbial cell walls. Anthropogenically influenced waste waters showed clear indication of fossil fuel derived substances by abundant occurrence of heterocyclic compounds. The comparison of fulvic acids from the contrasting aquatic environments manifested the already known conclusion that the fulvic acids consist of different pools with varying age (determined by ^{14}C data) and reactivity depending on their source and genesis in each aquatic ecosystem. Furthermore, the similarity of several takings of DOM from the bog water system suggested that DOM formation processes recur if the ecological conditions remain constant.

The formation of DOM has been studied in greater detail in the bog water system. Takings of several depths of *Sphagnum* peat were compared to the bulk DOM of the water. Even though the chromatograms of the peat and DOM showed similar pyrolysis products, it is obvious from the isotope ratios that the substances in the water must have been formed by different processes compared to those occurring in the peat. The combination of structural and isotope information of individual organic compounds demonstrated that a majority of pyrolysis products of DOM are relatively depleted in ^{13}C. It is here suggested that the compounds are formed *in situ* by the action of microorganisms in the water. Most probably a depletion is associated with the uptake of isotopically light compounds such as respired CO_2, CO_2 from oxidation of CH_4, or acetic acid. The depletion of ^{13}C in pyrolysis products of DOM compared to peat contradicts a simple solving mechanism of substances from the peat.

Ausführliche Zusammenfassung in deutscher Sprache

Gelöstes organisches Material (DOM) ist Bestandteil in allen Oberflächengewässern und ständiger Veränderung unterlegen. Die Zusammensetzung von DOM wird durch lokale biologische Quellen, wie z.B. Pflanzen, aber auch durch mikrobielle, geochemische und physikalische Prozesse im aquatischen Milieu und dem umgebenden System gesteuert. Die Variabilität potentieller Quellen resultiert in einem heterogenen Konglomerat, dessen organochemische Zusammensetzung charakteristische Merkmale des Ökosystems bildet. Innerhalb eines Schwerpunktprogramms der Deutschen Forschungsgemeinschaft (refraktäre organische Säuren in Gewässern, ROSIG) wurden daher Proben natürlicher Systeme (Moorwasser, Grundwasser, Bodensickerwasser) und anthropogen beeinflusster Systeme (Kläranlagenabwasser, Abwasser aus der Braunkohlepyrolyse) entnommen und als Referenzmaterial zu weiteren Untersuchungen zur Verfügung gestellt. Das Ziel der vorliegenden Arbeit war, Gemeinsamkeiten und Unterschiede im Hinblick auf Genese und Herkunft des DOM festzustellen.

Die Charakterisierung von Huminstoffen lässt sich vereinfachen, indem eine erste Separierung des Gemisches basierend auf Richtlinien der International Humic Substances Society (IHSS) durchgeführt wurde. Dieser methodische Ansatz führt zu einer Trennung des DOM aufgrund der pH-abhängigen Löslichkeit und der Adsorption an XAD-Harzen. Diese Fraktionen, Fulvin- und Huminsäuren, wurden vom ROSIG-Programm zur Verfügung gestellt und bildeten das Ausgangsmaterial für die vorliegenden Untersuchungen.

Veränderungen in den Verhältnissen stabiler Isotope sind Indikatoren für die Genese von organischem Material und für dessen Quelle, da die natürliche Isotopenhäufigkeit in organischen Verbindungen von physikalischen und chemischen Prozessen während der Biosynthese bestimmt wird. In der vorliegenden Arbeit wurde deshalb eine Methodik entwickelt, die in der Lage ist, Isotopenverhältnisse an strukturbildenden organischen Verbindungen dieser heterogenen Gemische im DOM zu messen (compound specific isotope analysis). Als Ausgangsverfahren wurde die Curie-Punkt Pyrolyse (773 K) zur thermischen Zersetzung von gefriergetrocknetem DOM gewählt. Ein an die Pyrolyseeinheit gekoppelter Gaschromatograph trennte die Pyrolyseprodukte, an denen on-line Isotopenverhältnisse des Kohlenstoffs ($^{13}C/^{12}C$, $\delta^{13}C$) gemessen wurden. Die Identifizierung der Pyrolyseprodukte erfolgte gleichzeitig in einem organischen Massenspektrometer über die für organische Verbindungen spezifischen Massenspektren.

Die Pyrolyse ist eine leicht zu handhabende und schnell anwendbare Möglichkeit, Proben, die mit nasschemischen Methoden schwer zu trennen sind, in einzelne Bestandteile zu

zersetzen. Die relativ einfache Probenvorbereitung vermindert zudem das Risiko von Kontamination und damit die Veränderung der ursprünglichen Isotopenverhältnisse. Während der thermischen Zersetzung entstehen allerdings intermolekulare Sekundärreaktionen, die es nicht erlauben, die ursprüngliche Struktur des organischen Materials zu erfassen, sondern nur die Zusammensetzung aufgrund charakteristischer Pyrolysebruchstücke nachzuvollziehen. Ein weiterer wichtiger Aspekt ist, dass ein Teil der Probe in dem Pyrolyseröhrchen als kohle- und teerartige Substanz zurückbleibt. Es war somit nicht möglich das gesamte organische Material zu betrachten. Korrelationen mit anderen Messergebnissen (Elementaranalyse, ^{13}C-NMR) legten die Vermutung nahe, dass der kohleartige Rest aus bereits kondensierter Form als aromatische Kohlenstoffverbindung vorlag, wohingegen die teerartige Ablagerung aliphatischen Verbindungen zugeschrieben werden konnte.

Wiederholungsmessungen an den Proben sprechen für die Konstanz der Pyrolysereaktionen. Die Standardabweichungen des δ^{13}C-Wertes schwanken zwischen 0,1‰ und 3‰ für die einzelnen Pyrolysebruchstücke. Das zeigt zum einen eine sehr gute Reproduzierbarkeit, andererseits konnte aber die Frage nicht beantwortet werden, warum einzelne Bruchstücke in ihrem δ^{13}C-Wert stark variieren. Quantitative Aussagen aufgrund der Peakflächen ließen sich nur an einem relativen Wert (% an Gesamtfläche) festmachen, da es keinen geeigneten internen Standard für die Pyrolyse von Festsubstanz in Verbindung mit Isotopenmessungen gibt. Massenbilanzen mussten entfallen, weil die große Menge an produzierten Gasen (bes. CO_2 und H_2O) aus systembedingten Gründen abgeleitet wurde. Im Gegensatz zur guten Reproduzierbarkeit der δ^{13}C-Werte, zeigten leichte Veränderungen der systemanalytischen Bedingungen großen Einfluss auf die Standardabweichungen der Flächenwerte.

Die Pyrolyse der isolierten Fulvinsäuren aus den fünf aquatischen Ökosystemen erzeugte hauptsächlich Bruchstücke von Kohlenhydraten und Lignin. Die Unterschiede im Isotopenverhältnis (δ^{13}C) der Bruchstücke entsprachen den natürlichen isotopischen Abständen dieser beiden Biopolymere in Pflanzen. Allerdings konnten an mehreren Kohlehydratbruchstücken Anreicherungen von ^{13}C festgestellt werden, die auf eine sekundäre Synthese durch Mikroorganismen hindeuteten. Besonders im Kläranlagenabwasser wurde eine erhöhte mikrobielle Aktivität durch Acetamid angezeigt, ein Pyrolysebruchstück mikrobieller Zellwände. Die anthropogen beeinflussten Abwässer kennzeichneten sich durch wiederholtes Auftreten heterozyklischer Verbindungen, die vermutlich auf einen Eintrag von fossilen Brennstoffträgern zurück zu führen sind. Im allgemeinen bestätigte sich die Vermutung, dass das organische Material aus diversen Pools unterschiedlichen Alters (^{14}C-Aktivität) und Reaktivität zusammengesetzt wird, abhängig von den Quellen und der Genese in den einzelnen aquatischen Systemen. Ähnlichkeiten in saisonal unterschiedlichen Proben des Moorwassers hingegen, deuten auf

eine Reproduzierbarkeit der genetischen Prozesse von DOM, wenn die ökologischen Grundbedingungen unverändert bleiben.

Im Vergleich von Pyrolysebruchstücken der Humin- und Fulvinsäure mit den Gesamt-DOM des Moorwassers zeigt sich ein prozentual hoher Anteil von Kohlenhydratbruchstücken im Gesamt-DOM und eine Anreicherung von Ligninbruchstücken in der Fulvinsäurefraktion, wahrscheinlich hervorgerufen durch das Isolationsverfahren. Anreicherungen in ^{13}C mehrerer Pyrolysebruchstücke deuten eine generell stärkere Modifikation der Fulvinsäuren im Vergleich zu den Huminsäuren an und stützen damit die These, dass Fulvinsäuren eine höhere biologische Verfügbarkeit haben.

Aufgrund seiner Stabilität wurde das Moorwassersystem im Hinblick auf die DOM-Genese genauer untersucht. Hierzu wurden mehrere Proben des *Sphagnum*-Mooses aus unterschiedlichen Tiefen entnommen und mit dem Gesamt-DOM verglichen. Obgleich die Chromatogramme der Moos- und Torfproben und des Wassers im wesentlichen die gleichen Pyrolysebruchstücke aufwiesen, wurde durch deren Isotopensignatur angezeigt, dass die Substanzen durch einen anderen Bildungsprozess entstanden sein mussten. Die Kombination von Strukturinformation und Isotopensignal ergab, dass eine deutliche Abreicherung von ^{13}C gegenüber ^{12}C in den meisten der Pyrolysebruchstücke des DOM vorliegt. Es liegt die Vermutung nahe, dass diese Abreicherung durch mikrobielle Aktivität unter Aufnahme 'leichter' Kohlenstoffquellen zustande gekommen ist. In Frage kommen dafür CO_2 aus Respiration, CO_2 aus der Oxidation von Methan (CH_4) und Essigsäure. Ein einfacher Lösungsmechanismus der Substanzen aus dem Torf scheint dagegen sekundär.

Die detaillierte Untersuchung des Hohlohsee-Systems zeigt, dass wichtige Informationen über die Bildung von DOM aus weiteren Systemparametern gezogen werden können. Untersuchungen potentiellen Ausgangsmaterials können vor allem das Ausgangssignal des Isotopenverhältnisses klären und damit wichtige Hinweise für die Interpretation der $\delta^{13}C$-Werte in den Pyrolysebruchstücken von DOM liefern. Dadurch ergibt sich der Bedarf an weiterer Forschung, um die Reproduzierbarkeit der Ergebnisse und deren Übertragbarkeit auf andere Systeme zu überprüfen.

Contents

1 Introduction

The need for interdisciplinary studies in microbiology, ecology, biochemistry, and modeling has developed with the increasing importance of global change and carbon flux research. In this context, investigations of humic substances (HS) have become a focal point in understanding the biological and (geo-) chemical processes which control carbon storage and release to the atmosphere.

Organic matter (OM) is composed of residues from a wide variety of organisms, e.g. microorganisms, plants, animals. Humic substances result from biological and chemical processes that take place during the reworking of this organic matter, and are found in soils and in terrestrial water systems (approx. 25% of total carbon bound in HS; Aiken, 1985). The broad diversity of input material to HS results in a highly complex and heterogeneous mixture of compounds, that can have a substantial influence on physical and chemical properties of the surrounding medium. In addition, organic matter binds large amounts of carbon in the terrestrial environment (Eswaran et al., 1993; Hedges et al., 1997) and, as a class of compounds, HS represent quantitatively important intermediate stages in the remineralization process from biologically-reduced carbon to CO_2. Therefore, the characterization of this assemblage with regard to functionality, structure, genesis, and fate has been the focus of numerous studies in soil science and analytical chemistry.

Recently, a growing attention was drawn to the role of HS in aquatic environments, i.e. dissolved organic matter (DOM), with respect to carbon flux balances. The composition of DOM (operationally defined as OM passing through a 0.45 μm filter) varies as a function of source and genesis. Besides autochthonous biotic productivity, inputs of HS from vegetation and soils account for large variations in composition (Hessen and Tranvik, 1998). Although a portion of DOM may aggregate and sediment out of the water column, most is found in dispersed forms and available for microbial consumption. Modifications by microorganisms during transport, partial degradation, and changing input sources create a complex and heterogeneous mixture of multiple organic compounds with different chemical properties (Hayes et al., 1989). The ecological importance of these organic compounds lies in the interaction between inorganic and organic compounds, i.e. cation exchange capacities and the binding of anthropogenic organic chemicals, the influence on chemical and physical properties of the environment such as redox potential, pH, and light attenuation, and in the limited accessibility of these biomolecules to enzymatic hydrolysis which results in slow turnover times. This ecological and technical significance of DOM in natural and anthropogenically influenced systems requires comparative studies of DOM characteristics and of its role in terrestrial carbon dynamics.

The present study has been developed within the context of the ROSIG-program (Refraktäre organische Säuren in Gewässern; english: ROSE – refractory organic substances in the environment), a special program funded by the Deutsche Forschungsgemeinschaft (DFG, Bonn, Germany) from 1994 to 2000. The objective of the program was to provide a standard reference of DOM to characterize DOM from contrasting aquatic ecosystems by comparative studies using different analytical methods. Special emphasis was given to structural investigations, biochemical and biological characterization, and molecular interactions. The samples were taken from groundwater, brown coal processing waste water, soil percolate, a waste water treatment plant, and bog water. All samples were separated into humic acids (HA) and fulvic acids (FA) before being provided to the working groups. The fact that different methods for isolation may lead to different characteristics of DOM was accounted for by standardized isolation procedure carried out at the Engler-Bunte-Institute, Universität Karlsruhe, Germany.

The ROSIG-reference material provided a sound basis for comparing the origin and genesis of DOM in contrasting environmental conditions. Origin and processes contributing to the formation of biochemically produced substances can be derived from their isotope signatures (see Section 2.3). Bulk isotope measurements of DOM do not entirely cope with the complex and heterogeneous composition of organic material. Thus it was required to elaborate a combination of analytical methods that separates the comprehensive mixture of DOM into its structural subunits and enables a direct, i.e. on-line, analysis for stable isotope ratios (also referred to as compound specific isotope analysis, CSIA). This was achieved by applying a combination of a degradative method followed by a chromatographic separation: pyrolysis-gas chromatography (Py-GC). The subunits were identified and analyzed for their isotopic signature by coupling an organic mass spectrometer (MS) and an isotope ratio-mass spectrometer (IRMS) to the Py-GC unit. The first such unit was set up at the Max-Planck-Institut für Biogeochemie, Jena, Germany, in October 1998.

The main objectives can be summarized as follows:

- to establish the applicability of combining two analytical systems (MS and IRMS) with a Py-GC unit,
- to determine the suitability of isotope analysis on pyrolysis products of DOM,
- to find common and dissimilar characteristics in fulvic acids of different aquatic systems,
- to investigate the formation of DOM in a defined natural system, and
- to determine the relevance of these results with respect to origin and genesis of DOM.

The results of the present work are divided in four chapters. Two chapters (Chapter 3 and 4) describe Curie-point pyrolysis and the analytical system, particularly addressing the

novelty of the method and critical considerations about pyrolysis. Chapter 5 discusses the results from the application of Py-GC/MS-IRMS to the ROSIG reference material and constitutes the need for additional analyses of possible sources for DOM as was realized for the bog water system (Chapter 6). A conclusive summary is given in Chapter 7. Basic aspects on humic substance formation, on the isolation of fulvic and humic acid, and on the application of stable isotope measurements are addressed in the following three sections of Chapter 2.

2 Theoretical background

2.1 Biochemical considerations of the formation of humic substances

Most theories about the formation of HS have developed from observations in soil science. Plant organic matter mainly consists of cellulose (15-50%), hemicellulose (10-40%), lignin (5-30%), proteins (2-15%), and lipids (Haider, 1996). Early diagenetic processes decompose labile plant material rapidly in aerobic soil environments with adequate water supplies. Oxidative and hydrolytic biodegradation of this dead plant material by microorganisms (mainly fungi and bacteria) is believed to be a primary source of HS (Stevenson, 1994). The degradation process is accompanied by secondary structural changes in organic material and release of CO_2. Degradation and consumption of OM by microorganisms also form new structural units, e.g. in bacterial and fungal biomass, which contribute to the HS. Other transformations may be induced by abiotic oxidation, photochemical processes, adsorption, and precipitation. Since the resulting biochemical structural units such as simple sugars, amino acids, fatty acids, and lignin building blocks (phenylpropane units) are commonly much smaller than HS, several researchers have suggested that HS ultimately are formed from a re-organization, polymerization and condensation of these small precursors by microbial activity (Flaig, 1988; Hatcher and Spiker, 1988; Hedges, 1988; Stevenson, 1994). Those biopolymers are thought to become less degradable (i.e. refractory). The resistance to further degradation is attributed to a loss of reactive functional groups as is the case in condensation processes, by self associations of the molecules, by protective associations with mineral colloids, and by entrapment in soil aggregates.

Current investigations on the formation of HS favor a mechanism based on the condensation of microbially-altered phenylpropane units, i.e. phenolic compounds or quinones with N-containing compounds (Stevenson, 1994). The number of possible precursor molecules for polyphenols is large. The most likely and frequent precursor polymer is lignin freed of its linkage with cellulose during decomposition. Another important source in addition to tannins and glycosides are microorganisms (Stevenson, 1994). Both actinomycetes and fungi have shown the ability to synthesize phenolic and hydroxy aromatic acids from non-aromatic carbon sources such as carbohydrates. The next step in the formation of HS is the oxidation of polyphenols to produce quinones, which then condense with each other or with amino acids to form synthetic polymers (Hedges, 1988). The melanoidin model, favored by marine scientists, allows for the formation of HS despite of a low abundance of phenolic compounds and fungi. It involves condensation reactions between simple sugars and amino acids initiated by the formation of a Schiff-

base. Nitrogenous polymers are then formed after a series of complex dehydration, rearrangement, and condensation reactions (Stevenson, 1994). Both models account for the majority of observations and the variety of characteristics of HS, and probably play a role in the formation of DOM. Nevertheless, HS formation is a dynamic process and it seems likely that synthetic and degradative processes occur simultaneously.

2.2 Classification and definition of DOM

The various ways of forming DOM cause the heterogeneity of the material which results in a range of different properties. This makes it difficult to assign a proper, generalized chemical definition. A more constructive approach is to infer average structure and functionality from average properties (Perdue, 1984). Three classes of DOM have been operationally isolated: fulvic acids (FA), humic acids (HA), and humin. All three fractions share the characteristics of being heterogeneous biomolecules which are yellow to brown or black in color, of high to moderate molecular weight (MW), and to a certain degree resistant to biodegradation (McKnight and Aiken, 1998). The primary difference lies in their solubility: FA are soluble under all pH conditions, HA are soluble above pH 2 (a standard value taken by water scientists), and humins are not soluble at any pH. The MW ranges from 500 Da (Dalton) for FA to more than 100,000 Da for HA (McKnight and Aiken, 1998). The size distribution covers a range of approximately 0.5 nm to 0.1 µm. In contrast to soil chemistry, the terms HS and non-humic substances (NHS) play a minor and different role. By definition, FA and HA comprise both HS and NHS such as peptides, sugars, nucleic acid residues, and fats which can be sorbed or co-precipitated with them (Hayes, 1998). NHS in dissolved organic matter are commonly referred to as the fraction that does not adsorb to an XAD-resin at a pH of 2 (see Section 5.2).

A significant part of DOM are organic acids. The acidic structural elements are predominantly carboxyl groups (-COOH), most abundant in FA. These groups are added to large biomolecules during oxidative degradation by microorganisms and affect the aqueous solubility (McKnight and Aiken, 1998). Other important functional groups are composed of hydroxyls (-OH), amines ($-NH_2$), esters, and ethers. Several attempts have been made to determine a general structure of humic substances based on these findings. Two proposed structures of a humic and a fulvic acid are given in Figures 2.1 and 2.2, both of which adequately represent the heterogeneous composition and the multitude of functional groups included. However, the determination of the structure of HA and FA is still under debate (Schulten et al., 1991; DeLeeuw and Hatcher, 1992; Schulten and Gleixner, 1999) and the question remains if there is any common structure at all.

In addition to functional and structural characteristics, elemental composition also varies depending on the fraction analyzed. For instance, FA are of higher O content and lower C

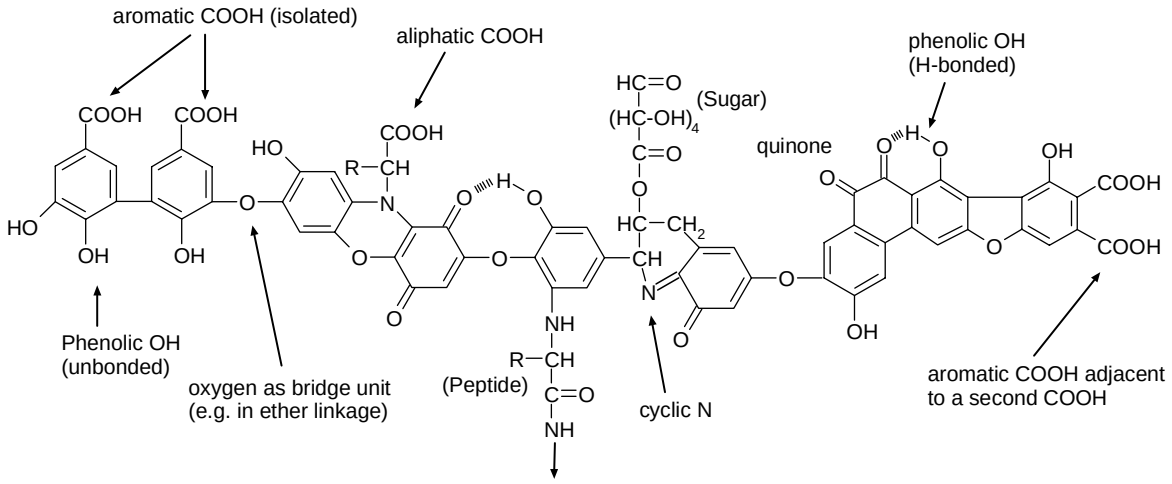

Figure 2.1: Hypothetical structure of humic acid (HA) showing free and bound phenolic OH groups, quinone structures, nitrogen and oxygen as bridge units, and carboxyl groups (COOH) variously placed on aromatic rings (after Stevenson, 1994).

content than humic acids. Much of the additional oxygen is bound in carboxyl and alcohol functional groups. Thus FA represent structures with greater hydrophilicity due primarily to the increased level of oxygen-containing functional groups. In contrast to soil HS where the HA fraction dominates, FA constitute >90% of riverine HS (Malcolm, 1990). In the present study, FA comprise the major fraction (60%-95%) of the HS (i.e. HA + FA) and between 10% and 35% of the total DOC (Frimmel and Abbt-Braun, 1999).

The polyfunctional property of DOM demands standardized preparation methods. Previous studies have demonstrated that even slight variations in measurement techniques led to different results and impeded interlaboratory comparisons (Frimmel, 1990). The most commonly employed standard isolation procedure uses non-ionic macroporous resins

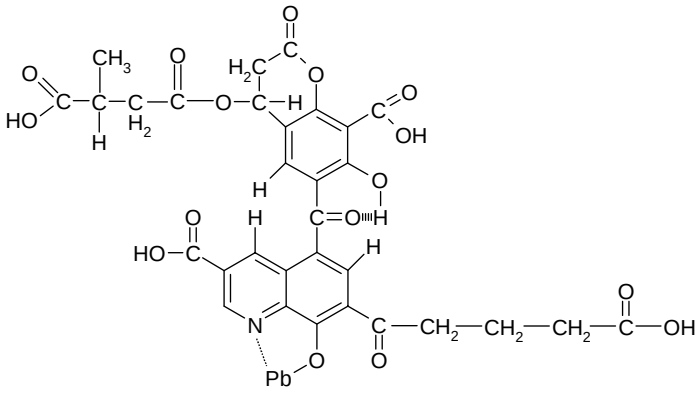

Figure 2.2: Proposed average structure model of Suwannee River fulvic acid (FA) containing a nitrogen metal-binding site (McKnight & Aiken, 1998).

(XAD 8) and was set up by the International Humic Substances Society (IHSS) based on the preparation method of Mantoura and Riley (1975). The isolation method is described in Section 8.2.

2.3 The significance of isotope measurements to determine origin and genesis of dissolved organic matter

Stable isotopes of H, C, N, O, S are a common and useful tool for environmental studies concerning formation processes. Although isotopes belong to the same chemical element by definition, their chemical and physical properties differ as a result of variations in atomic mass (isotope effect). Physical, chemical and biological processes change the original ratio of the isotopes (isotopic fractionation). The isotopic composition of natural organic compounds is influenced by the constraints of thermodynamic equilibrium and kinetic isotope effects on biosynthetic processes (Schmidt et al., 1995). Samples are measured against internal standard material and the deviation of the isotope ratio is expressed in parts per mil (δ notation). The international standard for carbon is PDB, a carbonate from a belemnite of the Cretaceous Pee Dee Formation in South Carolina.

The isotopic composition of plant material, the initial substrate for humification, results from carbon isotope fractionation during photosynthesis (Farquhar et al., 1989). The primary CO_2-fixing enzymes in plants discriminate against $^{13}CO_2$ thus leading to low $\delta^{13}C$ values relative to ambient CO_2. Plants with the C3 pathway of photosynthesis have δ-values ranging from –32‰ to –20‰, with a mean of –27‰, whereas values for C4 plants range from –17‰ to –9‰, with a mean value of –13‰. CAM plants (Crassulacean acid metabolism) are able to switch between the C3 and the C4 mode, thus reaching δ-values between –28‰ and –10‰ (Figure 2.3). Further fractionations of isotopes occur during plant metabolism. The isotopic composition of plant material varies between single plant sections such as leaves and roots, but also on a molecular level due to metabolic conversion occurring during photosynthesis. Lignins and other woody tissues are generally depleted in ^{13}C relative to carbohydrates by 3 to 6 ‰ (Leavitt and Long, 1986; Benner et al., 1987; Gleixner et al., 1993). Lipids are isotopically 'light' and most amino acids are 'heavy', with overall ranges often on the order of 5-10‰ (Degens, 1969; Blair et al., 1985; Benner et al., 1987) (Figure 2.4).

The detection of isotope discrimination can be used to determine the processes involved in the formation and decomposition of organic compounds (Hayes et al., 1990; Macko et al., 1990; Schmidt et al., 1993; Rieley, 1994; Lichtfouse et al., 1998). The change in the isotopic signal of individual compounds reflects biochemical conversion of corresponding source molecules (Macko et al., 1991; Balzer et al., 1997). This is best demonstrated for

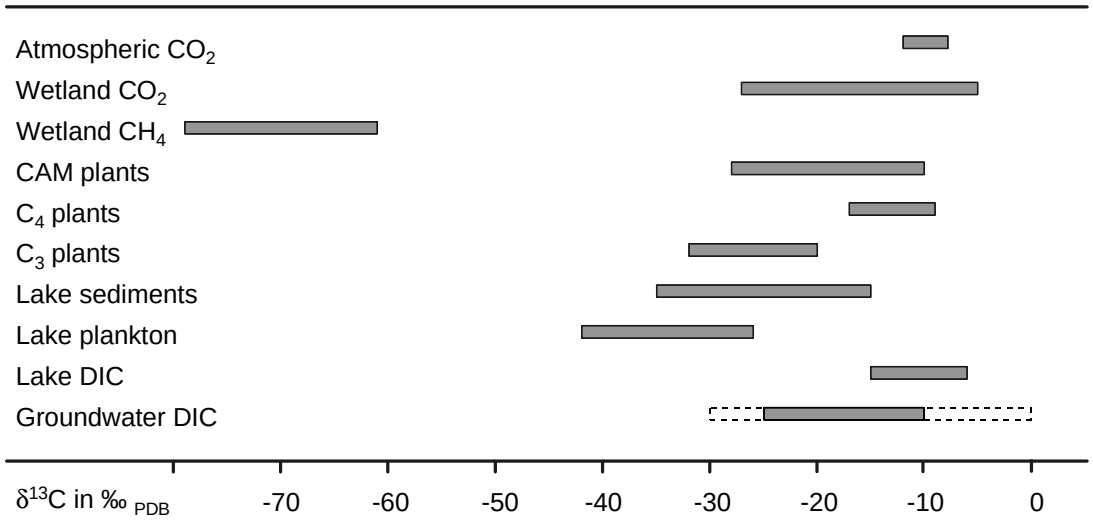

Figure 2.3: The range of $\delta^{13}C$ values for natural substances (based on values from Aravena et al., 1993, and Boutton, 1991).

the trophic level effect. The breakdown of compounds as a step in a nutritive series of an ecosystem, e.g. food chain, results in an enrichment of the heavier isotope in the organism (^{13}C) due to the loss of $^{12}CO_2$ in metabolic processes (DeNiro and Epstein, 1978). In contrast, constant values are believed to indicate a "preservation" of source molecules (Lichtfouse et al., 1998). Thus the structural units of HS are expected to carry isotopic clues of their origins and pathways. As a result, bulk isotope measurements are of limited use for understanding soil carbon biogeochemistry, as they contain little information that is specific to a given source or formation process. Observed changes of the bulk isotope signal can reflect different decomposition rates and/or changing compositions of organic molecules in the soil (Ågren et al., 1996; Miyajima et al., 1997). The use of compound specific isotope analysis, as applied in this study, is of further use when the isotopic composition of individual molecules can be traced or compared in a closely defined system with a known input, i.e. initial isotope signal of organic matter.

The relative abundance of carbon-bound, non-exchangeable deuterium (D or ^2H) in natural compounds is primarily influenced by local precipitation and, secondly, by the plant physiology (Schleucher, 1998). The isotopic signal is taken up by the roots from groundwater or precipitation. Evapotranspiration processes in the leaves cause a high enrichment of D in leave water. A secondary fractionation occurs during transfer of H into organic compounds (White, 1989). Carbohydrates are commonly depleted in D by 22‰ relative to available water (Epstein et al., 1976), whereas the most reduced compound classes, e.g. lipids, are characterized by the largest D depletion of around 120‰ ± 10‰ (Estep and Hoering, 1980; Smith and Ziegler, 1990).

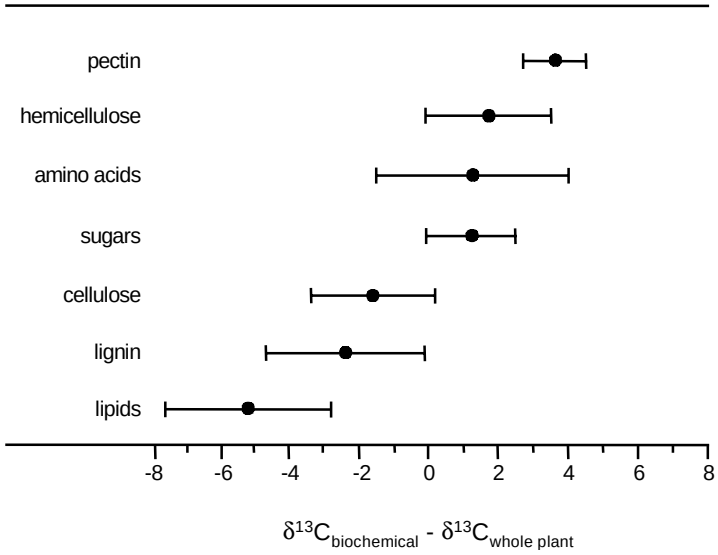

Figure 2.4: The variability of $\delta^{13}C_{PDB}$ in plant biochemical fractions relative to the $\delta^{13}C_{PDB}$ values of the whole plant from which they are extracted (adapted from Boutton, 1996).

The nitrogen cycle involves interactions of a vast range of organisms and different chemical and physical processes, thus it is difficult to generalize. Nitrogen-15 abundances of plants are mainly determined by the N-isotope signal of the corresponding primary source, basically NO_3^- made available from atmospheric nitrogen by N-fixing soil bacteria. Typical ^{15}N values for plant tissues range between –6‰ and +2‰ (Nadelhoffer and Fry, 1994). In general, soils are slightly enriched in ^{15}N relative to fresh litter and tissues. The enrichment in deeper soils (+8‰ ± 2‰) is believed to result from a discrimination against ^{15}N during mineralization coupled with an uptake of ^{15}N-depleted nitrogen by roots or loss from the soil by nitrate leaching and denitrification (Nadelhoffer and Fry, 1994, and references therein). Even higher enrichments are indicators for organic fertilizers such as manure (Schmidt et al., 1992), or for the origin of a higher level in the food chain. Heterotrophic microorganisms are responsible for a large fractionation due to their deaminating enzymes that cause a depletion of ^{15}N after uptake of amino acids and transferring them into proteins (Macko and Estep, 1984).

3 Basic aspects of Curie-point pyrolysis (Py)

Degradative methods such as pyrolysis have a strong impact on the original building blocks of the humic macromolecules. The technique has been widely used in investigations of humic substances over the past two decades but the considerable thermal reactions and rearrangements produced in the process inhibited a structural identification. Therefore, pyrolysis is of limited value when the structural evaluation is desired because the reaction products only partially reflect the structures of the building blocks and not so much the linkages (Saiz-Jimenez, 1996). However, Py-GC/MS has proved to be a powerful tool for characterizing natural organic mixtures (Nip et al., 1984; Boon et al., 1985; Schulten, 1987; Coban-Yildiz et al., 2000) and, particularly, polymeric substances not amenable to analysis by conventional wet chemical methods (Stankiewicz et al., 1998). It combines degradation, separation, and analytical evaluation of a heterogeneous, complex mixture. The method is fast and can be applied to small amounts of sample material. Subsequent isotope ratio-mass spectrometry (IRMS) analysis of the sample material demands that the analytical scheme does not produce isotope fractionation (Figure 3.1). A great advantage of pyrolysis is the fast and simple preparation of the sample material which limits the risk of

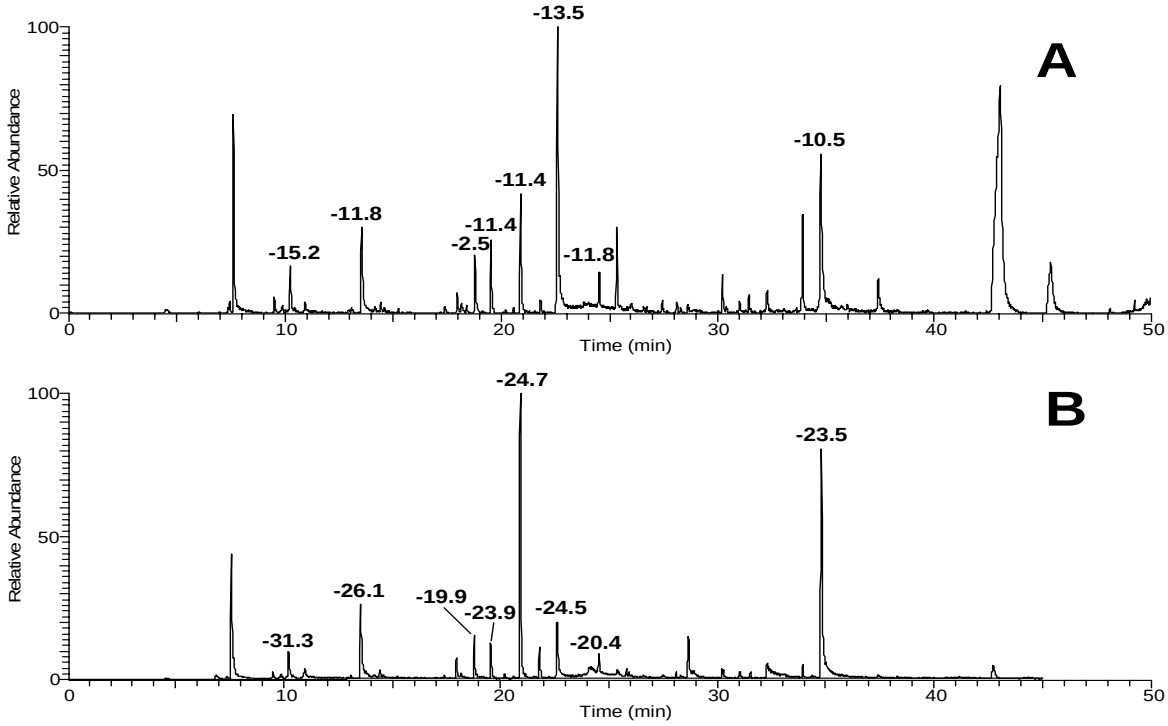

Figure 3.1: MS trace (total ion current) of a C3 (A) and C4 (B) sugar. $\delta^{13}C$ values of the pyrolysis products [‰ PDB] demonstrate the preservation of the original isotopic distance given by sugar derived from C4 and C3 plants.

contamination before analysis. The thermal fragmentation during pyrolysis has been proven to generate reaction products whose isotope values are reproducible and in the range expected for the natural occurring precursor (Gleixner and Schmidt, 1998; Gleixner et al., 1999; Schulten and Gleixner, 1999; Kracht and Gleixner, 2000).

3.1 Physico-chemical reactions of the pyrolytic process

Curie-point pyrolysis uses a high frequency field to get ferromagnetic alloys to reach their paramagnetic properties. At this point the alloy does not adsorb any more energy and remains at a specific temperature. In contrast to other flash pyrolysis methods, Curie-point pyrolysis requires a longer period of time to reach the Curie-point temperature (20-30 ms). This is important for the reproducibility of the procedure as the heat transport through the sample should be as fast as possible. During the time when the temperature is rising the first thermal reactions occur as three main reactions: 1) main-chain scission or depolymerization, 2) carbonization, and 3) side-group reactions, which mainly produce water and CO_2 in addition to SO_2, CO, and H_2 (Flynn and Florin, 1985; Moldoveanu, 1998) (Figure 3.2). The reactions also depend on the presence of additional reactants or catalysts which may modify the result of the pyrolytic reaction. The most common, unintentionally present reactants are most likely oxygen, hydrogen and water. These are produced in initial thermal reactions and may drive secondary reactions. Pyrolysis time should thus be kept short. Due to the heterolytic character of the pyrolysis reactions the presence of acidic or alkaline catalysts or salts may significantly influence the thermal degradation and the relative yield (Meuzelaar et al., 1982). Other catalyzing reactions may occur on the metal surface of the pyrolysis tube and during transport of the volatiles in the needle of the sample holder. A high flow rate reduces the residence time of the volatiles and can counter this effect. Considering the large number of different, possibly competing pyrolysis reactions that occur in highly complex biomaterials, the stability of the pyrolysis patterns of such materials is remarkable.

3.2 Typical pyrolysis products obtained from natural organic polymers

Pyrolysis of natural biopolymers has a long tradition and much detailed information on composite natural organic material is available. A comparison of the resulting products, however, must always take into account that variations in pyrolysis temperature may yield different pyrolysis products. The pyrolysis products essential in this study and commonly encountered upon Curie-point pyrolysis between 400-600 °C include fragments of carbohydrates, lignin, proteins, and lipids.

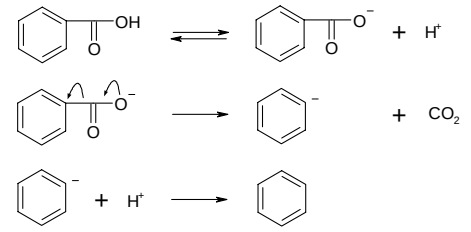

A)
Decarboxylation reaction of aromatic acids, i.e. benzoic acid

B)
Decarboxylation of beta-lactones, extrusion reaction

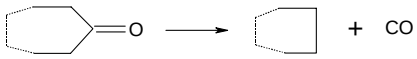

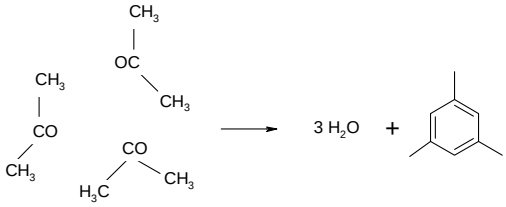

C)
Condensation of acetone with the formation of a molecule that is more stable at higher temperatures

D)
Free radical substitution, formation of polynuclear aromatic hydrocarbons from benzene

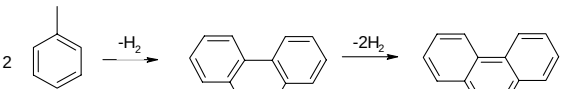

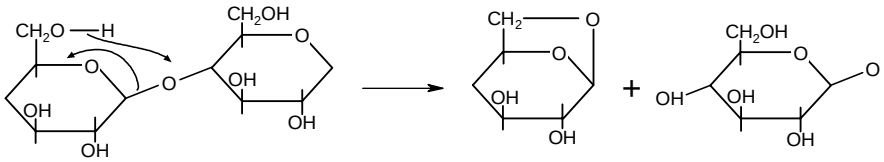

E) Transglycosidation reaction

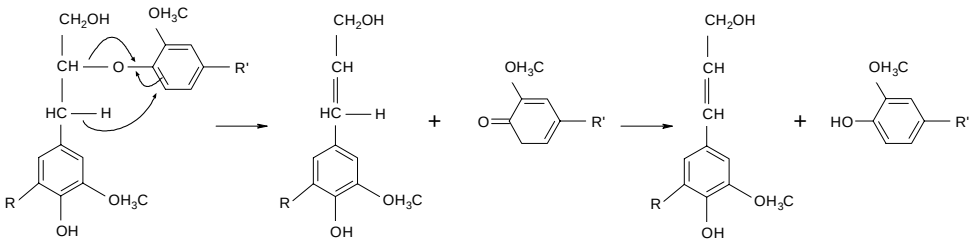

F) Possible reaction for lignin degradation

Figure 3.2: Selection of possible reactions occurring during pyrolysis of organic matter (adapted from Moldoveanu, 1998). A) and B): Side-group reactions; C) and D): carbonization, E): main-chain scisson, F): pyrolytic lignin degradation.

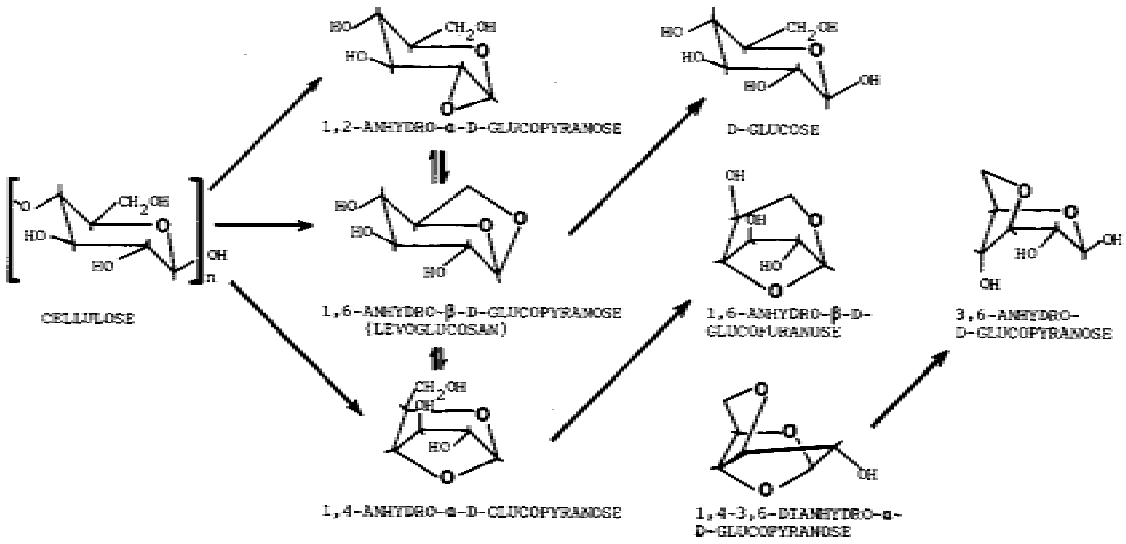

Figure 3.3: Initial reactions upon pyrolysis of cellulose showing depolymerization by transglycosidation (adapted from Irwin, 1982).

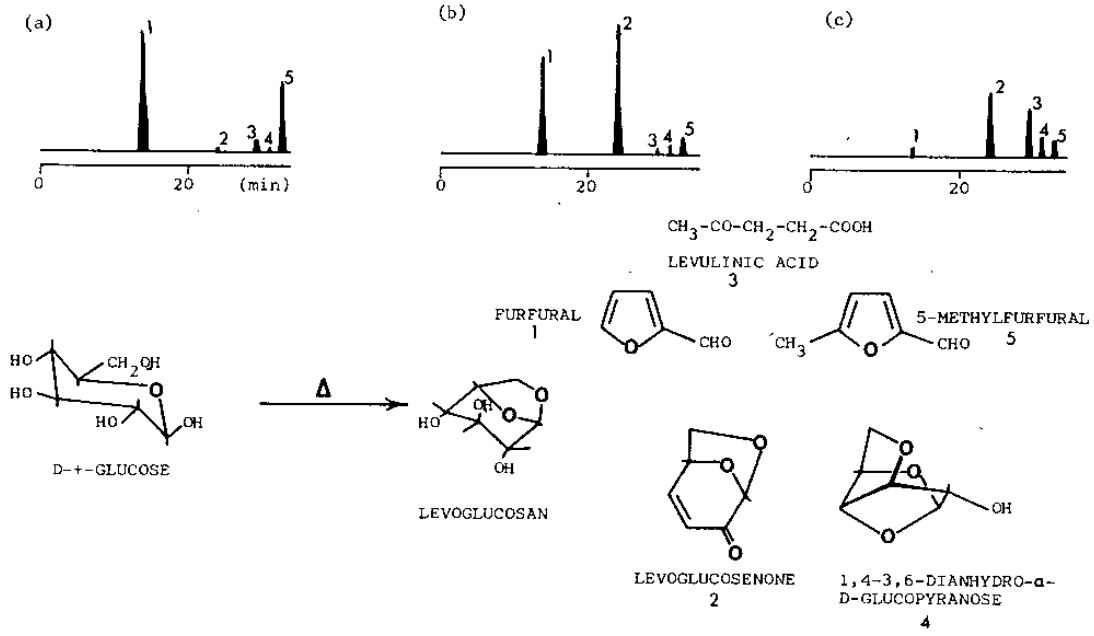

Figure 3.4: Curie-point pyrolysis of D-glucose, cellulose, and levoglucosan. The pyrolysis of monosaccharides shows essentially the same fragmentation but variation in product distribution: a) glucosan, b) cellulose, c) levoglucosan (adapted from Irwin, 1982).

Carbohydrates

Polymeric carbohydrates (e.g. polysaccharides such as in cellulose) are formed by bonding monosaccharide units through the elimination of a water molecule and the formation of an ether bond (Figure 3.2 E). The initial pyrolytic reactions thus involve a depolymerization and the release of adsorbed water with a series of inter- and intramolecular transglycosidation reactions (Figure 3.3). Among monosaccharides and aminosugars, cellulose and starch are the most probable polymers expected to occur in the samples. The total number of pyrolysis products from carbohydrates can be as large as 120. The most common product upon pyrolysis of cellulose and starch is levoglucosan ($C_6H_{10}O_5$). Other prevailing compound classes are anhydrosugars, furan derivatives, pyranones, acids and, acid esters. Cellulose in particular has been found to produce considerable amounts of gas, tar, and carbonaceous residue during pyrolysis (Irwin, 1982; Moldoveanu, 1998).

Lignin

Lignin can be considered a three-dimensional network polymer of phenylpropane units, the most common of which are 4-hydroxyphenylpropane, guaiacylpropane and syringylpropane. Thermal degradation by pyrolysis results basically in cleavage of internal linkages. The basic aromatic structure remains unaffected thus producing a number of alkylphenols and their methoxylated derivatives. Investigations on biodegraded lignin showed that side-chains were preferentially attacked by white-rot fungi (Martínez et al., 2001) yielding decreased proportions of syringyl-lignin units and increasing amounts of benzene derivatives as pyrolysis products (van Smeerdijk and Boon, 1987; Durig et al., 1991).

Proteins and lipids

The great majority of pyrolysis products found in the samples can be assigned to lignin and carbohydrate precursor material. Less abundant natural biopolymers such as amino acids, nucleic acids, and lipids produce only traces in the chromatogram. Some characteristic fragments shall be annotated.

The occurrence of nitrogen in pyrolysis products is the most likely indicator of amino acids or amino sugars as precursor material. Some fragments may also be produced from nucleic acids (Posthumus et al., 1974). Common pyrolysis products are pyrrole, nitrile and their derivatives, rarely heterocyclic amines, but also alkylphenols and alkylbenzenes have been reported (Stevenson, 1994).

Long-chain aliphatic compounds such as encountered in the class of lipids react upon pyrolysis by elimination and/or randomization of cleavage, the first of which is probably the elimination of a fatty acid residue. Principal products are most likely to be hydrocarbons such as alkanes and alkenes. Cyclization resulting in alkylaromatics has been reported upon pyrolysis of lipids in the presence of catalysts (Saiz-Jimenez, 1996).

4 Application and quality assessment of Py-GC/MS-IRMS

The degradative method must be interfaced with powerful techniques like gas chromatography and mass spectrometry in order to describe the polymeric and complex, variable structure of many natural compounds such as cellulose, lignin, but also whole bacterial or fungal organisms, bulk OM or DOM. The determination of natural abundances of stable isotopes in chromatographically separated volatiles has been greatly enhanced since the first commercial application of a system that couples isotope ratio monitoring with on-line combustion in 1988 (Brand, 1996). The combination of these techniques thus allows 1) a separation of a sample into structural units, 2) the identification of the units by mass spectra, and 3) the determination of their isotope ratios (compound specific isotope analysis). A coupling of these analytical techniques was achieved for the first time at the Max-Planck-Institut für Biogeochemie, Jena, Germany, in October 1998 (Figure 4.1).

4.1 Pyrolysis (Py)

The freeze-dried and milled sample material (0.2 to 1.0 mg) was filled in a ferromagnetic sample tube and then inserted into a glass liner of a Curie-point pyrolyzer (type 0316, Fischer, 53340 Meckenheim, Germany). The sample material was maintained in an inert atmosphere under constant He flow to eliminate any oxygen fixed to the sample material. Both sample holder and liner were manually placed in a conductor (Figure 4.2). An alternating magnetic flux causes a rapid temperature increase (20-30 ms) to a temperature level that is specific for the sample holder material (Curie-point). The alloy and dimensions of the holder used for this investigation allowed a temperature of 773 K, which was maintained for 9.9 s to initiate primary-bond fission and competing reactions before the volatile pyrolysis products were transferred to the injection chamber of the GC and onto

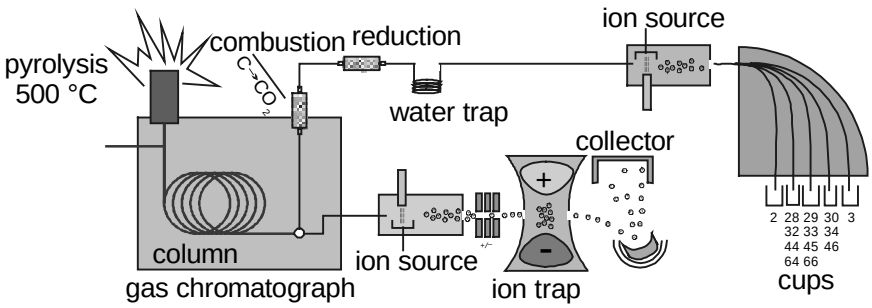

Figure 4.1: Scheme of the Py-GC/MS-IRMS system as it was set up for the present study. The fixed splitter at the exit of the GC column splits the eluting substances in an approx. ratio of 1:9 for simultaneous recording of mass spectra in the ion-trap MS and $\delta^{13}C$ values in the IRMS.

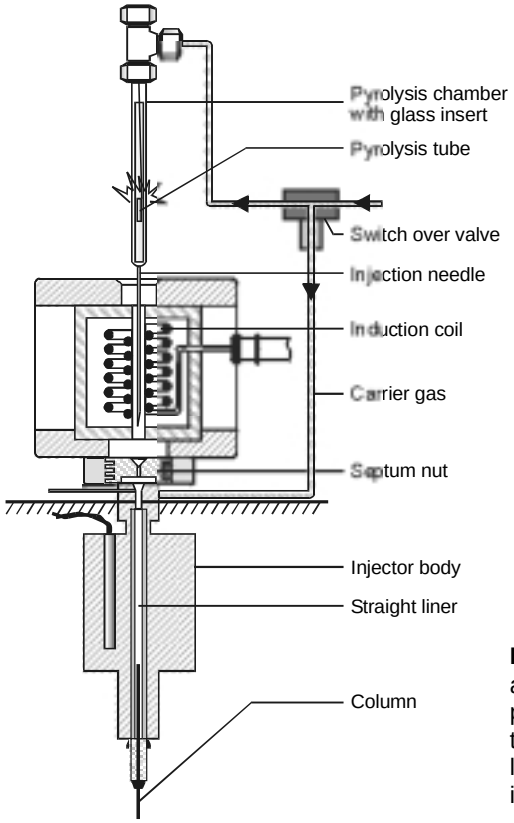

Figure 4.2: Scheme of the Curie-point pyrolysis device attached to the injector body of the GC as used in the present study. The injection needle must be inserted through the septum in the septum nut into the straight liner so that the pyrolysis tube is on a level with the induction coil.

the column.

Pyrolysis tubes were favored over wires for their higher sample capacity. The sample amount was chosen to achieve a balance between a sufficient signal intensity (signal-to-noise ratio) in the IRMS and column overload in the GC, which would raise the signal intensities above the range of linearity. Too much sample material can also impact the measurement reproducibility if the heat transport in the tube is slowed down or non-uniform such that the probability of secondary recombination reactions increases. Peak resolution and standard deviations of peak area improved when the amount of sample was kept as low as possible and nearly identical from sample to sample. The $\delta^{13}C$ values did not show variations with sample amount, thus confirming that no isotope fractionations occur by slight changes in analytical conditions.

Great care was required to avoid a 'memory effect', or contamination by leftover sample material from one analysis to the next. This problem was well observed in the initial experiments. In particular, the substance levoglucosenone, a carbohydrate pyrolysis product, appeared to remain in the pyrolysis system probably as tar and thus contaminated following samples. The potential contamination dilemma was overcome by adding a quartz glass insert in the pyrolysis chamber which captured the tar that was precipitated on its walls during pyrolysis and was replaced. The insert, however, may have increased the time required for the temperature to reach the Curie-point. The pyrolysis chamber and needle

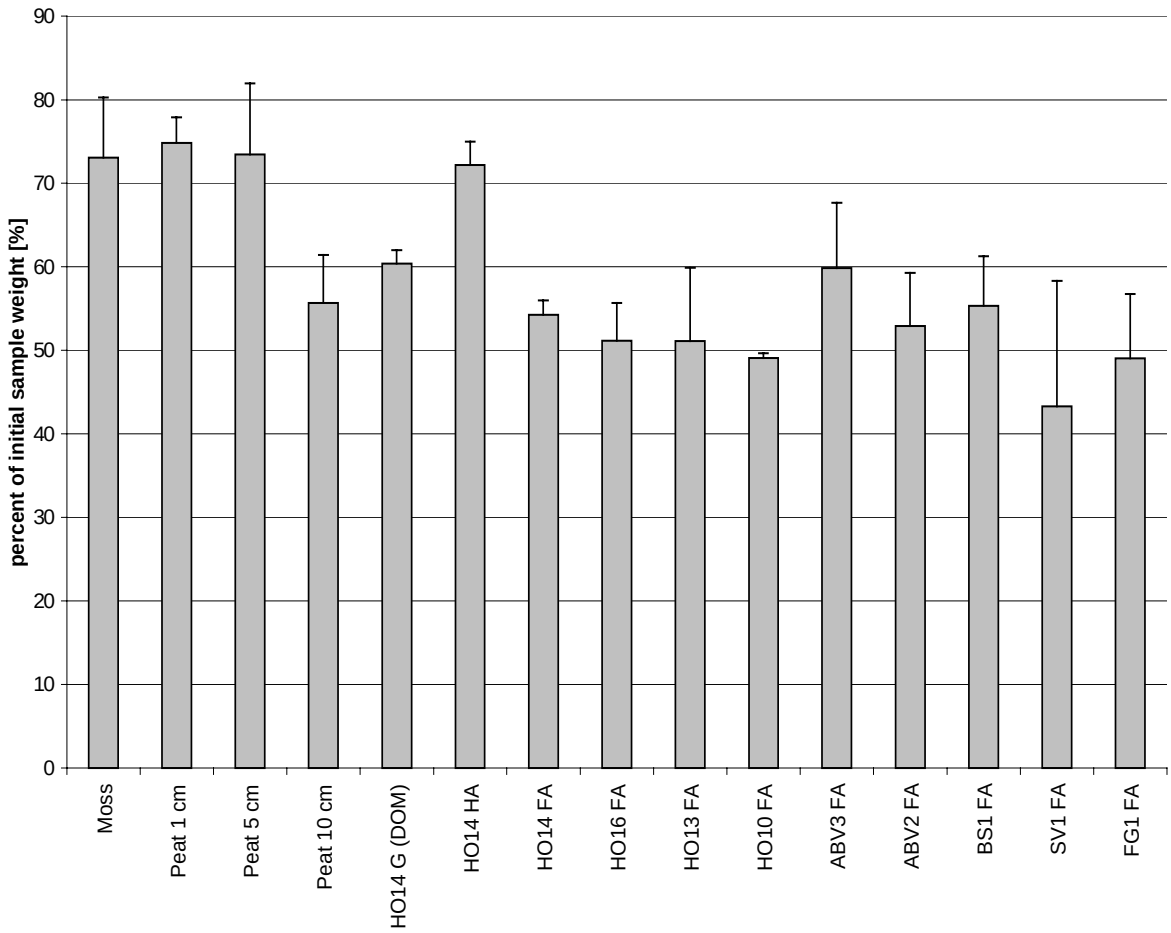

Figure 4.3: Yield of pyrolyzed substance for all samples analyzed in percentage of the initial sample weight including standard deviations. The loss of sample material is due to tar precipitating on the wall of the glass liner and to the carbonaceous residue remaining in the pyrolysis tube.

were cleaned by washing with acetone and a mixture of chloroform and methanol (1:1) in an ultrasonic bath after each run. The ferromagnetic pyrolysis tube was cleared of the remaining carbonaceous residue and annealed in the flame of a gas burner. Weighing before and after analysis confirmed proper removal of the residue.

The pyrolysis temperature impacts the behavior of the humic substances. Generally, an increase in temperature results in smaller and less characteristic fragments (Irwin, 1982). This study used a pyrolysis temperature of 773 K, which has been reported to be a good range to obtain a well-balanced distribution of pyrolysis products for polysaccharides and lignins and particularly for fulvic acids (Saiz-Jimenez, 1994).

One of the drawbacks of pyrolysis is that during pyrolysis only a relatively small amount of sample material is volatilized and subsequently analyzed. In the present study the pyrolyzed compounds represented 43%-60% of the initial sample material for the ROSIG fulvic acids (FA) and 56%-75% for the peat samples and the DOM from the bog lake Hohlohsee (Figure 4.3). The remaining material consisted of tar that precipitates in the

glass liner (up to 0.16 mg) and a coal-like carbonaceous residue in the pyrolysis tube. Pyrolysis of cellulose was reported to yield large amounts of tar (Irwin, 1982). Although the standard deviations of tar weight varied largely, the fulvic acids of the ground water and of the waste water effluents ABV2 and ABV3 appeared to precipitate the greatest amount of all FA samples. No data concerning tar are available for the peat samples. However, the visible precipitate of tar in the glass liner decreased with sample depth whereas the carbonaceous residue in the tube was highest in peat at 10 cm depth below the surface. These observations support the assumption that easily decomposable material such as cellulose is more abundant in upper peat layers and probably as well in ABV2, ABV3 and FG1. This was tested by correlating tar proportions yielded by pyrolysis with structural data obtained from NMR (Lankes and Lüdemann, 2001). The diagrams, however, suggest that the tar fraction results from aliphatic compounds such as found in lipids and not from carboxyl rich polymers such as cellulose (Figure 4.4, C and D). This may also explain the low amounts of aliphatic compounds observed in the samples after pyrolysis. It remains speculative to what extent this observation applies to the peat samples.

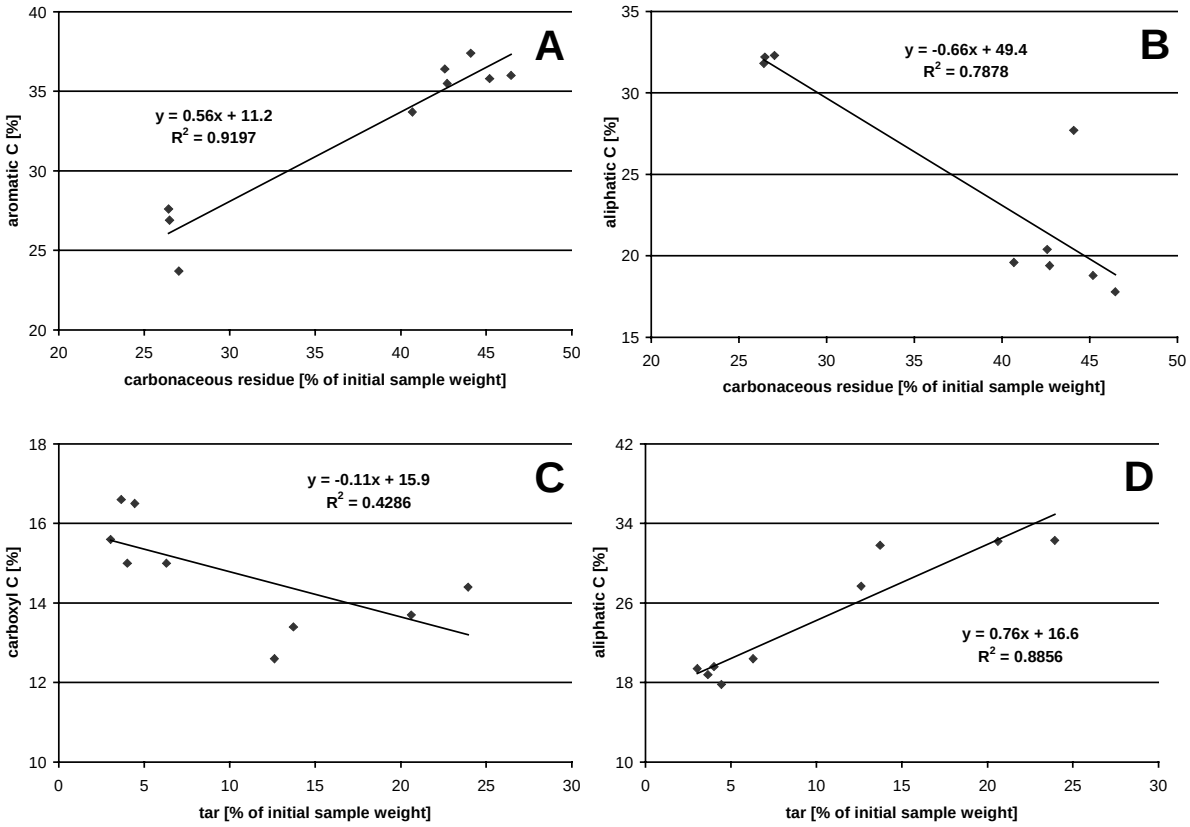

Figure 4.4: Correlation diagrams between structural NMR-data and residues of pyrolysis reactions. Data points are based on results obtained from pyrolysis of all fulvic acids of the ROSIG samples: A and B) carbonaceous residue in the pyrolysis tube, C and D) tar precipitated on the walls of the glass liner. NMR-data from Lankes and Lüdemann (2001) and listed in Appendix I.

The amount of the non-analyzable carbonaceous residue, on the other hand, is likely to be an indicator of already existent condensed organic matter as in the brown coal processing waste water SV1. Condensation of organic matter eventually results in an agglomeration of aromatic carbon, e.g. in coals, which is essentially inert due to strong C-C bindings and a deficiency of functional groups. The good correlation between relative amounts of carbonaceous residue and relative amounts of aromatic C obtained from NMR-data (Figure 4.4, A and B) is indicative of the aromatic character of the residue.

4.2 Gas chromatography (GC)

The crucial point in gas chromatography is the injection of the sample material with transmission onto the column. It depends on a combination of temperature gradients, flow of carrier gas, split ratio to prevent column overload, cleanliness, and accurate selection as well as assemblage of the different parts. The needle of the pyrolysis chamber was inserted into a simple straight liner (4 mm ID) of the injection chamber in the GC. The liner was filled with glass wool. The split flow controlled the amount of gas phase transferred onto the column. During progressive enhancement of the system, a retention gap was introduced between the injector and the column. This piece of 5 m of fused silica improved component separation, but resulted in a shift of peaks towards higher retention time and thus required a re-adjustment of retention time indices with former analyses. The BPX5 column (5% phenyl polysilphenylene-siloxane) used in this study is a durable multi-purpose column that is suitable for trace analysis of a broad range of substances, polar and non-polar. It also allows a high operating temperature of max. 643 K.

The pyrolysates were transferred to the GC by split injection (split ratio approx. 1:9) with a He flow of 1.6 ml/min. The volumetric flow rate was controlled electronically by the column head pressure (EPC). Separation of volatiles was accomplished on a BPX 5 column (60m x 0.32 mm, film thickness 1.0 µm, Scientific Glass Engineering, 64331 Weiterstadt, Germany) in an HP 5890 (76337 Waldbronn, Germany) using a temperature program of 309 K held for 5 min, temperature increase of 5 K/min to 543 K, followed by an instant rise of 30 K/min to a final temperature of 573 K. The injector temperature was set to 523 K. An outlet splitter (X-piece, Valco, VICI AG, 6214 Schenkon, Switzerland) at the exit of the column provides a fixed split of the effluents to the MS and the IRMS. Pressure differences, length, and inner diameters of the capillaries determine the ratio of the split. The ratio in this study was set approximately to 1:9, with one part being transferred to the ion-trap MS and nine parts to the IRMS.

4.3 Mass spectrometry (MS)

Mass spectrometry is commonly used for the identification of compounds due to their characteristic mass spectra. A comparison of mass spectra proved necessary to assure that substances eluting at similar retention times but in different samples were actually the same (Figure 4.5).

The two crucial parts of a mass spectrometer are the ionization and the separation of the masses. The ionization used in this study was performed by the most commonly applied electron impact (EI) resulting in positively charged fragments of a molecule exiting the GC column. Mass separation of the fragments is generally achieved in a magnetic field after acceleration. However, in contrast to single or double focussing MS the quadrupole ion trap used in this study keeps the ionized fragments in a mass analyzer cavity before they are ejected towards the ion detection system. Since mass spectra in spectra libraries for computer-aided search are based on other MS than ion trap MS, the identification of compounds can be more difficult. The reliability of mass spectra from the ion trap MS for library search was examined with a Py-GC/MS system used by the group of Prof. Dr. R. Schulten at the Institut für Bodenkunde, Universität Rostock. Slight shifts in the proportions of the intensities of the single masses were frequently observed (Figure 4.6). These shifts probably result from interactions of the fragments in the cavity of the ion trap mass analyzer which may produce further fragmentation. Thus several compounds are tentatively identified and marked with "(T)" if not confirmed by external standards or spectra from the literature (e.g. van Smeerdijk and Boon, 1987; Stout et al., 1988; Durig et al., 1991; Ralph and Hatfield, 1991). The complete list of mass spectra of the pyrolysis

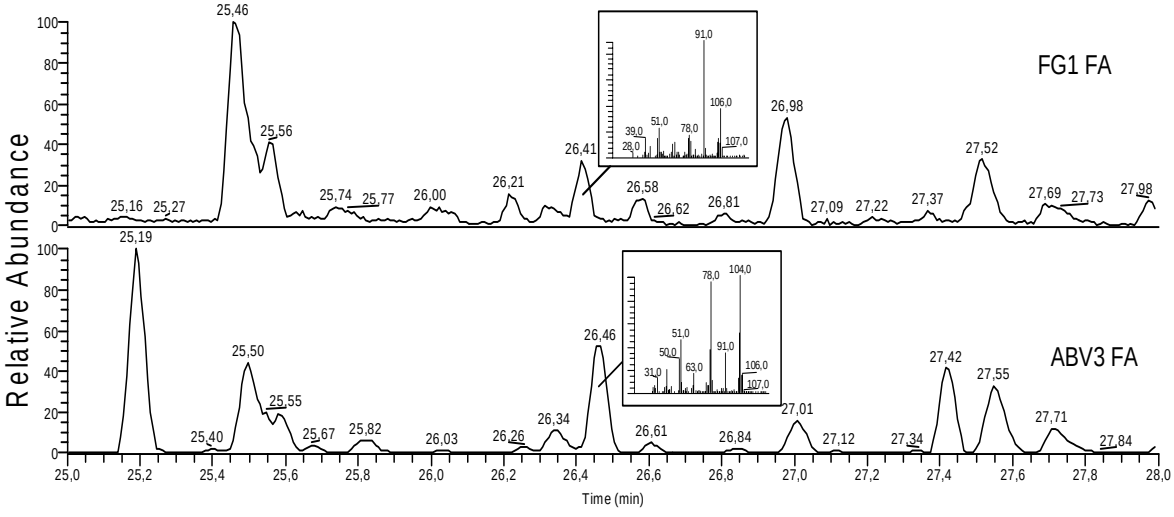

Figure 4.5: The comparison of mass spectra revealed that the substances eluting at a similar retention time (tR) in the groundwater FA (FG1, tR: 26,41) and the waste water FA (ABV3, tR: 26,46) are different. Note that there is an overall shift in tR of 3/100-4/100 min (industrial time) between the two samples due to analytical inaccuracies.

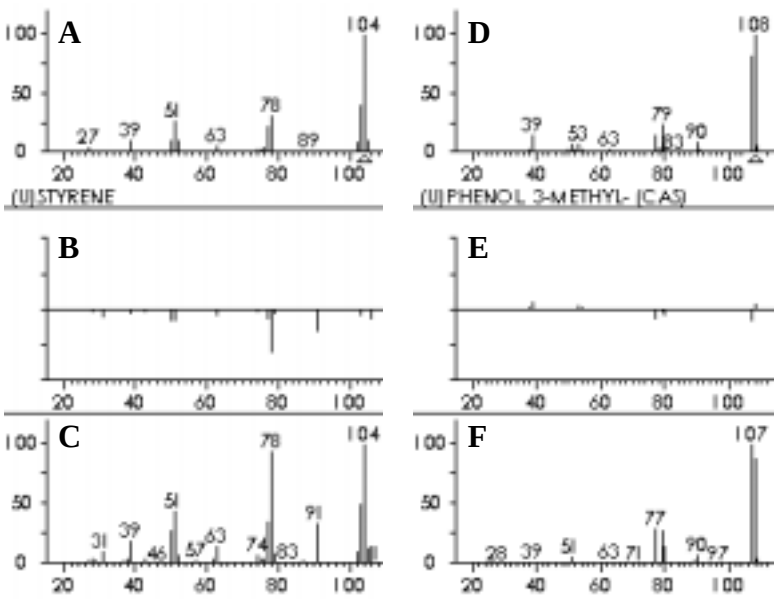

Figure 4.6: The results from the library search of two compounds (A, D) are compared to the spectra found in a sample analyzed by ion trap MS (C, F). The increase of mass fragments 78 in styrene and *m/z* 107 in 3-methylphenol is believed to be due to additional fragmentation in the mass analyzer cavity. The center row (B, E) presents the resulting spectrum after subtraction of A-C and D-F.

products is given in Appendix III. Chromatograms (total ion current, TIC) are shown in Appendix IV.

The ion-trap MS (GCQ, ThermoQuest, 63329 Egelsbach, Germany) was connected to the X-piece in the GC by a capillary of about 100 cm length (ID 0.1 mm) through a heated transfer line. The temperature of the transfer line was set to 543 K to avoid condensation of GC effluents. Transferred pyrolysis products entered the ion source (temperature set to 453 K) and were ionized by positive-ion electron impact (EI) with 70 eV ionization energy. The ion gauge pressure reached $1.2 \cdot 10^{-5}$ mbar. Mass spectra were obtained by scanning masses from *m/z* 26 to *m/z* 400. The scan time was 0.5 sec/scan.

4.4 Isotope ratio-mass spectrometry (IRMS)

Isotope ratio-mass spectrometer must be capable of measuring isotope ratios with highest possible precision and accuracy, particularly for measurements of naturally occurring isotope fractionations which can be as small as a few parts per million (ppm). In contrast to normal mass spectrometers such as ion-trap, quadrupole, and time-of-flight MS, IRMS uses simultaneous collection of all relevant ion beams in a multiple Faraday collector system to achieve highly precise results. The resolution of an IRMS, however, is lower so that complex molecules must be transferred into simple gases to keep the range of possible ionized masses narrow. For on-line measurements of stable isotopes the GC effluents were combusted to CO_2 and sent continuously to the mass spectrometer in a helium carrier stream. The method is also referred to as irmGC/MS (isotope ratio monitoring GC/MS) or GCCMS (GC Combustion MS). Compound specific isotope analysis (CSIA), as introduced in this study, required the adjustment of several parameters for precise measurements.

The system was equipped with a GC-Combustion Interface III (Finnigan MAT, 28197 Bremen, Germany). The interface maintained chromatographic conditions from the GC column exit to the ion source of the MS. The particular units of the interface ensured quantitative conversion of C to CO_2 without isotope fractionation, removal of H_2O in a Nafion®-tube, backflush of oxygen for re-oxidation of the combustion furnace and backflush of He to protect the ion source from undesired effluents. The oxidation furnace at the entrance of the combustion unit was equipped with CuO, NiO, and Pt wires and set at a temperature of 1233 K. An open split assembly at the end of the combustion interface was employed to transport the reaction product, i.e. CO_2, into the ion source and to introduce a reference gas under identical conditions. The design of open split assemblies allowed the dilution of reaction products with He to keep signal intensities in the range of linear operation and to reduce background signals. Therefore He pressure was set to 2 bar which corresponded to approximately 90 % of the effluent stream from the combustion interface to be transferred into the ion source. Linearity of response was achieved by keeping signal intensities in a range of 200 mV to 8000 mV (Figure 4.8).

$^{13}C/^{12}C$ analysis was done by converting the carbon of organic molecules into the elementary gas CO_2 and detecting ions of mass *m/z* 44, 45, and 46 corresponding to $^{12}C^{16}O_2$, $^{13}C^{16}O_2$, and $^{12}C^{16}O^{18}O$. The proportion of $^{12}C^{17}O^{16}O$ (*m/z* 45) was corrected automatically after Craig (1957). For $^{13}C/^{12}C$ ratio determination ISODAT 7.0 software (Finnigan MAT) was employed. The instantaneous rate of change of the signal was determined using a five point linear regression for each data point. Peak detection was prompted for start slope thresholds of 0.3 mV/s and 0.4 mV/s at the end and if the

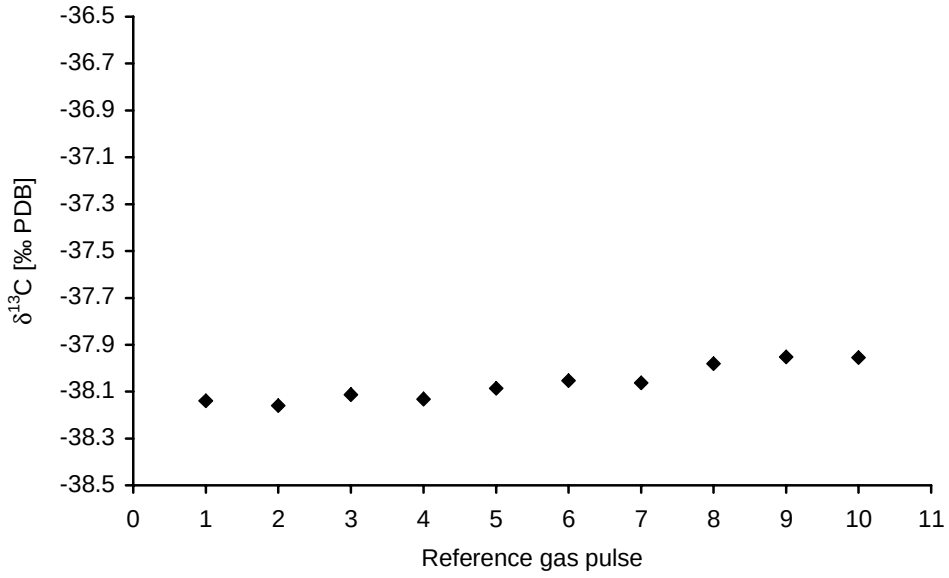

Figure 4.7: Linearity assessment of the reference gas pulse. On/off switch of the CO_2 reference gas ($\delta^{13}C$: -38.16‰) over a period of 6 min. Reference gas pressure was set to 1.0 bar, carrier gas pressure (He) was set to 2.0 bar. There is a slight shift towards higher δ-values with time (analyses performed by Rühlow).

amplitude was higher than 200 mV. Background subtraction was automatically applied using the dynamic background function (DyBGD) of the software. This function modeled the background of the whole chromatogram and has been chosen to account for the partly high backgrounds and the dense sequence of peaks that occurred after Py-GC of the samples (see also Figure 4.10).

The high amount of substances produced upon pyrolysis of DOM results in a chromatogram with a dense sequence of peaks. For precise isotope measurements, however, it is required that the peaks are properly resolved, i.e. the peak end slope returns

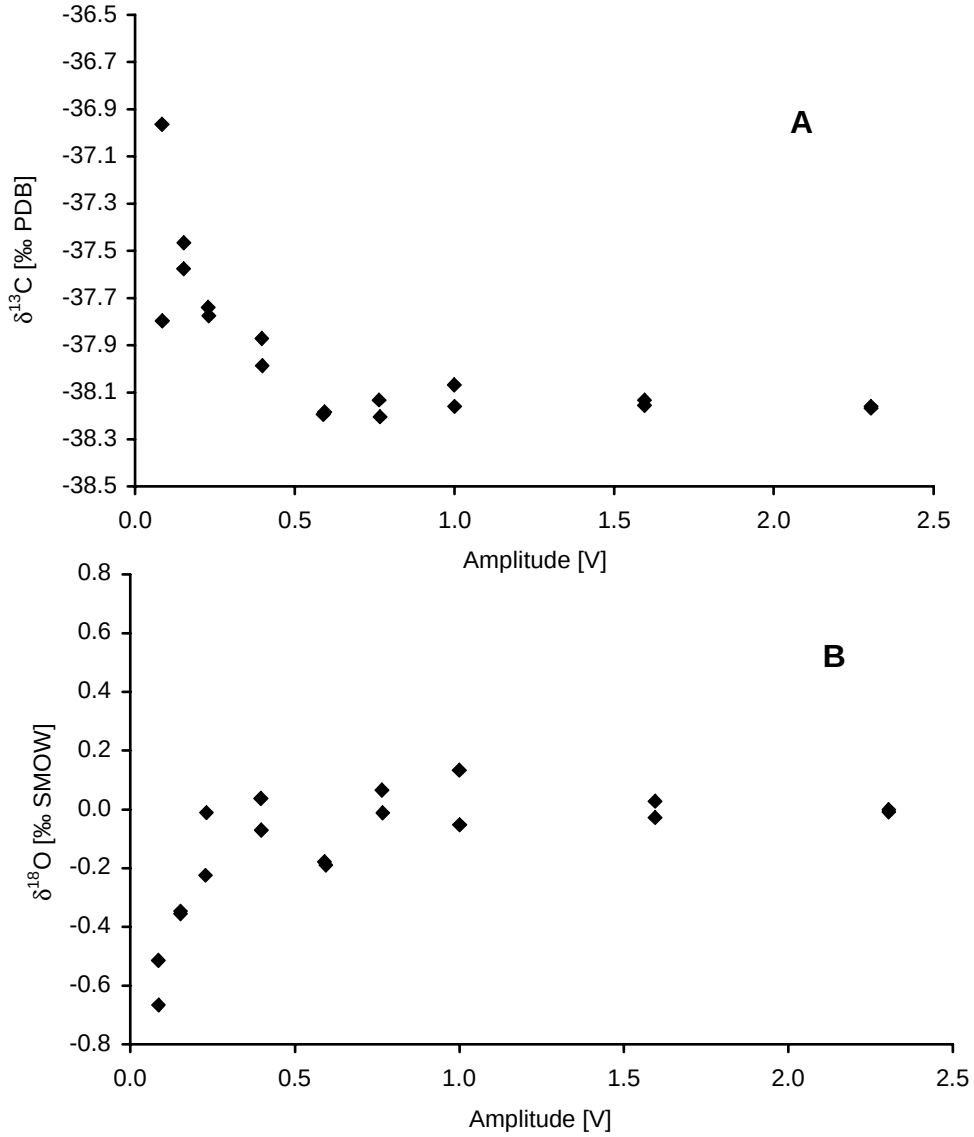

Figure 4.8: Test for range of linearity with respect to amplitude height. Reference gas pulses of CO_2 were set with increasing pressure (0.05 to 1.0 bar) resulting in increasing amplitude signals. The pressure of the carrier gas (He) was set to 2.0 bar. δ-values in good agreement with the known values of the reference gas ($\delta^{13}C$: -38.16‰ A; $\delta^{18}O$: 0.0‰ B) were reached with an amplitude height of 0.2 V thus setting the lower detection limit for pyrolysis products (analyses performed by Rühlow).

to the intensity of the background signal before the following peak starts. This was not the case for all eluted components. Consequently, several peaks had to be omitted from data interpretation. The remaining peaks had to be checked by comparison with the MS data to determine if an apparent single peak consists of two components, as can occur at co-elution. This would result in a mixing of two different $^{13}C/^{12}C$ ratios.

The range of standard deviations of ^{13}C signals of individual pyrolysis products is greater than what is commonly measured using modern IRMS. Several parameters are probably responsible, i.e. sample inhomogeneity and changing analytical conditions in one of the units which reduces reproducibility. For example, the oxidation furnace performance had to be checked regularly by external standard runs (caffeine) to account for the long-term shift in isotope ratios by decreasing oxidation efficiency. This effect is shown in Figure 4.9. After re-oxidation of the furnace the performance of the IRMS improved noticeably. Measurements with an external standard (caffeine, –51.8‰) resulted in an accuracy of ±0.4‰ and a reproducibility of ±0.2‰ to ±0.4‰ depending on the concentration of the standard (Figure 4.9). The slight signal drift during single runs (Figure 4.7) was accounted for by introducing reference gas peaks of CO_2 (–38.16‰) at the start and the end of a run.

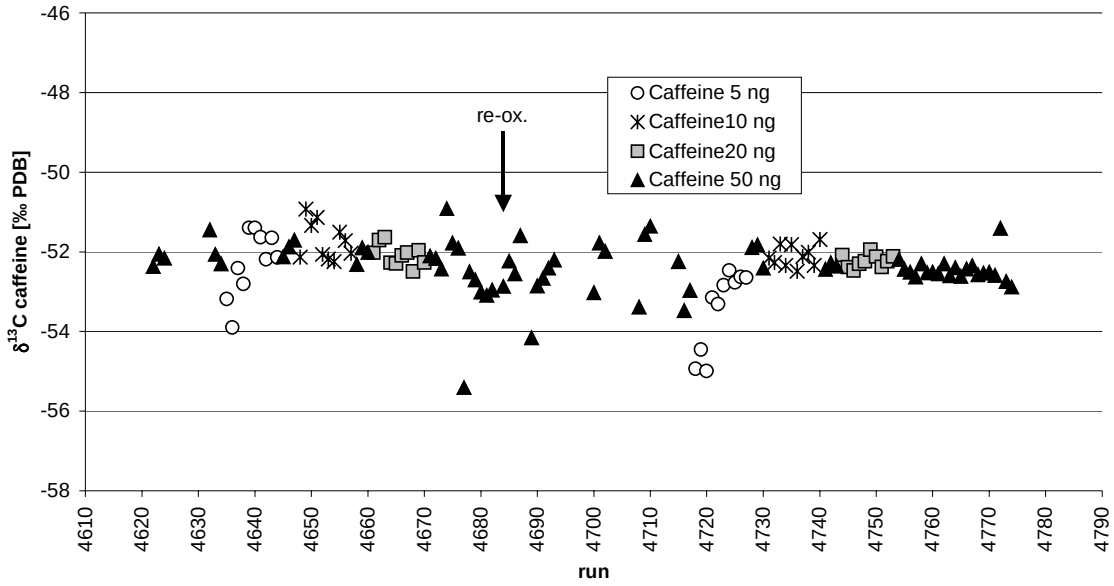

Figure 4.9: Long term observation (12 days) of the IRMS performance with an external standard of different concentrations (caffeine dissolved in ethyl acetate, -51.8‰). Best reproducibility was achieved at a concentration of 10-20 ng yielding amplitudes of 200 mV to 500 mV with standard deviations of 0.4‰ and 0.2‰, respectively. Accuracy was ±0.4‰ for both concentrations. Re-oxidation of the combustion furnace was carried out before run 4684 resulting in a higher reproducibility after excess oxygen was entirely removed from the system about 48 hours later (analyses performed by Rühlow).

4.4.1 Isotope data attainment and control

Samples were analyzed at least three times when there was sufficient sample material (except for the groundwater sample FG1 FA which was measured only twice) to determine standard deviations. Each run employed a sequence of 2-3 reference gas peaks at the beginning and at the end of the analysis, respectively, while the backflush was off. The $\delta^{13}C$ value of the CO_2 reference gas was –38.16‰. One of the reference gas peaks at the beginning and at the end, respectively, was set to this value for automatic data calculation, thus accounting for the influence of drift and background effects.

4.4.2 Quantitative calculations of pyrolysis products

Peak areas in chromatography are a measure of the quantity of a substance. Usually, a standard compound of known quantity is added to the sample whose peak area serves as a direct measure for the unknown substances. One of the drawbacks of pyrolysis is that there is no appropriate way of precisely adding a known amount of a substance to the sample nor is there any certainty on how the chosen substance interacts with the sample during pyrolysis. A promising result concerning internal standards for quantification of pyrolysis products was reported by Bocchini et al. (1997), who added a tributylbenzene solution in CH_2Cl_2 to the sample. This method, however, did not seem to be appropriate for the present study. Due to different setups of the pyrolyzers, an undesired evaporation of the standard solution before pyrolysis was expected and the standard itself was suspected to add additional carbon isotope signals to the samples. The lack of a standard could be overcome by normalization of peak areas to correct for differences in sample size. Relative amounts of individual pyrolysis products were calculated using the *m/z* 44 trace of the IRMS chromatogram for $\delta^{13}C$ analyses. Thus the amount of CO_2 produced by combustion of a single substance was normalized to the total amount of CO_2 in the analytical window

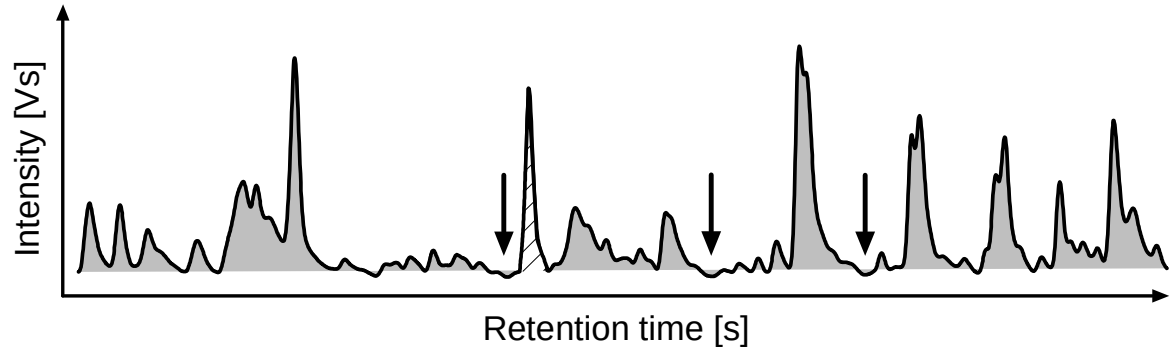

Figure 4.10: Example to explain the calculation of peak area normalization. The area of the peak is normalized by the total area in a certain time interval (shaded area, 900 – 2900 seconds in the IRMS chromatogram). Using the dynamic background function avoided negative area values, i.e. areas above the intensity of the signal as indicated in the figure by arrows.

(expressed in percentage of peak area to total area integrated over a fixed time interval, see Figure 4.10). This approach enables a direct comparison of the proportional amounts of a single pyrolysis product in the total pyrolyzed material. The standard deviation of the area values is partly insufficient to yield statistically significant statements. This problem has been encountered in numerous analyses since setting up the system and could only be limited if a set of samples is run during periods of identical analytical conditions. Slight changes in the analytical conditions (e.g. the exchange of the filament, pressure variations of the carrier gas, oxidation furnace), of the IRMS appeared to have a notable impact on the peak amplitude (or area) rather than on isotope values. The calculation of absolute amounts, i.e. normalized to 1 mg of sample weight, have been omitted due to even higher errors coming from additional inaccuracies during weighing. A complete mass balance was also not possible. The first peak of the chromatogram representing the low molecular weight volatiles such as water and CO_2 far exceeded the capacity of the IRMS ion source and had to be filtered out. It should be noted that the ratios of the peak intensities were not the same in the MS chromatograms as compared with the IRMS chromatograms (for comparison of MS and IRMS traces see Appendix IV). This reflected the difference in analytes used for detection, i.e. fragments of the molecule or its CO_2 produced from oxidation.

For $\delta^{13}C$ values of grouped pyrolysis products (Chapter 5 and 6), $\delta^{13}C$ values of individual products were weighted by peak areas, i.e. summed up and divided by the total area of the group. The value thus represents a 'bulk' value. Standard deviations are based on the regular, non-weighted δ-values and are elucidated by the quotation of ranges.

4.5 Analytical parameters and technical data of additional sample measurements

In addition to the compound specific isotope analysis performed by Py-GC/MS-IRMS, several framing parameters of bulk sample material have been determined particularly for the peat samples. Analytical parameters and technical data of these measurements are listed below. Data from elemental analysis of the ROSIG samples were provided by the working group of Dr. G. Abbt-Braun (Universität Karlsruhe). Structural information by ^{13}C-NMR was obtained from the working group around Prof. Dr. H.-D. Lüdemann (Universität Regensburg). Technical and analytical details are given in Frimmel and Abbt-Braun (1999) and Lankes (2001), respectively. These data sets were partly used in statistical calculations.

4.5.1 Bulk isotope analysis (EA-IRMS)

About 2 mg of sample material were placed in tin containers (LÜDI AG, 9230 Flawil, Switzerland) and combusted in an EA 1110 Elemental Analyzer (ThermoQuest, 20090 Rodano, Italy). CO_2 and N_2 were separated by GC and analyzed for ^{13}C and ^{15}N in a Delta^{Plus}XL isotope ratio mass spectrometer fitted with the Combustion Interface II (both from Finnigan MAT, 28197 Bremen, Germany). $\delta^{13}C$ and $\delta^{15}N$ values are expressed relative to international standards V-PDB and atmospheric air, respectively.

δD values were analyzed using about 10 mg of sample material in the same instrument, prepared at 1723 K in the conversion furnace and then measured. Values are expressed relative to V-SMOW. All samples were equally equilibrated to room air such that values can only be considered relative to one another.

Oxygen isotope analysis was performed under controlled pyrolysis conditions. About 4 mg of sample material were placed in Ag capsules (LÜDI AG, 9230 Flawil, Switzerland) and the bound oxygen was quantitatively converted at 1373 K to CO. After GC purification the gas was transferred to a VG MM 903 IRMS (VG, Middlewich, Great Britain). Values are expressed relative to V-SMOW.

The precision of bulk isotope measurements is: 0.16 ($\delta^{13}C$), 0.10 ($\delta^{15}N$), 0.8 ($\delta^{2}H$), and 0.14 ($\delta^{18}O$). These values are based on standard deviations of long term measurements of standard material (Werner and Brand, 2001).

4.5.2 Calculations

By international convention the isotope ratio is expressed in δ-values. It was introduced for the first time by McKinney et al. (1950) as the deviation of the isotope ratio relative to a standard (here, for example, $\delta^{13}C$):

$$\delta^{13}C_{sample}\ (‰) = (R_{sample} - R_{standard}) / R_{standard} \times 1000,$$

where R is the isotopic ratio of $[^{13}C]/[^{12}C]$. $R_{standard}$ is the defined isotope ratio of a standard sample, a limestone fossil of the Cretaceous Pee Dee Formation in South Carolina for $\delta^{13}C$ measurements, which is set to $\delta^{13}C = 0‰$ as the basis of the scale and has an absolute $^{13}C/^{12}C$ ratio of 0.0112372 (Craig, 1957). Standard samples for $\delta^{15}N$ (atmospheric air), $\delta^{2}H$ (Standard Mean Ocean Water, SMOW), and $\delta^{18}O$ (SMOW) or standards that have been calibrated against these are provided by the International Atomic Energy Agency (IAEA), Vienna, Austria, or the U.S. National Institute of Standards and Technology (NIST), Washington, D.C.

4.5.3 Elemental analysis (EA)

Elemental analysis of H, C, N, O, and S for the peat samples was performed in a vario EL (Elementar Analysensysteme GmbH, 63452 Hanau, Germany). For C, H, N, and S measurements, about 20 mg of sample material were placed in tin capsules (LÜDI AG, 9230 Flawil, Switzerland) and then transferred to a combustion tube. At a temperature of 1323 K, the carrier gas He was temporarily mixed with oxygen, and quantitative oxidation was achieved by a WO_3 catalyst. In a second tube filled with copper powder and set to a temperature at 1123 K, excess oxygen was removed and nitrogen oxides were reduced. A packing of silver wool adsorbed any halogens that were present. The produced gases N_2, SO_2, CO_2, and H_2O then passed through three columns which adsorbed water vapor, sulfur dioxide and carbon dioxide successively. N_2 was not influenced by adsorption processes and therefore was transferred directly to the thermal conductivity detector (TCD) for quantitative analysis. The remaining gases were released successively by temperature programming and integrated in the TCD. The elemental analyzer was calibrated with sulfonic acid and acetanilide; the standard deviation was less than 0.1 % absolute.

The determination of oxygen contents was accomplished in a second sample run. About 1.5 mg of sample material in tin capsules was pyrolyzed in a reductive atmosphere at 1453 K. Oxygen-containing radicals were converted to CO by gas sooth. Undesirable gases were subsequently adsorbed on NaOH and water vapor was removed. CO was separated from N_2 and CH_4 in a GC column at 313 K. After TCD measurement of N_2 and CH_4, CO was released at 403 K and quantitatively determined.

Problems with elemental analysis arose particularly for the determination of O and H due to the water content. All samples were freeze-dried and kept under vacuum prior to analysis. Nevertheless, investigations by Abbt-Braun et al. (1990) show that the water content of samples increased within a few minutes after removing them from the desiccator due to the hygroscopicity of humic substances. The amount of adsorbed water varies depending on the atmospheric humidity at the time. Since an adsorption of atmospheric water could not be ruled out, values have been corrected by assuming an H_2O-uptake of 8.1 % of the initial sample weight for all peat samples before analysis.

4.5.4 Thermogravimetry (TGA)

TGA was used to independently determine the ash content of the peat samples, HO14 G, HO14 FA, and HO14 HA. Between 2 and 5 mg of sample material were placed in Al_2O_3 crucibles and analyzed in a TGA851^e (Mettler-Toledo, 35396 Gießen, Germany). The temperature program was set to increase from an initial temperature of 298 K to 1273 K, at a rate of 20 K/min under N_2 atmosphere. Temperature was held constant at 1273 K for 5 minutes before atmosphere was switched to O_2 for another 5 minutes. As for elemental

analysis the adsorption of atmospheric water was accounted for by a subtraction of 8.1 % of the initial weight.

4.5.5 Statistical data handling

Multidimensional scaling (MDS) was applied to find a structural pattern in the set of ROSIG samples. The MDS procedure handles dissimilarity data from multiple sources. This is accomplished by assigning observations to specific samples in a conceptual space such that the distances between points in the space match the given dissimilarities as closely as possible. The basic parameters used were bulk isotope values, data from elemental analysis, and NMR. The data set and source are given in Appendix I.

The calculations were performed using SPSS 10.0.7 statistical software package. Distances from data were created by Euclidean distance measure and values were standardized to a range from 0 to1 when using data of different scales. Optional criteria were set to 0.001 for S-stress convergence, 0.005 for minimum S-stress value, and maximum iterations to 30.

4.5.6 Sample preparation and storage

All samples were kept in glass vials and under vacuum conditions in desiccators to avoid adsorption of atmospheric water. Peat samples and bulk DOM were freeze-dried in a E-C Super Modulyo (Edwards Hochvakuum GmbH, 35004 Marburg, Germany) and ground in a ball-mill before storage.

5 Results of the ROSIG samples

The reference materials of the ROSIG research program include dissolved organic matter (DOM) of five different aquatic environments in Germany (Figure 5.1, Table 5.1). Fulvic acids (FA), humic acids (HA) and non-humic substances were isolated from the DOM (see Section 5.2). All available HA and FA were analyzed for bulk isotope data. Py-GC/MS-IRMS was applied to the FA, the isolated humic acid fraction from the bog lake DOM (HO14 HA) and untreated DOM from the bog lake (HO14 G). A selection of eight ROSIG samples was additionally analyzed for radiocarbon (^{14}C).

5.1 Samples and sampling sites

The intention of the ROSIG program was to collect and compare DOM from different aquatic systems. Several working groups of the program participated in sampling and provided water samples of different origin which served as standard reference material for each working group. An overview of distinguishing characteristics of the samples is given in Table 5.1, details of the origin are described in the following paragraphs.

5.1.1 Groundwater (FG)

The groundwater sample was taken in a pumping station of a water company in the Fuhrberger Feld that supplies drinking water for the city of Hannover, Germany. The sampling was carried out in nitrogen atmosphere to avoid uncontrolled sorption reaction by precipitation of Fe- and Mn-compounds. The extensive groundwater recovery area comprises an unconfined aquifer consisting of 20-30 m thick unconsolidated fine- and

Table 5.1: Compilation of common characteristics of the individual ROSIG samples and introduction of the sampling codes used in the text. The sample code is followed by a number indicating the sequence of takings and the addendum FA for fulvic acid or HA for humic acid fraction.

Origin	DOC [mg/L]	Characteristics	Sample code
Groundwater	12	reductive conditions, lignite pebbles in aquifer, high DOC content	FG
Brown coal processing waste water	236	old, diagenetically and thermally altered organic matter	SV
Soil percolate	73	acidic humus rich forest floor (spruce)	BS
Waste water (secondary effluent)	10	anthropogenic input, microbially reworked	ABV
Bog water	25	high content of high molecular weight organic acids	HO

coarse-grained sand with gravelly sand lenses. These Quaternary sediments contain unevenly distributed lignitic pebbles of less than 5 mm in diameter. DOC concentrations vary between 5 and 17 mg C/L depending on local vegetation conditions and agricultural activities aboveground. The surface is covered with a sandy podzol of low humus content (Artinger et al., 2000). The location is described as nearly oxygen-free with bacterial denitrification and sulfate reduction reactions (Böttcher et al., 1992; Kölle, 1993).

5.1.2 Bog water (HO)

The Hohlohsee is part of a recently established natural preservation area on top of a mountain in the Black Forest, Germany (about 1000 m above sea level). The lake is only recharged by precipitation and the water level is kept to a maximum by natural overflow, thus water level fluctuations are small. The water depth is between 2-3 m. Typical bog vegetation (*Oxicocco-Sphagnetea*) consisting of shrub, grass, and moss species border the lake. Large parts of the lake are covered by several tens of centimeters of floating *Sphagnum* moss. The samples were taken from a water depth of 50 cm using a submersible pump.

5.1.3 Soil seepage water (BS)

The soil sample was taken from a Norway spruce litter-derived mor-type forest floor layer (O_a-horizon) in a stand at the edge of the Fichtelgebirge near Bayreuth, Germany. The soil type was classified as a Haplic Podzol after FAO nomenclature on epigneis as parent rock (Kaiser, pers. comm.). The sparse ground vegetation consisted of several grass species and shrubs (*Calamagrostis villosa*, *Carex sylvatica*, *Deschampsia flexuosa*, *Vaccinium myrtillus*). Dissolved organic matter was extracted by adding about 600 L of deionized H_2O to about 80 kg of soil material after sieving it to <2 mm. The procedure is described in more detail by Kaiser et al. (1996).

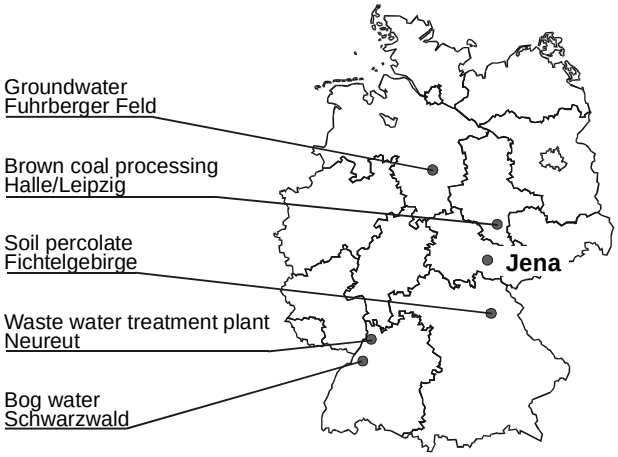

Figure 5.1: Map of Germany showing the sampling locations for the ROSIG reference material.

5.1.4 Waste water from a treatment plant (ABV)

The reference material was taken after the second treatment stage of a municipal waste water treatment plant at Neureut near Karlsruhe, Germany. Primary treatment involved removal of material by physical processes, i.e. screening, comminution, grit removal, and sedimentation. Secondary treatment removed particles by microbial consumption processes under aerated conditions. Sewage flow rates and input material vary over the course of the day and thus impede the predictability of waste water composition.

5.1.5 Waste water from brown coal processing (SV)

The sampling location “Vollert-Süd” near Hohenmölsen, Sachsen-Anhalt, Germany, used to serve as a reservoir for waste waters resulting from terrestrial brown coal and lignite processing. The whole area was subjected to extensive opencast mining until the 1990s. Processing of mined lignites usually involved low-temperature carbonization, i.e. the heating of lignite under air-exclusion to release volatile components (dry destillation). Due to high contents of phenolic compounds and anthropogenic humic substances these waste waters represented significant sources of hazards for groundwater contamination (Wießner et al., 1993).

5.2 Isolation procedure

The purpose of isolating the DOM was to simplify the standard reference materials and to gain better defined subsamples or fractions for investigations on reactions and structure. All original water samples were processed in the Engler-Bunte-Institut, Universität Karlsruhe, under the direction of Dr. G. Abbt-Braun. Each sample was filtered through a 0.45 µm cellulose nitrate filter before the isolation procedure. This step separated particulate organic matter (POM) from dissolved organic matter (DOM, <0.45 µm).

Humic acids (HA), fulvic acids (FA) and non-humic substances (NHS) were isolated from the standard reference material according to the IHSS-XAD-8 procedure (International Humic Substances Society) based on the Mantoura-Riley method (Mantoura and Riley, 1975). Acidified samples (HCl, pH = 2) were adsorbed on XAD-8 resin. Non-adsorbables were collected as NHS. Rinsing the XAD column with 0.2 *M* NaOH led to desorption. Repeated acidification of the solution (HCl, pH = 2) resulted in precipitation of the HA fraction which was filtered off. The remaining soluble FA fraction was adsorbed again on an XAD column, rinsed with 0.01 *M* HCl and double distilled water to remove chloride. Desorption was achieved again by rinsing the column with 0.2 *M* NaOH. In a final step the eluent passed a cation exchange resin in protonated form. The method is described in more detail by Frimmel and Abbt-Braun (1999).

5.3 Bulk isotope measurements of the ROSIG samples

5.3.1 Deuterium (D, ^{2}H)

Significant variations in δD in plants occur during biosynthesis (Epstein et al., 1976; Sternberg, 1989; Smith and Ziegler, 1990) but the initial isotope signal is given by the water that is taken up by plants. Isotopic ratios of H, as well as O, also exhibit pronounced seasonal and geographical variations in the isotopic ratios of precipitation (Ziegler, 1989; Lajtha and Marshall, 1994). It is thus probable that the isotopic composition of the different water samples created the first-order variations in the δD values of the FA and HA. A second cause of alteration to bulk δD values in DOM are varying proportions of differently-enriched compound classes. The third possibility - the exchange of hydroxyl hydrogen with atmospheric hydrogen during storage – has been overcome by keeping all samples under equal conditions for several months so that the small exchangeable amount

Table 5.2: Sampling date and bulk isotope values (in ‰) for all available ROSIG samples. Standard deviations (s.d.) are shown if based on at least three measurements, values are rounded (0.0 means s.d. <0.05). n.d. – not determined. Sample labeling: HO – bog lake Hohlohsee, ABV – secondary effluent from sewage plant, BS – soil percolate, FG – groundwater, SV – waste water from brown coal processing. Addendum: FA – fulvic acid, HA - humic acid, K – concentrate (by ultrafiltration), G – original water sample freeze dried.

	Sampling Date	δ^2H	s.d.	δ^{13}C	s.d.	δ^{15}N	s.d.	δ^{18}O	s.d.
HO10 HA	Oct. 94	-70.6	1.45	-26.5	0.1	-4.6	0.6	n.d.	—
HO10 FA	Oct. 94	-96.4	7.9	-26.6	0.1	-4.7	0.3	14.9	—
HO12 K	Jul. 96	-80.5	0.76	-26.4	0.1	-5.1	—	n.d.	—
HO13 HA	Aug. 96	n.d.	—	-27.0	0.0	n.d.	n.d.	n.d.	—
HO13 FA	Aug. 96	-87.7	0.80	-26.7	0.0	-12.3	—	n.d.	—
HO14 G	Jul. 97	-96.3	0.85	-26.3	0.3	-2.1	0.2	n.d.	—
HO14 HA	Jul. 97	-94.7	1.25	-26.9	0.0	-3.6	0.1	n.d.	—
HO14 FA	Jul. 97	-101.7	0.57	-26.7	0.1	-4.4	0.1	n.d.	—
HO16 G	Jul. 98	-93.3	0.68	-26.5	0.1	-3.8	—	n.d.	—
HO16 HA	Jul. 98	-100.0	0.93	-27.4	0.6	-3.5	—	n.d.	—
HO16 FA	Jul. 98	-102.0	0.04	-26.6	0.1	-5.1	—	n.d.	—
ABV2 FA	Mar. 95	-82.8	1.0	-26.2	0.0	0.3	0.1	13.4	—
ABV3 K	Apr. 99	-61.0	4.82	-22.0	0.1	14.5	—	n.d.	—
ABV3 FA	Apr. 99	-87.7	1.18	-27.3	0.0	-0.1	—	n.d.	—
BS1 HA	Nov. 95	-110.2	6.3	-25.5	0.5	-17.6	5.3	n.d.	—
BS1 FA	Nov. 95	-56.8	1.43	-26.1	0.4	7.3	4.2	14.8	—
FG1 FA	Jan. 96	-144.2	5.1	-27.7	0.0	-4.1	0.4	16.5	—
SV1 HA	May 95	-77.7	1.23	-24.9	0.2	27.2	1.5	n.d.	—
SV1 FA	May 95	-73.8	2.72	-24.3	0.4	24.8	0.0	15.3	—

of H is assumed to have equilibrated with the environment. The values should thus not be taken as absolute numbers but seen relative to one another.

δD (δ^2H) values of the samples varied largely between –56.8‰ and –144.2‰ (Table 5.2). All FA fractions of the Hohlohsee samples appear depleted in D compared to the HA fractions. This is most pronounced in HO10 and probably caused by a higher proportion of aliphatic compounds, e.g. lipids, in FA and lower amounts of aromatic, e.g. lignin, as well as carbohydrate related components as compared with HA. Evidence for this assumption is given by ^{13}C-NMR data (Lankes and Lüdemann, 2001). The samples HO13 and HO10 (taken in August and October, respectively) show a seasonal difference compared to the other Hohlohsee samples (taken in July), with a tendency towards higher δD values in the course of the summer. Summer precipitation is known to be enriched in D at higher latitudes (Ziegler, 1989; see also IAEA/WMO (1998), Global Network for Isotopes in Precipitation, station Feldberg/Schwarzwald) and the enrichment of D in the DOM of the bog water may be a response to the rain signal.

In contrast to the Hohlohsee samples, the FA of the soil percolate are notably enriched in D by 50‰ compared to the humic acid (BS1 HA). Even though there is again a predominance of aliphatic C in FA over HA in the soil percolate (Lankes and Lüdemann, 2001), the contrary enrichment of D must be caused by a different formation process. Carboxyl and amino groups which occur predominantly in FA readily exchange H and may be responsible for this effect. The soil percolate is of modern age (see ^{14}C data, Section 5.4) and thus compounds may be less refractory and, in turn, may be more susceptible to exchange H with the environment, for example with meteoric water. Another likely possibility results from the fact that the spruce tree sampling site creates a high input of lignin-derived organic matter, thus resulting in a general enrichment of D (White, 1989). A higher content of cellulose in the HA fraction, as indicated by a large amount of carbohydrates (Jahnel et al., 1998), may then lead to the observed depletion of D as compared with the FA fraction. A less significant enrichment of FA over HA is also observed in the brown coal waste water (SV1 FA: –73.8‰, SV1 HA: –77.7‰). More remarkable, however, is that the δD values of SV1 are uncommonly high when compared with typical data from coals (–110‰ ± 20‰ in: Whelan and Thompson-Rizer, 1993) and may indicate the contribution of another source of organic matter. FA from the two samplings of the waste water treatment plant do not differ much but show a distinct depletion of more than 20‰ compared with the concentrate. This indicates a preferential fractionation of substances by the isolation procedure. Finally, the groundwater is the most depleted (–144.2‰) of all samples. The Fuhrberger Feld aquifer contains lignitic wood residues (Böttcher et al., 1992) which may contribute to the DOM by solution processes (Artinger et al., 2000) although ^{14}C dating of the fulvic acids rather suggests input from

aboveground. It is thus more likely that the groundwater samples are rich in lipids, which is supported by a considerable amount of aliphatic C (Lankes and Lüdemann, 2001).

5.3.2 Carbon-13 (^{13}C)

The $\delta^{13}C$ values of all samples are in the range of –22.0‰ to –27.7‰ indicating C3 plant material as the original source. The relatively high value of –22.0‰ in the concentrate ABV3 K is consistent with a high turnover rate in sewage plants because every trophic level is isotopically enriched in the heavy isotope relative to the previous one within food chains (Gleixner and Schmidt, 1998). The value of the concentrate is significantly different from the fulvic acid fractions of ABV2 and ABV3 with values of –26.2‰ and –27.3‰, respectively. Effects of the isolation procedure with respect to enrichment and/or depletion of specific compound classes may favor the selective fractionation of isotopically 'light' substances in the FA samples, e.g. aliphatic or aromatic compounds. However, compared to the other samples, the sewage plant is much more affected by varying input material. Consequently, a greater range of $\delta^{13}C$ values can be expected. Considerable amounts of microbial biomass in the waste water FA are indicated by high total N contents, which are 2.92% for ABV2 FA and 2.18% for ABV3 FA (elemental analysis by Abbt-Braun et al.; see Appendix I). The ^{13}C signal in the groundwater FA fraction is the most depleted of all samples (–27.7‰) and is representative of different depths in the aquifer (Buckau et al., 2000). It also indicates that contribution of sedimentary organic matter as well as dissolved inorganic carbon is insignificant and that the main source of DOM is the podzolic humus layer. The highest enrichment in bulk ^{13}C is found in the waste water from the brown coal processing (SV1). A reference bulk value obtained from a possible source coal, a lignite from Hambach, Germany, was –25.6‰ (McRae et al., 1998) and thus close to –24.3‰ obtained from the FA.

5.3.3 Nitrogen-15 (^{15}N)

The $\delta^{15}N$ values for the Hohlohsee samples vary between –5.1‰ and –2.1‰ with a very low value of –12.3‰ for the sample HO13 FA. Fulvic acid fractions are slightly depleted in ^{15}N compared with HA (Table 5.1). The uptake of N by plants in a bog ecosystem is mainly limited to N from atmospheric deposition. Samples from the peat profile of the Hohlohsee (see Section 6.1) showed values around 0‰, a value expected for a low nitrogen ecosystem having only atmospheric deposition of nitrogen (Schmidt et al., 1992). N isotope values in soils, and thus in plants, can vary largely (Lajtha and Marshall, 1994). The variety of plant material as the source of humic substances is most likely the reason for the large variation of $\delta^{15}N$ values in the ROSIG samples. However, in contrast to the rather consistent values of the Hohlohsee samples, there are two notable features observed in the data set. First, the humic substances of the concentrate from the sewage plant (ABV3K) are enriched in ^{15}N by 14‰ relative to the FA. This is consistent with the high $\delta^{13}C$ and δD

values and, again, indicates a high trophic level of the concentrate. Second, the HA and FA of the brown coal processing water (SV1) are the most ^{15}N-enriched samples of the series (27.2‰ and 24.8‰, respectively). An enrichment of heavy isotopes in this sample is also indicated through the other stable isotopes. High amounts of hydrolyzable amino acids and carbohydrates as well as high N contents in ABV2 FA and SV1 FA indicate that both systems are biologically active (Frimmel and Abbt-Braun, 1999). These observations are indicative of microbial biomass and high trophic level. Again, striking differences between the FA and HA are observed in the soil percolate (BS1). The humic acids are depleted in ^{15}N by almost 25‰ compared to the fulvic acids. HA are found to be enriched in amino acids as compared to FA and the soil percolate has the highest proportion of all samples (Jahnel et al., 1998). These microbial products can be formed by heterotrophic bacteria with a strong discrimination against ^{15}N by up to 9‰ (Macko and Estep, 1984).

The $\delta^{18}O$ values of the FA in five selected samples vary between 13.4‰ and 16.5‰. Compared to plant material this enrichment of ^{18}O can be attributed to the secondary introduction of oxygen from O_2 in the course of the formation of FA (Gleixner and Schmidt, 1998). An introduction of ^{18}O through water-bound oxygen into carboxyl groups is also conceivable.

5.4 ^{14}C content of fulvic acids

The evaluation of ^{14}C data must always take into account that polymeric mixtures of old and young material can lead to an ambiguous determination of absolute ages as long as the proportion of these two pools are unknown. This is certainly the case with FA. Radiocarbon here is expressed as pMC – percent modern carbon – the difference in percent between the sample compared to that of a universal standard (oxalic acid, decay-corrected to 1950). Values above 100 pMC contain bomb-produced carbon and thus indicate that FA contain organic material that has been exposed to exchange with atmospheric $^{14}CO_2$ in the last 50 years. These values were measured in FA of the bog water and the soil seepage water (Table 5.3) which therefore comprise a certain amount of fresh organic matter.

For values below 100 pMC, the unknown ratio of post- and pre-bomb carbon leaves uncertainties about the composition of the pools. The secondary effluent from the waste water treatment plant (ABV2 FA) is particularly difficult to classify. Input material can range from ^{14}C 'dead' fossil fuels to material that has been digested several times and to fresh and young organic matter. The ^{14}C content of the groundwater (87.52 pMC) suggests ages above 50 years, i.e. post bomb-produced radiocarbon seems to play a minor role. The aquifer system consists of Quaternary fine- and coarse-grained and partly gravel sands and is unconfined with a water table 1-4 m below the surface. An input of soil organic carbon

Table 5.3: Bulk ^{13}C data and ^{14}C contents of fulvic acids (FA) extracted from different aquatic systems. Sample identification numbers as used in the text are given as well as a short description of the source of the sample (sample type). ^{14}C contents were measured on graphite targets in an accelerated mass spectrometer and were corrected for mass-dependent isotopic fractionation to –25‰ in $\delta^{13}C$. These values may deviate slightly from the $\delta^{13}C$ values analyzed by EA-IRMS. ^{14}C contents above 100% modern carbon (pMC) indicate bomb-produced radiocarbon (past 1950). It should be noted that the measured ^{14}C contents are based on samples that may contain young as well as old organic matter (see text for discussion). Values below 100% do not necessarily mean an absence of bomb-produced radiocarbon. Lab numbers are specific for the laboratories in charge with ^{14}C measurements and provide a simple backtracking of the samples.

Sample identification	Sample type	Sampling date	% of total DOC*	$\delta^{13}C$ ‰	^{14}C pMC	$\delta^{13}C$ used for corr. ‰	Lab No.
HO10 FA	bog water	10/94	31	-26.6±0.1	116.65±1.31	-26.3	J0062
HO13 FA	bog water	08/96	-	-26.7±0.0	n.d.	n.d.	-
HO14 FA	bog water	07/97	-	-26.7±0.0	n.d.	n.d.	-
HO16 FA	bog water	07/98	-	-26.6±0.1	n.d.	n.d.	-
BS1 FA	soil percolate	11/95	23	-26.1±0.4	116.35±1.11	-26.6	J0063
FG1 FA	ground water	01/96	32	-27.7±0.0	87.52±0.56	-27.7	J0060
ABV2 FA	secondary effluent	03/95	11	-26.2±0.0	94.96±0.60	-26.1	J0065
ABV3 FA	secondary effluent	04/99	-	-27.3±0.0	n.d.	n.d.	-
SV1 FA	brown coal processing	06/95	24	-24.3±0.4	5.52±0.10	-24.4	J0059

n.d. – not determined,
pMC – percent modern carbon,
s.d. is rounded: <0.05‰ indicated as ±0.0,
* data taken from Frimmel and Abbt-Braun (1999).

can be expected from both the humus poor podzols as well as from agricultural activities. The sandy sediments are free of carbonate (Buckau et al., 2000) so that a contribution of calcite dissolution to DOC can be excluded. The ^{14}C contents of FA measured in this study are in good agreement with values found by Artinger et al. (2000). In their study, both ^{14}C of total DOC and ^{3}H concentrations of the groundwater were representative of a young, oxidizing groundwater under recharge conditions with relatively high DOC concentrations. With around 5 pMC, the waste water from brown coal processing showed significantly high portions of old carbon. This value points out that the composition of FA is predominantly derived from the Tertiary brown coal.

5.5 Statistical approach and conclusive summary of bulk isotope measurements and ^{14}C data

Structural diversity, origin, and genesis of DOM cannot be easily resolved using bulk isotope values. A graphic representation of all observations based on the bulk isotope values are shown in the multivariate analysis of all ROSIG samples (Figure 5.2). A second analysis was performed considering additional results from elemental analysis and structural information from NMR by other working groups of the ROSIG program (Figure 5.3). Groundwater (FG1) and brown coal processing waste water (SV1) indicate a distinct

differentiation from the remaining samples. The main source of organic matter for FG1 is apparently relatively young material from the aboveground podzolic humus layer. SV1, on the other hand, originates from old and diagenetically altered material with a strong indication of a microbially active environment (Frimmel and Abbt-Braun, 1999) nourished by brown coal-derived carbon. Microbial biomass and biological activity are also likely to contribute to the isotope signals observed in the waste water ABV2 and ABV3. These two samples, however, indicate an association with the bog water samples from the Hohlohsee (HO) and not so much with SV1. Bog water and soil percolate represent systems with input of young, e.g. fresh organic material. Dissimilarities in FA as indicated in Figure 5.2 are

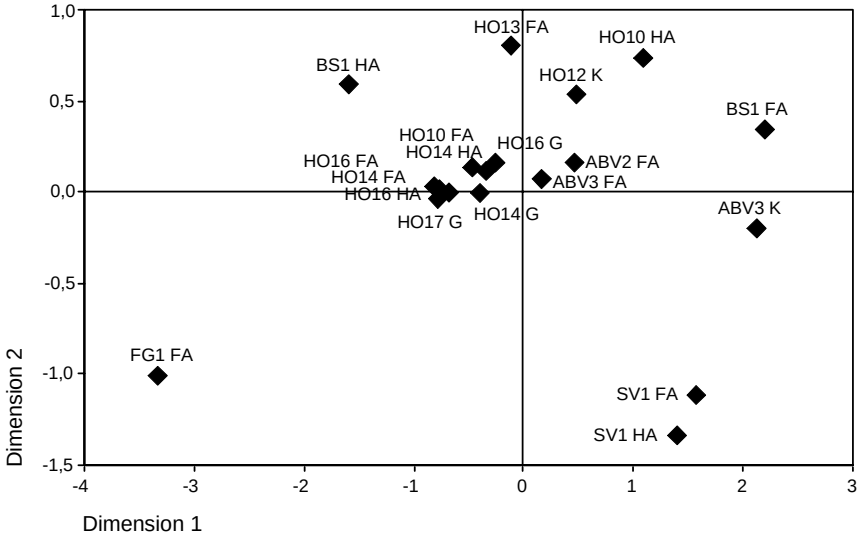

Figure 5.2: Multidimensional scaling (MDS) based on bulk isotope values. Data basis are values of Table 5.2. Details of the multivariate analysis are given in Section 9.4. S-stress value for this analysis: 0.002.

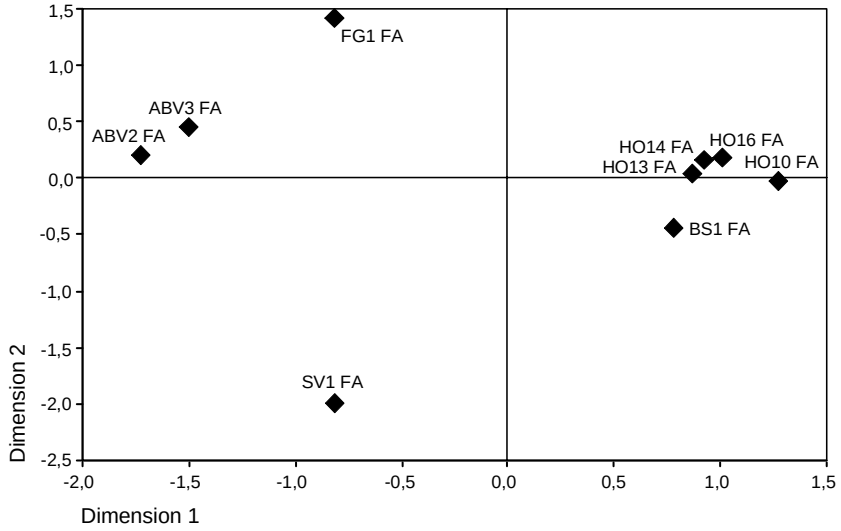

Figure 5.3: Multidimensional scaling based on bulk isotope values, data from elemental analysis and NMR data. The complete data set and data source is given in Appendix I. S-stress value for this analysis: 0.142, RSQ (squared correlation): 0.963.

most likely due to the difference in vegetation types. The bog water samples HO10 FA and HO13 FA are distinct from the other bog water samples in Figure 5.2. This is primarily due to the δD and $\delta^{15}N$ values. Seasonal variations may be responsible for this distinction. The concentrates HO12 K and ABV3 K do not reveal any close relation to their respective isolated fractions. An influence of preparation methods, e.g. ultrafiltration, on the composition of the original sample cannot be ruled out. Differences in isolated fractions are most obvious for the soil percolate BS1 FA and BS1 HA.

Structural information gained from NMR as well as elemental analyses emerge as indispensable for interpreting bulk isotope values. Several observations for the ROSIG samples, however, still remain ambiguous because there appear to be many sources of DOM. At this point isotopic information on structural building blocks may help to distinguish between different sources of organic matter.

5.6 Comparison of fulvic acids from the different aquatic systems by Py-GC/MS-IRMS

As many as 140 different pyrolysis products within all samples have been found with a minimum amplitude of 200 mV in the IRMS chromatograms. Only these substances gave reliable $\delta^{13}C$ values and were thus subject to identification. However, several substances had to be omitted due to co-elution. The remaining peaks were grouped into chemical classes of compounds to facilitate overview and comparison of the samples. The classes were determined following Zegouagh et al. (1999), using specific mass traces (i.e. alkylphenols: *m/z* 94 + 107 + 108 + 121 + 122; alkylbenzenes: *m/z* 78 + 92 + 106 + 120; alkylpyrroles: *m/z* 67 + 80 + 94 among alkylcyclopentenones and alkylcyclopentenes). Alkylmethoxyphenols and carbohydrates were grouped by mass spectra identification or based on results found in the literature, respectively. All five classes represent between 43% and 67% of the area of all pyrolysis products which gave a peak amplitude higher than 200 mV in the IRMS trace and are treated separately in the following paragraphs. The listing of mass spectra of all pyrolysis products is given in Appendix III.

The remaining products consist primarily of heterocyclic compounds such as indole and benzofurandiones, and dicyclic compounds such as naphthalene, azulene and indene and their methylated derivatives. Sulfur-containing compounds like thiophene were also identified. These products are exclusively found in the anthropogenically-influenced waste waters (ABV2, ABV3 and SV1) and occur naturally in a multitude of essential oils in plants and in products of fossil fuels (e.g. oil, coal). Pyrolysis of macerals yielded essentially the same products (Stankiewicz et al., 1996). It is thus likely that these materials are responsible as precursor material for the pyrolysis products. ABV2 is also

interesting for its very prominent acetamide peak. This substance was found upon pyrolysis of peptidoglycans which occur in microbial and fungal cell walls (da Cunha et al., 2000).

Several possible alkanes and alkenes were also present in ABV2 but have been omitted because of uncertainties in identification and missing results of methylation by TMAH to determine if the precursor material are fatty acid derivatives. Their contribution is estimated at about 4% based on peak areas of all peaks with a minimum amplitude of 200 mV. Further pyrolysis products comprise substances such as phenol, toluene, derivatives of butanal and various acids which can have several precursors. The complete list of all identified pyrolysis products is given in Appendix II.

5.6.1 Alkylphenols and methoxyphenols

As the second most abundant naturally occurring compound in biomass after cellulose, lignin is an important source of DOM. Pyrolysis of lignin and degraded lignin commonly produces alkylphenols and methoxyphenols (Meuzelaar et al., 1982; Saiz-Jimenez and DeLeeuw, 1986; van Smeerdijk and Boon, 1987) in addition to benzenediols (van Heemst et al., 2000). The latter were not encountered in any of the samples. Alkylphenols, on the other hand, have also been reported upon pyrolysis of macromolecules rich in tyrosine moieties resulting from the degradation of cross-linked proteins (van Heemst et al., 1999). However, the appearance of 2-methoxyphenol (peak no. *51*), 2-methoxy-4-methylphenol (*61*), 4-ethyl-2-methoxyphenol (*74*) or 4-vinyl-2-methoxyphenol (*78*) in all samples except for the groundwater (FG1) and the brown coal processing waste water (SV1) strongly suggests an input from lignin derived material. A lack of methoxyphenols and benzenediols may thus indicate that most lignin has already been degraded. In addition, the absence of methoxyphenols is observed in samples with the lowest ^{14}C content (FG1 and SV1, Table 5.5). As possible lignin-derived pyrolysis products in these two samples, alkylphenols had mean weighted $\delta^{13}C$ values of –27.4‰ and –25.9‰, respectively (Table 5.4). Two alkylphenols occurred in both samples: ethylphenol (*58*) and methylphenol (*50*). Both compounds are depleted in ^{13}C in the groundwater sample, both individually and compared with SV1 (by 2.8‰ and 1.5‰, respectively). In general, proteins are slightly more enriched in ^{13}C compared with lignin (Schmidt et al., 1995). Thus, the observed alkylphenols in the brown coal processing water are more likely derived from cross-linked proteins than the same two compounds in the groundwater. These alkylphenols in SV1 may represent old and transformed material as was previously observed in DOM (van Heemst et al., 1999). The highest relative amount of methoxyphenols was observed in the

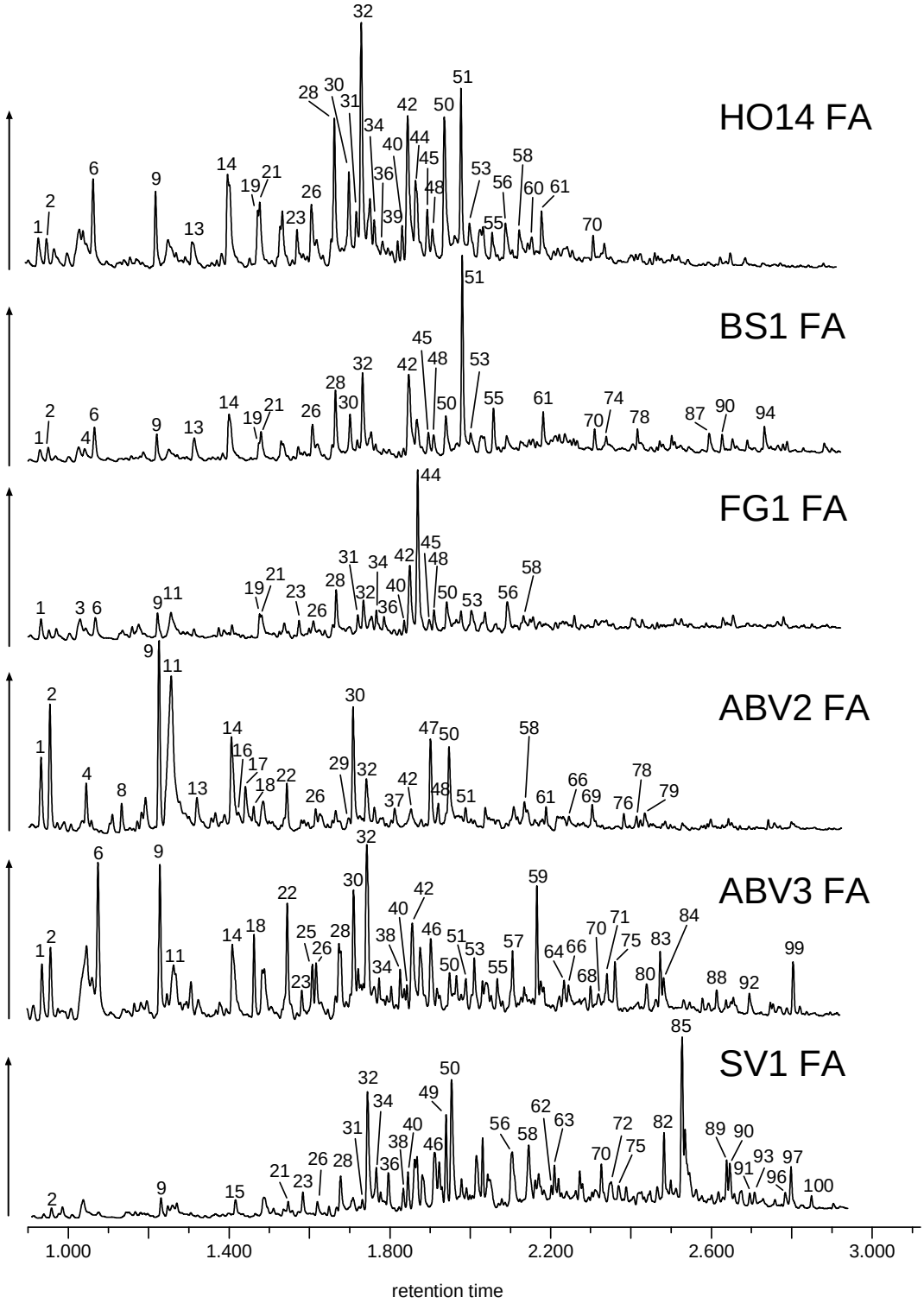

Figure 5.4: IRMS chromatograms (*m/z* 44) of isolated fulvic acids (FA) of DOM from contrasting aquatic systems. Numbers refer to pyrolysis products listed in Appendix I. Only those pyrolysis products were identified whose intensities reached a minimum amplitude of 200 mV in the IRMS chromatograms. HO14 FA (bog water FA) is representative for all bog water samples. Peak amplitudes are relative to the highest peak in the chromatogram and differ due to different enlargement factors of the chromatograms.

soil percolate and second highest in the bog water samples (Table 5.5, Figure 5.6). Both sample types represent young and thus probably least degraded DOM. With increasing age the amount of these substances decreases. Thus, it seems reasonable to assume that lignin-derived material is decomposed with time in aquatic ecosystems.

5.6.2 Alkylbenzenes

C_0-C_3 alkylbenzenes were monitored by mass chromatography using masses *m/z* 78 + 92 + 106 + 120. This approach also yielded C_2-alkylbenzofuranones and C_2-alkylisobenzofurandiones which occurred exclusively in the waste water of the brown coal processing and were included in this class. The origin of alkylbenzenes is questionable. Biosynthetic precursors in soils are nearly excluded because most microorganisms producing alkylbenzenes are found in extreme environments. Burning of biomass and deposition of smoke and particles after forest fires are likely sources, but they may be produced as artifacts upon pyrolysis of aliphatic precursors (Saiz-Jimenez, 1996). All three waste waters contained relatively high amounts of this class of compounds. Pyrolysis of kerogens, coals, and asphaltenes can also produce alkylbenzene related to the aromatic moieties in macromolecules (Hartgers et al., 1994). The exact precursors are unknown, but the additional occurrence of heterocyclic and dicyclic compounds in the waste waters suggest fossil fuel products as a conceivable source. $\delta^{13}C$ values vary strongly and therefore imply multiple sources. However, the high depletion of ^{13}C in some individual compounds (toluene, ethylmethylbenzene, styrene) could indicate fossil fuel-derived aromatics.

Alkylbenzenes are also reported as pyrolysis products from lignin and biodegraded lignin (van Smeerdijk and Boon, 1987; Durig et al., 1991). They represent part of the refractory organic matter in DOM and particulate organic matter of marine systems (van Heemst et al., 2000). The presence of methoxyphenols and alkylphenols in the bog water and soil seepage water as well as similar $\delta^{13}C$ values in these three compound classes may thus suggest a mutual source such as lignin for these two samples.

5.6.3 Carbohydrates

Furan derivatives, furaldehydes, alkylcyclopentenones, derivatives of pyranone (i.e. 4-hydroxy-5,6-dihydro-2H-pyran-2-one in this study), levoglucosenone and a dianhydro-rhamnose isomer are typical pyrolysis products of carbohydrates, monosaccharides,

Table 5.4: Mean weighted $\delta^{13}C$ values and standard deviations (s.d.) of compound classes. Numbers are calculated from individual $\delta^{13}C$ values of *n* compounds. The complete data set is given in Appendix II.

Sample type	Bog water					Bog water					Bog water					Bog water				
Sample identification	HO10 FA					HO13 FA					HO14 FA					HO16 FA				
	$\delta^{13}C$ ‰	s.d.	min ‰	max ‰	*n*	$\delta^{13}C$ ‰	s.d.	min ‰	max ‰	*n*	$\delta^{13}C$ ‰	s.d.	min ‰	max ‰	*n*	$\delta^{13}C$ ‰	s.d.	min ‰	max ‰	*n*
Alkylbenzenes	-27.6	1.6	-28.7	-25.1	*4*	-26.7	4.0	-29.0	-20.9	*4*	-27.4	2.2	-29.3	-23.1	*6*	-27.7	1.4	-28.4	-25.4	*4*
Alkylphenole	-27.1	0.4	-27.3	-26.5	*4*	-27.9	0.5	-28.2	-27.1	*3*	-28.3	0.6	-28.7	-27.3	*4*	-27.5	0.8	-28.2	-26.0	*5*
Alkylpyrrole																				
Carbohydrates	-24.3	1.2	-25.7	-22.4	*5*	-24.4	4.5	-26.3	-15.6	*5*	-24.3	1.1	-25.8	-22.8	*7*	-24.4	1.1	-25.8	-23.4	*6*
Methoxyalkylphenols	-28.1		-29.2	-27.6	*2*	-27.8		-30.2	-27.0	*2*	-27.7		-29.0	-27.2	*2*	-26.5		-26.5	-26.4	*2*

Sample type	Ground water					Soil percolate					Secondary effluent					Secondary effluent					Brown coal processing				
Sample identification	FG1 FA					BS1 FA					ABV2 FA					ABV3 FA					SV1 FA				
	$\delta^{13}C$ ‰	s.d.	min ‰	max ‰	*n*	$\delta^{13}C$ ‰	s.d.	min ‰	max ‰	*n*	$\delta^{13}C$ ‰	s.d.	min ‰	max ‰	*n*	$\delta^{13}C$ ‰	s.d.	min ‰	max ‰	*n*	$\delta^{13}C$ ‰	s.d.	min ‰	max ‰	*n*
Alkylbenzenes	-29.1	0.8	-29.9	-28.2	*3*	-27.1	1.8	-28.7	-25.1	*3*	-31.6	2.9	-34.5	-27.9	*4*	-27.2	3.0	-34.0	-21.4	***11***	-23.9	3.0	-30.3	-20.1	***12***
Alkylphenole	-27.4	0.9	-28.1	-26.3	*4*	-28.1		-28.5	-27.2	*2*	-31.8		-32.2	-30.0	*2*	-28.0		-28.5	-26.9	*2*	-25.9	0.9	-26.6	-24.9	*3*
Alkylpyrrole											-26.1	4.3	-29.2	-20.7	*3*										
Carbohydrates	-26.9	1.0	-28.8	-26.0	*5*	-22.6	4.2	-25.2	-13.9	*6*	-23.8	2.3	-26.9	-20.5	*8*	-28.9	2.8	-27.1	-19.2	*7*	-22.6	2.0	-25.4	-20.8	*4*
Methoxyalkylphenols						-29.1	2.0	-29.8	-25.6	*4*	-29.6	1.4	-30.9	-28.2	*3*	-28.4		-28.4	-28.4	*1*					

Table 5.5: Peak areas of compound classes in percent of the total area in the analytical window. Numbers are summed up from individual peak areas of *n* compounds. The complete data set is given in Appendix II.

Sample type	Bog water		Bog water		Bog water		Bog water		Ground water		Soil percolate		Secondary effluent		Secondary effluent		Brown coal processsing	
Sample identification	HO10FA		HO13FA		HO14FA		HO16FA		FG1FA		BS1FA		ABV2FA		ABV3FA		SV1FA	
	area %	*n*	area %	*n*	area %	*n*	area %	*n*	area %	*n*	area %	*n*	area %	*n*	area %	*n*	area %	*n*
Alkylbenzenes	3.1	*5*	3.5	*5*	3.0	*6*	2.8	*4*	3.6	*4*	1.9	*3*	7.1	*4*	12.3	*11*	14.9	*13*
Alkylphenole	4.8	*4*	4.0	*3*	4.3	*4*	6.8	*5*	5.1	*4*	2.2	*2*	5.3	*3*	3.5	*3*	9.0	*4*
Alkylpyrrole													1.2	*3*				
Carbohydrates	11.0	*8*	11.5	*7*	14.3	*10*	13.6	*9*	9.9	*5*	13.5	*8*	13.1	*9*	15.6	*9*	3.0	*4*
Methoxyalkylphenols	2.2	*2*	3.8	*2*	3.6	*2*	3.2	*2*			8.0	*4*	1.1	*3*	0.7	*1*		
Sum of area	21.1		22.7		25.3		26.4		18.6		25.5		27.8		32.1		26.9	
% area all peaks >200 mV*	37.6		51.7		39.0		43.1		40.7		41.9		41.3		65.9		63.2	
%	56.1		43.9		64.7		61.3		45.8		61.0		67.3		48.7		42.5	
Total area*	178.3		140.4		187.1		186.5		149.8		168.4		298.0		203.3		248.2	

* in analytical window 900-2900 sec.

and polysaccharides such as cellulose and starch (van der Kaaden et al., 1983; van Smeerdijk and Boon, 1987; Pouwels et al., 1989; Stankiewicz et al., 1997b; Huang et al., 1998). They totaled up to 15 pyrolysis products found in all samples, with variable relative amounts (see Appendix II). Most individual carbohydrate markers are detected in the bog water (10 in HO14 FA), but relative amounts are in a narrow range throughout all samples except for the groundwater (9.9%) and the brown coal processing waste water (SV1 FA) with only 3% (Table 5.5, Figure 5.6).

An interesting feature is the large variation of carbohydrate-derived pyrolysis products expressed in the mean weighted $\delta^{13}C$ values. Bog water FA were all in a narrow range with mean values of around –24‰ (Table 5.4). The same holds true for the groundwater but in this sample the compound class was slightly depleted compared to the bog water carbohydrates. The $\delta^{13}C$ values of the individual pyrolysis products from the bog water FA are in a typical range of carbohydrates between –22.4‰ and –26.3‰ (except for levoglucosenone in HO13, Appendix II). The carbohydrate markers in the remaining samples showed much higher variations.

Levoglucosenone

Levoglucosenone (*55*) was encountered in four samples: in the bog water samples HO14 ($\delta^{13}C$: –22.8‰) and HO13 (–15.6‰), in the secondary effluent ABV3 (–19.2‰) and the soil seepage BS1 (–13.9‰). This compound is a polysaccharide marker for both cellulose and microorganisms (Stout et al., 1988). The occurrence of this substance in the FA of the bog water is surprising because results by Kracht and Gleixner (2000) (see also Chapter 6 and Appendix V), showed that, although this substance occurred in a peat profile from the lake's edge, it was not retrieved in the bulk DOM of the water. The isolation procedure for the FA fraction from bog water DOM obviously enriched this substance. $\delta^{13}C$ values of levoglucosenone from the peat samples varied between –23.0‰ and –22.4‰ and are thus in agreement with HO14 FA (–22.8‰), indicating a possible dissolution of the precursor compound from the peat into the water body. However, the high enrichment of ^{13}C in levoglucosenone of the bog water sample HO13 suggests a microbial origin, with an enrichment due to the trophic level effect as is supposed for the high $\delta^{13}C$ value in the secondary effluent. The extent to which levoglucosenone is derived from cellulose or from microorganisms is an open question. The same holds for the soil seepage water which was taken from a spruce tree stand in the Fichtelgebirge, Germany. Carbohydrates in this sample have been found to be around –21‰ (Kaiser, pers. comm.) which is in fair agreement with the calculated mean weighted $\delta^{13}C$ value of –22.9‰. Levoglucosenone as a pyrolysis product of extracted cellulose from four Siberian pine trees showed $\delta^{13}C$ values between –22.4‰ and –17.9‰ (bulk cellulose between –23‰ and –24‰, unpublished data). Although this variation is quite large like the two bog water samples, a value of

around –13‰, as was found in the soil seepage water, again rather suggests a proportion of microbially-derived material in the sample

5.6.4 Alkylpyrroles

Nitrogen-containing compounds make up only small portions of all pyrolysis products observed in the chromatograms (Figure 5.6). In this study they were only encountered to measurable extents in the FA of the secondary effluent ABV2: Methylpyrrole (*16*), acetylpyrrole (*29*) and an unknown product (*76*) identified only by using specific mass traces for alkylpyrroles. The δ-values of the individual products vary greatly (–29.2‰, –20.7‰ and –25.9‰, respectively), and thus add up to a 'bulk' value of –26.1‰ with a high standard deviation (Table 5.4). The precursors of the alkylpyrroles are most likely N-containing compounds such as chitin, proteins and macromolecules present in cell walls. In ABV2, alkylphenols that can be derived from degraded cross-linked proteins (van Heemst et al., 1999) were also found. Usually alkylphenols derived from proteins are linked to old, degraded material. The high ^{13}C depletion in alkylphenols found in ABV2 (around –32‰), however, rather suggested lignin as a source. Acetamide, a very pronounced peak in this sample, (see discussion below) suggests that at least chitin contributed to N-containing precursor material. From the high variation in δ-values, however, it is concluded that the three pyrolysis products were derived from different, yet unknown precursors. Only the unknown substance with a $\delta^{13}C$ value of –25.9‰ was in a range close to acetamide (–24.8‰) and thus may also be derived from chitin.

Acetamide

The nitrogen-containing acetamide is the most prominent peak in the secondary effluent ABV2 (*11*, Figure 5.4). This substance was also identified as a pyrolysis product of pure cultures of the bacterium *Bacillus sphaericus* and the fungus *Cladosporium cladosporioides* (Gleixner, unpublished data). It has been detected in pyrolysis products of riverine particulate organic matter and related to peptidoglycans of microbial and fungal cell walls, diatoms, algae and aquatic animals (da Cunha et al., 2000). This broad peak with a mean $\delta^{13}C$ value of –24.8 ± 0.1‰ (n=3) has a relative peak area of 9.6 ± 1.2 and therefore exceeds all compound classes except for carbohydrates (Table 5.5). It is thus a good biomarker for microorganisms in the secondary effluent of the waste water. This substance was also found above the detection limit in ABV3 but did not yield accurate $\delta^{13}C$ values. The occurrence of this pyrolysis product in the fall sample of the bog water fulvic acid HO10 FA with a $\delta^{13}C$ value of –15.5 ± 0.9‰ may indicate an increase in microorganisms in the bog water during the summer period. The enrichment of ^{13}C in this amino sugar fragment by about 9‰ compared with acetamide in ABV2 is noteworthy. Carbohydrates and amino acids are commonly in the same $\delta^{13}C$ range relative to plant bulk values (see Figure 2.4). A positive isotope fractionation effect of up to 11‰ during the

synthesis of amino acids, however, was reported from bacteria grown on different substrates and related to respiration of organic substances in the Krebs cycle (Macko and Estep, 1984). Both negative and positive shifts in $\delta^{13}C$ appear to depend on the substrate used by microorganisms, and not so much on the species.

5.7 Differences and common characteristics of fulvic acids

The strongest similarities are observed between the four bog water FA samples. Although collected in different years and months, bulk $\delta^{13}C$ values and mean weighted $\delta^{13}C$ values of the different compound classes record a very stable system over time. Closest to this system are results from the soil seepage water. The generation of this water in a spruce

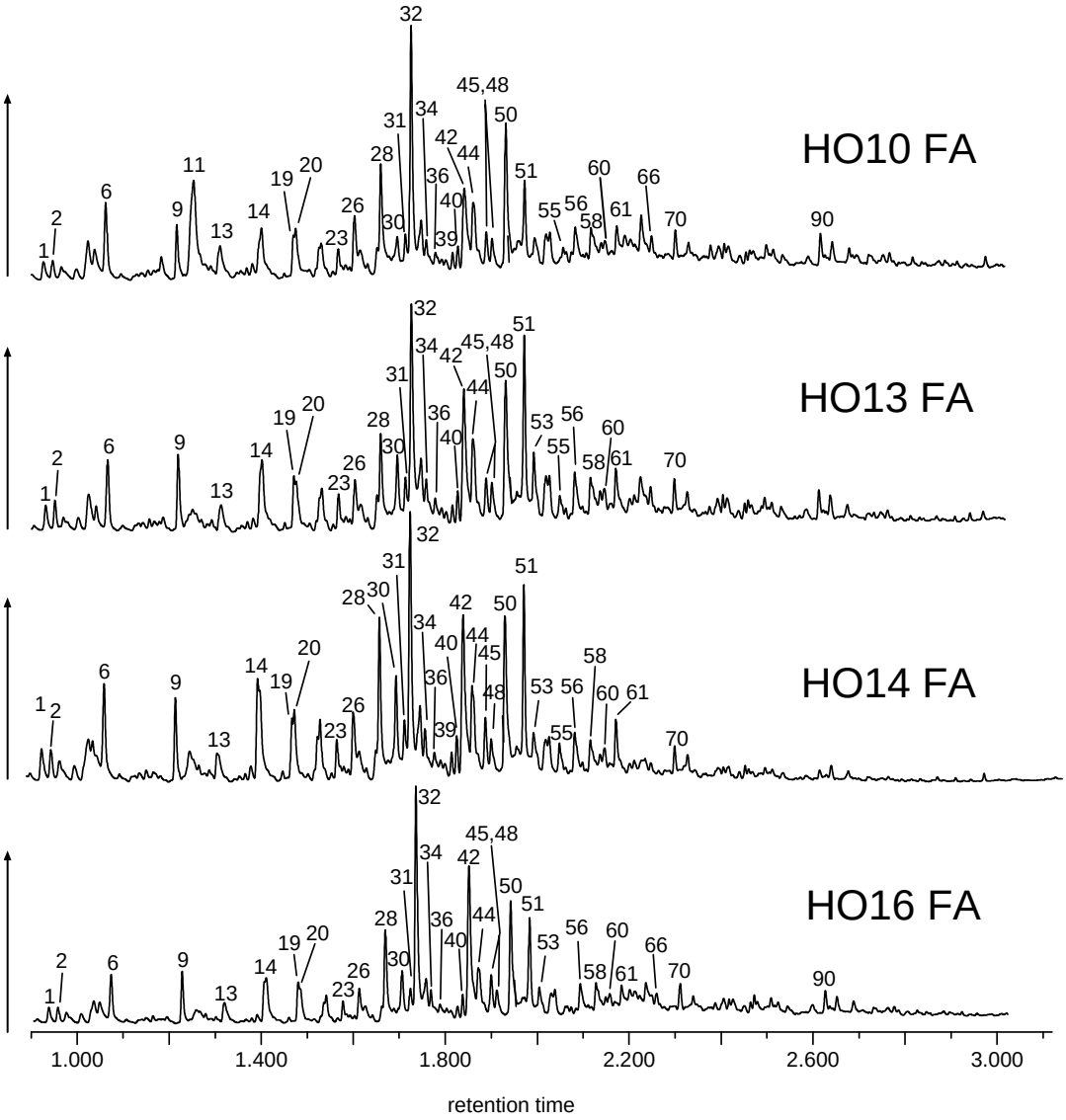

Figure 5.5: IRMS trace (*m/z* 44) of the four bog water fulvic acids. Numbers refer to peaks listed in Appendix II.

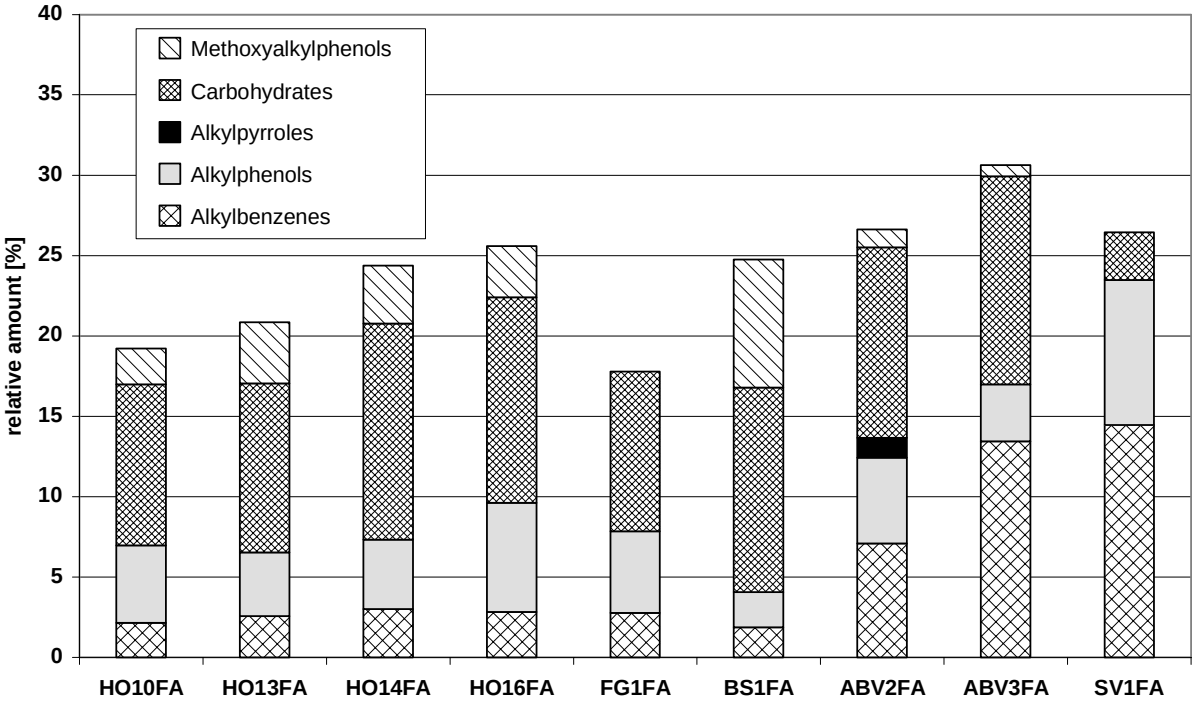

Figure 5.6: Relative amounts of compound classes for all isolated fulvic acids (FA) of the aquatic ecosystems. The values are based on peak areas as determined by IRMS chromatograms. Numbers are given in Table 5.4 and in Appendix II. Sample identification is explained in Table 5.2.

stand is mirrored by a higher amount of methoxyphenols. Both systems contain considerable amounts of fresh organic material as indicated by the ^{14}C data.

The groundwater FA differ from the bog water and the soil seepage water in bulk ^{13}C, ^{14}C and in the lack of methoxyphenols as lignin markers. The 1‰-shift in bulk ^{13}C could result from different proportions of carbohydrates and lignin-derived material, which usually differ naturally by a few per mil (Benner et al., 1987). However, typical pyrolysis products of lignin such as methoxyphenols were not encountered in the groundwater FA and thus cannot account for the slight depletion. This is remarkable in so far as the reductive environment of the aquifer should favor a preservation of lignin derived material. Mean weighted $\delta^{13}C$ values of the compound classes (Table 5.4) as well as observations on individual pyrolysis products clearly show that carbohydrate-derived compounds are depleted by 2‰ - 4‰ relative to the same compounds in the bog water. The $\delta^{13}C$ signatures of dissolved inorganic carbon (DIC) in this aquifer system are around –27‰ and thus indicate that the mineralization of lignitic wood residues contributes to the DIC and that dissolution of calcite is unimportant (Buckau et al., 2000). These depleted lignitic wood residues may serve also as an additional source for microbial biosynthesis of carbohydrates and thus influence the bulk ^{13}C value. The absence of methoxyphenols, however, indicates that a dissolution of the lignite and peat pebbles in the aquifer is unlikely.

The anthropogenically-influenced waste waters ABV2, ABV3 and SV1 were the most contrasting samples, both amongst each other and compared with other systems. Bulk $\delta^{13}C$ values indicated that the brown coal processing water (SV1) comprised higher amounts of ^{13}C-enriched compounds, which was also reflected by the compound classes (Table 5.4). This is surprising because, in general, chemically- and microbially-mediated reactions during diagenesis result in the formation of geopolymers that are depleted in ^{13}C due to a loss of ^{13}C-enriched carboxyl groups (Macko et al., 1993). This loss of carboxyl groups should occur during carbonization prior to extinguishing by water, and favor an enrichment of aromatic compounds. An enrichment of aromatic products is the only notable similarity between those three samples: a high portion of alkylbenzenes and the occurrence of hetero- and dicyclic compounds most probably derived from fossil fuel products. The precursor material for the alkylbenzenes, however, seems to be different. Alkylbenzenes in the brown coal processing water (SV1) are enriched by 3‰ compared with ABV3 and by almost 8‰ compared with ABV2. Individual compounds vary by up to 13‰. As part of the refractory organic matter, this pool most likely consists of comparable structural units, i.e. cyclic, but is generated from different precursor material.

Differences in source material could cause variability in the carbohydrate isotopic signal as well. Precursor material can be plant or microorganism-derived. Clear hints of microbial biomass have only been encountered in the secondary effluent ABV2, and not so much in ABV3 collected at the same place under comparable conditions four years later. The decomposition of organic material by microorganisms, as may be expected in a waste water treatment plant, should result in a release of 'light' respired $^{12}CO_2$ and be reflected in an enrichment of ^{13}C (trophic level effect). Although this is not indicated by the bulk values, the mean weighted $\delta^{13}C$ values of the carbohydrates in ABV2 suggest an input of microbially synthesized material. The clear hints on microbial biomass in ABV3 (Frimmel and Abbt-Braun, 1999) are only reflected by acetamide, a pyrolysis product of bacterial cell walls (see Section 5.6.4). Except for a high nitrogen content, the absence of N-containing pyrolysis products and an unusual depletion of ^{13}C for carbohydrates are rather contradictory. Additional information on this particular sample by other analytical techniques applied in the ROSIG project are only available from solid state high-resolution ^{13}C- and ^{15}N-NMR (Lankes and Lüdemann, 2001). In their study no significant differences have been observed between ABV2 FA and ABV3 FA.

5.8 Comparison of a fulvic and a humic acid fraction with bulk DOM (HO 14)

IRMS chromatograms of isolated fulvic acid (FA) and humic acid fractions (HA) show different characteristics (Figure 5.7). Pyrolysis products above the detection limit of

200 mV in the IRMS chromatogram of the humic acid fraction are dominated by two major peaks: phenol and 2-methoxyphenol, thus reducing the number of detectable peaks to 18 (Table 5.5). In contrast, pyrolysis products of the FA are distributed more evenly and yield 32 peaks. A grouping of all identified products into compound classes according to their origin results in a more efficient comparison. The relative quantification of aromatic compounds (lignin-derived pyrolysis products, alkylphenols and alkylbenzenes) in the HA fraction is 18% of the pyrolyzed material whereas the same compounds make up 11% of the FA fraction (Figure 5.8). This predominant aromatic character of HA as compared with FA is in agreement with results from previous studies (Stevenson, 1994; Schulten, 1999; González-Vila et al., 2001). In the case of the FA sample, carbohydrate-related pyrolysis products are the main contributors comprising 13% of the pyrolyzed material. In addition to the classified compounds, two more compounds could be identified in the FA: an alkane/alkene likely to be derived from lipids, and benzofuran, a compound encountered upon pyrolysis of coumarone-indene resins (Luke, 1973). The low amount of

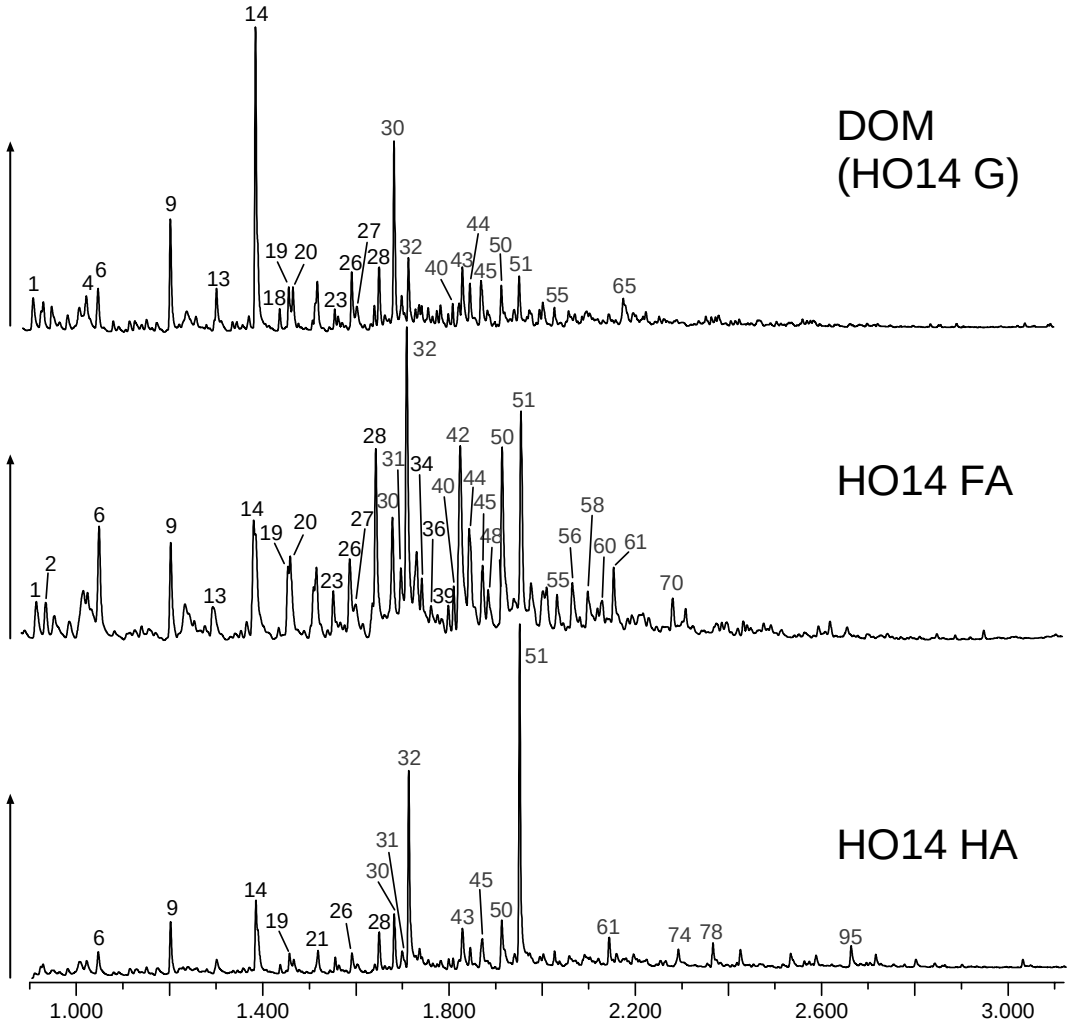

Figure 5.7: IRMS chromatograms (*m/z* 44) of dissolved organic matter (DOM) from a bog lake (Hohlohsee sample HO14) and its isolated fulvic (FA) and humic acids (HA). Numbers of the peaks refer to pyrolysis products listed in Table 5.5.

alkanes/alkenes generated upon pyrolysis contrasts with findings of a relatively high contribution of aliphatics (Joly et al., 2000; González-Vila et al., 2001) but may be attributed to differences in analytical conditions, e.g. the GC column or pyrolysis temperature. In general, these results again suggest that a variety of heterogeneous materials, dominated by lignin and carbohydrates, are components of the humic and fulvic acid fractions.

Isolation procedures naturally result in enrichments of certain compound classes. It is thus not surprising, that several pyrolysis products of the HA and FA fraction were not detected in the DOM. These comprise predominantly compounds ascribed to lignin. In contrast, two compounds related to lipids were only found in the DOM (methylbutanal and 1-dodecene). Main constituents of the DOM are carbohydrates (15%), followed by a considerable amount of alkylbenzenes (4%, Figure 5.8). A conclusion with regard to effects of the isolation procedure on the fractions may not be drawn.

Differences in isotope values of single pyrolysis products should not be expected if it is assumed that the FA and HA fractions can be isolated without an isotope fractionation

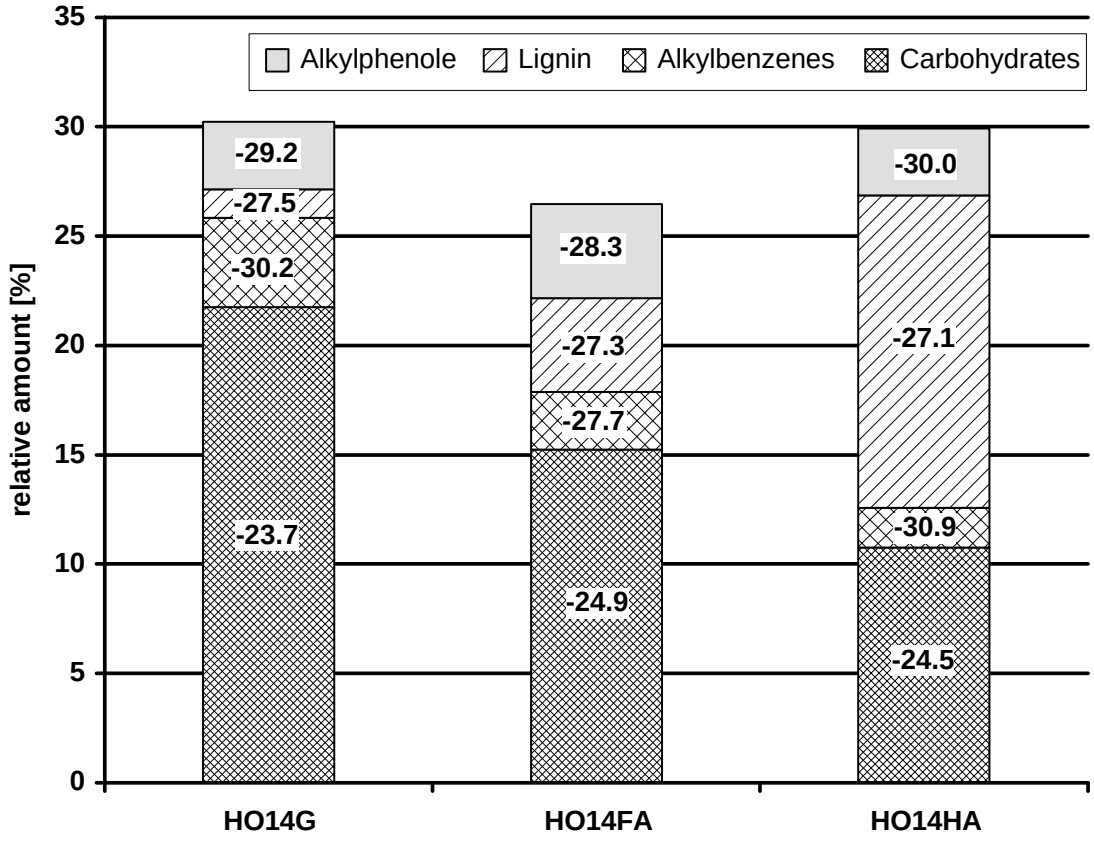

Figure 5.8: Relative amounts of compound classes for dissolved organic matter from bog water (HO14 G) and isolated fulvic (FA) and humic acids (HA). The values are based on peak areas as determined by IRMS chromatograms. 'Bulk' $\delta^{13}C$ values of compound classes are given in the bars. Numbers refer to values in Table 5.5.

effect. Considering the mean weighted isotope values for classified compounds again demonstrates the enrichment of ^{13}C in carbohydrate-related compounds relative to aromatics (Figure 5.7). The differences between FA, HA, and DOM can be attributed to varying compositions. Pyrolysis products not detected in one sample may influence the 'bulk' value in the other. However, there are also differences of $\delta^{13}C$ values of single pyrolysis products. In all three samples, all compounds except for methylsuccinic anhydride indicate a slight enrichment of ^{13}C in the fulvic acid fraction (Figure 5.8). This tendency may not be statistically significant but corresponds to findings that FA are more strongly modified than HA (Hatcher and Spiker, 1988; Jahnel et al., 1998). Two additional pyrolysis products are found exclusively in the HA and FA fraction: 2-methlyphenol (peak no. *45*) and 2-methoxy-4-methylphenol (*61*). Comparison of their δ-values reveals an enrichment of ^{13}C in the HA fraction, which is particularly high for 2-methoxy-4-methylphenol (4.5‰). These findings seem to indicate that modified substances, independent of compound classes, do not exclusively occur in FA. Particularly the enrichment of ^{13}C in a lignin-derived pyrolysis product such as 2-methoxy-4-methylphenol contradicts findings that lignin in HA is less altered than compared to those of corresponding FA (Ertel and Hedges, 1984).

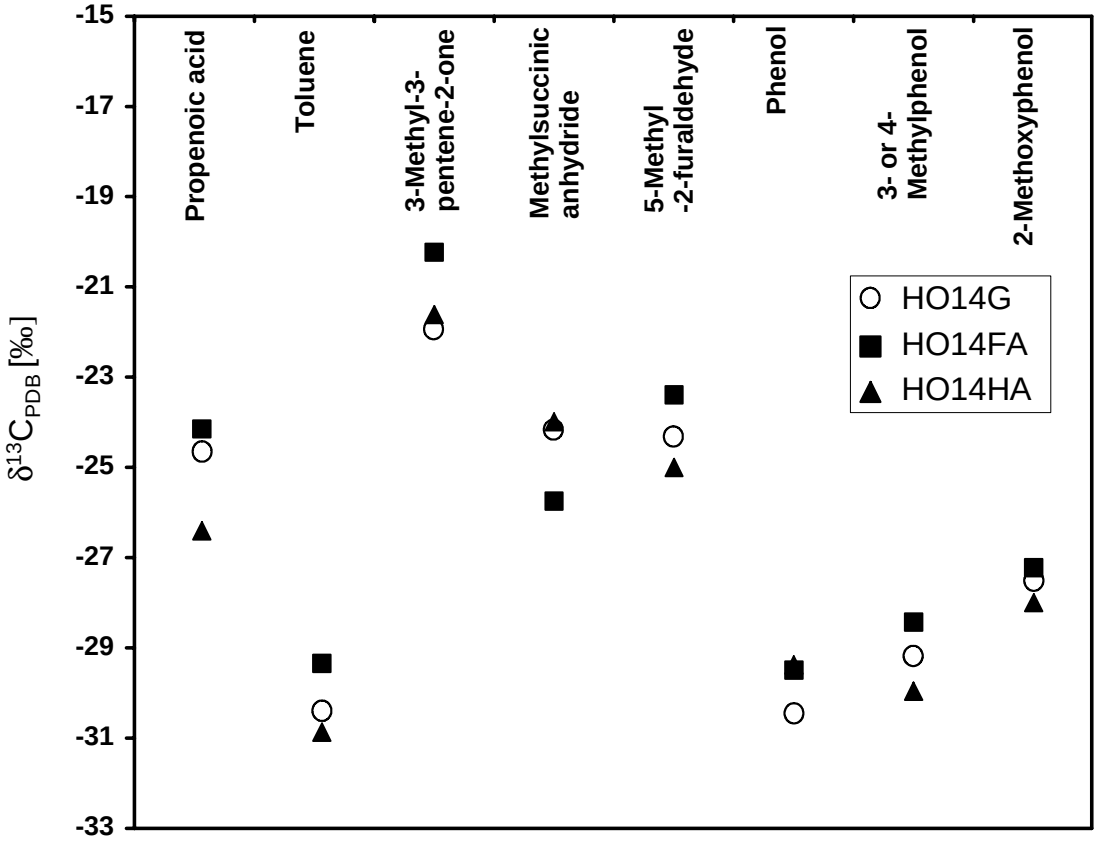

Figure 5.9: $\delta^{13}C$ values of pyrolysis products that occur in all three samples: dissolved organic matter (HO14 G), isolated fulvic (FA) and humic acids (HA).

Table 5.5: Relative amount (% area) and $\delta^{13}C$ values (‰) of pyrolysis products from dissolved organic matter (DOM), isolated fulvic acids (FA) and humic acids (HA) from bog lake water (HO14). Standard deviations (s.d.) as well as number of replicates (*n*) are given. Values are rounded: s.d.=0.0 means <0.05; — means less than three replicates. (T) stands for tentative identification. The number of replicates can vary with analytical conditions due to detection thresholds. Missing data indicate peak below detection threshold in all runs. ∗ means peak detectable but no reliable isotope signal or area value determined because of co-elution.

	DOM (HO14 G)						HO14 FA						HO14 HA						Pyrolysis product	Compound class
no.	rel. amt.	s.d.	*n*	$\delta^{13}C$	s.d.	*n*	rel. amt.	s.d.	*n*	$\delta^{13}C$	s.d.	*n*	rel. amt.	s.d.	*n*	$\delta^{13}C$	s.d.	*n*		
1	1.1	—	*2*	-29.4	—	*2*													3-Methylbutanal	
2							0.4	—	*1*	-25.6	—	*1*							Benzene	alkylbenzenes
4	∗	∗		∗	∗		∗	∗		∗	∗								Dimethylfuran	PS
6	1.3	0.3	*4*	-24.7	0.3	*4*	1.4	0.1	*3*	-24.1	0.1	*3*	1.4	—	*2*	-26.4	—	*2*	Propenoic acid	PS
9	3.1	0.8	*4*	-31.3	1.5	*7*	1.0	0.0	*3*	-29.3	0.5	*3*	1.8	0.2	*4*	-30.9	0.4	*4*	Toluene	alkylbenzenes
13	0.3	0.1	*4*	-25.4	1.4	*4*	∗	∗		∗	∗								2(5H)-Furanone	PS
14	1.3	2.5	*5*	-23.7	1.2	*8*	∗	∗		∗	∗		∗	∗		∗	∗		2-Furaldehyde	PS
18	0.6	—	*1*	-26.3	—	*1*													Ethylbenzene	alkylbenzenes
19	1.1	—	*2*	-23.4	—	*2*	∗	∗		∗	∗		0.8	—	*1*	-24.7	—	*1*	Dimethylbenzene	alkylbenzenes
20	1.1	0.3	*3*	-29.1	0.6	*3*	∗	∗		∗	∗								Methylfuranone (isomer)	PS
21	∗	∗		∗	∗		∗	∗		∗	∗		1.1	—	*1*	-28.0	—	*1*	Dimethylbenzene	alkylbenzenes
23	0.5	—	*1*	-23.7	—	*1*	0.4	—	*2*	-23.1	—	*2*							2-Methyl-2-cyclopenten-1-one	PS
26	1.5	0.7	*5*	-21.9	0.3	*5*	0.9	0.0	*3*	-20.2	0.1	*3*	0.9	—	*1*	-21.6	—	*1*	3-Methyl-3-penten-2-one (T)	PS
27	1.0	0.5	*3*	-27.7	0.2	*3*	0.5	—	*1*	∗	∗								Methylfuranone (isomer)	PS
28	1.7	0.4	*5*	-24.1	0.7	*5*	2.2	—	*2*	-25.8	—	*2*	1.2	0.1	*4*	-24.0	0.7	*4*	Methlysuccinic anhydride	PS
30	3.8	0.4	*5*	-24.3	1.3	*8*	1.6	—	*2*	-23.4	—	*2*	1.8	0.2	*4*	-25.0	0.2	*4*	5-Methyl-2-furaldehyde	PS
31							0.7	—	*2*	-25.3	—	*2*	0.9	—	*1*	-24.3	—	*1*	Benzaldehyde	Lig
32	2.4	0.6	*5*	-30.4	0.6	*8*	2.8	—	*2*	-29.5	—	*2*	7.0	1.4	*4*	-29.4	1.2	*4*	Phenol	mixed
34							0.8	—	*2*	-28.1	—	*2*							Trimethylbenzene	alkylbenzenes
36							0.4	—	*1*	-26.4	—	*1*							Benzofuran	
39							0.2	—	*1*	-23.1	—	*1*							Methyl-(1-methylethyl-)-benzene	alkylbenzenes
40	0.4	—	*1*	-27.8	—	*1*	0.3	0.0	*3*	-25.9	2.2	*3*							Ethylmethylbenzene	alkylbenzenes
42							3.7	0.7	*3*	-24.1	0.5	*3*							Unknown polysaccharide marker	PS
43	3.2	0.7	*3*	-24.3	0.5	*3*							1.6	0.3	*4*	-24.1	1.2	*4*	5-Methyl-2-acetylfuran	PS
44	1.1	—	*2*	-26.7	—	*2*	1.5	0.1	*3*	-29.3	0.9	*3*							2,3-Dimethyl-2-cyclopenten-1-one	PS
45	1.9	0.9	*4*	∗	∗		0.7	0.0	*3*	-28.2	0.9	*3*	1.1	—	*2*	-27.0	—	*2*	2-Methylphenol	alkylphenol
48							0.7	0.1	*3*	-29.6	1.1	*3*							Unknown	PS
50	1.2	0.2	*3*	-29.2	0.8	*5*	2.3	0.1	*3*	-28.4	0.5	*3*	2.0	0.3	*4*	-30.0	2.4	*4*	3- or 4-Methylphenol	alkylphenol
51	1.3	0.5	*3*	-27.5	0.9	*3*	2.7	0.8	*3*	-27.2	0.2	*3*	9.4	1.9	*4*	-28.0	1.0	*4*	2-Methoxyphenol	Lig
55	1.1	—	*2*	-17.9	—	*2*	0.4	—	*1*	-22.8	—	*1*							Levoglucosenone	PS
56							0.7	0.0	*3*	-27.3	1.0	*3*							Dimethylphenol	alkylphenol
58							0.7	—	*1*	-28.7	—	*1*							Ethylphenol	alkylphenol
60							0.8	—	*1*	-29.1	—	*1*							Alkane/Alkene(T)	Lip
61							0.9	0.0	*3*	-29.0	0.2	*3*	0.9	—	*2*	-24.4	—	*2*	2-Methoxy-4-methylphenol	Lig
65	1.5	0.9	*3*	-28.2	1.5	*3*													1-Dodecene	Lip
70							0.4	0.0	*3*	-26.4	0.8	*3*							2-Coumaranone	alkylbenzenes
74													0.8	—	*1*	-23.3	—	*1*	4-Ethyl-2-methoxyphenol	Lig
78													1.1	0.1	*3*	-26.9	1.8	*3*	4-Vinyl-2-methoxyphenol	Lig
95													1.2	—	*2*	-27.3	—	*2*	1-(4-Hydroxy-3-methoxyphenyl)-ethanone	Lig

6 The Hohlohsee study

The formation of DOM has been studied in greater detail in one of the systems that has shown consistency over several years: the bog water system Hohlohsee (Kracht and Gleixner, 2000; Appendix V). The combination of structural analysis and isotope measurements of DOM and possible precursors can provide more detailed information on the genesis of DOM. In contrast to the fractions of humic substances investigated in the ROSIG reference material, the samples from the Hohlohsee represent the whole organic matter of the peat and the complete DOM of the bog water. Although the Hohlohsee is surrounded by different types of vegetation as possible source material for the DOM, the *Sphagnum* moss was chosen because of its close and extensive contact to the water (Figure 6.1).

6.1 Moss and peat samples

Peats are suitable for investigations because of the small variety of species adapted to the nitrogen poor and acidic conditions of the soil. The living top layer at the bog lake Hohlohsee is dominated by *Sphagnum* species, with some Ericaceae and *Eriophorum* species. In June 1998, during the sampling of the Hohlohsee bog water (HO14), samples of

Figure 6.1: The bog lake Hohlohsee (Schwarzwald, Germany, facing west) and its extensive *Sphagnum* moss vegetation. Typical bog vegetation (*Oxicocco-Sphagnetea*) consisting of shrub, grass, and moss species border the lake. The water was sampled from 50 cm depth of the surface water. Picture taken with permission from Abbt-Braun from the official ROSIG web page (http://ebiwat24.ciw.uni-karlsruhe.de/Specials/Rosig/probenahmeorte.html).

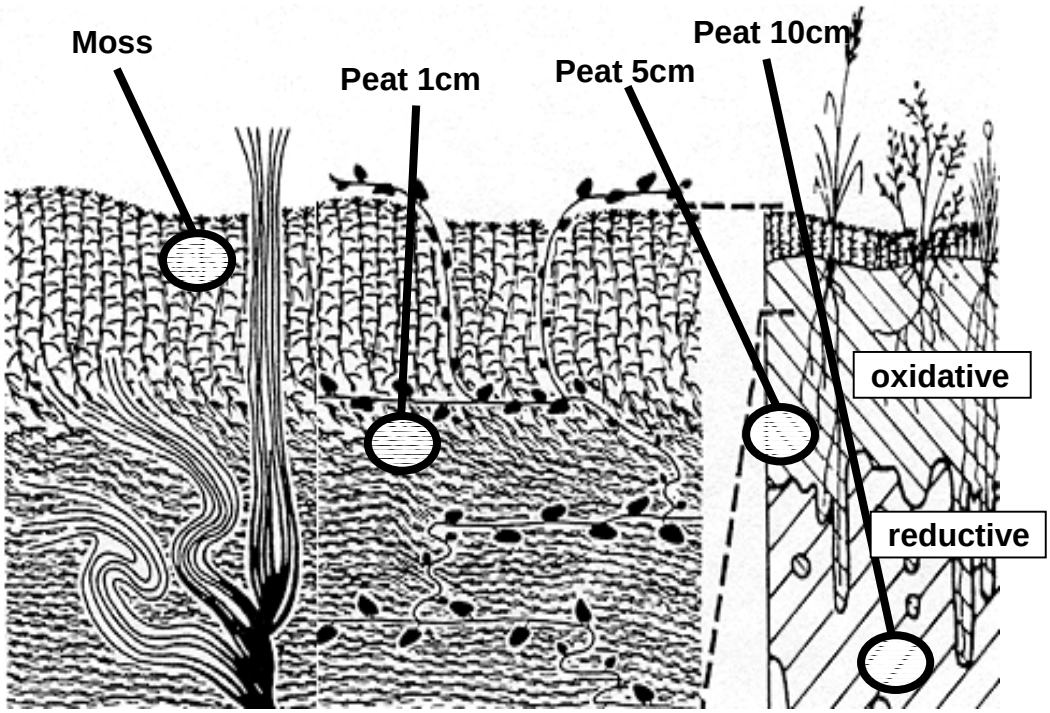

Figure 6.2: Sketch representing sampling depths and approximate environmental situation at the time of peat sampling. Boundary between oxidative and reductive conditions is subject to water level fluctuations. Drawing modified after Göttlich, 1990.

the *Sphagnum* dominated peat were taken as possible precursor material for humic substances in the bog water (descriptions of bog water sampling and environment are given in Section 5.1.2). Peat samples were taken from various depths with *Sphagnum* moss under different conditions (Figure 6.2). The uppermost layer of fresh moss and peat from 1 cm depth are well above the water surface, peat from 5 cm depth is affected by water level fluctuations while peat from 10 cm is permanently water saturated. The different stages of decomposition of the *Sphagnum* moss were indicated by a decrease in particle size. The samples were also characterized by a change of color from green (living top layer) to yellow in the middle layers, to brown and dark brown in the deepest layer which was accompanied by increasing decomposition. A contamination of rootlets, as can occur in peat by other bog inhabiting species like heathers, could be nearly excluded, at least for the uppermost layers, because the degradation stage was too low and fine roots could be separated easily from the abundant mass of peat moss.

6.2 Bulk elemental analyses

The carbon content of the moss and peat samples increases with depth in the profile from 48.4% in the *Sphagnum* layer to 52.2% at 10 cm depth, while the amount of oxygen and hydrogen decreases from 41.9% to 27.7% and from 5.8% to 4.9%, respectively (Table 6.1).

The major differences in composition are found between the peat at 10 cm and the overlying layers. In an O/C and H/C diagram (Figure 6.3) these differences represent a dehydration process affecting the sample at 10 cm depth (van Krevelen, 1993), i.e. a primary loss of hydroxyl groups. Alternatively, the observed shift can be explained by different decomposition rates of biomolecules. Moss and peat at 1 and 5 cm depth show H/C ratios close to cellulose (H/C: 1.67) whereas peat at 10 cm depth plots close to a region representative for phenylpropanes. Since cellulose is readily degraded (Deines, 1980; Benner et al., 1987), this shift may also imply that the upper 5 cm are in an early stage of degradation. Alternatively, the permanent water saturation of peat at 10 cm depth might inhibit particularly oxidative degradation of phenolic substances (Haider, 1996) and consequently result in the accumulation of these substances. However, the high ash content in peat at 10 cm compared with the other samples indicates the progressive mineralization

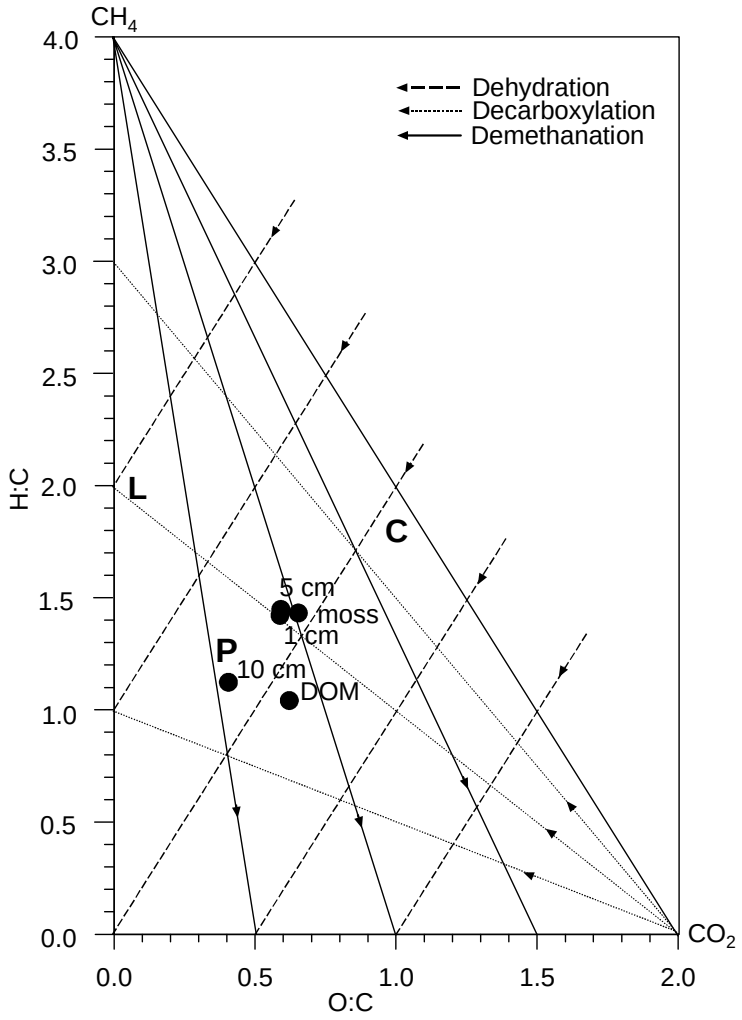

Figure 6.3: Molar ratios of O/C versus H/C of bulk samples from *Sphagnum* moss, peat of given depth and dissolved organic matter (DOM) from bog lake water. Positions of important biological compounds such as carbohydrates (C), lignins (P, phenylpropanes) and lipids (L) are indicated. See text for discussion. The lines represent different condensation reactions in the formation of coal (after van Krevelen, 1993).

Table 6.1: Elemental composition (C, N, S, H, and O) in weight percent and bulk isotope analyses ($\delta^{13}C$ and $\delta^{15}N$) of *Sphagnum* moss, different layers of peat and dissolved organic matter (DOM) from bog lake water with standard deviations (s.d.).

	%C	%N	%S	%H	%O	%ash	sum	$\delta^{15}N$	s.d.	$\delta^{13}C$	s.d.
Moss	48.4	1.2	0.1	5.8	41.9	1.7	99.1	0.1	0.4	-26.3	0.8
Peat 1cm	48.4	2.7	0.4	5.7	38.3	5.6	101.1	0.1	0.5	-26.5	0.7
Peat 5cm	49.6	1.2	0.4	6.0	39.4	2.2	98.8	-0.7	0.3	-26.1	0.4
Peat 10cm	52.2	2.0	0.3	4.9	27.7	13.3	100.4	0.4	0.1	-26.9	0.2
DOM	48.0	1.3	1.5	4.2	39.6	7.9	102.5	-2.1	0.2	-26.3	0.3

with depth.

The nitrogen content in the peat profile varies from 1.2% in the moss to 2.0% at 10 cm depth with a notable enrichment of 2.7% at 1 cm depth (Table 6.1). These variations of total N are assumed to reflect the different microbial activities within the profile. This inference is supported by the enrichment of amino acids at the surface in peat samples (Macko et al., 1990). However, the varying N contents of the samples from the Hohlohsee could also be influenced by the changing conditions, e.g. the change from oxygenated to reduced conditions as can be expected by water level fluctuations in peat from 10 to 5 cm. Products from nitrification and denitrification processes can account for the total N decrease from peat 10 cm to peat 5 cm. Nitrous oxide (N_2O), for example, has been found to be mainly produced at the water/air boundary (Schmidt et al., 1992) and subsequently released to the atmosphere. It can only be speculated on the processes behind the N variations, but microbial activity is most likely to be the cause of N variations. This is also discussed below in combination with $\delta^{15}N$ values.

The elemental composition of DOM in the water sample differs from that of the peat samples (Table 6.1, Figure 6.3). Slightly lower amounts of H may indicate fewer aliphatic structures in DOM. Sulfur in the bog water is enriched by one order of magnitude compared to nearly constant values in the peat profile. This enrichment can be attributed to atmospheric input of sulfuric acid, as acid rain has been a known problem in the Black Forest for the last 20 years. Isotopic evidence for predominant atmospheric input of S in two forested catchments in the Black Forest has also been reported (Mayer et al., 1995).

6.3 Bulk isotope measurements

The $\delta^{13}C$ values of the bulk samples were consistently around –26‰ (Table 6.1) with only minor variations within the standard deviation. In contrast to the atomic ratios, the constancy in $\delta^{13}C$ over the peat profile indicates that structural changes play only a minor role. Obviously, an accumulation of lignins, as has been reported previously in low

oxygenated, water-saturated soils based on ^{13}C depletions (Deines, 1980; Benner et al., 1987), does not occur. This would be consistent with findings that lignins are absent from *Sphagnum* (Lewis et al., 1999) and, hence, from *Sphagnum*-derived peat, but contradicts the observations from the elemental analysis which indicated an enrichment of phenylpropanes (Figure 6.3).

The $\delta^{15}N$ values in the peat profile were about 0‰, a value expected for a low nitrogen ecosystem having only atmospheric deposition of nitrogen (Schmidt et al., 1992). The slight shift of ^{15}N in peat 5 cm may be due in part to an occurrence of isotopically depleted amino acids in bacteria and fungi. It is possible that the nitrogen content, particularly above the water level, varies with the production of amino acids by bacterial and fungal growth and that isotope variations are caused by interaction of several biochemical reactions (Macko and Estep, 1984). Further analyses using N-isotope signatures of pyrolysis products from amino acids could be helpful to identify these processes.

The $\delta^{13}C$ value of the DOM (bog water) exactly matches the value for the soil organic matter (SOM) fraction and therefore suggests that it is directly released from the SOM pool. In contrast, the $\delta^{15}N$ value of DOM is notably depleted by 2‰ relative to the SOM pool. This strongly contradicts a simple solving mechanism from the peat. As partly discussed above and reported by Macko and Estep (1984) and Claus et al. (1999), this ^{15}N depletion is likely to result from microbial interactions. Alternatively, an uptake of isotopically "light" N from atmospheric nitrogen fixed by azotrophic microorganisms or the consumption of isotopically depleted N_2O is also conceivable.

The influence of microbial interactions during the formation of the organic material may be detected by compound specific isotope measurements. The system designed for this study allows the determination of $\delta^{13}C$ values, thus identifying the input of microbially produced substances masked by bulk isotope values.

6.4 Py-GC/MS-IRMS of peat samples and DOM from the bog lake

As with the ROSIG fulvic acid samples, only major peaks in the IRMS-chromatograms were identified using the ion-trap MS, since these were the only peaks suitable for simultaneous isotope ratio determinations. The relative amounts of pyrolysis products from the peat and DOM samples are given in Table 6.2. The complete listing of mass spectra of the pyrolysis products is given in Appendix III. More than 60% of the major pyrolysis products investigated for this study are derivatives of furan and phenol. Additionally, some derivatives of benzene, pyran and cycloalkenones could be identified. Furan and furaldehyde derivatives are mainly pyrolysis products of polysaccharides (Irwin, 1982; van Smeerdijk and Boon, 1987; Stout et al., 1988; Pouwels et al., 1989; Durig et al., 1991). The

other group of important pyrolysis products are derivatives of phenol which are generated from various compounds of the shikimic acid pathway.

Substances with low retention time in the chromatogram, e.g. furan derivatives, become less dominant, whereas peaks in the "phenol region", e.g. retention time between 1800 s and 2500 s, increase with depth down the profile (Figure 6.4). This shift in the molecular composition is consistent with the bulk elemental measurements (Table 6.1, Figure 6.3), as it suggests that phenols - mainly the methoxylated lignin derivatives - are preserved in the humification process of *Sphagnum* (Benner et al., 1987; Spiker and Hatcher, 1987; Stout et al., 1988). In contrast, the relative loss of carbohydrate pyrolysis products and the relative accumulation of pyrolysis products from phenolic compounds in the profile are not consistent with bulk $\delta^{13}C$ ratios, as these structural changes would result in ^{13}C depletion over the peat profile (Benner et al., 1987; Gleixner and Schmidt, 1998). This may suggest that pyrolysis products from different depths in the profile have different precursors, e.g. carbohydrates from *Sphagnum* in the upper horizons and from microorganisms in the deeper horizons.

The chromatogram of the DOM consists mainly of substances identifiable at the beginning of the chromatogram, e.g. toluene, furaldehyde, 5-methylfuraldehyde and phenol (Figure 6.2, Table 6.2). Compounds with high retention time and higher molecular weight, e.g. pyrolysis products of phenolic compounds and higher lipids, are less abundant.

6.4.1 Combined information of structure and isotopic content: Py-GC/MS-IRMS

The main objective of the Hohlohsee study was to combine structural information from Py-GC/MS with the isotope content of the pyrolysis products in order to understand different biogeochemical processes at the molecular level. The $\delta^{13}C$ values and standard deviations for 52 pyrolysis products are given in Table 6.2. Mean standard deviation for all measurements was 1.3‰. Classification was done in the same way as with the ROSIG samples (Figure 6.6): 25 pyrolysis products could be attributed to carbohydrates, eight were ascribed to lignin. The latter included methoxyalkylphenols and alkylbenzenes, as it was assumed that lignin is the most likely source for alkylbenzenes in this environment. A third class comprises five alkylphenols. The sums and weighted δ-values are based on the pyrolysis products which gave reliable data. Products marked with * in the table were excluded from calculations in all samples.

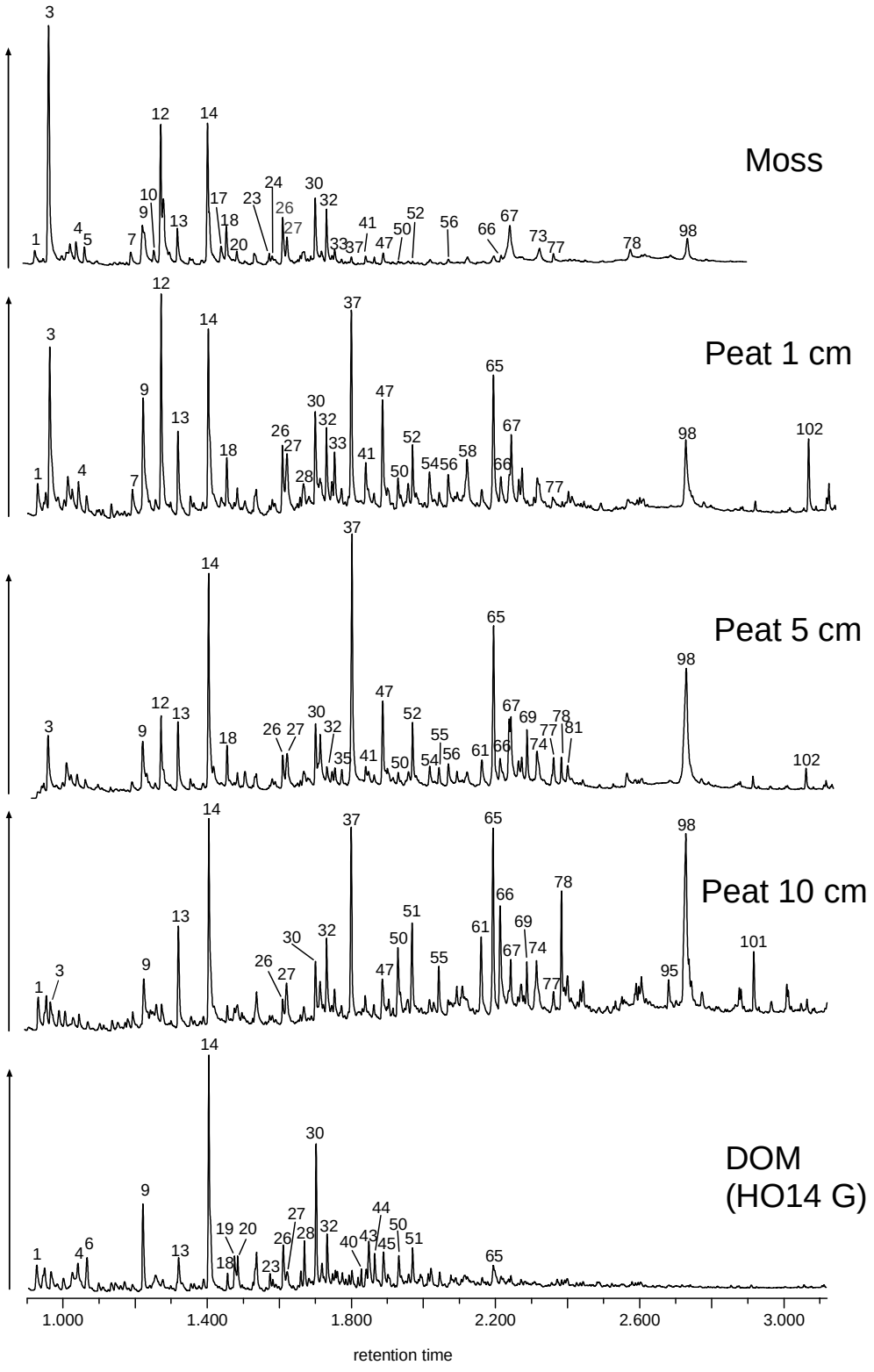

Figure 6.4: Representative CO_2 trace (*m/z* 44) of pyrolysis products from *Sphagnum* moss, peat and dissolved organic matter (DOM) obtained from IRMS. Numbers refer to peaks listed in Table 6.2. It should be noted that peaks can appear larger due to magnification.

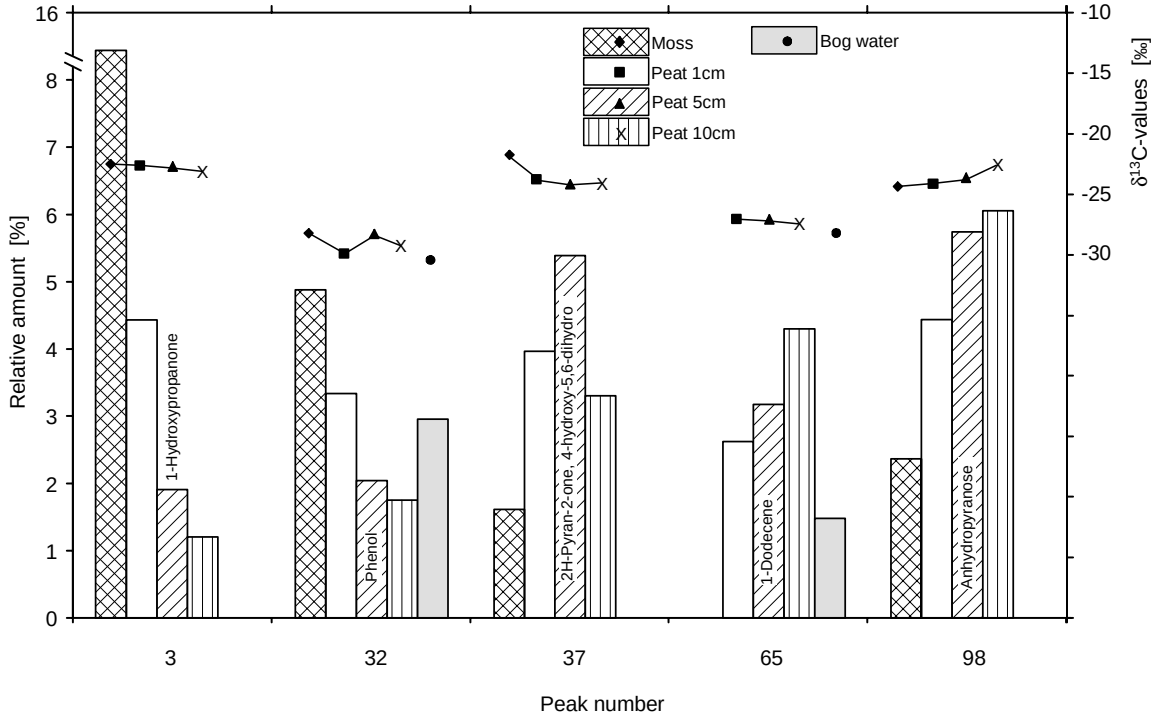

Figure 6.5: Relative peak area (bars) and $\delta^{13}C$ values (symbols) of selected pyrolysis products, e.g. 2-hydroxypropanone, phenol, 4-hydroxy-5,6-dihydro-2H-pyran-2-one, 1-dodecene and anhydropyranose from *Sphagnum* moss, peat and DOM from bog water. Peak numbers and values refer to numbers in Table 6.2 (partly modified after Kracht and Gleixner, 2000).

6.4.1.1 Biogeochemical processes as inferred from selected compounds

Specific processes during humification are distinguishable by the combination of data yielded by peak areas and isotope values of pyrolysis products. They will be introduced before the two main groups of carbohydrate and lignin derived pyrolysis products are discussed in the following two sections. The processes are best demonstrated by five pyrolysis products from the depth profile: 1-hydroxypropanone, phenol, 4-hydroxy-5,6-dihydro-2H-pyran-2-one, 1-dodecene and anhydropyranose. Their relative amounts and $\delta^{13}C$ values are given in Figure 6.5. The relative amounts of 1-dodecene (peak no. *65*) and anhydropyranose (*98*) increase with profile depth, a pattern most distinctly observed for anhydropyranose. Simultaneously, the isotopic content of the anhydropyranose increases with profile depth (Figure 6.5), suggesting that this compound is formed as an anabolic product of microorganisms in the profile. The slight increase of ^{13}C is likely due to the trophic level effect which leads to an enrichment of ^{13}C in metabolic products of microorganisms relative to their source molecules. The isotopic composition of 1-dodecene is relatively constant with depth. No isotope value could be determined for the fresh moss sample, as this compound was below the detection limit.

The precursor of 1-dodecene is not favored by microbial degradation and hence selectively preserved in the humification process. The $\delta^{13}C$ values of 4-hydroxy-5,6-dihydro-2H-pyran-2-one (*37*) decrease from –21.7‰ in the moss to relatively constant values around –24‰, accompanied by a decrease in relative amounts in the peat at 10 cm. This pyrolysis product is most likely derived from a pentose. Since the source of this carbohydrate could be plants as well as microorganisms, the isotope effect may be caused by an introduction and/or replacement of carbohydrates from bacteria and fungi. A similar fractionation effect has been described for individual carbohydrates in *Sphagnum* peat by Macko et al. (1991) and must be related to a formation of microbial carbohydrates (biosynthesis) with a contrary isotope effect compared to the trophic level effect. A possible formation process is the use of a 'light' source molecule such as CH_4, which is produced by methanogenic bacteria in the anoxic layers of the peat and provides a substrate for methane-oxidizing bacteria. The decrease in relative amounts of 4-hydroxy-5,6-dihydro-2H-pyran-2-one in the peat at 10 cm must then be attributed to a higher rate of utilization (Table 6.3).

The amounts of 1-hydroxypropanone (*3*) and phenol (*32*) show a decrease from *Sphagnum* moss to peat, but only the δ-value of 1-hydroxypropanone remains constant. This is conceivable for substances which are gradually degraded. The ^{13}C values of phenol do not show a distinct tendency with depth. This pyrolysis product has obviously several precursors (Tsuge and Marsubara, 1985; Stout et al., 1988; Pouwels et al., 1989).

These results demonstrate that the additional isotope information is valuable to verify the structural results. Most precursors of the pyrolysis products must have been subject to

Tabelle 6.3: Processes occurring during humification of *Sphagnum* moss as indicated by Py-GC/MS-IRMS analyses. +: increasing (i.e. enrichment of ^{13}C), —: decreasing (i.e. depletion of ^{13}C), const.: constant, i.e. within standard deviation of 1‰. Δ ‰ values indicate the shift of $\delta^{13}C$ from *Sphagnum* to peat at 10 cm depth (modified after Kracht & Gleixner, 2000).

relative amount	***$\delta^{13}C$ of individual products***	***Process assumed***
+	+ (Δ +1.7 ‰)	formation of microbial biomass (trophic level effect) e.g. Anhydropyranose
+	– (Δ -2.0 ‰)	biosynthesis of microbial carbohydrates e.g. 4-Hydroxy-5,6-dihydro-2H-pyran-2-one
+	const.	selective preservation, e.g. 1-Dodecene
–	not distinct	mixed sources, e.g. Phenol
–	const.	slow degradation, e.g. 1-Hydroxypropanone

(bio-) chemical conversion in the humification process. For example, pyrolysis products of carbohydrates at different depths of the profile have different sources, e.g. remaining carbohydrates from plants and accumulating carbohydrates from microorganisms. The only components in this study that indicate selective preservation are 1-dodecene, a potential product of lipids, and 2-furaldehyde.

6.4.1.2 Carbohydrates in moss and peat samples

The sum of all identified carbohydrate derivatives indicates a constant decrease from surface *Sphagnum* to the peat at 10 cm (Figure 6.6). The mean weighted δ-values decrease from –22.2‰ in the moss sample and to a fairly constant value of around –23‰ in the peat samples. Carbohydrates are known to be readily biodegraded from litter but are produced by bacterial or fungal growth at the same time. Thus, ascertaining the origin of pyrolysis products from the decay of plant material and from the growth of fungi or other microorganisms is difficult. The only indication is given by isotope data. Mean weighted δ-values already indicate that some carbohydrates are derived from different sources than those for the carbohydrates found in fresh moss. A close look at the 25 identified pyrolysis products of carbohydrates (indicated as 'PS' in Table 6.2) reveals different behavior. Ten are found in all peat samples (peak no. *3*, *13*, *14*, *26*, *27*, *30*, *37*, *47*, *67*, *98*). Of the remaining substances, six are detected exclusively in the moss (*10*, *17*, *20*, *23*, *24*, *73*). Most substances fall below detection limit at deeper depths in the profile, which suggests that they are biodegraded. Their δ-values, however, exhibit different tendencies. Furaldehyde (*14*), 4-hydroxy-5,6-dihydropyranone (*37*), its methylated derivative (*52*), and anhydropyranose (*98*) all show an increase in $\delta^{13}C$ with increasing depth. This is also the case for levoglucosenone (*55*), which is detected at 5 cm and 10 cm depth.

Several substances that initially occur in the moss are not only biodegraded but must be also replaced by a new source, most likely from microorganisms. This effect is indicated by increasing $\delta^{13}C$ values and may be attributed to the trophic level shift. The observed depletion in ^{13}C as demonstrated by hydroxymethylcyclopentenone (*41*) suggests the use of a 'light' source molecule supposedly by methane-oxidizing bacteria. This isotope effect is also demonstrated by the two derivatives of pyranone (*37*, *52*) which also increase with depth. The relative amount of 2-furaldehyde also increases but keeps a fairly constant $\delta^{13}C$ value, thus indicating that this substance is not produced with depth. It rather seems to be selectively preserved, an unexpected behavior given that carbohydrates are preferentially used by microorganisms as carbon sources. Anhydropyranose, a pyrolysis product of cellulose, is one of the substances that shows a distinct increase with depth. This increased yield of anhydropyranose with depth has been observed previously by Stout et al. (1988), and related to either a microbially-induced disruption of the crystalline framework of

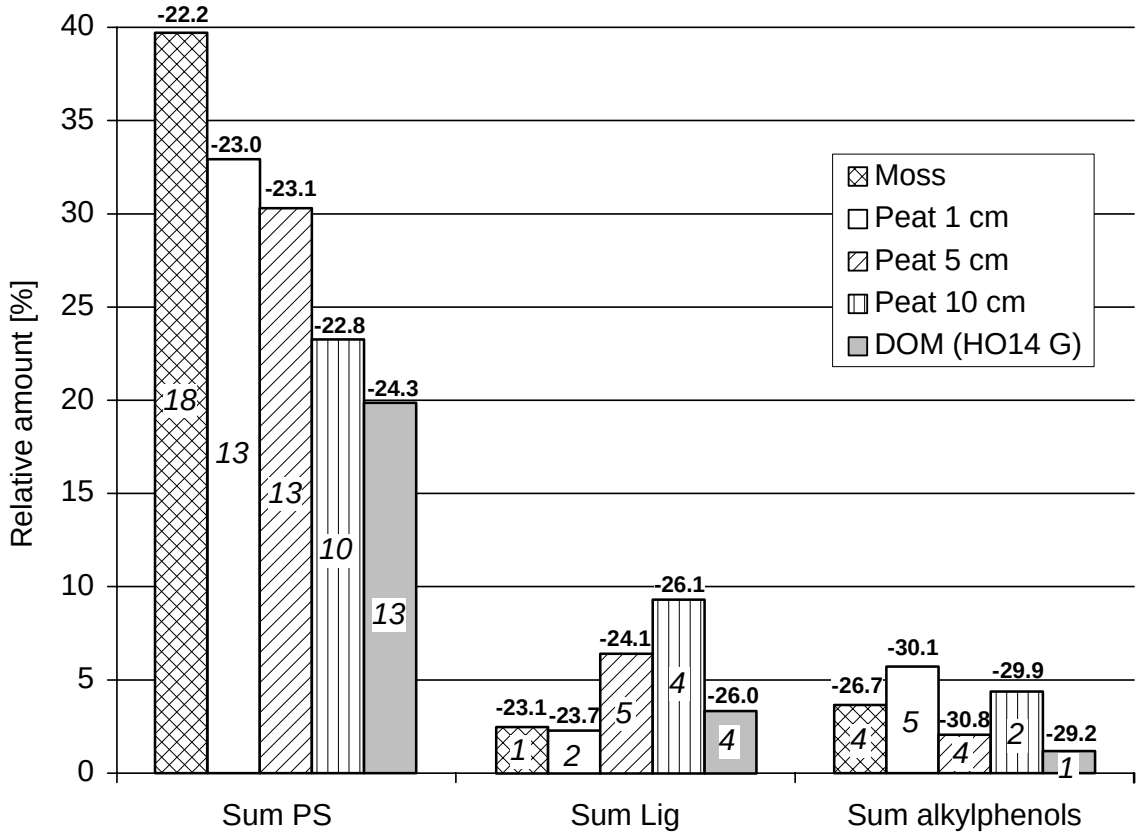

Figure 6.6: Relative amounts of specific compound classes in peat samples and DOM. 'Bulk' $\delta^{13}C$ values for the compound classes are given on top of the bars. Italic numbers in the bars refer to the number of pyrolysis products used for area calculations. PS – Polysaccharides; Lig – Lignin.

cellulose or the contribution of anhydrosugars (e.g. anhydropyranose) from micro-organisms. The additional isotope information in these results support the assumption of a microbial contribution. The slight increase of ^{13}C in anhydropyranose with depth can be attributed to the trophic level effect.

In summary, these results suggest that the carbohydrate content continuously decreases with depth from the surface. The changes in $\delta^{13}C$ values, however, indicate that two major processes in humification interact: biodegradation and substance formation.

6.4.1.3 Alkylphenols and lignin derived compounds in moss and peat samples

Phenolic compounds and alkylbenzenes are usually produced upon flash pyrolysis of lignins. Alkylphenols, however, may have different sources and were thus separately classified. In general, lignins have a low biodegradability in soils and are mainly degraded in oxygenated environments (Lewis et al., 1999). This corresponds to a general increase of lignin-derived compounds with depth, as observed in the peat samples (Figure 6.6). Alkylphenols and lignin-derived compounds added together show a clear increase in relative abundance with depth (6.8%, 8.1%, 8.6%, 13.4% with increasing depth), thus explaining the isolated position of the peat at 10 cm in the van Krevelen-diagram (Figure

6.3) Weighted mean $\delta^{13}C$ values of lignin-derived pyrolysis products show a depletion of ^{13}C from –23.1‰ in the moss to –26.1‰ at 10 cm. A similar trend is observed for the alkylphenols, ranging from –26.7‰ in the moss to –29.9‰ in the peat at 10 cm. Overall the alkylphenols are more depleted in ^{13}C than the lignin-derived compounds by approximately 3‰. Both classes show a general depletion in ^{13}C relative to pyrolysis products from carbohydrates.

Although lignins are reportedly absent from *Sphagnum* moss, phenolic compounds like sphagnum acid (p-hydroxy-β[carboxymethyl]-cinnamic acid) are part of the plant (Lewis et al., 1999). Of the substances found in the fresh moss, pyrolysis products such as phenol, vinylphenol and isopropenylphenol can be attributed to sphagnum acid (van Smeerdijk and Boon, 1987; Stankiewicz et al., 1997a; van der Heijden et al., 1997). Specific lignin markers such as alkylmethoxyphenols were not detected in the pure fresh moss. Only ethylbenzene may be indicative of lignin derived pyrolysis products. However, these results are a good indication that a contamination of the *Sphagnum* sample by lignin-containing plants did not occur, and occurrence of lignin-like polyphenolic structures in *Sphagnum* can be excluded.

Methoxylated phenols, i.e. 2-methoxy-4-methylphenol (methyl guaiacol, peak no. *61*), 4-ethyl-2-methoxyphenol (ethylguaiacol, *74*) and 4-vinyl-2-methoxyphenol (vinyl guaiacol, *78*), first appear in deeper layers of the profile (Figure 6.4). It is most unlikely that these compounds - which are indicative for coniferyl lignin in the peat - are produced in the peatification process. This suggests that the deeper layers of the peat are contaminated with rootlets from angiosperms.

Interestingly, the δ-values of the methoxylated phenols have an unexpected pattern. In contrast to the known general ^{13}C depletion of phenols relative to carbohydrates, 2-methoxy-4-methylphenol and 4-ethyl-2-methoxyphenol are strongly enriched in ^{13}C. Their $\delta^{13}C$ values are between –19‰ and –22.6‰ in peat 5 and 10 cm, whereas 4-vinylphenol (*66*) and its methoxylated form (*78*) show the expected depletion in ^{13}C (around –30‰ in all samples, Table 6.2). It thus seems unlikely that 4-vinyl-2-methoxyphenol is derived

Table 6.2, right: Relative amount (% area) and $\delta^{13}C$ values (‰) of pyrolysis products from *Sphagnum* moss, peat, and dissolved organic matter (DOM) from bog lake water. Standard deviations (s.d.) as well as number of replicates (*n*) are given. Values are rounded: s.d.=0.0 means <0.05; — means less than three replicates. (T) stands for tentative identification. The number of replicates can vary with analytical conditions due to detection thresholds. Missing data indicate peak below detection threshold in all runs. ∗ means peak detectable but no reliable isotope signal or area value determined because of co-elution.

	Moss						Peat 1 cm						Peat 5 cm						Peat 10 cm						DOM (HO14 G)						Pyrolysis product	Source
no.	area (norm)	s.d.	*n*	$\delta^{13}C$	s.d.	*n*	area (norm)	s.d.	*n*	$\delta^{13}C$	s.d.	*n*	area (norm)	s.d.	*n*	$\delta^{13}C$	s.d.	*n*	area (norm)	s.d.	*n*	$\delta^{13}C$	s.d.	*n*	area (norm)	s.d.	*n*	$\delta^{13}C$	s.d.	*n*		
1	1.2	0.0	*3*	-25.7	0.6	*3*	1.0	0.1	*3*	-28.5	2.1	*3*							1.0		*1*	-28.6		*2*	1.1	0.0	*2*	-29.4		*2*	3-Methylbutanal	
3	15.4	0.9	*4*	-22.5	0.8	*8*	4.4	0.9	*4*	-22.6	2.0	*7*	1.9	0.2	*5*	-22.8	1.5	*8*	1.2		*1*	-23.3		*1*							1-Hydroxypropanone	PS
4	1.8		*2*	-25.7		*2*	0.9	0.0	*2*	-24.1		*2*													*	*		*	*		Dimethylfuran	PS
5	1.1		*2*	-19.6		*2*																									Unknown	
6																									1.3	0.3	*4*	-24.7	0.3	*4*	Propenoic acid	PS
7	1.1	0.0	*3*	-21.9	1.1	*3*	0.9		*2*	-24.9		*2*																			Pyrrole (T)	Prot
9	*	*		*	*		*	*		*	*		*	*		*	*		2.0	0.3	*4*	-28.1	0.9	*7*	3.1	0.8	*4*	-31.3	1.5	*7*	Toluene	mixed
10	1.0	0.1	*3*	-21.6	0.5	*3*																									1-Pentene-1-one	PS
12	*	*		*	*		4.1	1.2	*4*	-20.8	1.4	*7*	1.1	0.1	*3*	-17.6	2.5	*6*													2-Propanone	PS
13	2.6	0.2	*4*	-20.4	1.0	*4*	1.9	0.4	*4*	-22.0	1.7	*7*	2.7	0.6	*4*	-21.7	1.0	*7*	2.4	0.1	*4*	-22.3	1.4	*7*	0.3	0.1	*4*	-25.4	1.4	*4*	2(5H)-Furanone	PS
14	1.3	0.0	*4*	-23.4	1.4	*8*	2.2	1.7	*4*	-23.6	0.7	*7*	5.2	0.7	*5*	-22.6	0.7	*8*	5.1	0.2	*4*	-23.2	0.3	*7*	1.3	2.5	*5*	-23.7	1.2	*8*	2-Furaldehyde	PS
17	1.6	0.1	*3*	-18.2	0.5	*3*																									2-Furanmethanol	PS
18	2.5	0.3	*4*	-23.1	0.7	*4*	1.0	0.2	*4*	-23.7	2.0	*4*	0.7	0.1	*5*	-22.9	0.8	*7*							0.6	0.0	*1*	-26.3		*1*	Ethylbenzene	Lig
19																									1.1	0.0	*2*	-23.4		*2*	Dimethylbenzene	Lig
20	0.9	0.0	*3*	-23.5	0.7	*3*																			1.1	0.3	*3*	-29.4	0.6	*3*	Methyl-2(xH)-furanone	PS
23	0.3	0.2	*3*	-20.2	2.6	*3*																			0.5	0.0	*1*	-23.7		*1*	2-Methyl-2-cyclopenten-1-one	PS
24	0.4	0.3	*3*	-22.3	4.9	*3*																									Methylfuraldehyde (T)	PS
26	2.8	0.1	*4*	-19.3	1.9	*4*	1.4	0.1	*4*	-18.9	0.7	*5*	0.6	0.1	*5*	-15.8	1.8	*6*	0.6	0.0	*1*	-15.2		*1*	1.5	0.7	*5*	-21.9	0.3	*5*	3-Methyl-3-penten-2-one	PS
27	2.3	0.5	*4*	-24.8	1.8	*4*	2.3	0.2	*4*	-24.8	1.9	*5*	1.5	0.5	*3*	-24.8	0.8	*5*	1.3	0.0	*1*	-23.8		*1*	1.0	0.5	*3*	-27.7	0.2	*3*	Methyl-2(xH)-furanone	PS
28							*	*		*	*														1.7	0.4	*5*	-24.1	0.7	*5*	Methlysuccinic anhydride	PS
30	4.1	0.1	*4*	-22.9	0.9	*5*	1.8	0.2	*3*	-22.7	1.0	*5*	1.4	0.2	*3*	-20.1	1.2	*6*	1.3	0.1	*4*	-23.6	1.0	*7*	3.8	0.4	*5*	-24.3	1.3	*8*	5-Methyl-2-furaldehyde	PS
32	4.1	0.9	*4*	-28.3	0.9	*7*	3.0	1.4	*4*	-29.9	1.1	*6*	2.0	0.8	*5*	-28.3	1.2	*8*	1.7	0.2	*4*	-29.2	1.7	*4*	2.4	0.6	*5*	-30.4	0.6	*8*	Phenol	mixed
33	1.0	0.0	*3*	-27.9	0.4	*3*	1.2	0.1	*3*	-26.1	0.8	*3*																			3-Methyl-2-cyclohexen-1-one	
35													0.5	0.0	*2*	-16.8		*2*													Unknown	
37	1.0	0.0	*3*	-21.7	2.0	*3*	4.1	0.2	*4*	-23.6	1.8	*6*	5.5	1.0	*5*	-24.1	0.9	*8*	3.5	0.4	*4*	-23.7	0.9	*7*							4-Hydroxy-5,6-dihydro-2H-pyran-2-one	PS
40																									0.4	0.0	*1*	-27.8		*1*	Ethylmethylbenzene	Lig
41	1.2	0.0	*3*	-21.2	1.8	*3*	1.3	0.3	*4*	-20.6	7.8	*4*	0.8	0.0	*1*	-25.2		*1*													2-Hydroxy-3-methyl-2-cyclopenten-1-one	PS
43																									3.2	0.7	*3*	-24.3	0.5	*3*	5-Methyl-2-acetylfuran	PS
44																									1.1	0.0	*2*	-26.7		*2*	2,3-Dimethyl-2-cyclopenten-1-one	PS
47	*	*		*	*		2.4	0.1	*3*	-24.0	2.0	*5*	1.7	0.4	*3*	-23.0	1.9	*6*	*	*		*	*		*	*		*	*		Dianhydrorhamnose	PS
50	0.1		*2*	-27.0		*2*	1.9	0.0	*2*	-34.3		*2*	1.2	0.2	*3*	-34.7	2.6	*3*	1.2	0.2	*4*	-28.5	3.5	*4*	1.2	0.2	*3*	-29.2	0.8	*5*	3- or 4-Methylphenol	alkylphenol
51													1.2	0.0	*2*	-22.0		*2*	1.9	0.2	*4*	-25.3	1.4	*4*	1.3	0.5	*3*	-27.5	0.9	*3*	2-Methoxyphenol	Lig
52	0.6		*1*	-22.4		*1*	1.4	0.1	*4*	-24.1	0.8	*3*	1.5	0.2	*3*	-25.4	0.4	*6*													Methyl-4-hydroxy-5,6-dihydro-2H-pyran-2-one	PS
54							0.9	0.0	*3*	-22.8	0.7	*3*	0.5	0.0	*1*	-23.4		*1*													3-Acetoxypyridine	Prot
55													0.5	0.1	*3*	-23.0	0.7	*6*	1.0	0.1	*3*	-22.2	0.9	*6*	1.1	0.0	*2*	-17.9		*2*	Levoglucosenone	PS
56	1.3		*1*	-23.3		*1*	0.6	0.2	*3*	-21.1	1.2	*3*	0.6	0.0	*1*	-23.9		*1*													Dimethylphenol	alkylphenol
58							0.1	0.0	*3*	-31.6	1.4	*3*																			Ethylphenol	alkylphenol
61													1.4	0.5	*3*	-19.0	1.2	*6*	2.0	0.0	*1*	-21.4	2.6	*3*							2-Methoxy-4-methylphenol	Lig
65							2.8	0.5	*4*	-27.1	1.2	*6*	3.1	0.4	*5*	-27.1	1.1	*8*	3.9	0.3	*4*	-27.4	0.6	*7*	1.5	0.9	*3*	-28.0	1.5	*3*	1-Dodecene	Lip
66	1.8		*1*	-28.4		*1*	2.2	0.6	*3*	-29.4	0.5	*4*	0.2	0.1	*3*	-29.7	0.8	*6*	3.2	0.0	*2*	-30.4	0.1	*3*							4-Vinylphenol	alkylphenol
67	2.9	2.7	*3*	-25.6	0.7	*3*	*	*		*	*		*	*		*	*		1.6	0.4	*3*	-26.4	2.8	*3*							5-Hydroxymethyl-2-furaldehyde	PS
69													1.0	0.2	*5*	-23.5	1.7	*8*	0.9	0.1	*3*	-25.7	1.9	*4*							Alkane/Alkene (T)	
73	1.1	1.0	*3*	-23.9	2.0	*3*																									Anhydroxylose	PS
74							*	*		*	*		1.8	1.2	*5*	-20.8	1.7	*8*	2.1	0.0	*2*	-22.6	1.1	*5*							4-Ethyl-2-methoxyphenol	Lig
77	0.5		*2*	-29.0		*2*	0.9	0.0	*2*	-28.1		*2*	0.1	0.0	*5*	-27.3	1.4	*6*													Isopropenylphenol	alkylphenol
78													1.5	0.4	*5*	-30.9	1.4	*8*	2.0	0.4	*4*	-30.5	1.0	*5*							4-Vinyl-2-methoxyphenol	Lig
81													0.9	0.3	*5*	-19.9	1.3	*8*													Unknown	
86	0.9	0.9	*3*	-24.4	0.3	*6*																									Unknown	
95																			1.2	0.0	*1*	-28.0		*1*							1-(4-Hydroxy-3-methoxyphenyl)-ethanone	Lig
98	1.2	1.1	*4*	-24.1	0.4	*4*	4.4	1.4	*4*	-24.1	0.7	*6*	5.7	1.6	*4*	-23.6	0.4	*8*	6.0	1.2	*4*	-22.4	1.1	*7*							Anhydropyranose	PS
101																			1.1	0.2	*4*	-32.3	0.8	*6*							Unknown	
102				-26.7		*1*	0.0	0.0	*2*	-33.1	1.0	*5*	0.0	0.0	*0*	-30.9	1.1	*3*													Unknown	

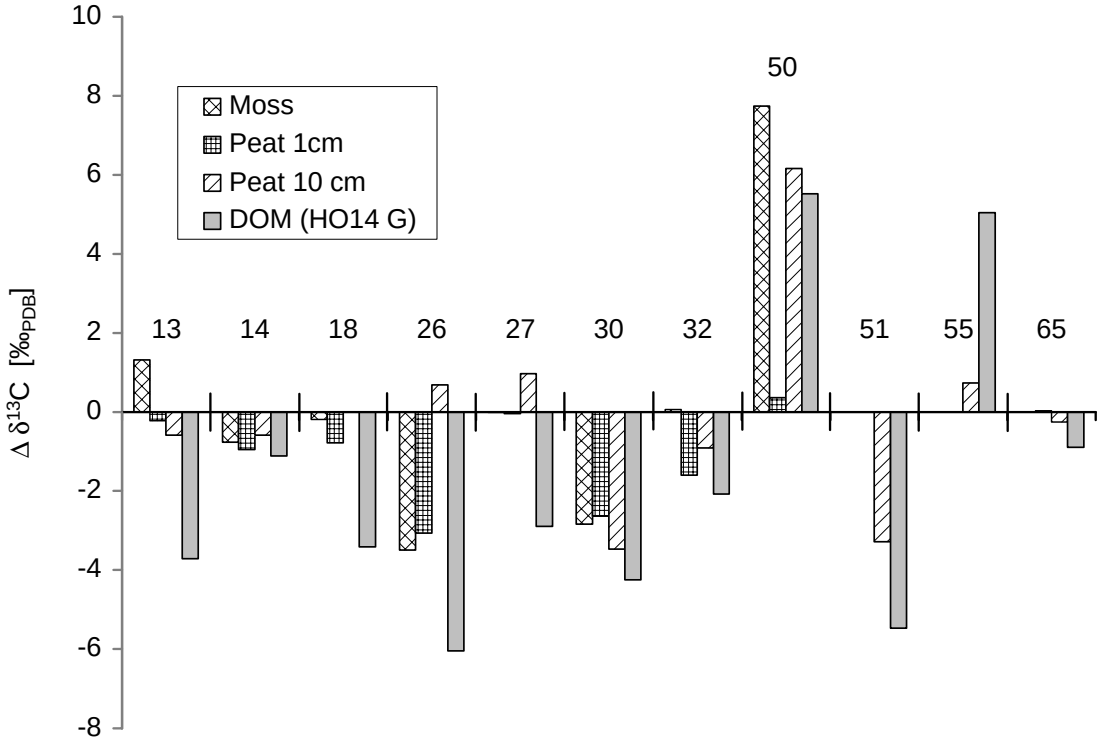

Figure 6.7: Shift of isotopic content in selected pyrolysis products. δ-values indicate an enrichment (positive values) or a depletion of ^{13}C (negative values) relative to the same pyrolysis products in peat at 5 cm depth. Numbers on top of the bars correspond to pyrolysis products listed in Table 6.2.

from the same source like the other two methoxylated forms. In fact, the comparably low δ-values suggest that both vinylphenolic compounds originate from another source. The pyrolysis product 4-isopropenylphenol (*77*), the biomarker for sphagnum acid (–29.0‰ in moss), could act as a precursor for 4-vinylphenol and thus explains its occurrence in the uppermost layers of the peat. However, a secondary methoxylation of 4-vinylphenol by microorganisms at 5 cm or during pyrolysis is unlikely. Furthermore, 4-isopropenylphenol is strongly depleted in the moss and at the first cm, yet in the peat at 5 cm the component is enriched by 1.7‰. This points to a subsequent biogeochemical conversion of this biomarker.

6.4.2 Pyrolysis products of DOM compared to peat

Isotope information on pyrolysis products can be employed to address the question of DOM formation, and possibly determine whether pyrolysis products from DOM are related to the peat. In contrast to the ^{13}C bulk isotope analyses, a significant difference between the DOM and the peat samples could be found by Py-GC/MS-IRMS. Of the substances studied, 21 in the DOM gave detectable isotope signals. 12 of those can be attributed to carbohydrates, four are pyrolysis products of lignin and the remaining five cannot be

clearly identified with respect to the precursor material except for 1-dodecene. Five compounds are exclusively detected in the DOM: dimethyl benzene (*19*) and ethylmethyl benzene (*40*) as lignin derived pyrolysis products and propenoic acid (*6*), methylacetyl furan (*43*), and dimethyl cyclopentenone (*44*) as carbohydrate markers. Pyrolysis products of carbohydrates in DOM are depleted in ^{13}C and clearly less abundant relative to the peat samples (Figure 6.6). Furthermore, the chromatogram of DOM is less complex (Figure 6.4). Biodegradation and photolysis of precursors are likely to cause a decrease in pyrolyzable biomolecules (Tranvik, 1998). However, $\delta^{13}C$ values of pyrolysis products in DOM indicate a different source for their precursors. The organic matter in DOM could be formed *in-situ* by microorganisms in the water. The potential of microorganisms to either enrich or deplete the isotopic composition of organic matter has been reported earlier (Macko and Estep, 1984; Macko et al., 1991; Claus et al., 1999). Oxygen depletion is a common feature in oligotrophic lakes and provides conditions for anaerobic microbial metabolism. Fermentative bacteria produce acetate, H_2 and CO_2 which supply the substrate for methanogenic bacteria. Most probably the depletion of ^{13}C in pyrolysis products of DOM is associated with the uptake of isotopically light compounds such as respired CO_2, CO_2 from oxidation of CH_4, or acetic acid (van der Meer et al., 1998; Schulten and Gleixner, 1999). Nevertheless, stronger evidence for these processes could be given by additional measurements and takings of different depths and locations.

7 Summary and conclusive aspects

7.1 Technical and methodological aspects

Investigations of complex and often diffuse (bio)chemical systems require a different analytical approach aimed at the detection of a wide range of compounds rather than a selective analysis of compounds. This requirement is especially true if no prior knowledge exists of the kind of compounds involved in the properties of such systems. The advantages of pyrolysis as a degradation technique for complex, polymeric organic material has already been addressed. Although the reactions during thermal fragmentation remain basically theoretical, they are highly reproducible and thus the method became applicable as a 'fingerprinting' analysis. In addition, it could be shown that the isotope values of pyrolysis products represent the isotopic differences known from their particular precursors, e.g. lignin and carbohydrates. Results from Py-GC/MS-IRMS of a C3- and a C4-sugar demonstrated that all pyrolysis products keep their natural isotopic difference of 9‰-13‰ (Figure 3.1). Thus, arbitrary isotope fractionation during pyrolysis can be ruled out and isotopic differences in identical pyrolysis products traced in a profile like at the Hohlohsee must indicate biogeochemical processes.

The most striking drawback, however, is that it is not possible to investigate the complete sample material. The uninvestigated portions remain with the carbonaceous residue in the pyrolysis tube and the condensation of non-volatile, relatively high molecular weight and polar compounds on the inner wall of the glass insert. High pyrolysis yields in material like the top *Sphagnum* moss layer suggest that fresh, less degraded organic matter is more easily pyrolyzed, probably due to a higher amount of reactive groups than compared with highly decomposed, condensed substances. Pyrolysis yields correlate well with the H:C ratios shown in the van Krevelen-diagram suggesting a decrease of pyrolyzed material with increasing aromatic proportions in the sample. The correlation of ^{13}C-NMR data and pyrolysis yields, however, indicated that the tar fraction precipitated on the walls of the glass liner is probably derived from aliphatic compounds and not from cellulose.

Comparable problems occur in samples with substances protected through associations with mineral colloids as is primarily the case in soil samples. Investigations on naturally labeled fields (C3-C4 vegetation change) using Py-GC/MS-IRMS demonstrated that the pyrolysis products comprise a pool of material with turnover times of up to 200 years (Gleixner et al., 1999; Gleixner et al., 2001). The old and for microbial respiration less favorable organic material thus evades from a closer investigation through the analytical system. This restricts investigations on the so-called millennium carbon pool which is an important component in estimating global carbon fluxes. The application of MS to large

biomolecules and synthetic polymers has been limited due to low volatility and thermal instability of these materials. New, recently developed soft ionization techniques such as electrospray ionization (ESI) or matrix assisted laser desorption/ionization (MALDI) coupled to high resolution MS, tandem MS (MS/MS), or time-of-flight (TOF) MS can be able to fill that gap.

Quality control and reproducibility have progressively evolved for the system used. Some of the major improvements since the set up of the Py-GC/MS-IRMS unit were the installation of a switch valve that regulated the carrier stream between pyrolysis unit and GC. This improved particularly the standard deviations of the peak area values. The introduction of external standard runs enabled early observations of shifts in isotope signals due to changes in the analytical conditions. The coupling of different analytical systems is always connected with a high effort of routine maintenance. System errors are likely to occur because the probability is multiplied by the number of devices coupled together. This also impedes maintaining identical analytical conditions for sample runs. So far, all experiments were started manually. The installation of a pyrolysis autosampler to reduce man-made inaccuracy failed to date because of severe memory effects and carryover problems

The complex nature of the investigated material leads to an extended amount of data. With respect to isotope data, this amount must be restricted to those peaks that deliver proper values. Not all of the remaining well-resolved pyrolysis products can be assigned to a distinct precursor molecule. Some are even derived from different sources and thus degrade the significance of the isotopic signal. Another limitation arose when well-resolved pyrolysis products were not the same in different samples thus impeding a comparison. A focussing on a selection of compound classes could limit the amount of data and thus increase the number of well-resolved peaks although sample pretreatment such as extraction procedures come along with the risk of contamination and a change in isotope ratios. Further improvement may be given by data analysis techniques. First applications of data reprocessing and pattern recognition have already been introduced for Py-MS analysis (Meuzelaar et al., 1982; Tas and Vandergreef, 1994). More recent developments in neural network applications are promising (Goodacre, 1994; Goodacre et al., 1996). Statistical evaluation was impeded in the present study because most appropriate procedures require a solid database of several sample runs. Further restrictions were given by an incomplete set of isotope data due to varying numbers of well-resolved peaks within the set of samples.

7.2 Research aspects

The presented results demonstrated the possibilities of a fast and easily applicable analytical method to source identification and biogeochemical processes as inferred from shifts in ^{13}C-signals. Main focus was lain on questions addressing the origin and genesis of DOM rather than obtaining structural information. Bulk isotope analyses have shown limitations when interpreting the formation of complex and heterogeneous mixtures such as DOM. Differences in composition as identifiable by natural isotopic differences of biopolymers may be masked. The comparison of fulvic acids from contrasting aquatic environments manifested the already known conclusion that the formation of humic substances strongly depends on the input organic matter. Furthermore, the similarity of several takings of DOM from the Hohlohsee system suggested that DOM formation processes recur if the ecological conditions remain constant. Pyrolysis behavior and ^{13}C-signals of several pyrolysis products indicate that portions of the DOM can be attributed to new production during early diagenetic stages. Further such detailed studies are required to confirm the reproducibility of the results in space and time and to answer the question if such processes can be assigned to other aquatic systems.

There is also isotopic indication of processes that occur in the humification of *Sphagnum* moss and peat. None of the processes could be distinctly assigned to specific compound classes and repeated measurements are required to support the findings, e.g. rapid degradation of carbohydrates or selective preservation of lipids. Another limitation arises from the use of relative amounts of pyrolysis products. This approach is sufficient for a comparison of samples such as the fulvic acids. The exact determination of processes in a depth sequence, however, requires a quantitative evaluation in absolute increase or decrease of a specific pyrolysis product in addition to the change in isotope signal. This problem can be overcome by the development of internal standards which causes difficulties to date in sample preparation, possible introduction of new carbon (i.e. contamination), and unpredictable interferences in pyrolytic reactions.

Substituted aromatics such as benzenes, phenols, and furans form the majority of pyrolysis products found in all samples. Interestingly, the amount of carbohydrate-derived pyrolysis products was high in most samples, only the FA of brown coal processing water were dominated by aromatic compounds indicating input from condensed organic matter of the lignites processed. Carbohydrates, however, are commonly considered labile and readily-degradable compounds. The evident occurrence of this class arises the question to what extent DOM is refractory. Refractory in the sense of unaffected (or less affected) by microbial degradation seems unlikely. In fact, the results from this study suggest that DOM, i.e. the fulvic acids, consists of different pools with varying age and reactivity depending on the source and genesis in each aquatic ecosystem. The very low signal of ^{14}C activity in the microbially active DOM of the brown coal processing water is a good hint at

the carbon source used by microbial activity. Microorganisms seem to introduce new carbon only to an insignificant amount and feed on the old organic matter. Evidence for the incessant change of organic matter was also given by the peat sequence. The combination of relative amounts and isotopic content of pyrolysis products indicates several processes that take place in humification. A better knowledge of the processes will eventually help to refine models for the soil carbon cycle. This could be particularly elemental if turnover processes for specific compound classes such as carbohydrates and lignins become quantifiable.

Some models for humic substance formation have been linked to the change in molecular weight. Two types have been discussed, one assuming the formation of humic substances by degradation of plant produced biopolymers (biopolymer degradation, BD), the other deducing the formation of larger structures from a condensation of small, enzymatically degraded molecules (abiotic condensation, AC) (Hatcher and Spiker, 1988; Hedges, 1988). Thus it has been reasoned that smaller fractions, i.e. fulvic acids, derive from humic acids (BD model) or fulvic acids condense/repolymerize to the larger humic acids (AC). Enrichments of ^{13}C in pyrolysis products from the comparison of the humic and a fulvic acid of the bog water DOM indicate that fulvic acids may be more strongly modified thus giving preference to the biopolymer degradation pathway. The condensation pathway, however, bases on the polymerization of aromatic molecules such as modified lignin structures, microbially synthesized polyphenols or their enzymatically oxidized products quinones. There is evidence for aromatic building blocks in all samples. Some lignin-derived pyrolysis products even indicate modifications by a strong enrichment of ^{13}C, i.e. phenol derivatives in the peat samples and in the FA fraction of the brown coal processing waste water (SV1 FA). Consent to the melanoidin model favored by marine scientist is also given. Even though pyrolysis products of amino acids were barely identified, there is indication of browning reaction products given by sugar-derived furans in all samples. The degradative analytical approach by Curie-point pyrolysis, however, impedes a clear conclusion on how the precursor compounds were linked to each other and to what extent pyrolysis products represent original structural building blocks.

7.2.1 Relevance to other research areas

Isotope signatures of pyrolysis products may have practical application in other fields. This has already been demonstrated for calculations of turnover times using naturally labeled organic matter (Gleixner et al., 1999; Gleixner et al., 2001). The clear isotopic difference of biomolecules produced from C3 and C4 plants is distinctly distinguishable by Py-GC/MS-IRMS. Pyrolysis products from C3 and C4 sugar have been found to differ between 11‰ and 17‰ thus easily exceeding the standard deviations encountered in the

present study. Another comparable investigation to the Hohlohsee study with respect to origin of DOM in swamp water was carried out by Lu et al. (2000). Using Py-GC/MS among other techniques, they concluded that swamp humic substances are derived from surrounding soils because humic substances from swamp water and from soil in the surrounding area of the swamp were identical. This corresponds to the results from the bog lake Hohlohsee in so far as that pyrolysis products in Hohlohsee-DOM were also found in the peat samples. Only indication by isotope signals revealed that different processes occur in the formation of DOM.

Another possible application for Py-GC/MS-IRMS is related to open questions about the fate of terrestrial organic carbon in the ocean (Hedges et al., 1997). The application of stable carbon isotopes of bulk samples in source studies includes several complications. Preferential assimilation or preservation of different biochemicals owing varying isotope signatures in individual organisms as well as C3 and C4 carbon may result in mixtures that isotopically resemble marine organic matter. Recent age determinations of riverine DOM and particulate organic matter proved that organic carbon entering the oceans is aged and degraded (Raymond and Bauer, 2001). This contrasts the general belief of young and relatively fresh organic carbon delivered to the oceans and asks for further investigations as dissolved organic carbon in the oceans is one of the biggest reservoirs in the global carbon cycle (Ludwig, 2001).

References

ABBT-BRAUN, G., SCHMIEDEL, U., FRIMMEL, F.H., 1990. Elemental Analysis of Isolated Fulvic Acids from Different Origin. Vom Wasser 75, 59-73.

ÅGREN, G.I., BOSATTA, E., BALESDENT, J., 1996. Isotope Discrimination during Decomposition of Organic Matter: A Theoretical Analysis. Soil Science Society of America Journal 60, 1121-1126.

AIKEN, G.R., 1985. Isolation and Concentration Techniques for Aquatic Humic Substances. In: Aiken, G. R., McKnight, D. M., Wershaw, R. L., McCarthy, P. (Eds.), Humic substances in soil, sediment, and water. Geochemistry, Isolation, and Characterization, 363-385. John Wiley, New York.

ARAVENA, R., WARNER, B.G., CHARMAN, D.J., BELYEA, L.R., MATHUR, S.P., DINEL, H., 1993. Carbon isotopic composition of deep carbon gases in an ombrogenous peatland, Northwestern Ontario, Canada. Radiocarbon 35(2), 271-276.

ARTINGER, R., BUCKAU, G., GEYER, S., FRITZ, P., WOLF, M., KIM, J.I., 2000. Characterization of groundwater humic substances: influence of sedimentary organic carbon. Applied Geochemistry 15(1), 97-116.

BALZER, A., GLEIXNER, G., GRUPE, G., SCHMIDT, H.L., SCHRAMM, S., TURBANJUST, S., 1997. In vitro decomposition of bone collagen by soil bacteria - the implications for stable isotope analysis in archaeometry. Archaeometry 39(Part 2), 415-429.

BENNER, R., FOGEL, M.L., SPRAGUE, E.K., HODSON, R.E., 1987. Depletion of ^{13}C in lignin and its implication for stable isotope studies. Nature 329, 708-710.

BLAIR, N., LEU, A., MUNOZ, E., OLSEN, J., KWONG, E., MARAIS, D.D., 1985. Carbon Isotopic Fractionation in Heterotrophic Microbial Metabolism. Applied and Environmental Microbiology 50(4), 996-1001.

BOCCHINI, P., GALLETTI, G.C., CAMARERO, S., MARTINEZ, A.T., 1997. Absolute Quantitation of Lignin Pyrolysis Products Using an Internal Standard. Journal of Chromatography 773(1-2), 227-232.

BÖTTCHER, J., STREBEL, O., KÖLLE, W., 1992. Redox Conditions and Microbial Sulfur Reactions in the Fuhrberger Feld Sandy Aquifer. In: Matthess, G., Frimmel, F. H., Hirsch, P., Schulz, H. D., Usdowski, E. (Eds.), Progress in Hydrogeochemistry. Springer-Verlag, Berlin, pp. 219-226.

BOON, J.J., GENUIT, W., VANDERVALK, F., DALLINGA, J., KORNIG, S.A., EISMA, D., 1985. Characterization of Particulate Organic-Matter from the Estuaries of the Eems, Rhine and Gironde by Pyrolysis-MS, Pyrolysis-MSMS, Pyrolysis-GCMS Techniques. Abstracts of Papers of the American Chemical Society 189(APR-), 44-GEOC.

BOUTTON, T.W., 1991. Stable Carbon Isotope Ratios of Natural Materials: II. Atmospheric, Terrestrial, Marine, and Freshwater Environments. In: Coleman, D.C., Fry, B. (Eds.), Carbon Isotope Techniques. Academic Press, San Diego, pp. 173-185.

BOUTTON, T.W., 1996. Stable Carbon Isotope Ratios of Soil Organic Matter and Their Use as Indicators of Vegetation and Climate Change. In: Boutton, T. W., Yamasaki, S.-i. (Eds.), Mass Spectrometry of Soils. Marcel Dekker, Inc., New York, pp. 47-82.

BRAND, W.A., 1996. High Precision Isotope Ratio Monitoring Techniques in Mass Spectrometry. Journal of Mass Spectrometry 31, 225-235.

BUCKAU, G., ARTINGER, R., GEYER, S., WOLF, M., FRITZ, P., KIM, J.I., 2000. Groundwater in-situ generation of aquatic humic and fulvic acids and the mineralization of sedimentary organic carbon. Applied Geochemistry 15(6), 819-832.

CLAUS, H., GLEIXNER, G., FILIP, Z., 1999. Formation of humic-like substances in mixed and pure cultures of aquatic microorganisms. Acta Hydrochimica et Hydrobiologica 27(4), 200-207.

COBAN-YILDIZ, Y., CHIAVARI, G., FABBRI, D., GAINES, A.F., GALLETTI, G., TUGRUL, S., 2000. The chemical composition of Black Sea suspended particulate organic matter: pyrolysis-GC/MS as a complementary tool to traditional oceanographic analyses. Marine Chemistry 69(1-2), 55-67.

CRAIG, H., 1957. Isotopic standards for carbon and oxygen and correction factors for mass spectrometric analysis of carbon dioxide. Geochimica et Cosmochimica Acta 12, 133-149.

DA CUNHA, L.C., SERVE, L., GADEL, F., BLAZI, J.L., 2000. Characterisation of riverine particulate organic matter by pyrolysis-gas chromatography-mass spectrometry. The Science of the Total Environment 256(2-3), 191-204.

DEGENS, E.T., 1969. Biogeochemistry of Stable Isotopes. In: Eglinton, G., Murphy, M. T. J. (Eds.), Organic Geochemistry - Methods and Results. Springer-Verlag, New York, pp. 304-329.

DEINES, P., 1980. The isotopic composition of reduced organic carbon. In: Fritz, P., Fontes, J. C. (Eds.), Handbook of Environmental Isotope Geochemistry, Volume 1 - The Terrestrial Environment, A, 1. Elsevier, Amsterdam, pp. 329-406.

DELEEUW, J.W., HATCHER, P.G., 1992. A Chemical Structure For Humic Substances - Reply. Naturwissenschaften 79(7), 331-331.

DENIRO, M.J., EPSTEIN, S., 1978. Influence of diet on the distribution of carbon isotopes in animals. Geochimica et Cosmochimica Acta 42, 495-506.

DURIG, J.R., CALVERT, G.D., ESTERLE, J.S., 1991. Particle Size Fraction and Downhole Depositional Trends of a Tropical Domed Peat Deposit as Determined by Pyrolysis GC / FT-IR / FID and Pyrolysis GC / MS. Journal of Analytical and Applied Pyrolysis 18, 293-324.

EPSTEIN, S., YAPP, C.J., HALL, J.H., 1976. Determination of the D/H ratios of non-exchangeable hydrogen in cellulose extracted from aquatic and land plants. Earth and Planetary Science Letters 30, 241-251.

ERTEL, J.R., HEDGES, J.I., 1984. The lignin component of humic substances: Distribution among soil and sedimentary humic, fulvic, and base-insoluble fractions. Geochimica et Cosmochimica Acta 48(10), 2065-2074.

ESTEP, M.E., HOERING, T.C., 1980. Biogeochemistry of the stable hydrogen isotopes. Geochimica et Cosmochimica Acta 44, 1197-1206.

ESWARAN, H., VANDENBERG, E., REICH, P., 1993. Organic-Carbon in Soils of the World. Soil Science Society of America Journal 57(1), 192-194.

FARQUHAR, G.D., EHLERINGER, J.R., HUBICK, K.T., 1989. Carbon isotope discrimination and photosynthesis. Annual Review of Plant Physiology and Plant Molecular Biology 40, 503-537.

FLAIG, W., 1988. Generation of Model Chemical Precursors. In: Frimmel, F. H., Christman, R. F. (Eds.), Humic Substances and Their Role in the Environment, 41. John Wiley & Sons, Chichester, pp. 75-92.

FLYNN, J.H., FLORIN, R.E., 1985. Degradation and Pyrolysis Mechanisms. In: Liebman, S. A., Levy, E. J. (Eds.), Pyrolysis and GC in Polymer Analysis, 29. Marcel Dekker, Inc., New York, pp. 149-208.

FRIMMEL, F.H., 1990. Characterization of Organic Acids in Freshwater: A Current Status and Limitations. In: Perdue, E. M., Gjessing, E. T. (Eds.), Organic Acids in Aquatic Ecosystems, 48. John Wiley & Sons, Chichester, pp. 5-23.

FRIMMEL, F.H., ABBT-BRAUN, G., 1999. Basic characterization of reference NOM from Central Europe - Similarities and differences. Environment International 25(2-3), 191-207.

GLEIXNER, G., BOL, R., BALESDENT, J., 1999. Molecular insight into soil carbon turnover. Rapid Communications in Mass Spectrometry 13(13), 1278-1283.

GLEIXNER, G., DANIER, H.J., WERNER, R.A., SCHMIDT, H.-L., 1993. Correlations between the ^{13}C Content of Primary and Secondary Plant Products in Different Cell Compartments and That in Decomposing Basidomycetes. Plant Physiology 102, 1287-1290.

GLEIXNER, G., POIRIER, N., BOL, R., BALESDENT, J., 2001. Molecular dynamics of organic matter in a cultivated soil. Organic Geochemistry, in review.

GLEIXNER, G., SCHMIDT, H.-L., 1998. On-Line Determination of Group-Specific Isotope Ratios in Model Compounds and Aquatic Humic Substances by Coupling Pyrolysis to GC-C-IRMS. In: Stankiewicz, B. A., Van Bergen, P. F. (Eds.), Nitrogen-Containing Macromolecules in the Bio- and Geosphere, 707, Washington, DC, pp. 34-46.

GONZÁLEZ-VILA, F.J., LANKES, U., LÜDEMANN, H.D., 2001. Comparison of the information gained by pyrolytic techniques and NMR spectroscopy on the structural

features of aquatic humic substances. Journal of Analytical & Applied Pyrolysis 58, 349-359.

GOODACRE, R., 1994. Characterisation and Quantification of Microbial Systems Using Pyrolysis Mass Spectrometry: Introducing Neural Networks to Analytical Pyrolysis. Microbiology Europe 2(2), 16-22.

GOODACRE, R., NEAL, M.J., KELL, D.B., 1996. Quantitative Analysis of Multivariate Data Using Artificial Neural Networks - a Tutorial Review and Applications to the Deconvolution of Pyrolysis Mass Spectra. Zentralblatt für Bakteriologie - International Journal of Medical Microbiology Virology Parasitology & Infectious Diseases 284(4), 516-539.

GÖTTLICH, K., 1990. Moor- und Torfkunde. Schweizerbart'sche Verlagsbuchhandlung, Stuttgart.

HAIDER, K., 1996. Biochemie des Bodens. Enke Verlag, Stuttgart.

HARTGERS, W.A., DAMSTE, J.S.S., DE LEEUW, J.W., 1994. Geochemical Significance of Alkylbenzene Distributions in Flash Pyrolysates of Kerogens, Coals, and Asphaltenes. Geochimica et Cosmochimica Acta 58, 1759-1775.

HATCHER, P.G., SPIKER, E.C., 1988. Selective Degradation of Plant Biomolecules. In: Frimmel, F. H., Christman, R. F. (Eds.), Humic Substances and Their Role in the Environment, 41. John Wiley & Sons, Chichester, pp. 59-74.

HAYES, J.M., FREEMAN, K.H., POPP, B.N., HOHAM, C.H., 1990. Compound-Specific Isotopic Analyses - a Novel Tool For Reconstruction of Ancient Biogeochemical Processes. Organic Geochemistry 16(4-6), 1115-1128.

HAYES, M.H.B., 1998. Humic Substances: Progress Towards More Realistic Concepts of Structure. In: Davies, G., Ghabbour, E. A., Khairy, K. A. (Eds.), Humic Substances - Structures, Properties and Uses, Spec. Publ. 228. The Royal Society of Chemistry, Cambridge, pp. 1-27.

HAYES, M.H.B., MACCARTHY, P., MALCOLM, R.L., SWIFT, R.S., 1989. Humic Substances II - In Search of Structure. In. John Wiley & Sons, Chichester, pp. 764.

HEDGES, J.I., 1988. Polymerization of Humic Substances in Natural Environments. In: Frimmel, F. H., Christman, R. F. (Eds.), Humic Substances and Their Role in the Environment, 41. John Wiley & Sons, Chichester, pp. 45-58.

HEDGES, J.I., KEIL, R.G., BENNER, R., 1997. What Happens to Terrestrial Organic Matter in the Ocean? Organic Geochemistry 27(5-6), 195-212.

HESSEN, D.O., TRANVIK, L.J., 1998. Aquatic Humic Matter: from Molecular Structure to Ecosystem Stability. In: Hessen, D. O., Tranvik, L. J. (Eds.), Aquatic Humic Substances, 133. Springer, Berlin, pp. 333-342.

HUANG, Y., EGLINTON, G., VAN DER HAGE, E.R.E., BOON, J.J., BOL, R., INESON, P., 1998. Dissolved organic matter and its parent organic matter in grass upland soil horizons

studied by analytical pyrolysis techniques. European Journal of Soil Science 49(1), 1-15.

IRWIN, W.I., 1982. Analytical Pyrolysis. Marcel Dekker, Inc., New York.

JAHNEL, J.B., ILIEVA, P., ABBT-BRAUN, G., FRIMMEL, F.H., 1998. Amino Acids and Carbohydrates in Refractory Organic Acids. Vom Wasser 90, 205-216.

JOLY, H.A., LI, H.B., BELZILE, N., 2000. Pyrolysis gas chromatography - mass spectrometry of humic substances extracted from Canadian lake sediments. Canadian Journal of Chemistry 78(1), 51-63.

KAISER, K., GUGGENBERGER, G., ZECH, W., 1996. Sorption of DOM and DOM fractions to forest soils. Geoderma 74(3-4), 281-303.

KÖLLE, W., 1993. Huminstoffe - Erfolge und offene Fragen der Wasserversorgungspraxis. In: Frimmel, F. H., Abbt-Braun, G. (Eds.), Refraktäre organische Säuren in Gewässern - Ergebnisse eines Rundgesprächs am 2. und 3. Juli 1990, XII. VCH, Weinheim, pp. 107-118.

KRACHT, O., GLEIXNER, G., 2000. Isotopic analysis of pyrolysis products from *Sphagnum* peat and dissolved organic matter from bog water. Organic Geochemistry 31(7-8), 645-654.

LAJTHA, K., MARSHALL, J.D., 1994. Sources of variation in the stable isotopic composition of plants. In: Lajtha, K., Michener, R. H. (Eds.), Stable Isotopes in Ecology and Environmental Sciences. Blackwell Scientific Publications, Oxford, pp. 1-21.

LANKES, U., 2001. Festkörper-NMR-Spektroskopie zur Charakterisierung von refraktären organischen Säuren in Gewässern. Dissertation, Naturwissenschaftliche Fakultät III Biologie und vorklinische Medizin. Universität Regensburg, Regensburg, pp. 249.

LANKES, U., LÜDEMANN, H.-D., 2001. Structural Characterization of Refractory Organic Substances by Solid State High-Resolution ^{13}C and ^{15}N Nuclear Magnetic Resonance. In: Frimmel, F. H., Abbt-Braun, G. (Eds.), Refractory Organic Substances (ROS) in the Environment, in press. John Wiley & Sons, Chichester.

LEAVITT, S.W., LONG, A., 1986. Stable-carbon isotope variability in tree foliage and wood. Ecology 67(4), 1002-1010.

LEWIS, N.G., DAVIN, L.B., SARKANEN, S., 1999. The Nature and Function of Lignins. In: Pinto, M. B. (Ed.) Carbohydrates and Their Derivatives Including Tannins, Cellulose, and Related Lignins, 3. Elsevier, Amsterdam, pp. 618-745.

LICHTFOUSE, E., CHENU, C., BAUDIN, F., LEBLOND, C., DA SILVA, M., BEHAR, F., DERENNE, S., LARGEAU, C., WEHRUNG, P., ALBRECHT, P., 1998. A Novel Pathway of Soil Organic Matter Formation By Selective Preservation of Resistant Straight-Chain Biopolymers - Chemical and Isotope Evidence. Organic Geochemistry 28(6), 411-415.

LU, X.Q., HANNA, J.V., JOHNSON, W.D., 2000. Source indicators of humic substances: an elemental composition, solid state C-13 CP/MAS NMR and Py-GC/MS study. Applied Geochemistry 15(7), 1019-1033.

LUDWIG, W., 2001. Carbon cycle - The age of river carbon. Nature 409(6819), 466-467.

LUKE, B.G., 1973. Pyrolysis-Gas Chromatography of Coumarone-Indene and Cyclopentadiene Resins. Journal of Chromatographic Science 11(8), 435-438.

MACKO, S.A., ENGEL, M.H., HARTLEY, G., HATCHER, P., HELLEUR, R., JACKMAN, P., SILFER, J., 1991. Isotopic compositions of individual carbohydrates as indicators of early diagenesis of organic matter. Chemical Geology 93, 147-161.

MACKO, S.A., ENGEL, M.H., PARKER, P.L., 1993. Early Diagenesis of Organic Matter in Sediments. In: Engel, M. H., Macko, S. A. (Eds.), Organic Geochemistry - Principles and Application, 11. Plenum Press, New York, pp. 211-224.

MACKO, S.A., ESTEP, M.L.F., 1984. Microbial alteration of stable nitrogen and carbon isotopic composition of organic matter. Organic Geochemistry 6, 787-790.

MACKO, S.A., HELLEUR, R., HARTLEY, G., JACKMAN, P., 1990. Diagenesis of organic matter - a study using stable isotopes of individual carbohydrates. Organic Geochemistry 16, 1129-1137.

MALCOLM, R.L., 1990. Variations Between Humic Substances Isolated from Soils, Stream Waters, and Groundwaters as Revealed by ^{13}C-NMR Spectroscopy. In: MacCarthy, P., Clapp, C. E., Malcolm, R. L., Bloom, P. R. (Eds.), Humic Substances in Soil and Crop Sciences: Selected Readings. American Society of Agronomy, Madison, pp. 13-35.

MANTOURA, R.F.C., RILEY, J.P., 1975. Analytical Concentration of Humic Substances From Natural Waters. Analytica Chimica Acta 76(1), 97-106.

MARTÍNEZ, A.T., CAMARERO, S., GUTIÉRREZ, A., BOCCHINI, P., GALLETTI, G.C., 2001. Studies on wheat lignin degradation by Pleurotus species using analytical pyrolysis. Journal of Analytical & Applied Pyrolysis 58, 401-411.

MAYER, B., FEGER, K.H., GIESEMANN, A., JÄGER, H.J., 1995. Interpretation of Sulfur Cycling in Two Catchments in the Black Forest (Germany) Using Stable Sulfur and Oxygen-Isotope Data. Biogeochemistry 30(1), 31-58.

MCKINNEY, C.R., MCCREA, J.M., EPSTEIN, S., ALLEN, H.A., UREY, H.C., 1950. Improvements in mass spectrometers for the measurements of small differences in isotope abundance ratios. Review of Scientific Instruments 21, 724-730.

MCKNIGHT, D.M., AIKEN, G.R., 1998. Sources and Age of Aquatic Humus. In: Hessen, D. O., Tranvik, L. J. (Eds.), Aquatic Humic Substances, 133. Springer, Berlin, pp. 9-39.

MEUZELAAR, H.L.C., HAVERKAMP, J., HILEMAN, F.D., 1982. Pyrolysis Mass Spectrometry of Recent and Fossil Biomaterials - Compendium and Atlas. Elsevier, Amsterdam.

MIYAJIMA, T., WADA, E., HANBA, Y.T., VIJARNSORN, P., 1997. Anaerobic Mineralization of Indigenous Organic Matters and Methanogenesis in Tropical Wetland Soils. Geochimica et Cosmochimica Acta 61(17), 3739-3751.

MOLDOVEANU, S.C., 1998. Analytical Pyrolysis of Natural Organic Polymers. Elsevier, Amsterdam.

NADELHOFFER, K.J., FRY, B., 1994. Nitrogen isotope studies in forest ecosystems. In: Lajtha, K., Michener, R. H. (Eds.), Stable Isotopes in Ecology and Environmental Sciences. Blackwell Scientific Publications, Oxford, pp. 22-44.

NIP, M., DELEEUW, J.W., SCHENCK, P.A., MEUZELAAR, H.L.C., GIVEN, P.H., 1984. Curie-Point-Py-MS and Curie-Point-Py-GC-MS as Analytical Tools to Identify Substructures of Bio-Polymers, Lignites and Coals. Fresenius Zeitschrift für Analytische Chemie 318(6), 444-445.

PERDUE, E.M., 1984. Analytical Constraints on the Structural Features of Humic Substances. Geochimica et Cosmochimica Acta 48(7), 1435-1442.

POSTHUMUS, M.A., NIBBERING, N.M.M., BOERBOOM, A.J.H., SCHULTEN, H.R., 1974. Pyrolysis Mass-Spectrometric Studies On Nucleic-Acids. Biomedical Mass Spectrometry 1(5), 352-357.

POUWELS, A.D., EIJKEL, G.B., BOON, J.J., 1989. Curie-Point Pyrolysis Capillary Gas-Chromatography High-Resolution Mass-Spectrometry of Microcrystalline Cellulose. Journal of Analytical and Applied Pyrolysis 14(4), 237-280.

RALPH, J., HATFIELD, R.D., 1991. Pyrolysis-GC-MS Characterization of Forage Materials. Journal of Agricultural and Food Chemistry 39(8), 1426-1437.

RAYMOND, P.A., BAUER, J.E., 2001. Riverine export of aged terrestrial organic matter to the North Atlantic Ocean. Nature 409(6819), 497-500.

RIELEY, G., 1994. Derivatization of Organic-Compounds Prior to Gas-Chromatographic Combustion-Isotope Ratio Mass-Spectrometric Analysis - Identification of Isotope Fractionation Processes. Analyst 119(5), 915-919.

SAIZ-JIMENEZ, C., 1994. Analytical Pyrolysis of Humic Substances - Pitfalls, Limitations, and Possible Solutions. Environmental Science & Technology 28(11), 1773-1780.

SAIZ-JIMENEZ, C., 1996. The Chemical Structure of Humic Substances: Recent Advances. In: Piccolo, A. (Ed.), Humic Substances in Terrestrial Ecosystems. Elsevier, Amsterdam, pp. 1-44.

SAIZ-JIMENEZ, C., DELEEUW, J.W., 1986. Lignin Pyrolysis Products - Their Structures and Their Significance as Biomarkers. Organic Geochemistry 10(4-6), 869-876.

SCHLEUCHER, J., 1998. Intramolecular Deuterium Distributions and Plant Growth Conditions. In: Griffiths, H. (Ed.), Stable Isotopes: Integration in Biological, Ecological and Geochemical Processes. βIOS Scientific Publisher, Oxford, pp. 63-73.

SCHMIDT, H.-L., BUTZENLECHNER, M., ROSSMANN, A., SCHWARZ, S., KEXEL, H., KEMPE, K., 1993. Inter- and intramolecular isotope correlations in organic compounds as criterion for authenticity identification and origin assignment. Zeitschrift für Lebensmittel Untersuchung und Forschung 196, 105-110.

SCHMIDT, H.-L., KEXEL, H., BUTZENLECHNER, M., SCHWARZ, S., GLEIXNER, G., THIMET, S., WERNER, R.A., GENSLER, M., 1995. Non-statistical isotope distribution in natural compounds: Mirror of their biosynthesis and key for their origin assignment. In: Wada,

E., Yoneyama, T., Minagawa, M., Ando, T., Fry, B. D. (Eds.), Stable Isotopes in the Biosphere. Kyoto University Press, Kyoto, pp. 17-35.

SCHMIDT, H.-L., VOERKELIUS, S., AMBERGER, A., 1992. Nitrogen and Oxygen Isotopes as Indicators for Nitrification and Denitrification. In: Matthess, G., Frimmel, F. H., Hirsch, P., Schulz, H. D., Usdowski, E. (Eds.), Progress in Hydrogeochemistry. Springer-Verlag, Berlin, pp. 212-219.

SCHULTEN, H.R., 1987. Pyrolysis and Soft Ionization Mass-Spectrometry of Aquatic-Terrestrial Humic Substances and Soils. Journal of Analytical and Applied Pyrolysis 12(2), 149-186.

SCHULTEN, H.R., 1999. Analytical pyrolysis and computational chemistry of aquatic humic substances and dissolved organic matter. Journal of Analytical and Applied Pyrolysis 49(1-2), 385-415.

SCHULTEN, H.-R., GLEIXNER, G., 1999. Analytical pyrolysis of humic substances and dissolved organic matter in aquatic systems: Structure and origin. Water Research 33(11), 2489-2498.

SCHULTEN, H.R., PLAGE, B., SCHNITZER, M., 1991. A Chemical Structure For Humic Substances. Naturwissenschaften 78(7), 311-312.

SMITH, B.N., ZIEGLER, H., 1990. Isotopic Fractionation of Hydrogen in Plants. Botanica Acta 103(4), 335-342.

SPIKER, E.C., HATCHER, P.G., 1987. The Effects of Early Diagenesis On the Chemical and Stable Carbon Isotopic Composition of Wood. Geochimica et Cosmochimica Acta 51(6), 1385-1391.

STANKIEWICZ, B.A., HUTCHINS, J.C., THOMSON, R., BRIGGS, D.E.G., EVERSHED, R.P., 1997a. Assessment of Bog-body Tissue Preservation by Pyrolysis-Gas Chromatography/Mass Spectrometry. Rapid Communications in Mass Spectrometry 11(17), 1884-1890.

STANKIEWICZ, B.A., KRUGE, M.A., MASTALERZ, M., 1996. A Geochemical Study of Macerals From a Miocene Lignite and an Eocene Bituminous Coal, Indonesia. Organic Geochemistry 24(5), 531-545.

STANKIEWICZ, B.A., MASTALERZ, M., KRUGE, M.A., VAN BERGEN, P.F., SADOWSKA, A., 1997b. A comparative study of modern and fossil cone scales and seeds of conifers: A geochemical approach. New Phytologist 135(2), 375-393.

STANKIEWICZ, B.A., VAN BERGEN, P.F., SMITH, M.B., CARTER, J.F., BRIGGS, D.E.G., EVERSHED, R.P., 1998. Comparison of the analytical performance of filament and Curie- point pyrolysis devices. Journal of Analytical and Applied Pyrolysis 45(2), 133-151.

STERNBERG, L.S.L., 1989. Oxygen and Hydrogen Isotope Ratios in Plant Cellulose: Mechanisms and Applications. In: Rundel, P. W., Ehleringer, J. R., Nagy, K. A. (Eds.), Stable Isotopes in Ecological Research, 68. Springer-Verlag, Berlin, pp. 124-141.

STEVENSON, F.J., 1994. Humus Chemistry - Genesis, Composition, Reactions. John Wiley & Sons, Inc., New York.

STOUT, S.A., BOON, J.J., SPACKMAN, W., 1988. Molecular aspects of the peatification and early coalification of angiosperm and gymnosperm woods. Geochimica et Cosmochimica Acta 52, 405-414.

TAS, A.C., VANDERGREEF, J., 1994. Mass Spectrometric Profiling and Pattern Recognition. Mass Spectrometry Reviews 13(2), 155-181.

TRANVIK, L.J., 1998. Degradation of Dissolved Organic Matter in Humic Waters by Bacteria. In: Hessen, D. O., Tranvik, L. J. (Eds.), Aquatic Humic Substances, 133. Springer, Berlin, pp. 259-283.

TSUGE, S., MARSUBARA, H., 1985. High-resolution pyrolysis-gas chromatography of proteins and related materials. Journal of Analytical and Applied Pyrolysis 8, 49-64.

VAN DER HEIJDEN, E., BOON, J.J., RASMUSSEN, S., RUDOLPH, H., 1997. Sphagnum Acid and its Decarboxylation Product Isopropenylphenol as Biomarkers for Fossilised *Sphagnum* in Peats. Ancient Biomolecules 1(2), 93-107.

VAN DER KAADEN, A., HAVERKAMP, J., BOON, J.J., DE LEEUW, J.W., 1983. Analytical pyrolysis of carbohydrates. I. Chemical interpretation of matrix influences on pyrolysis-mass spectra of amylose using pyrolysis-gas chromatography-mass spectrometry. Journal of Analytical and Applied Pyrolysis 5(3), 199-220.

VAN DER MEER, M.T.J., SCHOUTEN, S., SINNINGHE DAMSTÉ, J.S., 1998. The effect of the reversed tricarboxylic acid cycle on the ^{13}C contents of bacterial lipids. Organic Geochemistry 28(9/10), 527-533.

VAN HEEMST, J.D.H., MEGENS, L., HATCHER, P.G., DE LEEUW, J.W., 2000. Nature, origin and average age of estuarine ultrafiltered dissolved organic matter as determined by molecular and carbon isotope characterization. Organic Geochemistry 31(9), 847-857.

VAN HEEMST, J.D.H., VAN BERGEN, P.F., STANKIEWICZ, B.A., DE LEEUW, J.W., 1999. Multiple sources of alkylphenols produced upon pyrolysis of DOM, POM and recent sediments. Journal of Analytical and Applied Pyrolysis 52, 239-256.

VAN KREVELEN, D.W., 1993. Coal -Typology, Physics, Chemistry, Constitution. Elsevier, Amsterdam.

VAN SMEERDIJK, D.G., BOON, J.J., 1987. Characterisation of subfossil *Sphagnum* leaves, rootlets of Ericaceae and their peat by pyrolysis-high-resolution gas chromatography-mass spectrometry. Journal of Analytical and Applied Pyrolysis 11, 377-402.

WERNER, R.A., BRAND, W.A., 2001. Referencing strategies and techniques in stable isotope ratio analysis. Rapid Communications in Mass Spectrometry 15(7), 501-519.

WHELAN, J.K., THOMPSON-RIZER, C.L., 1993. Chemical Methods for Assessing Kerogen and Protokerogen Types and Maturity. In: Engel, M. H., Macko, S. A. (Eds.), Organic Geochemistry - Principles and Applications, 11. Plenum Press, New York, pp. 289-353.

WHITE, J.W.C., 1989. Stable Hydrogen Isotope Ratios in Plants: A Review of Current Theory and Some Potential Applications. In: Rundel, P. W., Ehleringer, J. R., Nagy, K. A. (Eds.), Stable Isotopes in Ecological Research, 68. Springer-Verlag, Berlin, pp. 142-162.

WIEßNER, A., KUSCHK, P., WEIßBRODT, E., STOTTMEISTER, U., PÖRSCHMANN, J., KOPINKE, F.-D., 1993. Charakterisierung des Wassers und des Sedimentes einer Braunkohle-Schwelwasserdeponie. Wasser-Abwasser-Praxis 6, 375-379.

ZEGOUAGH, Y., DERENNE, S., LARGEAU, C., BERTRAND, P., SICRE, M.A., SALIOT, A., ROUSSEAU, B., 1999. Refractory organic matter in sediments from the North-West African upwelling system: abundance, chemical structure and origin. Organic Geochemistry 30(2-3), 101-117.

ZIEGLER, H., 1989. Hydrogen Isotope Fractionation in Plant Tissues. In: Rundel, P. W., Ehleringer, J. R., Nagy, K. A. (Eds.), Stable Isotopes in Ecological Research, 68. Springer-Verlag, Berlin, pp. 105-123.

ACKNOWLEDGEMENT

First of all, I owe great thanks to my supervisor Gerd Gleixner who provided the topic and shared his wealth of knowledge with me. He was also available for fruitful and extensive discussions at any time and inspired several new approaches and experiments.

Prof. Dr. G. Büchel from the Institut für Geowissenschaften, Friedrich-Schiller-Universität, Jena, deserves thank for his co-operation and collaborative obligingness and the time he sacrificed for an external PhD-student.

I am also grateful to Prof. Dr. Dr. F. H. Frimmel and Dr. G. Abbt-Braun, who seamlessly guided the ROSIG-Program. They supervised sampling and sample preparation of the ROSIG reference material. Much of this work was done by Axel Heidt.

The lab work was greatly facilitated and enhanced by the experience and help of Steffen Rühlow and many advice on mass spectrometers by Willi Brand, Roland Werner and their staff B. Rothe, S. Bräunlich, and H. Geilmann. They were also in charge with the bulk isotope measurements. Bulk elemental analyses were performed by I. Hilke. Thank you.

First steps in gas-isotope ratio-mass spectrometry were taken under the guidance of Prof. Dr. H.-R. Schulten of the Institut für Bodenkunde, Universität Rostock, and his team. Dr. G. Jandl introduced me into the techniques of Py-GC/MS. Thank you for the time in Rostock. Dr. Klaus Kaiser and Ulrich Lankes, are gratefully acknowledged on behalf of all other scientists of the ROSIG-program who provided helpful information on the samples and sampling parameters.

Besides the other MPI working group members Christiane Kramer, Jan Rothe and, for too short a time, Natacha Poirier, who contributed to a productive and entertaining atmosphere and intense discussions, there are two persons of the Max-Planck-Institute that deserve particular mentioning: Ali Telz helped a great deal in sample preparation and Dr. Karen Kohfeld's comments on the manuscript played an important role in improving it, not only for the English language. Special thanks also to Jens Radke - the only other geologist in the institute! - for spending technically-inspiring hours of tackling GC-IRMS problems in the lab and with a few beers afterwards.

A personal thanks goes to Ike who gave her consent to letting me go to Jena for three years and thus provided the basis for a solid and continual weekend-relationship during this period.

This work was funded by the Deutsche Forschungsgemeinschaft (DFG), Bonn-Bad Godesberg (Gl 1-5 and Gl 1-6). A perfect scientific working environment, instrumental equipment and administrative support was provided by the Max-Planck-Gesellschaft.

Ich erkläre, dass ich die vorliegende Arbeit selbständig und nur unter Verwendung der angegebenen Hilfsmittel und Literatur angefertigt habe.

Jena, 04.06.2001

Curriculum Vitae

Name : K R A C H T, Oliver
Geburtsdatum : 08. Mai 1967 in Frankfurt/Main

1973-77	Grundschule in Bonn
1977-86	Gymnasium
1986	Abiturabschluss
1988-89	Studium an der Rhein. Friedrich-Wilhelms-Universität, Bonn, Fachbereich: Geologie/Paläontologie
1989-97	Universität Hannover Fachbereich: Geologie/Paläontologie
Dezember 1991	Vordiplom
1992-93	Studium ("graduate study") an der University of Nevada, Reno, Department of Geological Sciences, Mackay School of Mines
Februar 1997	Abschluss des Studiums als Diplom-Geologe
Mai – August 1997	Praktikum und geologische Tätigkeiten bei Fa. GEO-data, Dienstleistungsgesellschaft für Geologie, Hydrologie und Umweltanalytik
Oktober 1997 – März 1998	Forschungsaufenthalt an der Australian National University, Canberra
Mai 1998 – Juni 1998	zweimonatige Einstellung bei der Fa. GEO-data
September 1998 – Juli 2001	Anfertigung der Dissertation am Max-Planck-Institut für Biogeochemie, Jena

Appendix I

Basic data set used for statistical evaluation (multidimensional scaling) of ROSIG samples (see Section 5.5 for results).

	Bulk isotope data			Elemental analysis [1]				Integration of ^{13}C spectra from CPMAS-NMR [2]			
	δ^2H	$\delta^{13}C$	$\delta^{15}N$	H	C	N	O	S	Carbonyl groups	Carboxyl groups	Aromatic C	Aliphatic C
	‰	‰	‰	%	%	%	%	%	%	%	%	%
HO10 FA	-96.4	-26.6	-4.7	3.66	52.71	0.66	41.45	0.69	3.6	16.5	36.0	17.8
HO13 FA	-87.7	-26.7	-12.3	3.95	52.92	0.68	38.20	0.01	3.4	15.0	36.4	20.4
HO14 FA	-101.8	-26.7	-4.4	4.07	53.02	0.62	41.51	0.00	3.3	15.6	35.5	19.4
HO16 FA	-102.0	-26.6	-5.1	4.10	52.69	0.89	40.28	0.00	3.4	16.6	35.8	18.8
ABV2 FA	-82.8	-26.2	0.3	5.03	50.58	2.92	33.20	0.00	1.9	13.7	26.9	32.2
ABV3 FA	-87.7	-27.3	-0.1	5.16	52.36	2.18	32.89	2.60	1.9	13.4	27.6	31.8
BS1 FA	-56.8	-26.1	7.3	3.62	53.30	1.06	41.80	0.00	2.7	15.0	33.7	19.6
FG1 FA	-144.2	-27.7	-4.1	4.85	55.62	1.43	31.85	1.62	3.3	14.4	23.7	32.3
SV1 FA	-73.8	-24.3	24.8	3.95	50.99	1.80	25.57	9.51	3.6	12.6	37.4	27.7

1) Data from Abbt-Braun (unpublished).

2) Data from Lankes & Lüdemann (2001).

Appendix II

The tables list all pyrolysis products found in the ROSIG samples. The numbers refer to the numbers in the text. Relative amount (% area) and $\delta^{13}C$ values (‰) of pyrolysis products from dissolved organic matter (DOM), isolated fulvic acids (FA) and humic acids (HA) from bog lake water (HO14). Standard deviations (s.d.) as well as number of replicates (*n*) are given. Values are rounded: s.d.=0.0 means <0.05; _ means less than three replicates. (T) stands for tentative identification. The number of replicates can vary with analytical conditions due to detection thresholds. Missing data indicate peak below detection threshold in all runs. ∗ means peak detectable but no reliable isotope signal or area value determined because of co-elution.

	HO10 FA				HO13 FA				HO14 FA				HO16 FA				BS1 FA				FG1 FA				ABV2 FA				ABV3 FA				SV1 FA				Pyrolysis product	Compound class
no.	rel. amt.	s.d.	$\delta^{13}C$	s.d.	rel. amt.	s.d.	$\delta^{13}C$	s.d.	rel. amt.	s.d.	$\delta^{13}C$	s.d.	rel. amt.	s.d.	$\delta^{13}C$	s.d.	rel. amt.	s.d.	$\delta^{13}C$	s.d.	rel. amt.	s.d.	$\delta^{13}C$	s.d.	rel. amt.	s.d.	$\delta^{13}C$	s.d.	rel. amt.	s.d.	$\delta^{13}C$	s.d.	rel. amt.	s.d.	$\delta^{13}C$	s.d.		
1									0.5	—	-24.1		0.6	—	25.0	—					0.9	—	-26.9	—	1.6	0.1	-30.4	0.5	1.0	0.3	-27.1	3.5					Methylbutanal	
2									0.4	—	-25.6	—					0.6	—	-25.1	—					2.5	0.1	-27.9	0.2	1.2	0.3	-26.7	2.6	0.4	—	-30.3	—	Benzene	alkylbenzene
4	1.0	0.0	-25.6	1.1	0.9	—	-26.5	—	*	*	*	*	0.8	0.1	-24.9	1.4	0.8	—	-27.0	—					1.2	0.1	-23.8	0.5	*	*	*	*					Dimethylfuran	PS
6	1.6	0.1	-25.0	1.1	1.3	0.1	-25.8	1.4	1.4	0.1	-24.1	0.1	1.4	0.1	-23.4	0.8	1.3	0.1	-24.8	1.2	1.4	—	-26.7	—					3.6	0.1	*	*					Propenoic acid	PS
9	0.9	0.1	-27.8	1.5	1.0	0.1	-28.6	1.2	1.0	0.0	-29.3	0.5	1.1	0.1	-28.3	0.9	0.8	0.1	-27.5	2.5	1.1	—	-29.9	—	3.1	0.2	-34.5	0.1	2.3	0.5	*	*	0.6	0.0	-28.7	1.5	Toluene	alkylbenzene
11	3.5	0.0	-15.5	0.9																	2.8	—	-18.9	—	9.6	1.2	-24.8	0.1	2.2	0.4	*	*					Acetamide	
13	1.1	0.0	*	*					0.6	—	*	*	0.8		*	*	1.1	0.1	*	*					1.0	0.0	-27.1	0.5									2(5H)-Furanone	PS
14	1.7	0.1	*	*	2.1	0.1	*	*	2.3	0.0	*	*	2.1	0.2	*	*	2.3	0.1	-21.2	1.5					2.9	0.0	-24.3	0.1	1.7	0.2	-22.0	2.1					2-Furaldehyde	PS
15																																	0.6	0.0	-22.5	0.5	2-Methylfuran	PS
16																									0.5	—	-29.2	—									2-Methylpyrrole	alkylpyrrole
17																									1.3	0.1	-23.5	0.6									2-Furanmethanol	PS
18																									0.6	0.0	-30.1	0.6	1.1	0.2	-28.5	2.1					Ethylbenzene	alkylbenzene
19	*	*	*	*	*	*	*	*	*	*	*	*	*	*	*	*	*	*	*	*	*	*	*	*	*	*	*	*	*	*	*	*	*	*	*	*	Dimethylbenzene isomer	
21	*	*	*	*	*	*	*	*	*	*	*	*	*	*	*	*	*	*	*	*	*	*	*	*	*	*	*	*	*	*	*	*	*	*	*	*	Dimethylbenzene isomer	alkylbenzene
22																									0.9	0.1	-32.3	0.9	2.0	0.3	-26.7	1.8					Styrene	alkylbenzene
23	0.4	—	-24.2	—					0.4	—	-23.1	—	0.4	0.0	-23.4	0.6					0.7	—	-28.8	—					0.5	—	-23.7	—	0.7	0.0	-24.3	1.0	2-Methylcyclopenten-1-one	PS
25																													0.9	0.1	-26.0	1.2					1-Methylethenylbenzene	alkylbenzene
26	1.0	0.1	-21.1	0.7	0.8	0.1	-21.5	0.5	0.9	0.0	-20.2	0.1	0.8	0.0	-20.8	0.5	1.1	0.0	-20.6	1.2	0.9	—	-27.0	—	0.5	0.0	-22.1	0.7	0.9	0.1	-26.0	1.4	0.5	0.0	-21.5	2.1	3-Methyl-3-penten-2-one (T)	
28	2.9	—	-24.9	—	2.2	0.4	-26.3	0.8	2.2	—	-25.8	—	2.2	—	-25.5	—	2.3	0.2	-25.2	2.3	3.2	—	-27.3	—					1.9	—	-27.1	—	1.3	0.1	-20.8	0.6	Methylsuccinic anhydride	PS
29																									0.3	—	-20.7	—									N-Acetylpyrrole (T)	alkylpyrrole
30					1.6	0.1	-25.6	0.4	1.6	—	-23.4	—	1.5	—	-24.8	—	1.6	0.1	-23.8	1.9					2.6	0.1	-24.1	0.5	1.7	—	-23.6	—					5-Methylfuraldehyde	PS
31	0.6	—	-25.7	—					0.7	—	-25.3	—	0.8	—	-25.8	—					1.1	—	-27.3	—									0.4	—	-25.4	—	3-Methyl-2-cyclopenten-1-one (T)	PS
32	6.3	3.5	-27.4	1.0	4.6	0.8	-29.0	1.5	2.8	—	-29.5	—	5.3	0.4	-29.9	0.0	2.9	0.3	-31.0	1.7	1.7	—	-31.1	—	1.8	0.4	-30.5	1.4	*	*	*	*	3.5	0.1	-30.9	0.6	Phenol	
34	0.7	—	-28.7	—	0.8	—	-29.0	—	0.8	—	-28.1	—	0.8	—	-28.4	—					1.3	—	-28.7	—					0.8	—	-28.1	—	0.5	0.0	-25.4	0.8	Trimethylbenzene	alkylbenzene
36									0.4	—	-26.4	—									1.0	—	-30.6	—									0.9	0.0	-26.2	1.1	Benzofuran (T)	
37																									0.5	0.0	-20.5	2.9									4-Hydroxy-5,6-dihydro-2H-pyran-2-one	PS
39									0.2	—	-23.1	—																									Methyl-(1-methylethyl-)-benzene	alkylbenzene
40	0.2	—	-25.1	—	0.3	—	-23.5	—	0.3	0.0	-25.9	2.2	0.4	0.1	-25.4	0.4					0.4	—	-28.2	—					0.4	—	-34.0	—	0.7	0.0	-21.4	1.2	Ethylmethylbenzene	alkylbenzene
42	1.8	0.3	-22.4	0.6	2.8	0.4	-23.0	0.5	3.7	0.7	-24.1	0.5	3.7	0.5	-23.7	0.5	3.1	0.2	-23.2	0.5	3.5	—	-26.0	—	0.7	0.0	-26.9	2.0	2.5	—	-23.6	—					Unknown polysaccharide marker	PS
44	1.4	0.1	-28.0	0.2	1.8	0.2	-28.3	0.4	1.5	0.1	-29.3	0.9	1.5	0.1	-28.8	0.8	1.4	0.0	-28.7	0.8	6.4	—	-18.5	—					1.4	—	-29.1	—	1.2	0.1	-23.0	0.2	2,3-Dimethyl-2-cyclopenten-1-one	
45	0.6	0.0	-27.2	0.9	0.6	0.0	-27.7	1.8	0.7	0.0	-28.2	0.9	0.9	0.0	-27.7	0.3	0.7	0.0	-27.2	0.9	0.7	—	-27.9	—													2-Methylphenol	alkylphenol
46																													1.5	—	-28.4	—	2.0	0.0	-20.1	0.2	Butylbenzene	alkylbenzene
47																									1.8	0.1	-21.7	0.5									Dianhydrorhamnose isomer	PS
48	0.5	—	-29.6	—					0.7	0.1	-29.6	1.1	0.7	0.0	-30.2	1.5	0.7	0.1	-33.4	1.3	1.1	—	-28.7	—	0.4	0.0	-30.3	1.4					1.1	0.0	-21.6	0.3	Unknown	
49																																	1.8	0.0	-26.1	0.2	Unknown	
50	2.6	0.1	-27.3	0.7	2.5	0.2	-28.2	1.1	2.3	0.1	-28.4	0.5	3.0	0.3	-28.2	0.4	1.5	0.1	-28.5	0.7	1.7	—	-28.1	—	2.9	0.5	-32.2	0.7	0.8	0.1	-26.9	0.7	3.6	0.1	-26.6	0.4	3- or 4-Methylphenol	alkylphenol
51	1.5	0.1	-27.6	0.3	2.9	0.0	-27.0	0.7	2.7	0.8	-27.2	0.2	2.5	0.2	-26.5	0.7	5.7	1.2	-29.4	1.1					0.4	0.0	-28.9	1.1	0.7	—	-28.4	—					2-Methoxyphenol	Lig
53					1.2	0.0	-29.4	1.0					1.0	0.2	-28.9	1.7	0.9	—	-31.7	—	1.5	—	-27.6	—					1.2	0.2	-29.3	0.8					Unknown	

	HO10 FA				HO13 FA				HO14 FA				HO16 FA				BS1 FA				FG1 FA				ABV2 FA				ABV3 FA				SV1 FA				Pyrolysis product	Source
no.	rel. amt.	s.d.	$\delta^{13}C$	s.d.	rel. amt.	s.d.	$\delta^{13}C$	s.d.	rel. amt.	s.d.	$\delta^{13}C$	s.d.	rel. amt.	s.d.	$\delta^{13}C$	s.d.	rel. amt.	s.d.	$\delta^{13}C$	s.d.	rel. amt.	s.d.	$\delta^{13}C$	s.d.	rel. amt.	s.d.	$\delta^{13}C$	s.d.	rel. amt.	s.d.	$\delta^{13}C$	s.d.	rel. amt.	s.d.	$\delta^{13}C$	s.d.		
55					0.5	—	-15.6	—	0.4	—	-22.8	—					1.0	0.1	-13.9	1.2									0.7	0.1	-19.2	0.7					Levoglucosenone	PS
56	0.8	0.1	-26.8	0.9	0.8	—	-27.1	—	0.7	0.0	-27.3	1.0	0.9	0.0	-26.0	0.9					1.7	—	-26.3	—									*	*	*	*	Dimethylphenol isomer	alkylphenol
57																													1.1	0.1	-26.7	0.6					Pentylbenzene	alkylbenzene
58									0.7	—	-28.7	—	1.1	0.0	-26.7	1.1					0.9	—	-28.0	—	1.8	0.6	*	*					2.3	0.0	-25.2	0.4	Ethylphenol	alkylphenol
59																													2.0	0.5	-28.5	0.5					Unknown	alkylphenol
61	0.7	0.1	-29.2	1.8	0.9	0.1	-30.2	1.8	0.9	0.0	-29.0	0.2	0.7	0.0	-26.4	2.1	1.3	0.1	-29.8	0.7					0.5	0.0	-30.9	0.9									2-Methoxy-4-methylphenol	Lig
62																																	0.6	0.1	-24.9	1.1	Dimethylphenol isomer	alkylphenol
63																																	0.9	0.0	-20.7	0.6	Unknown	
64																													0.6	—	-24.9	—					Naphthalene (T)	
66	0.8	0.1	-26.5	0.4									0.9	—	-27.3	—									0.6	0.0	-30.0	1.1	0.7	—	*	*					4-Vinylphenol	alkylphenol
68																													0.3	—	-29.2	—					Hexylbenzene	alkylbenzene
69																									0.6	0.0	-27.5	0.8									Alkene/alkene (T)	
70	0.4	—	-26.5	—	0.5	—	-20.9	—	0.4	0.0	-26.4	0.8	0.5	0.0	-26.8	0.7	0.5	0.0	-28.7	1.9									0.7	—	-21.4	0.0	1.3	0.1	-26.0	0.2	2-Coumaranone	alkylbenzene
71																													0.9	0.3	-27.8	2.7					Unknown	
72																																	1.1	0.0	-26.0	0.3	Unknown	alkylbenzene
74																	0.5	—	-26.8	—																	4-Ethyl-2-methoxyphenol	Lig
75																													1.1	0.3	-28.9	2.8	0.7	0.1	-26.4	0.2	Unknown	
76																									0.4	0.1	-25.9	0.4									Unknown	alkylpyrrole
78																	0.5	0.0	-25.6	2.6					0.2	—	-28.2	—									4-Vinyl-2-methoxyphenol	Lig
79																									0.5	0.0	-26.1	0.5									1H-Indol	
80																													0.5	—	-27.1	—					1-Phenyl-2-cyclopenten-1-ol	PS
82																																	1.5	0.0	-23.3	0.6	3-Methyl-2(3H)-benzofuranone isomer	alkylbenzene
83																													0.7	0.1	-25.9	1.6					Methylnaphthalene	
84																	0.5	—	-38.1	—									1.1	0.4	-28.8	2.9					1,3-Isobenzofurandione	
85																																	3.7	0.2	-23.1	0.2	3-Methyl-2(3H)-benzofuranone isomer	alkylbenzene
87																	0.7	—	-23.4	—																	4-Hydroxy-3-methoxybenzaldehyde	
88																													0.4	—	-29.1	—					Ethylnaphthalene	
89																																	0.9	—	-21.7	—	Unknown	
90	0.5	—	-24.5	—									0.5	—	-25.3	—	0.5	—	-24.0	—									0.6	—	-24.4	—	2.7	1.3	-25.4	1.3	4-Methyl-1,3-isobenzofurandione	
91																																	0.3	0.1	-20.8	2.0	Unknown	
92																													0.5	—	-27.6	—					Dimethylnaphthalene	
93																																	0.5	0.1	-22.2	0.9	Dimethyl-2(3H)-benzofuranone	alkylbenzene
94																	0.9	—	-28.1	—																	Acetovanillone	
96																																	0.7	0.2	-23.1	0.3	Unknown	
97																																	1.7	0.5	-25.2	0.3	4,7-Dimethyl-1,3-isobenzofurandione isomer	alkylbenzene
99																													1.2	—	-27.7	—					Methylbutyl-trimethylbenzene	alkylbenzene
100																																	0.5	0.2	-27.1	2.0	4,7-Dimethyl-1,3-isobenzofurandione isomer	alkylbenzene

Appendix III

Appendix III lists all mass spectra of the pyrolysis products obtained by ion trap mass spectrometry. The numbers refer to the peak numbers used in the text. Identification of the mass spectra was processed by using mass spectra libraries (Wiley 6.0 with NIST extension). Additional confirmation was given by external standards and comparison of mass spectra in the literature (see Section 4.3). Substances not clearly identified are denoted as tentative (T).

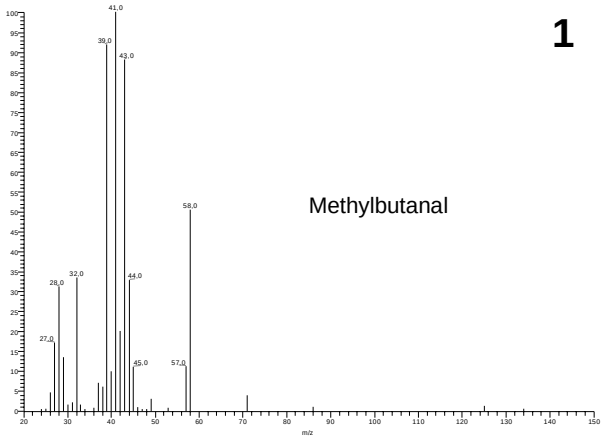
1
Methylbutanal
m/z

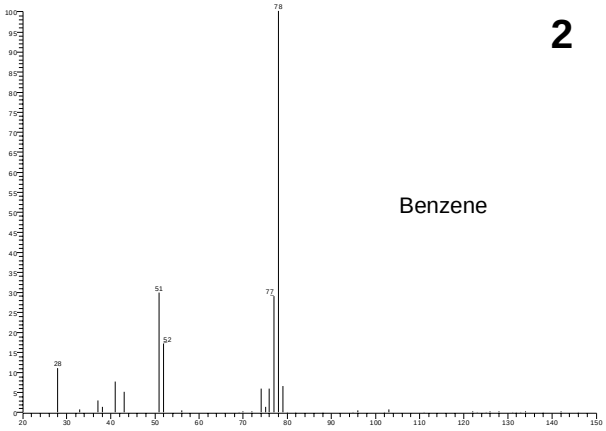
2
Benzene
m/z

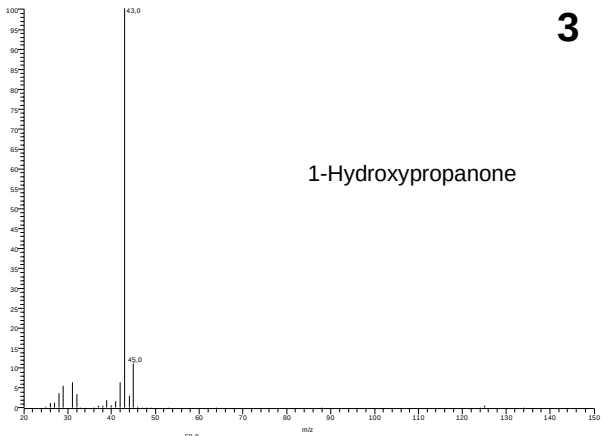
3
1-Hydroxypropanone
m/z

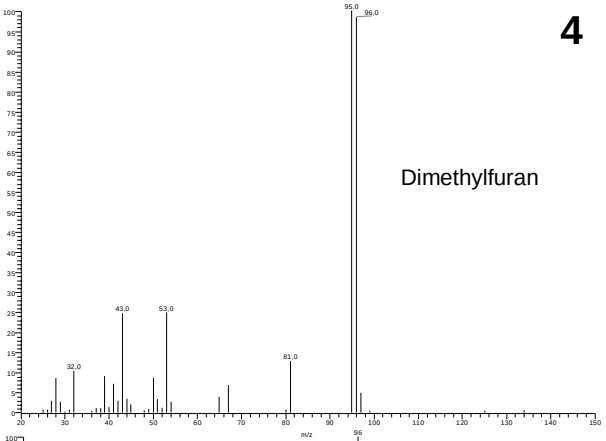
4
Dimethylfuran
m/z

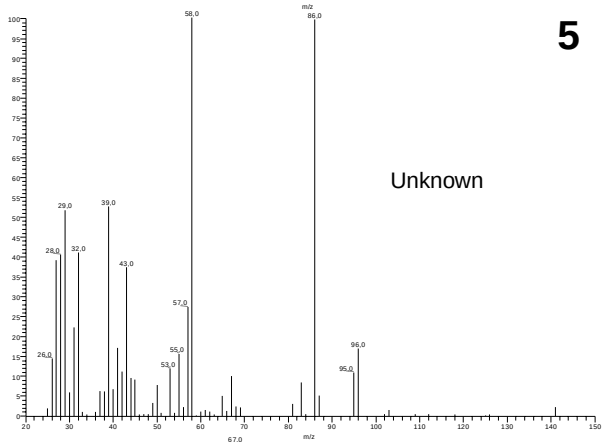
5
Unknown
m/z

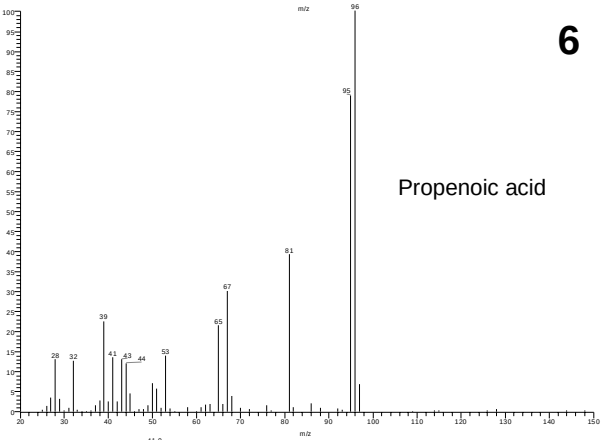
6
Propenoic acid
m/z

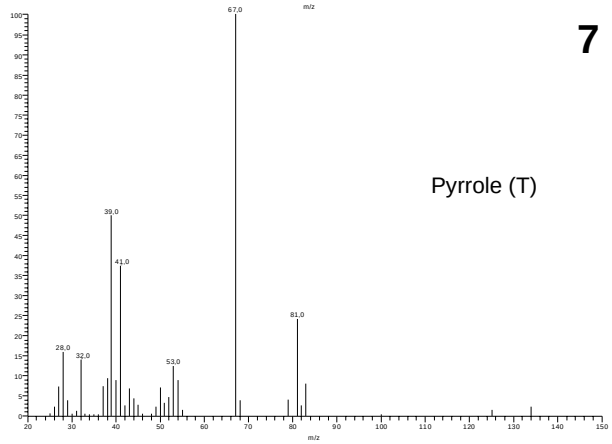
7
Pyrrole (T)
m/z

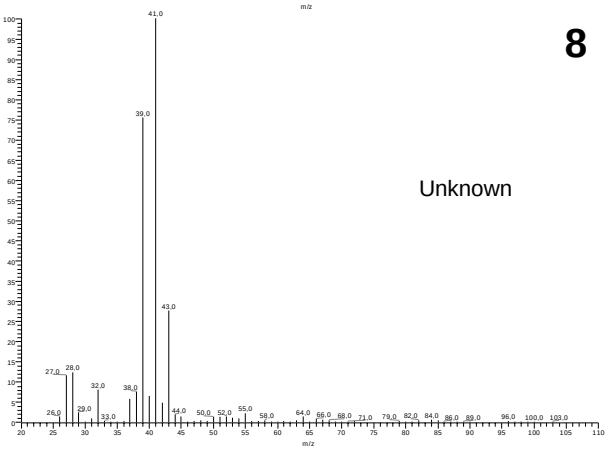
8
Unknown
m/z

9

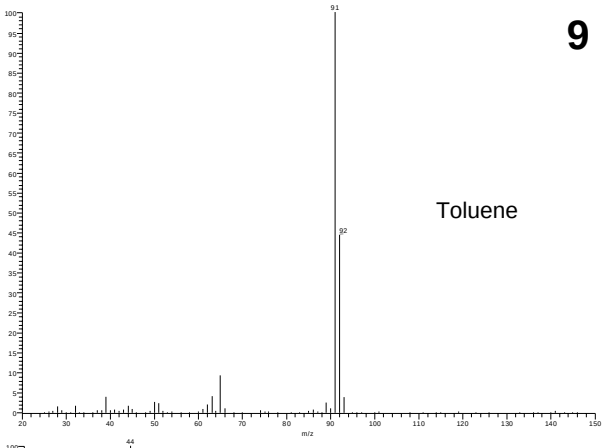

Toluene

10

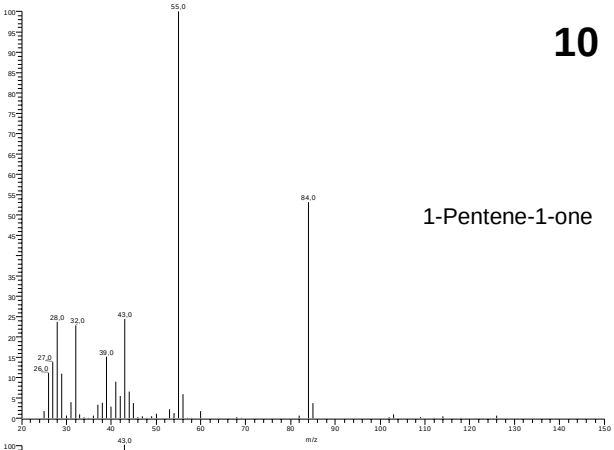

1-Pentene-1-one

11

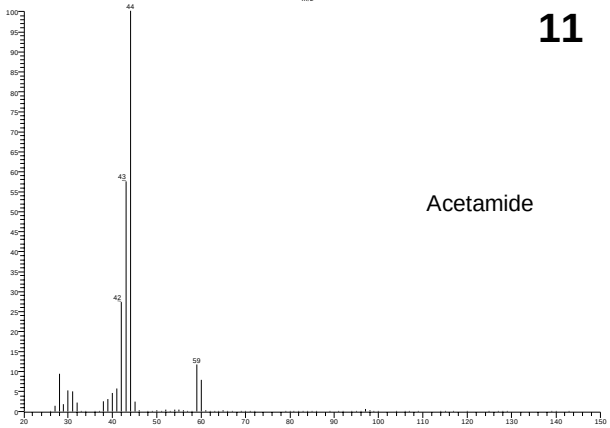

Acetamide

12

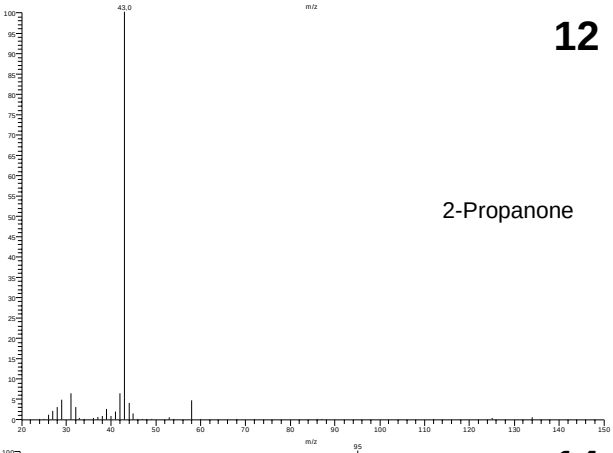

2-Propanone

13

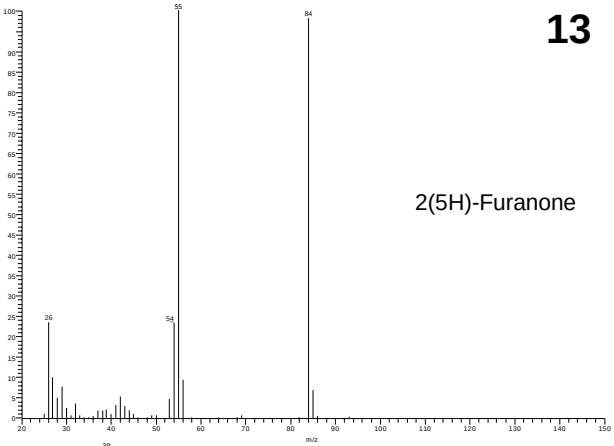

2(5H)-Furanone

14

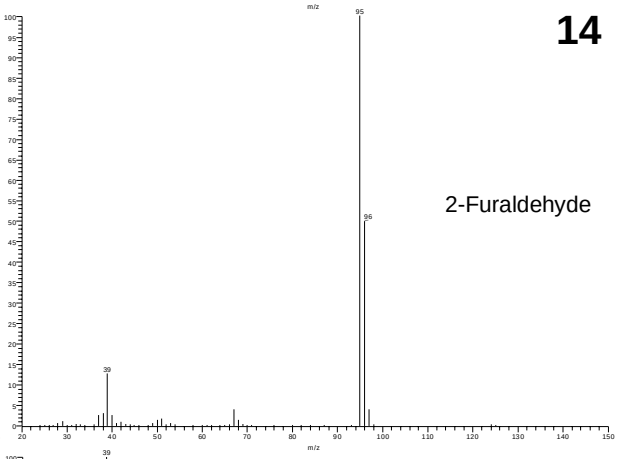

2-Furaldehyde

15

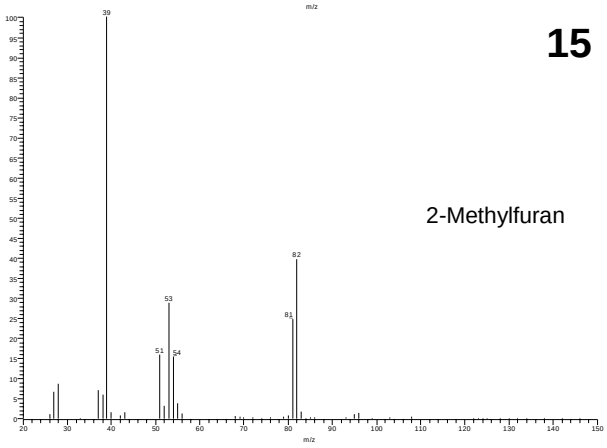

2-Methylfuran

16

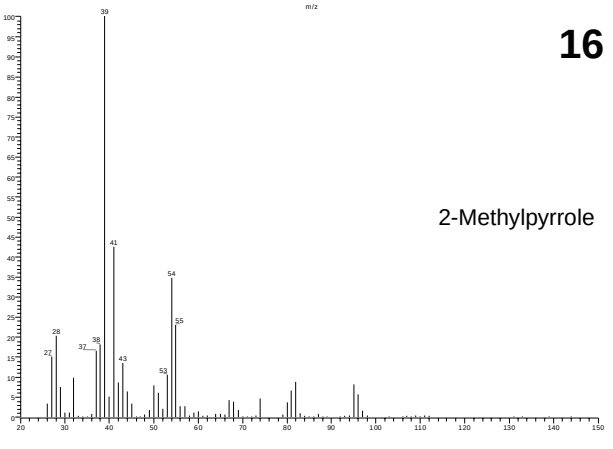

2-Methylpyrrole

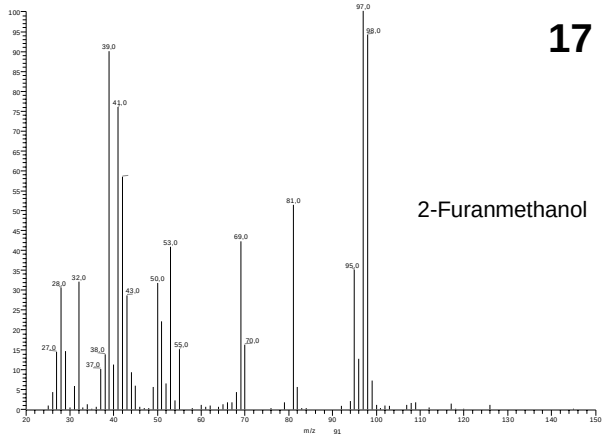
17
2-Furanmethanol

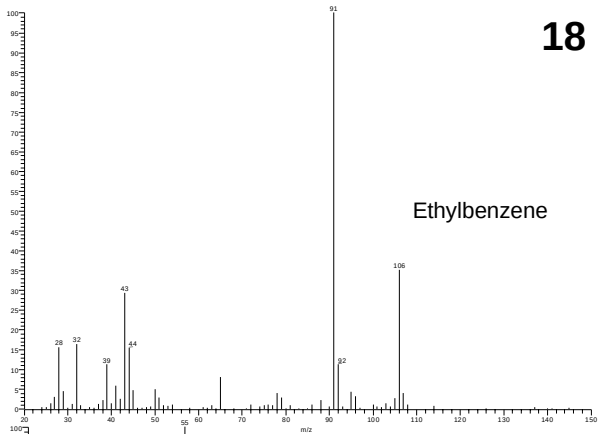
18
Ethylbenzene

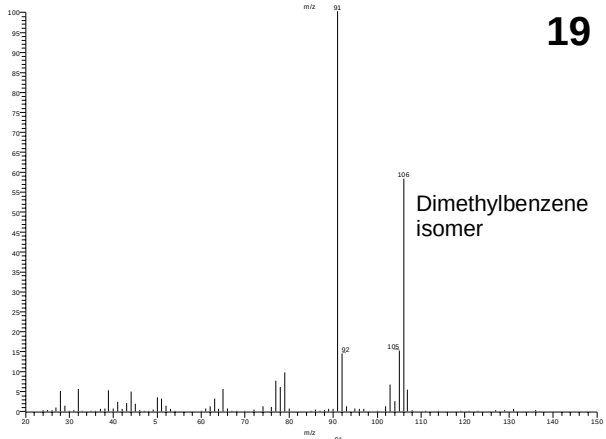
19
Dimethylbenzene
isomer

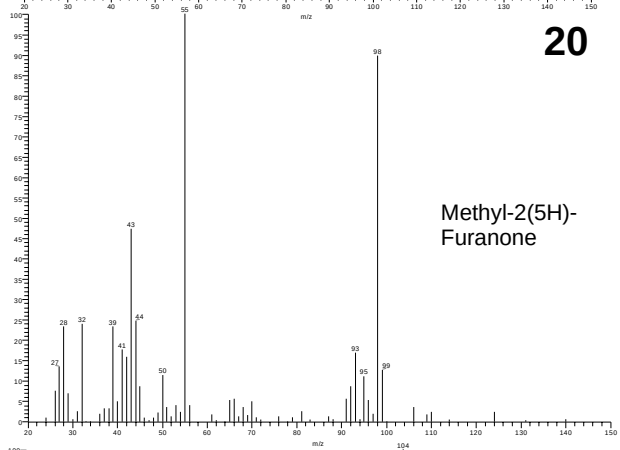
20
Methyl-2(5H)-
Furanone

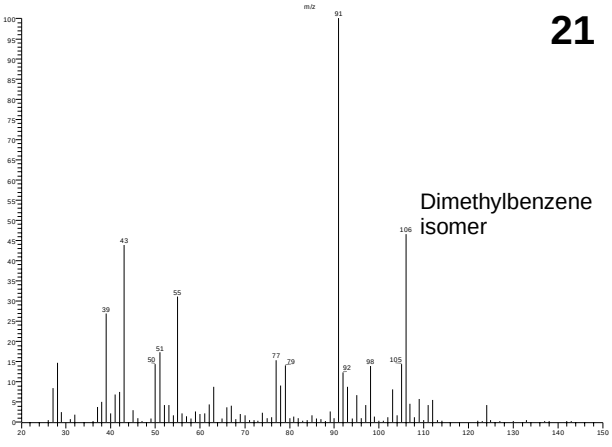
21
Dimethylbenzene
isomer

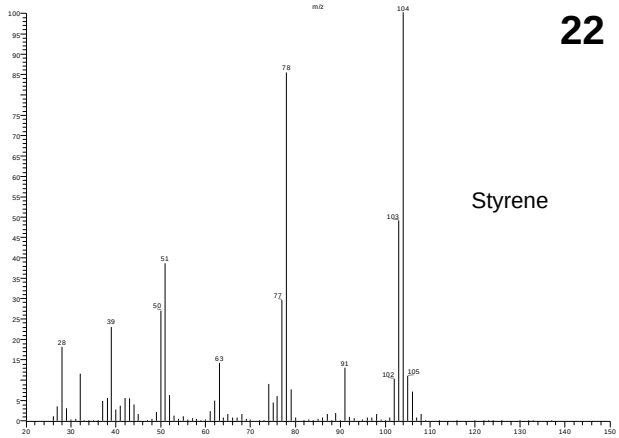
22
Styrene

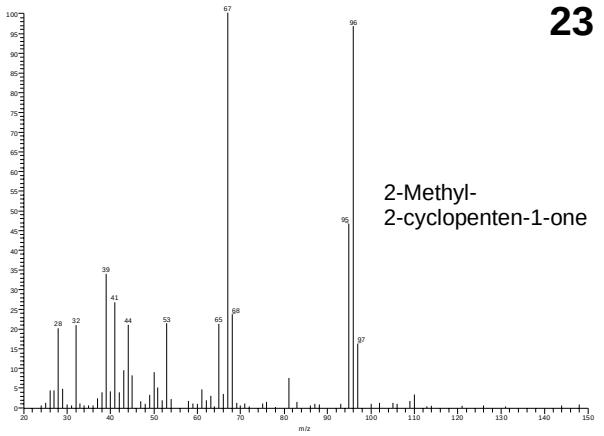
23
2-Methyl-
2-cyclopenten-1-one

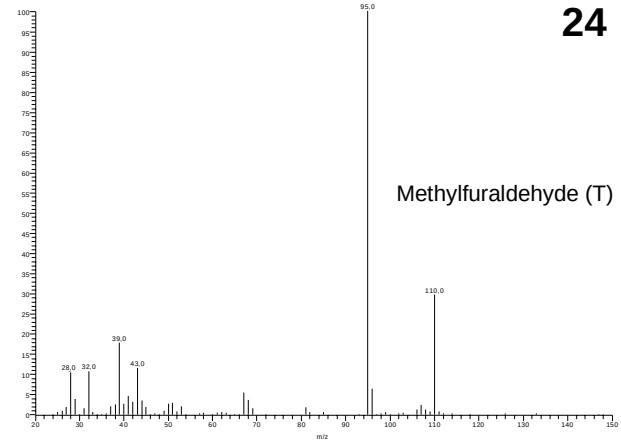
24
Methylfuraldehyde (T)

25

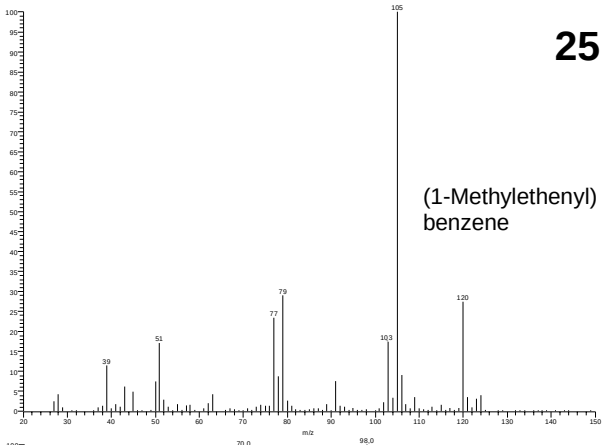

(1-Methylethenyl) benzene

26

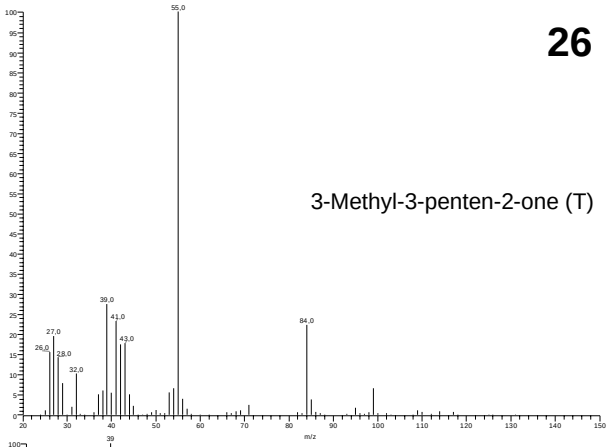

3-Methyl-3-penten-2-one (T)

27

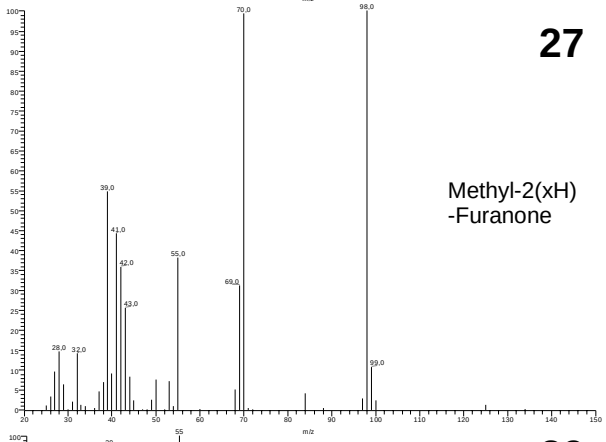

Methyl-2(xH) -Furanone

28

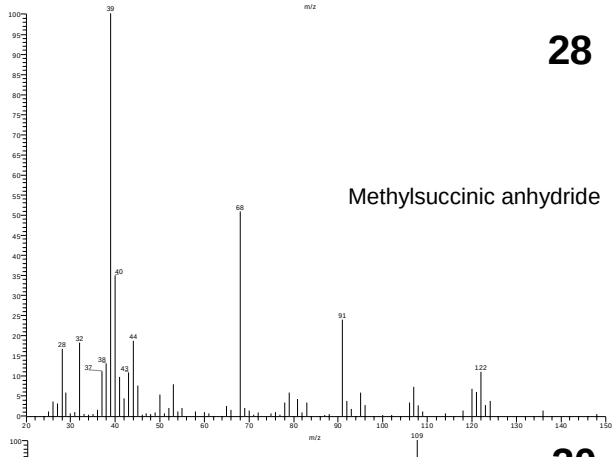

Methylsuccinic anhydride

29

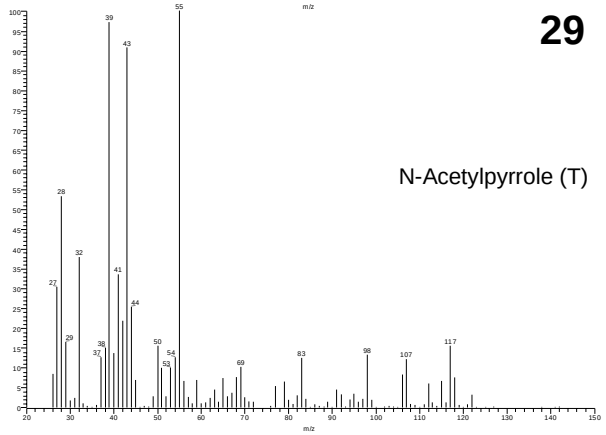

N-Acetylpyrrole (T)

30

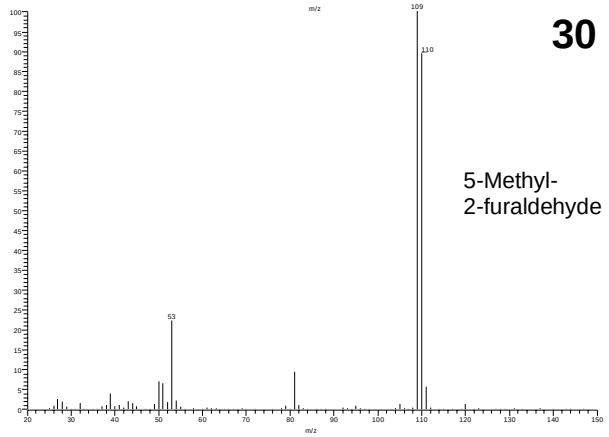

5-Methyl- 2-furaldehyde

31

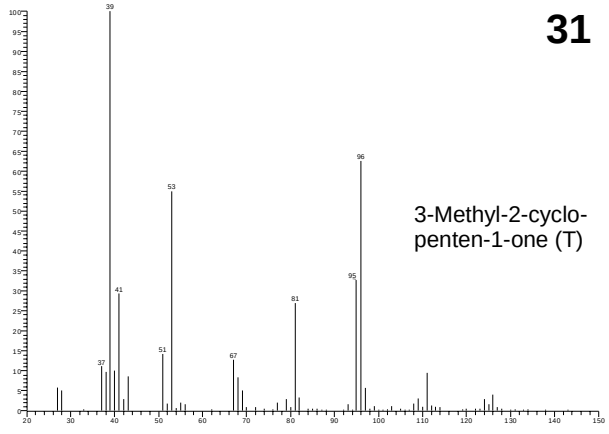

3-Methyl-2-cyclo- penten-1-one (T)

32

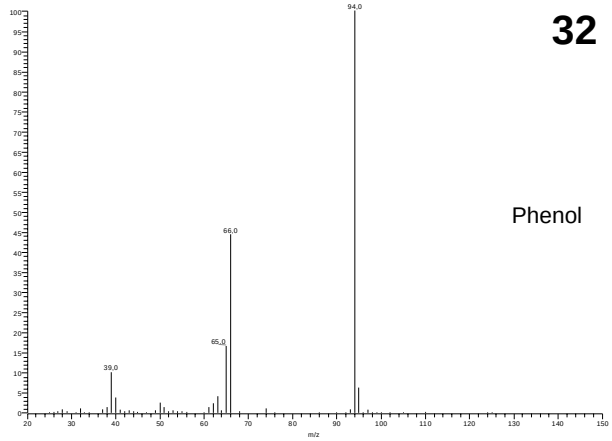

Phenol

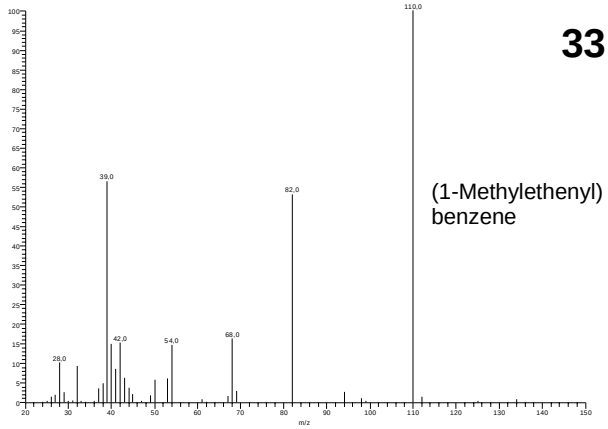
33
(1-Methylethenyl)
benzene
110,0
39,0
82,0
42,0
54,0
68,0
28,0
m/z

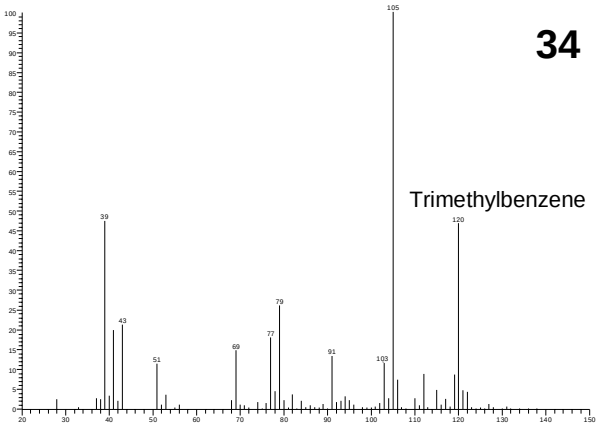
34
Trimethylbenzene
105
39
120
79
43
77
69
91
51
103
m/z

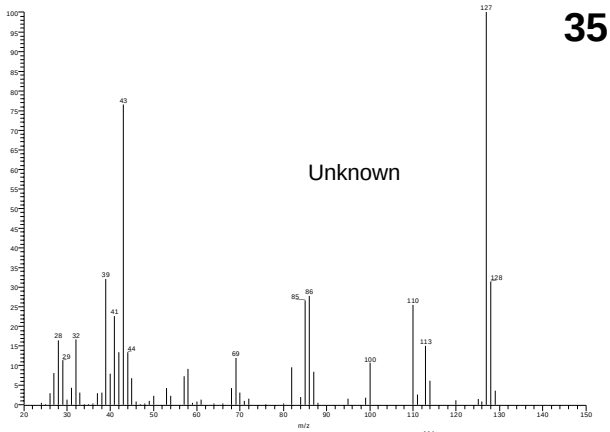
35
Unknown
127
43
39
128
41
86
85
110
28
32
44
29
69
100
113
m/z

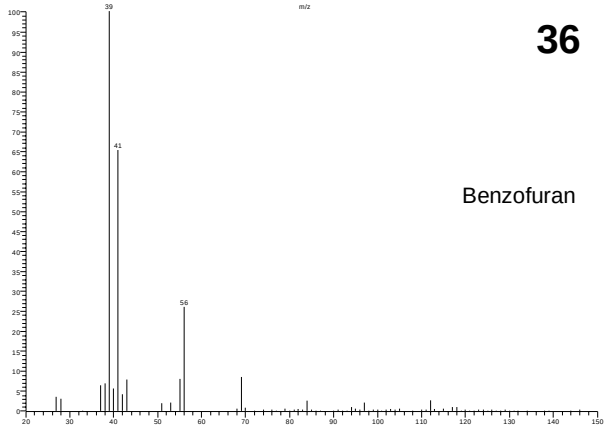
36
Benzofuran
39
41
56
m/z

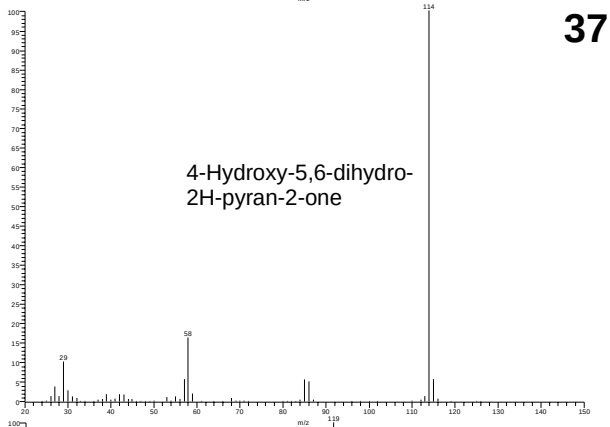
37
4-Hydroxy-5,6-dihydro-
2H-pyran-2-one
114
58
29
m/z

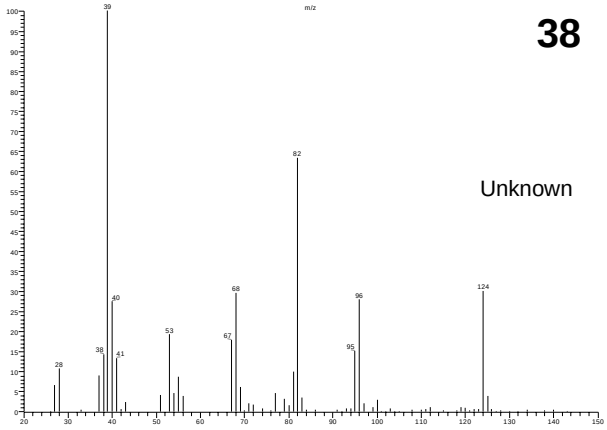
38
Unknown
39
82
40
68
53
67
96
124
38
41
95
28
m/z

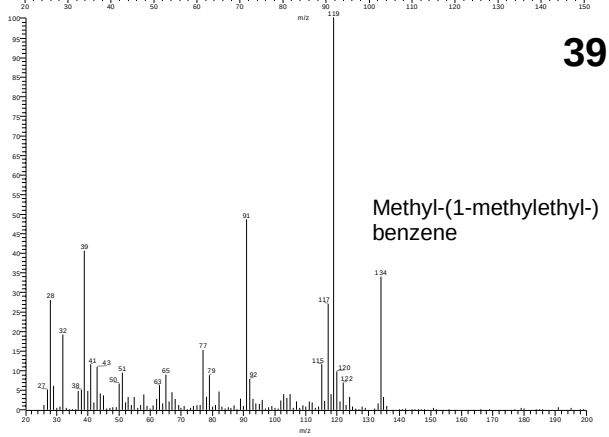
39
Methyl-(1-methylethyl-)
benzene
119
91
39
134
28
117
32
77
41
43
51
115
65
79
92
120
122
27
38
50
63
m/z

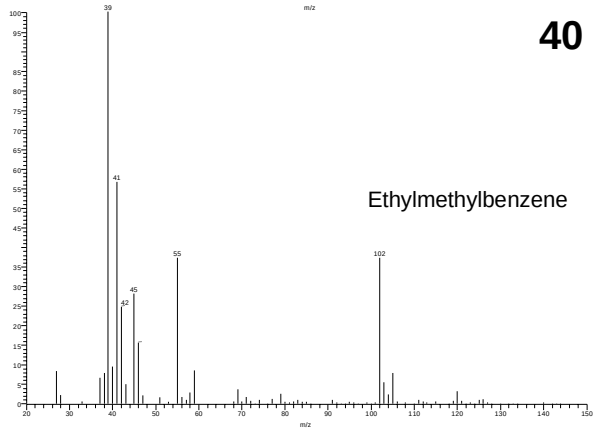
40
Ethylmethylbenzene
39
41
55
102
45
42
m/z

41

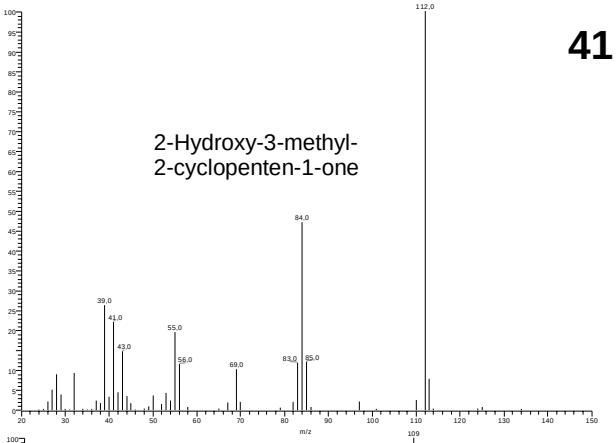

2-Hydroxy-3-methyl-
2-cyclopenten-1-one

42

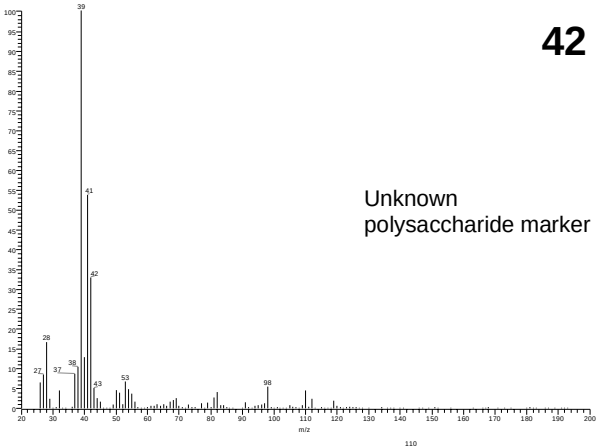

Unknown
polysaccharide marker

43

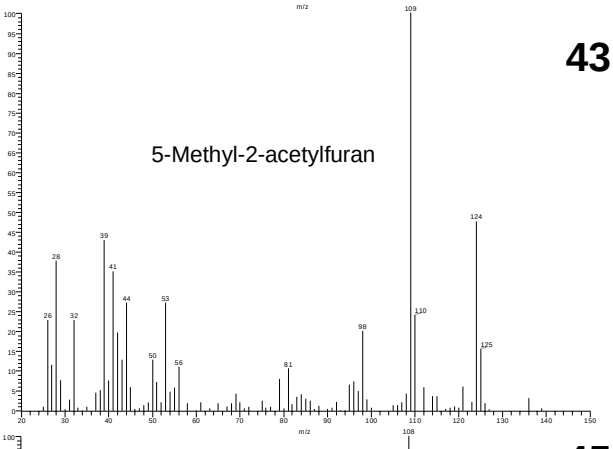

5-Methyl-2-acetylfuran

44

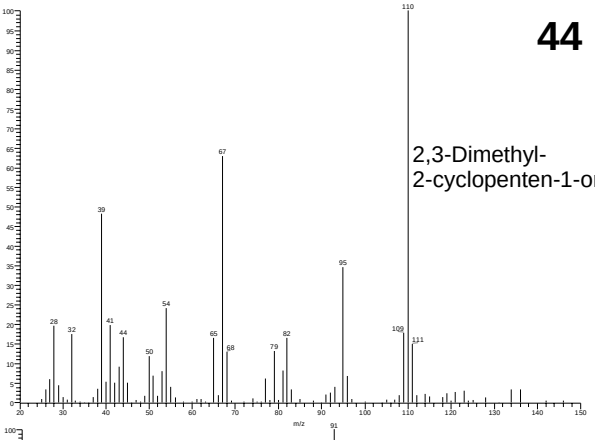

2,3-Dimethyl-
2-cyclopenten-1-one

45

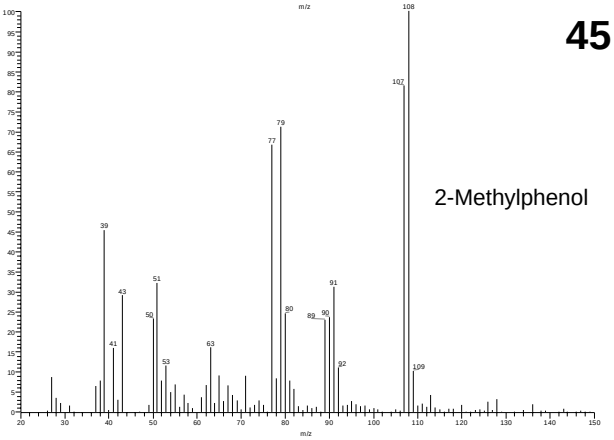

2-Methylphenol

46

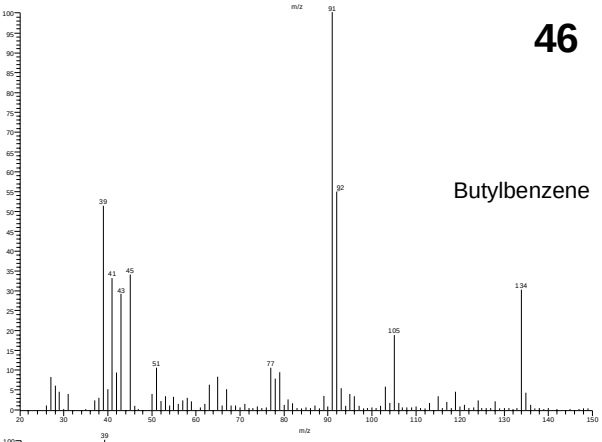

Butylbenzene

47

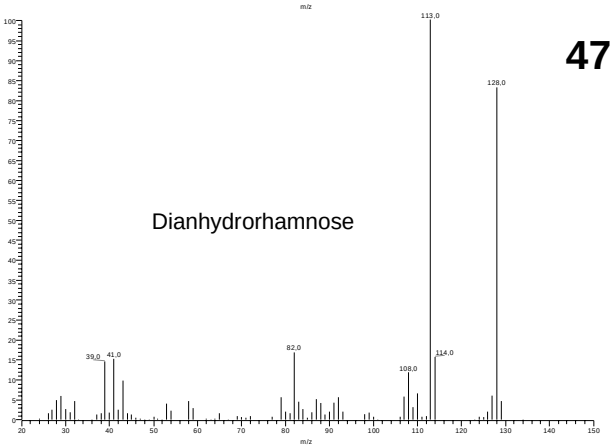

Dianhydrorhamnose

48

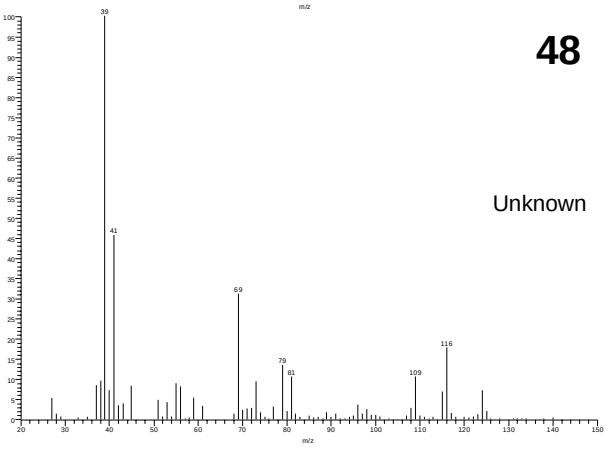

Unknown

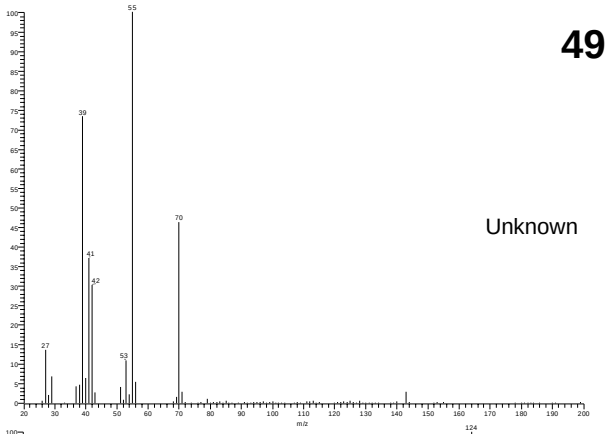
49
Unknown

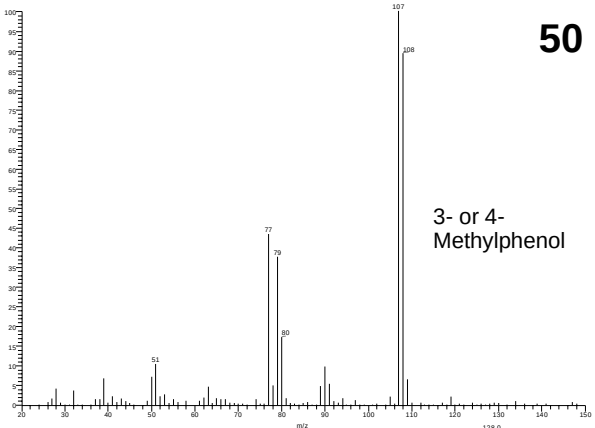
50
3- or 4-
Methylphenol

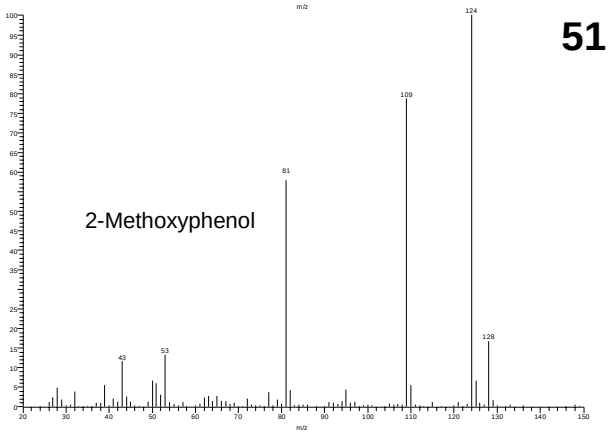
51
2-Methoxyphenol

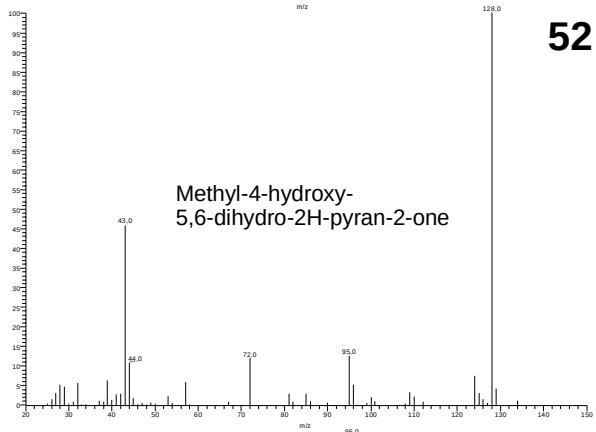
52
Methyl-4-hydroxy-
5,6-dihydro-2H-pyran-2-one

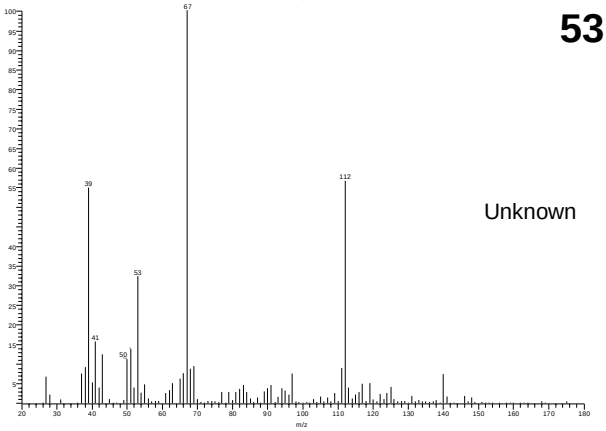
53
Unknown

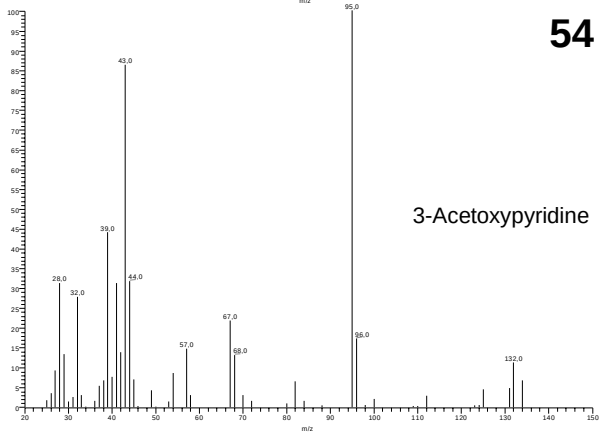
54
3-Acetoxypyridine

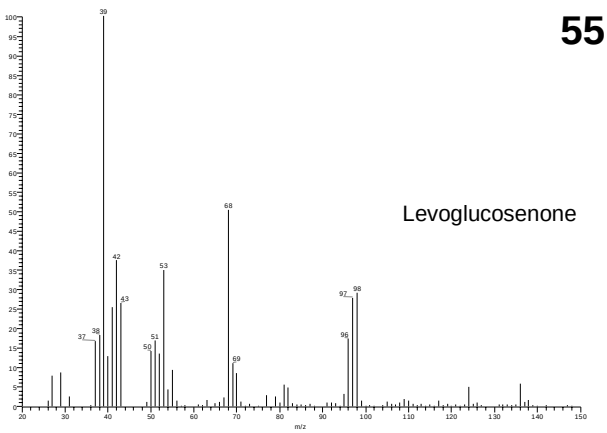
55
Levoglucosenone

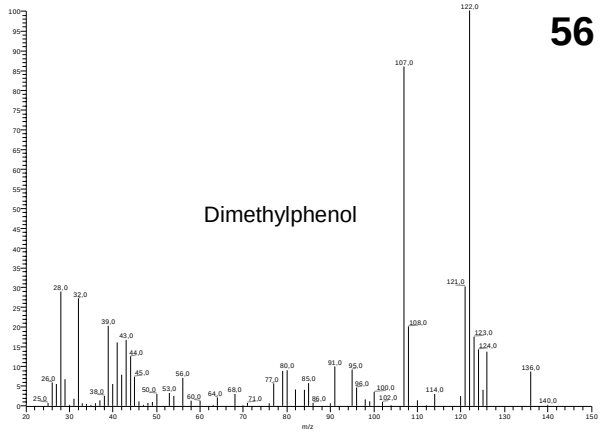
56
Dimethylphenol

57

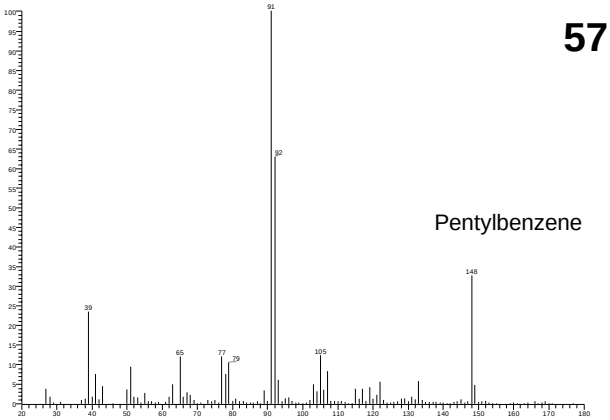

Pentylbenzene

58

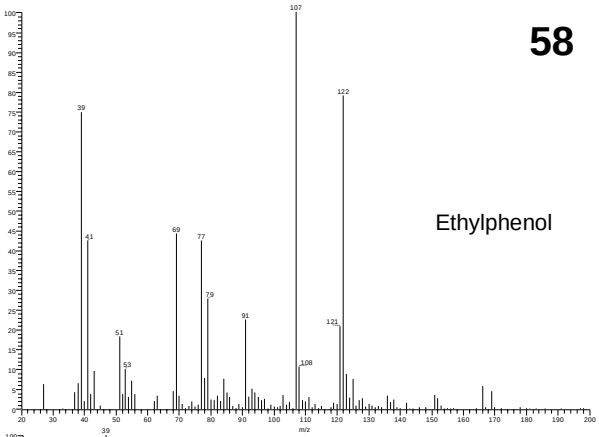

Ethylphenol

59

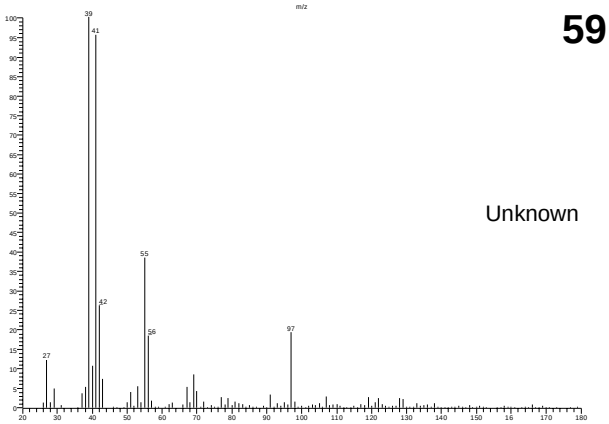

Unknown

60

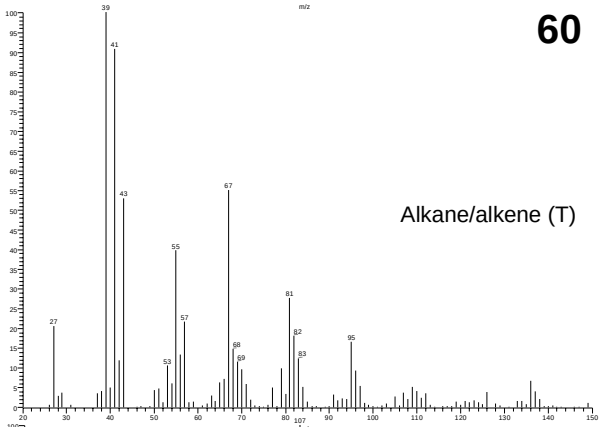

Alkane/alkene (T)

61

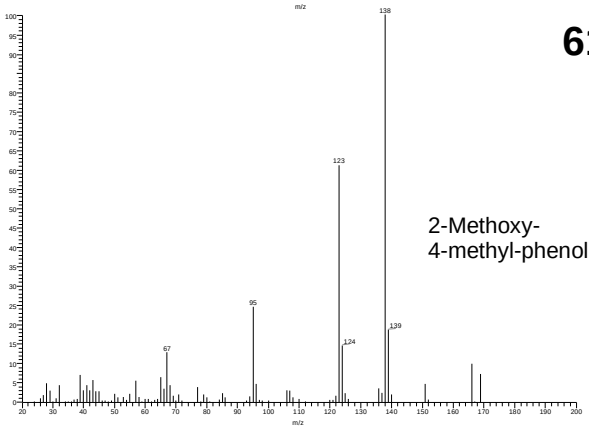

2-Methoxy-
4-methyl-phenol

62

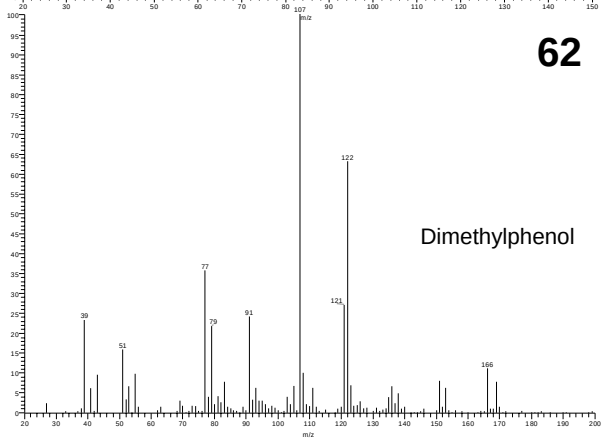

Dimethylphenol

63

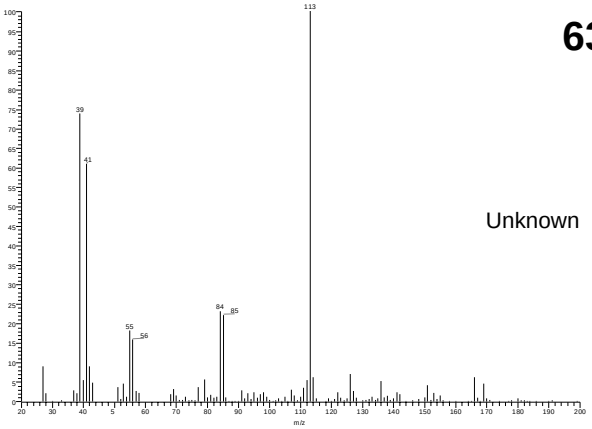

Unknown

64

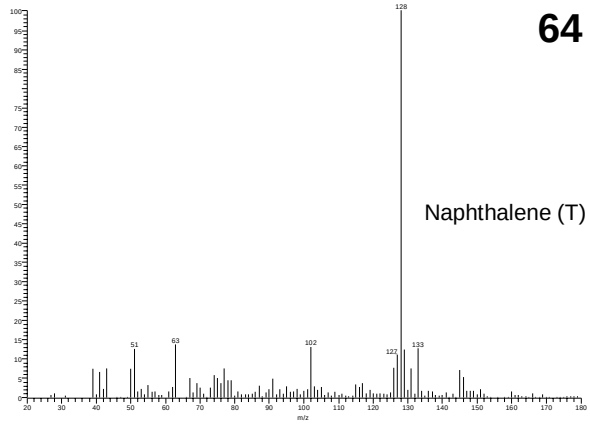

Naphthalene (T)

65

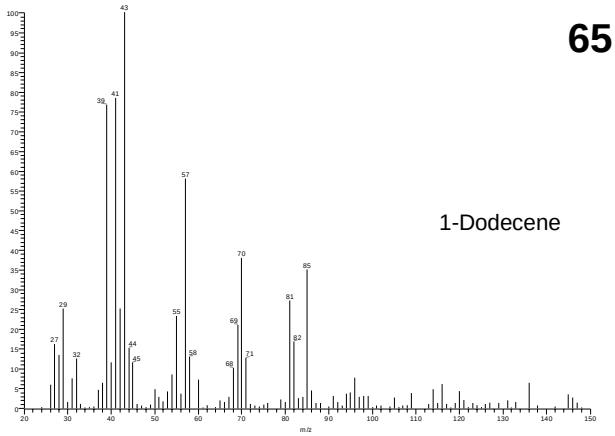

1-Dodecene

66

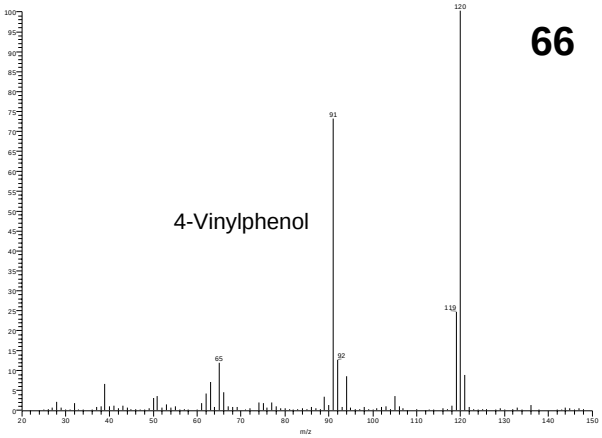

4-Vinylphenol

67

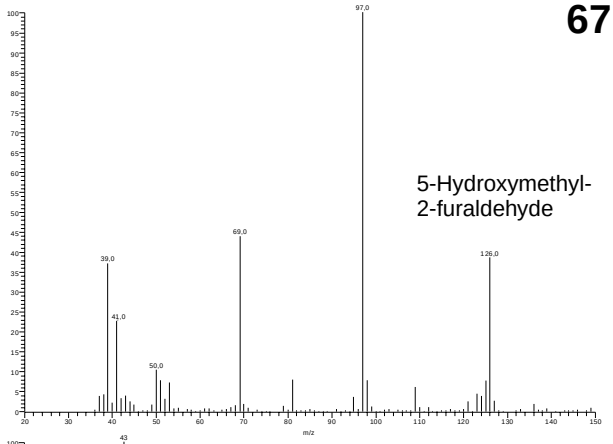

5-Hydroxymethyl-
2-furaldehyde

68

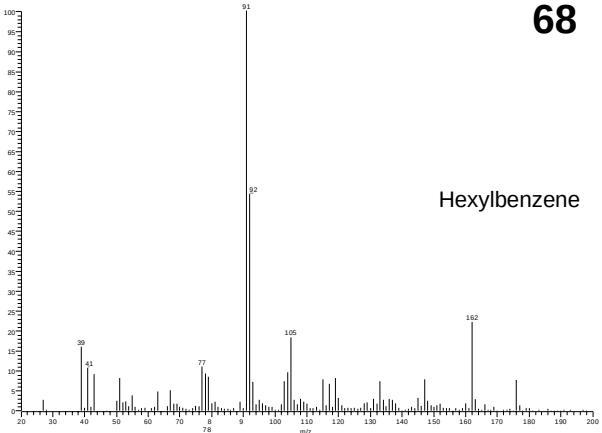

Hexylbenzene

69

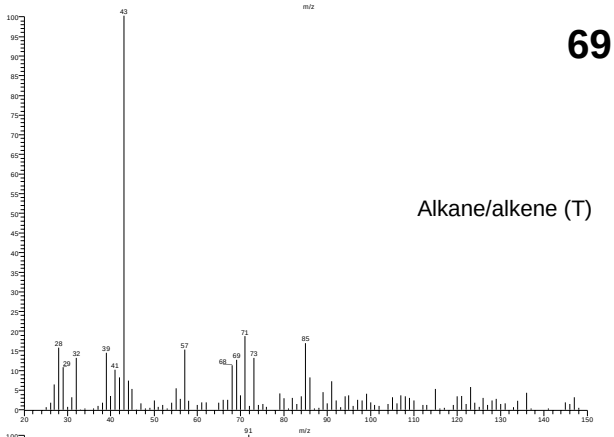

Alkane/alkene (T)

70

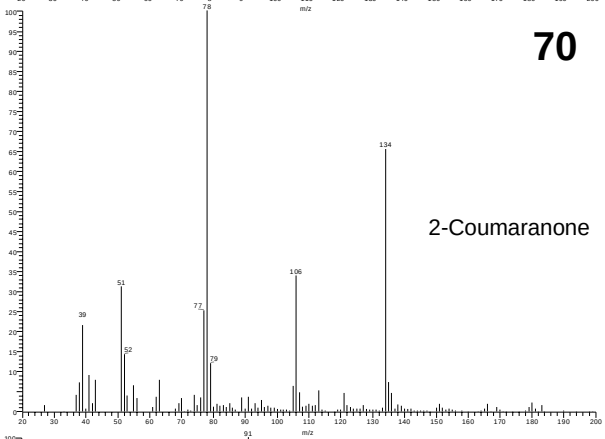

2-Coumaranone

71

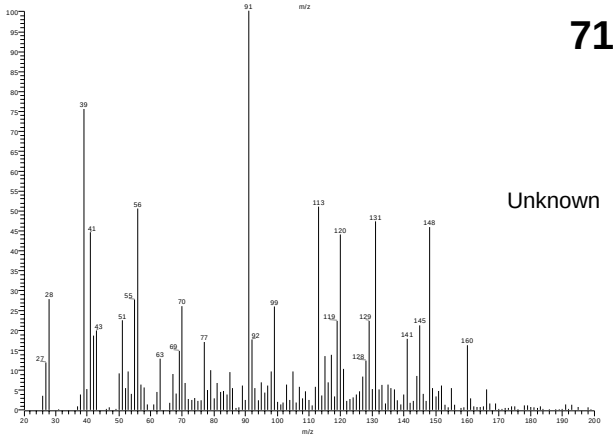

Unknown

72

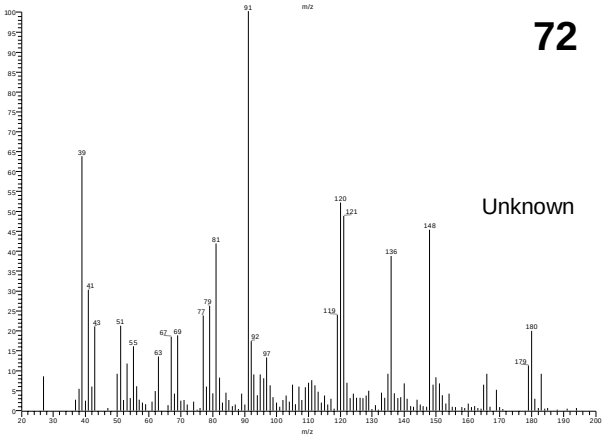

Unknown

73

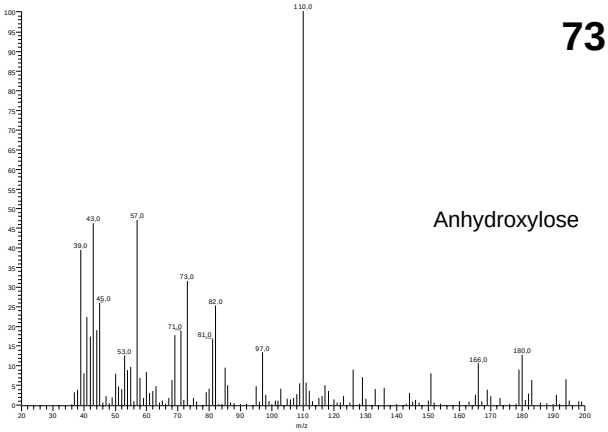

Anhydroxylose

74

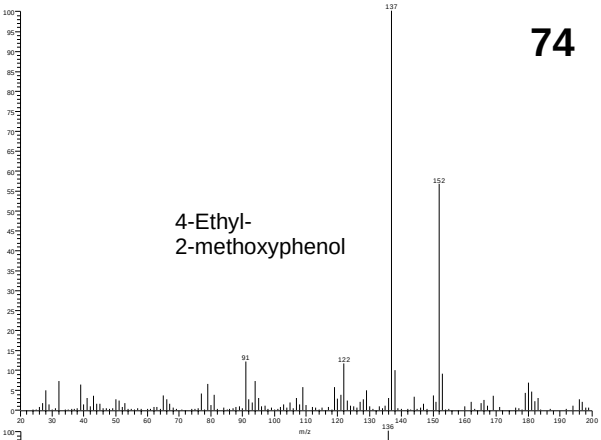

4-Ethyl-
2-methoxyphenol

75

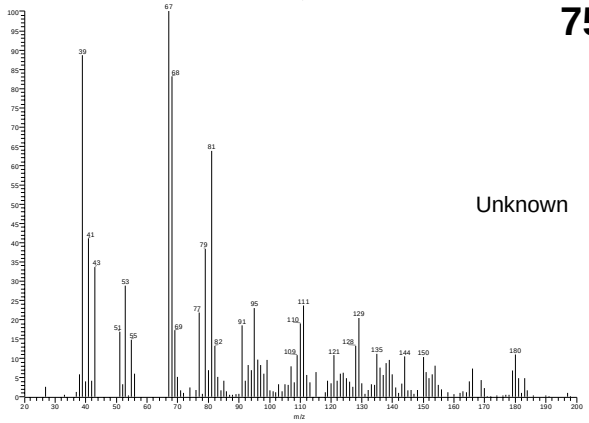

Unknown

76

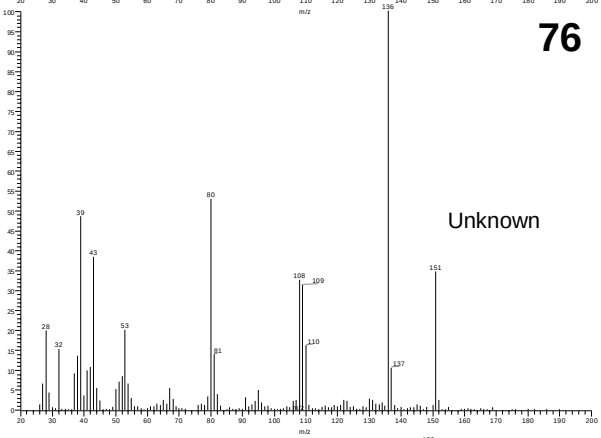

Unknown

77

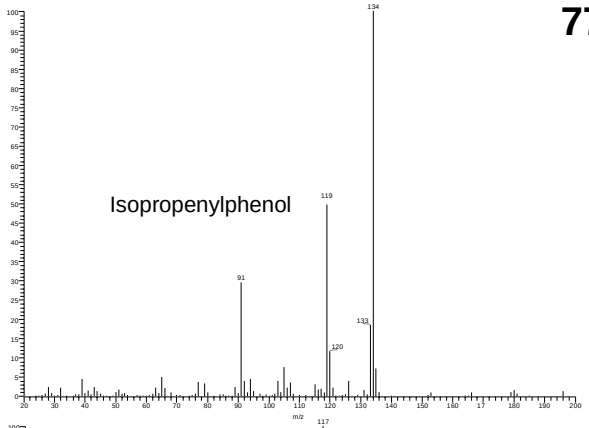

Isopropenylphenol

78

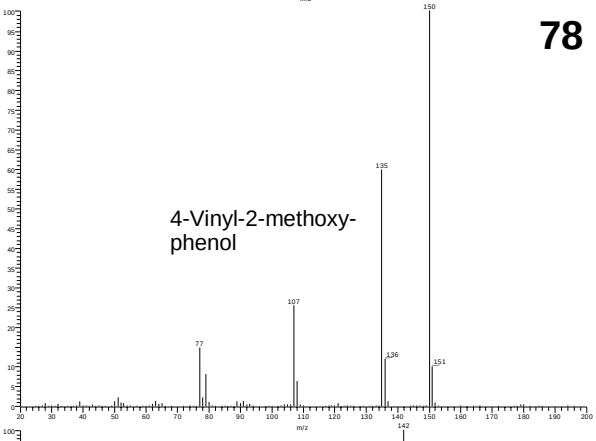

4-Vinyl-2-methoxy-
phenol

79

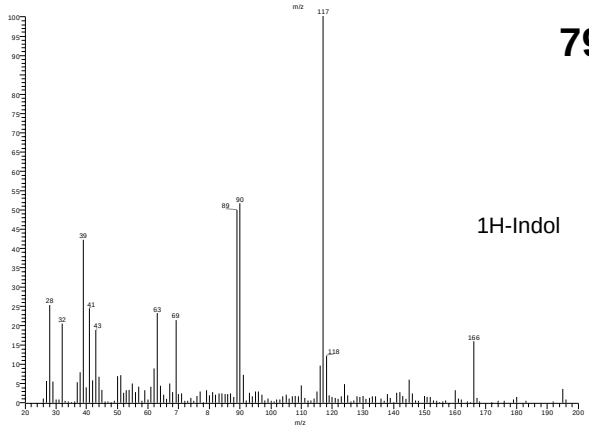

1H-Indol

80

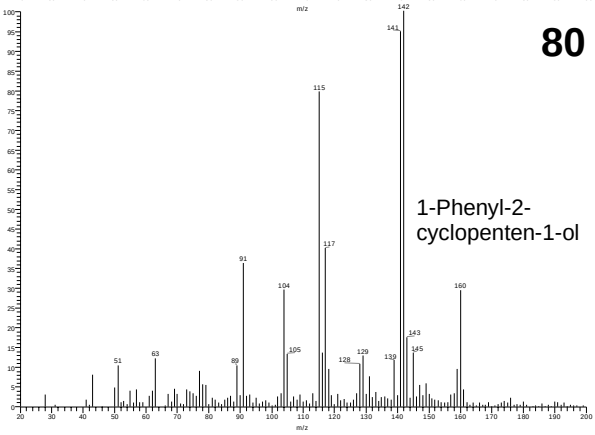

1-Phenyl-2-
cyclopenten-1-ol

81

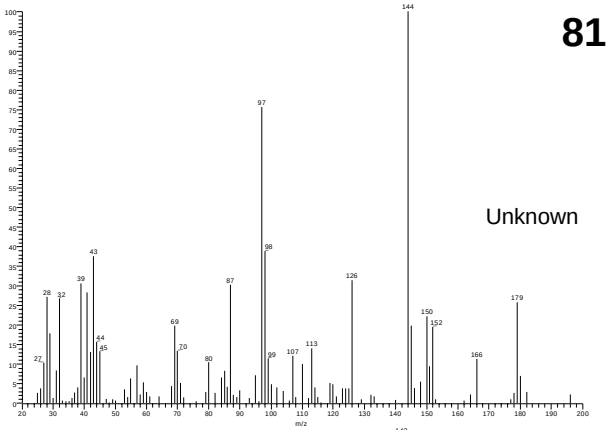

Unknown

82

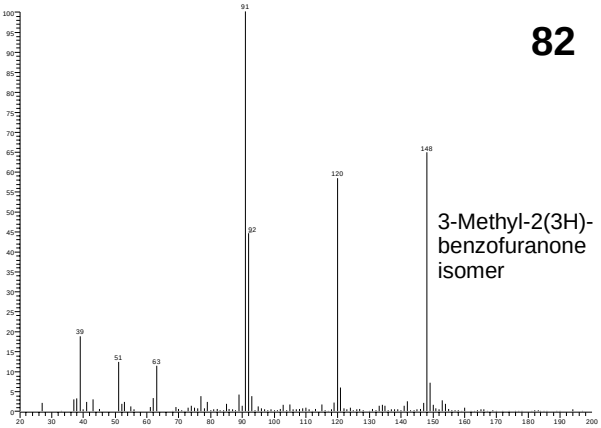

3-Methyl-2(3H)-benzofuranone isomer

83

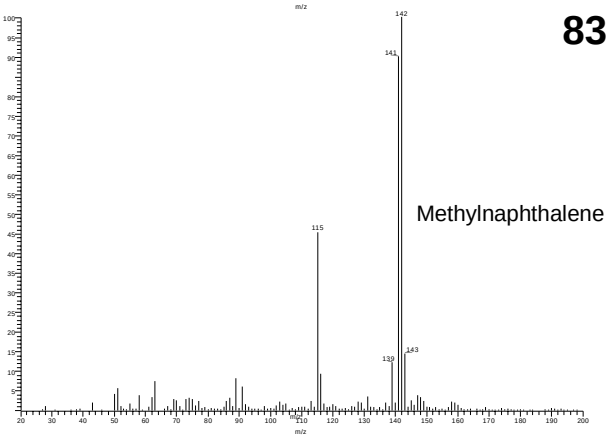

Methylnaphthalene

84

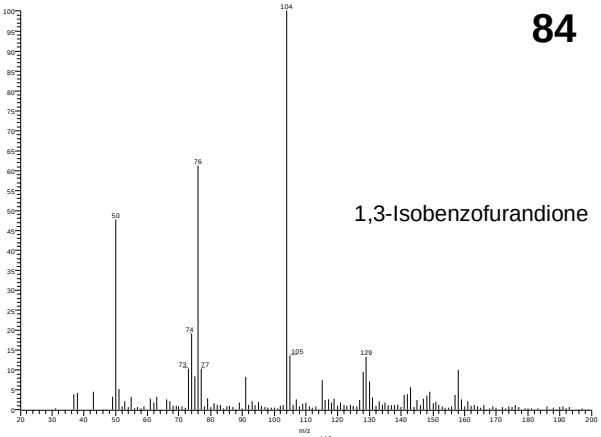

1,3-Isobenzofurandione

85

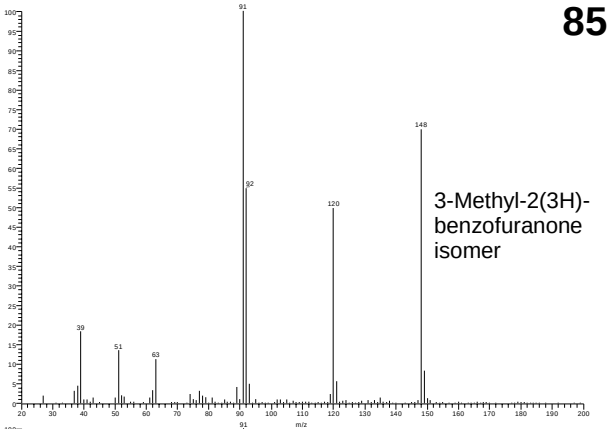

3-Methyl-2(3H)-benzofuranone isomer

86

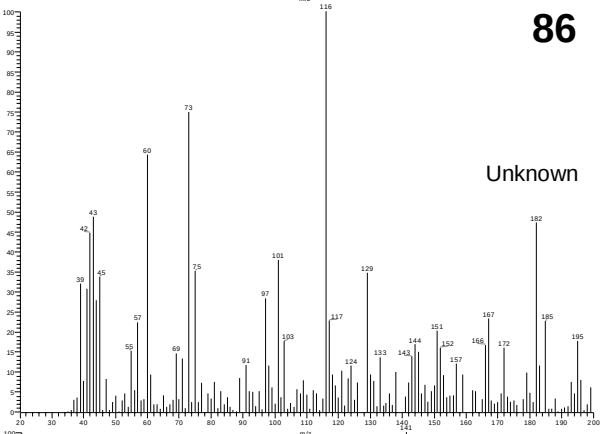

Unknown

87

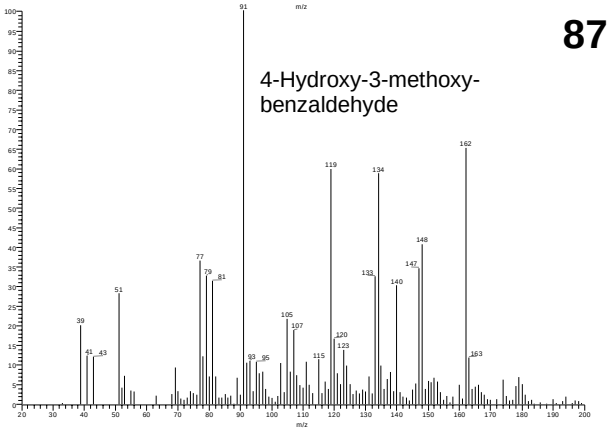

4-Hydroxy-3-methoxy-benzaldehyde

88

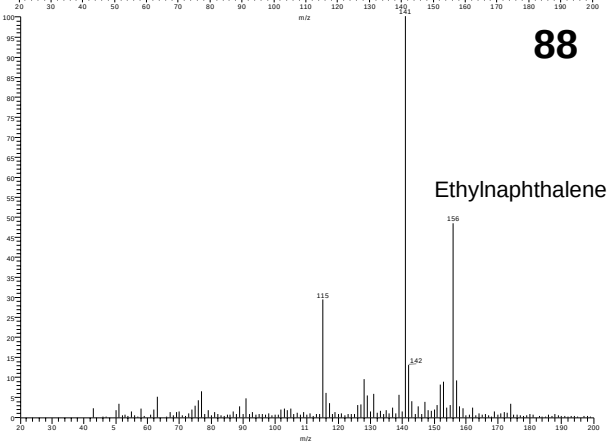

Ethylnaphthalene

89

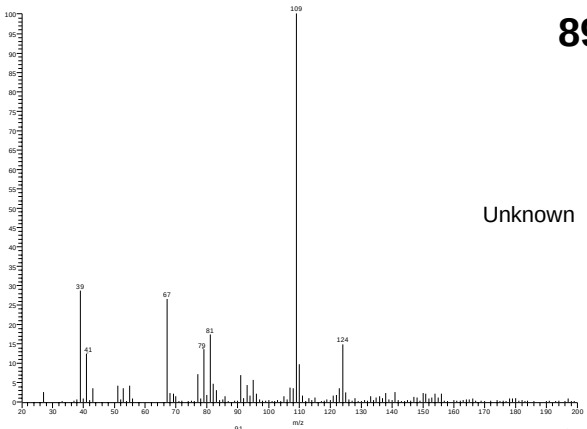

Unknown

90

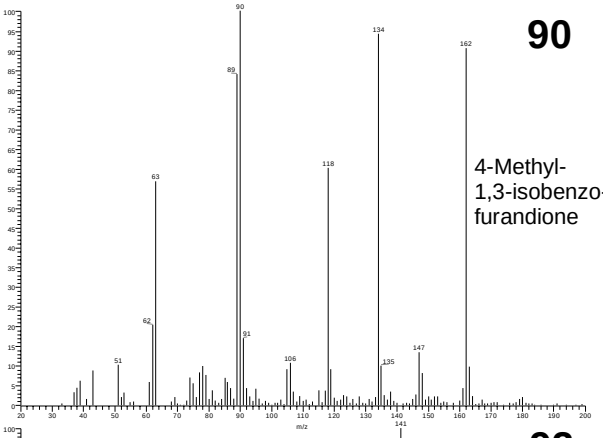

4-Methyl-
1,3-isobenzo-
furandione

91

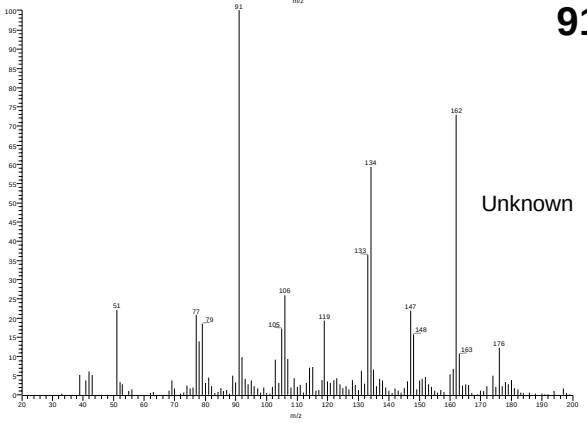

Unknown

92

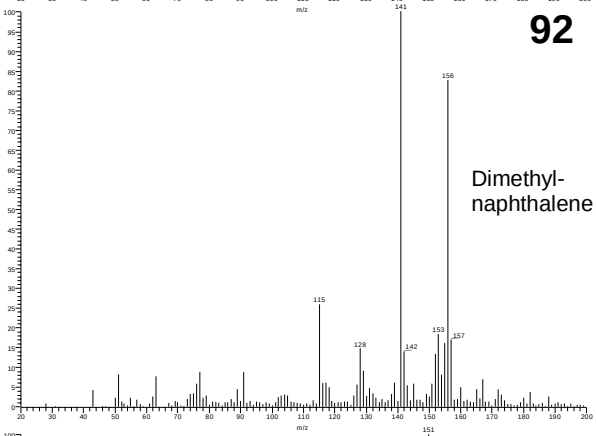

Dimethyl-
naphthalene

93

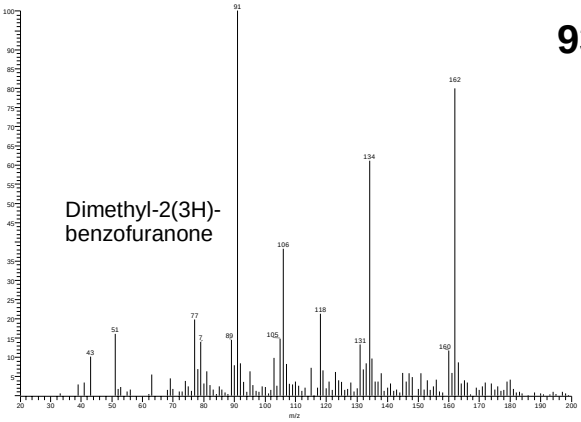

Dimethyl-2(3H)-
benzofuranone

94

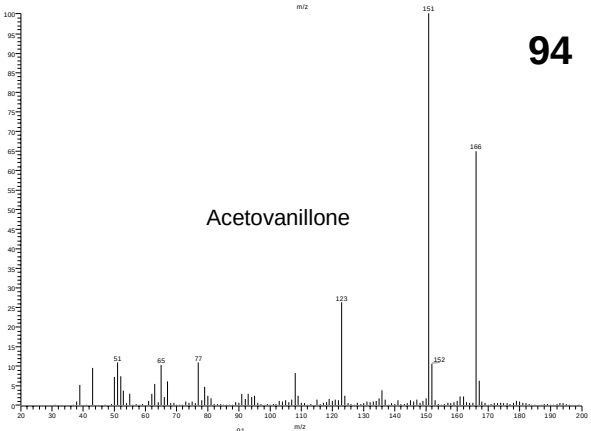

Acetovanillone

95

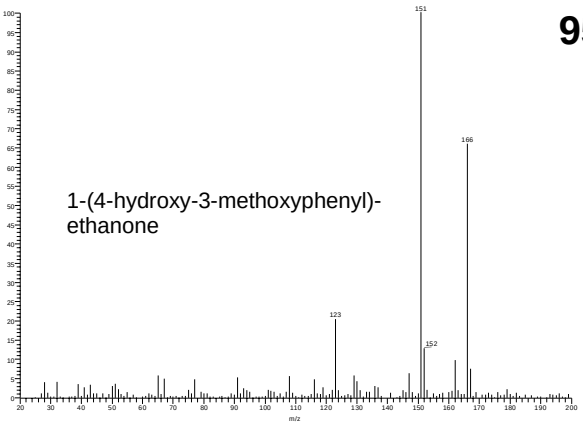

1-(4-hydroxy-3-methoxyphenyl)-
ethanone

96

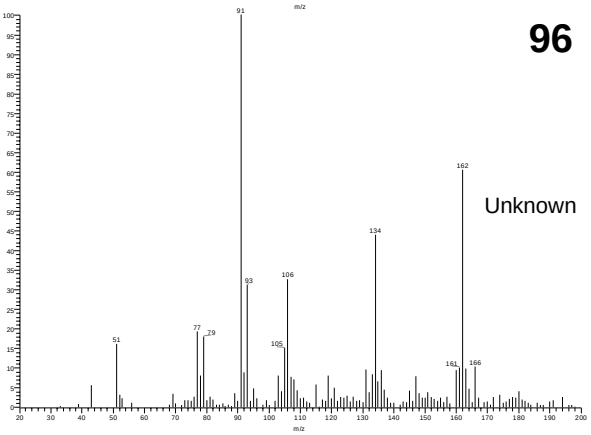

Unknown

97

4,7-Dimethyl-
1,3-isobenzofurandione
isomer

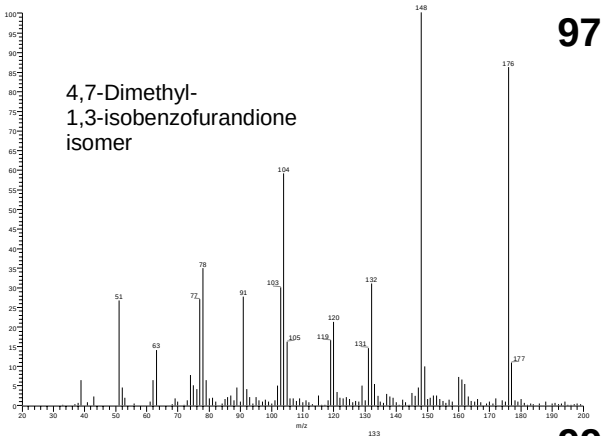

98

Anhydropyranose

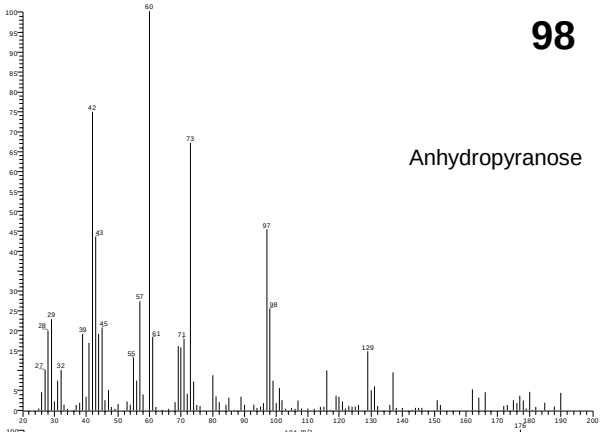

99

Methylbutyl-trimethyl-
benzene

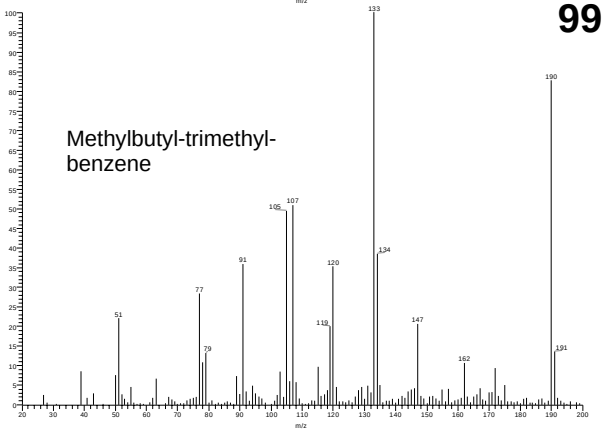

100

4,7-Dimethyl-
1,3-isobenzofurandione
isomer

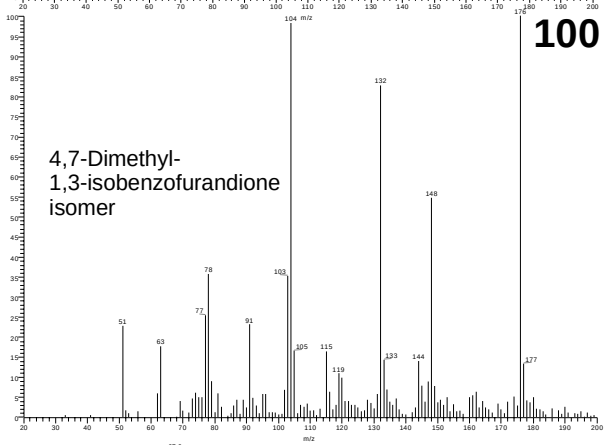

101

Unknown

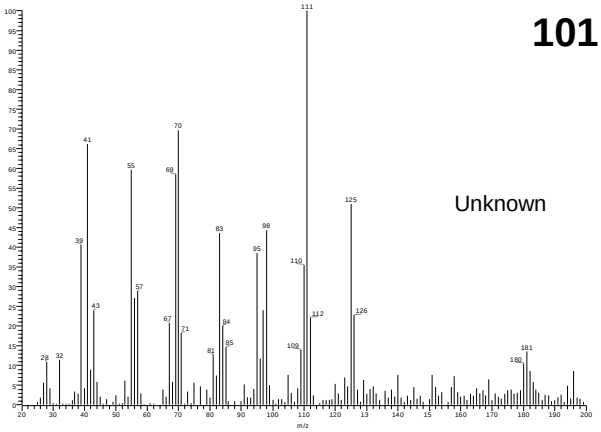

102

Unknown

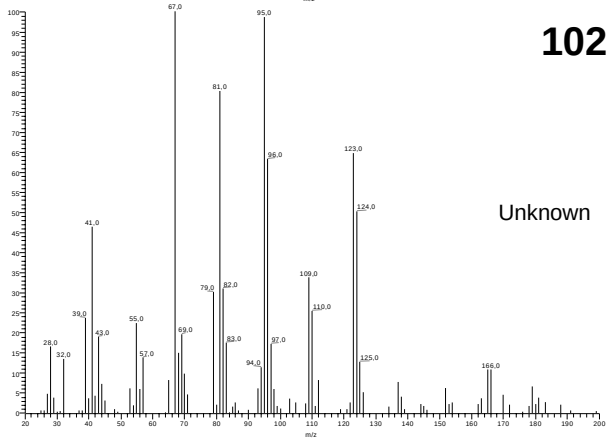

Appendix IV

Chromatograms of the ion trap-mass spectrometer (GCQ) and isotope ratio-mass spectrometer of the samples are compared in Appendix IV. Upper chromatograms represent IRMS traces (*m/z* 44) and include numbers denoting pyrolysis products mentioned in the text. Mass spectra of the pyrolysis products are given in Appendix III. MS chromatograms of the same run are normalized to 100% intensity and represent the total ion current (TIC). Due to the difference in analytes used for detection, the proportion of the peaks may vary in the chromatograms.

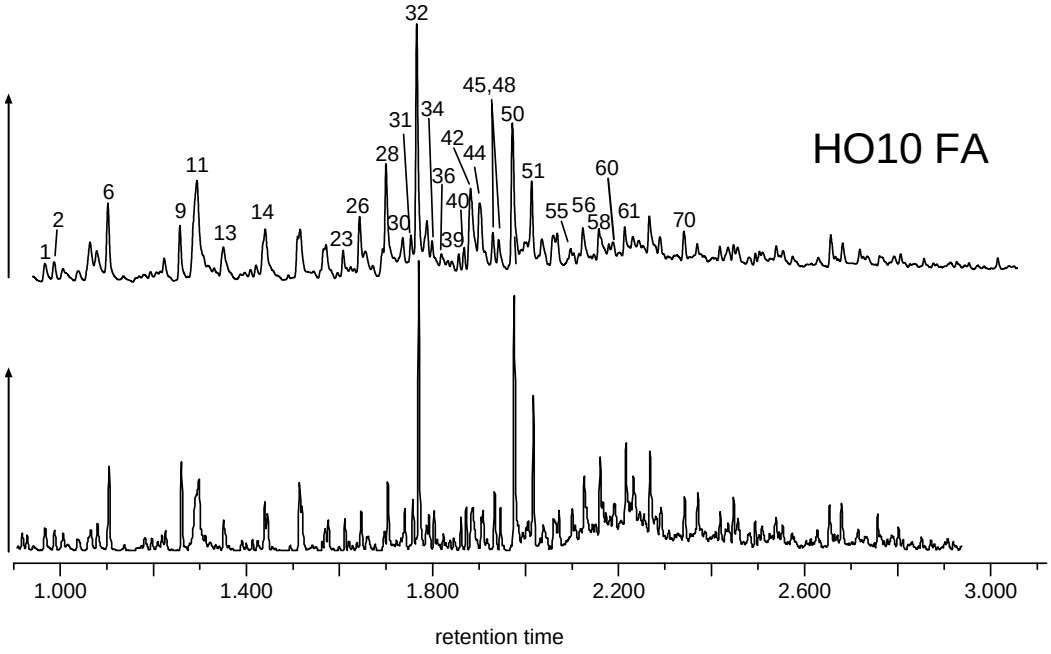
HO10 FA
1
2
6
9
11
13
14
23
26
28
30
31
32
34
36
39
40
42
44
45,48
50
51
55
56
58
60
61
70
1.000
1.400
1.800
2.200
2.600
3.000
retention time

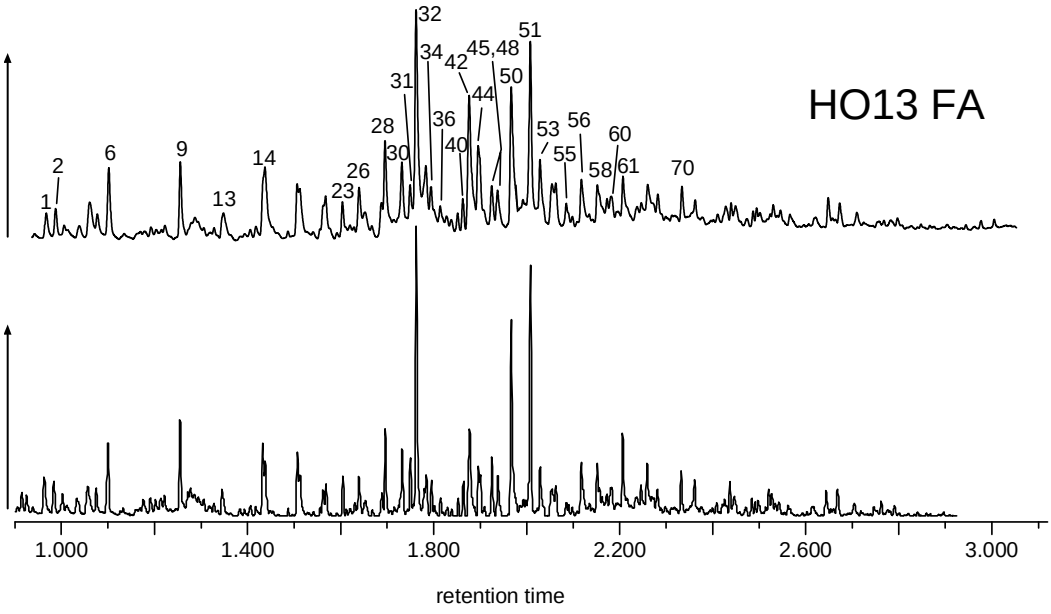
HO13 FA
1
2
6
9
13
14
23
26
28
30
31
32
34
36
40
42
44
45,48
50
51
53
55
56
58
60
61
70
1.000
1.400
1.800
2.200
2.600
3.000
retention time

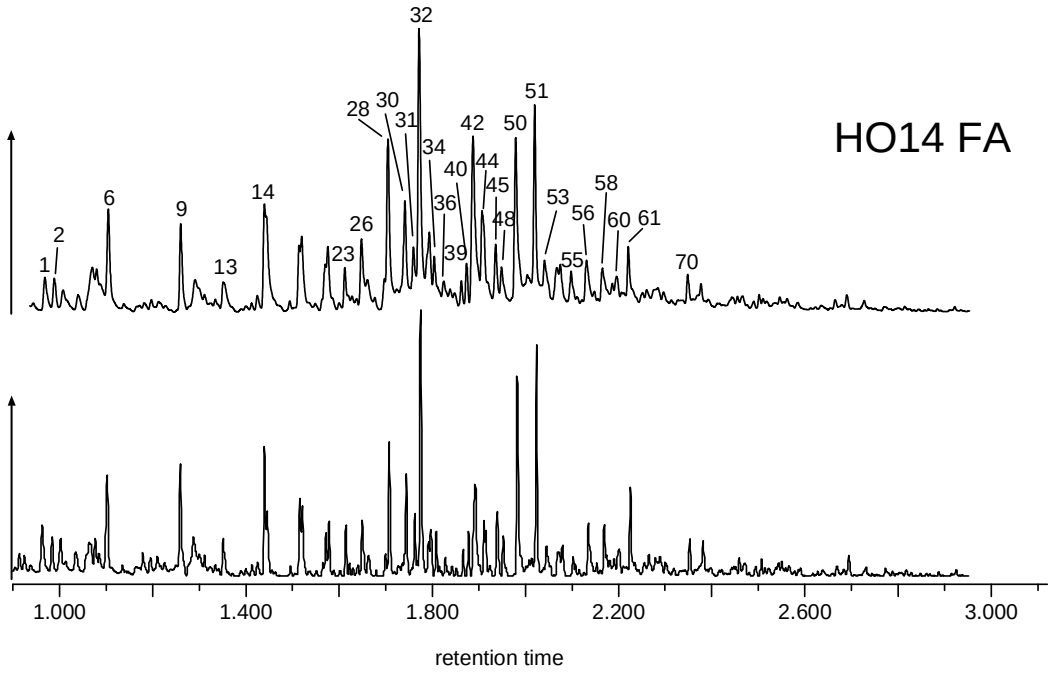
HO14 FA
1
2
6
9
13
14
23
26
28
30
31
32
34
36
39
40
42
44
45
48
50
51
53
55
56
58
60
61
70
1.000
1.400
1.800
2.200
2.600
3.000
retention time

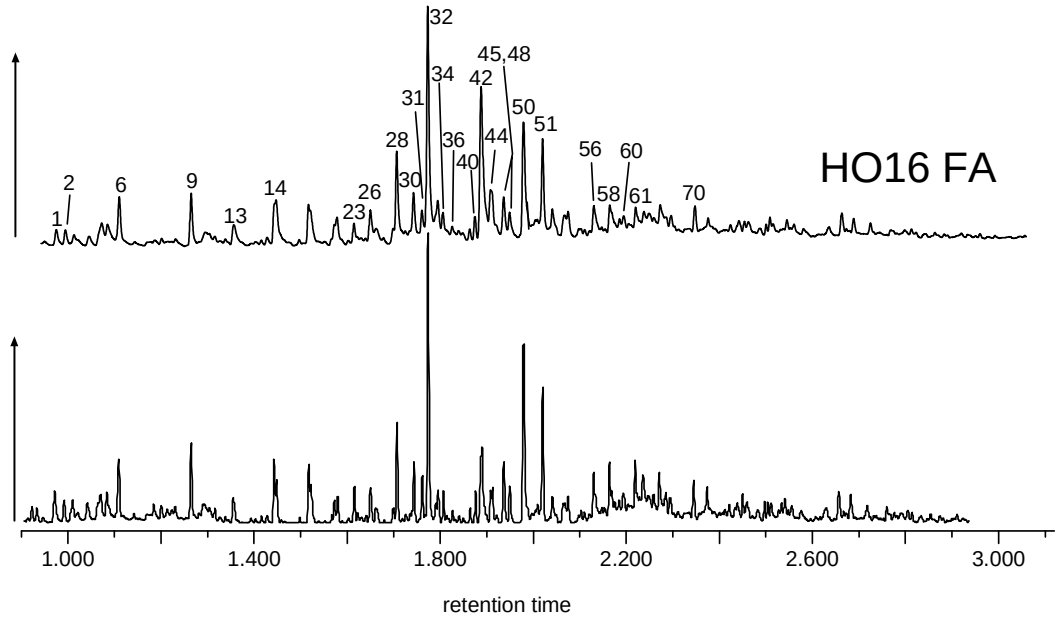
HO16 FA
1
2
6
9
13
14
23
26
28
30
31
32
34
36
40
42
44
45,48
50
51
56
58
60
61
70
1.000
1.400
1.800
2.200
2.600
3.000
retention time

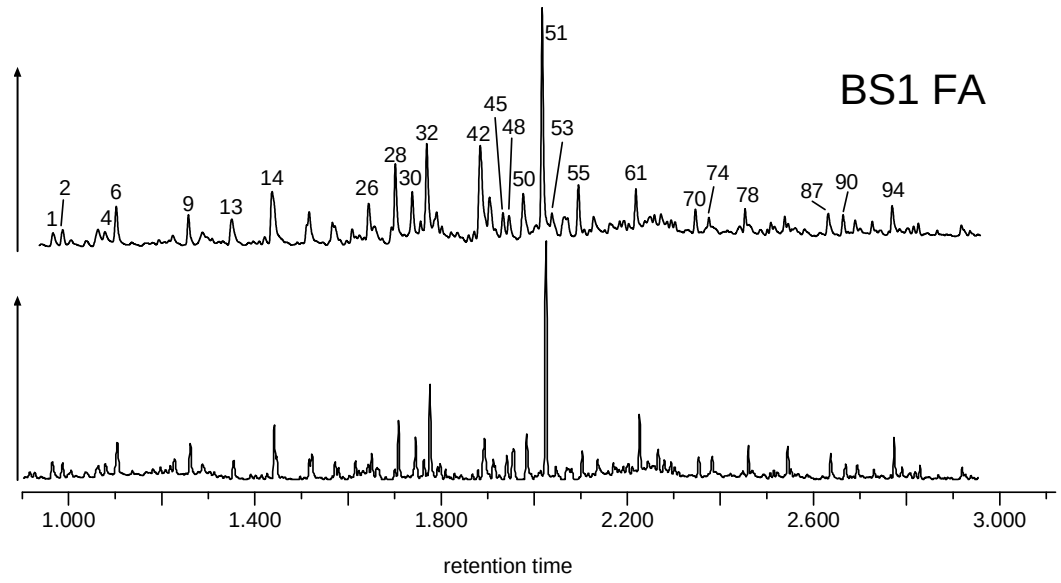
BS1 FA
1
2
4
6
9
13
14
26
28
30
32
42
45
48
50
51
53
55
61
70
74
78
87
90
94
1.000
1.400
1.800
2.200
2.600
3.000
retention time

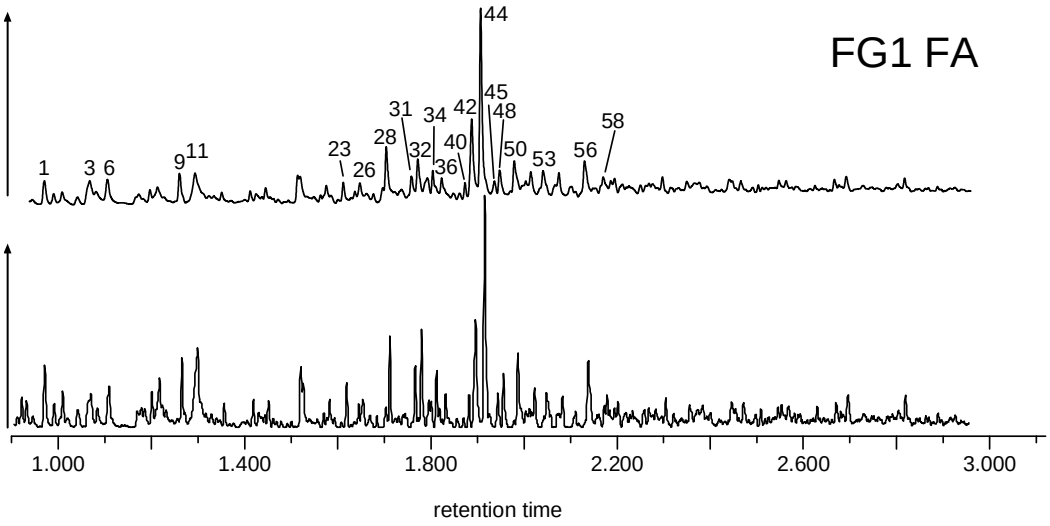
FG1 FA
1
3
6
9
11
23
26
28
31
32
34
36
40
42
44
45
48
50
53
56
58
1.000
1.400
1.800
2.200
2.600
3.000
retention time

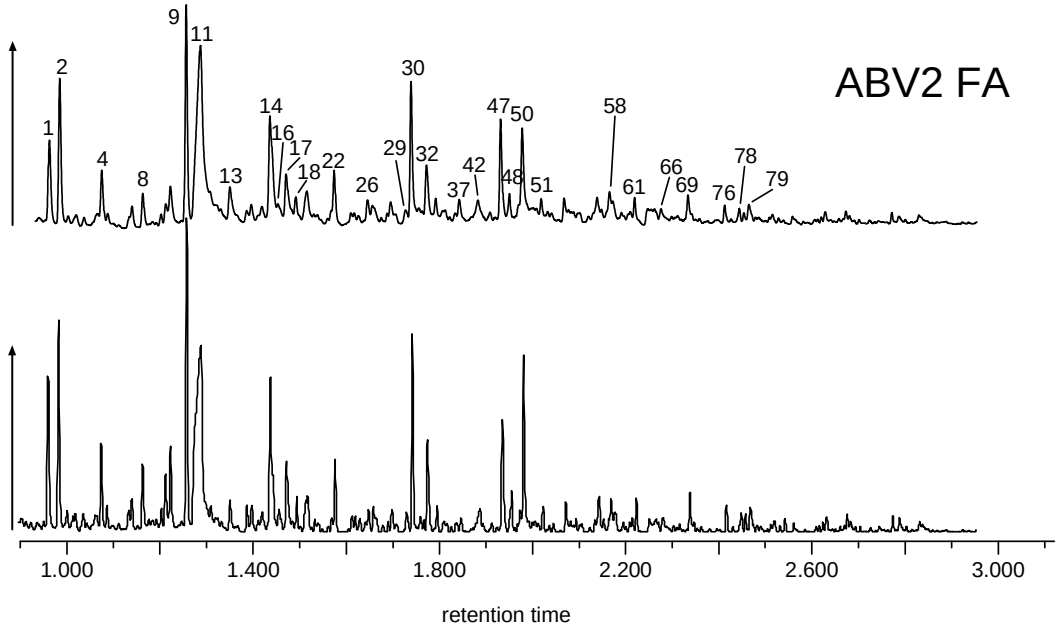
ABV2 FA
1.000
1.400
1.800
2.200
2.600
3.000
retention time

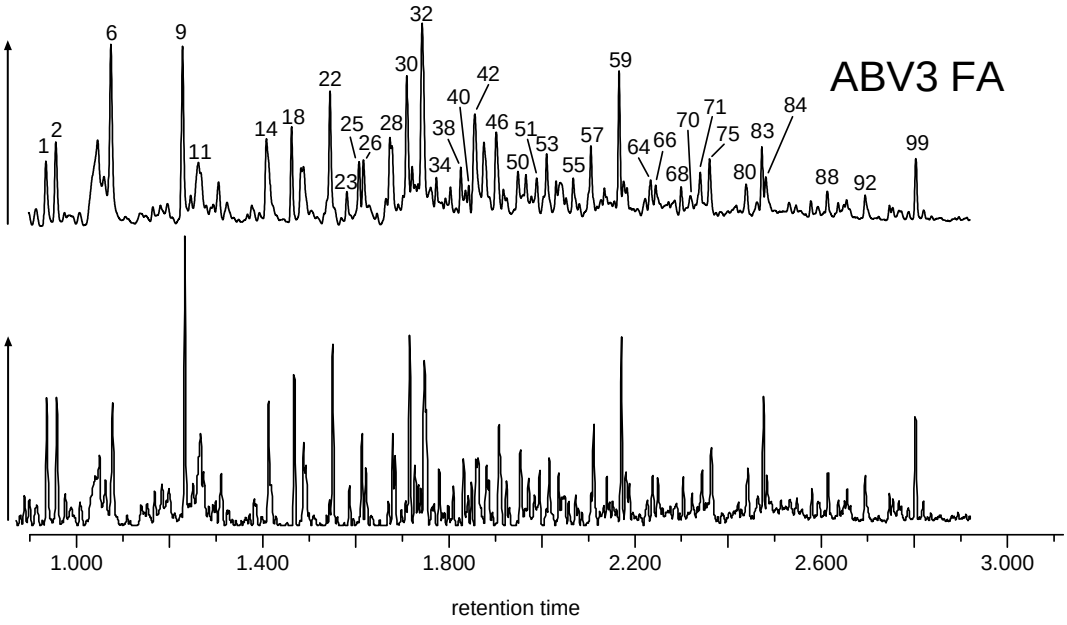
ABV3 FA
1.000
1.400
1.800
2.200
2.600
3.000
retention time

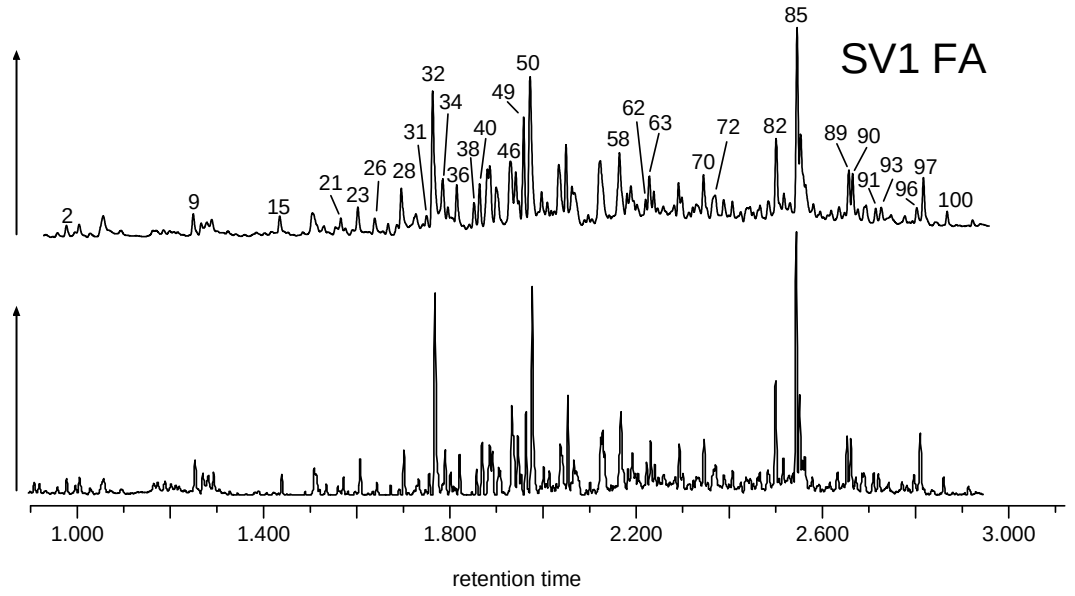
SV1 FA
85
32
50
49
34
62
63
72
82
31
40
58
89
90
38
46
70
93
97
26
28
21
36
91
96
23
9
15
2
100
1.000
1.400
1.800
2.200
2.600
3.000
retention time

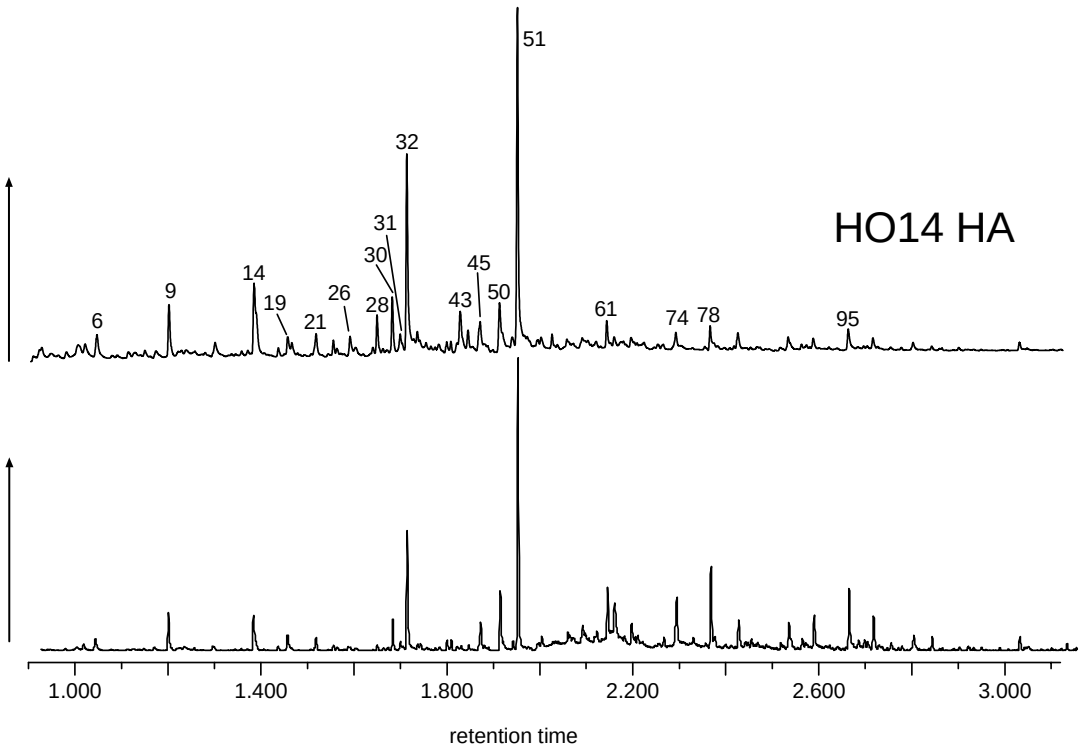
HO14 HA
51
32
31
30
45
14
9
26
19
43
50
61
74
78
6
21
28
95
1.000
1.400
1.800
2.200
2.600
3.000
retention time

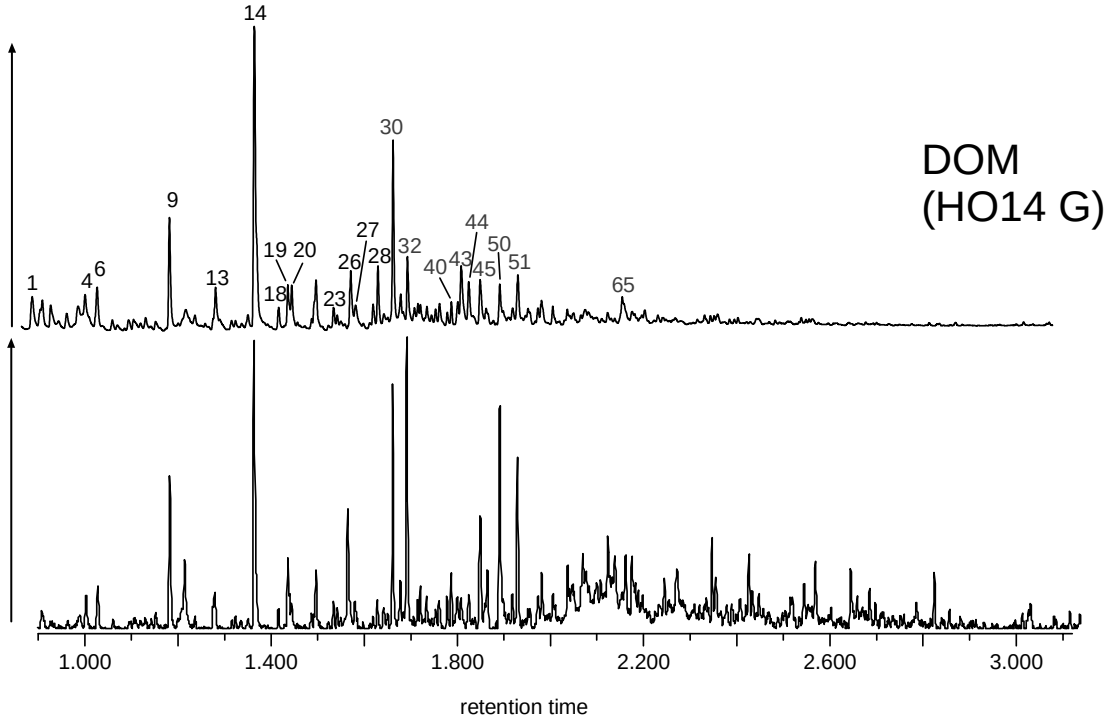
DOM
(HO14 G)
1
4
6
9
13
14
18
19
20
23
26
27
28
30
32
40
43
44
45
50
51
65
1.000
1.400
1.800
2.200
2.600
3.000
retention time

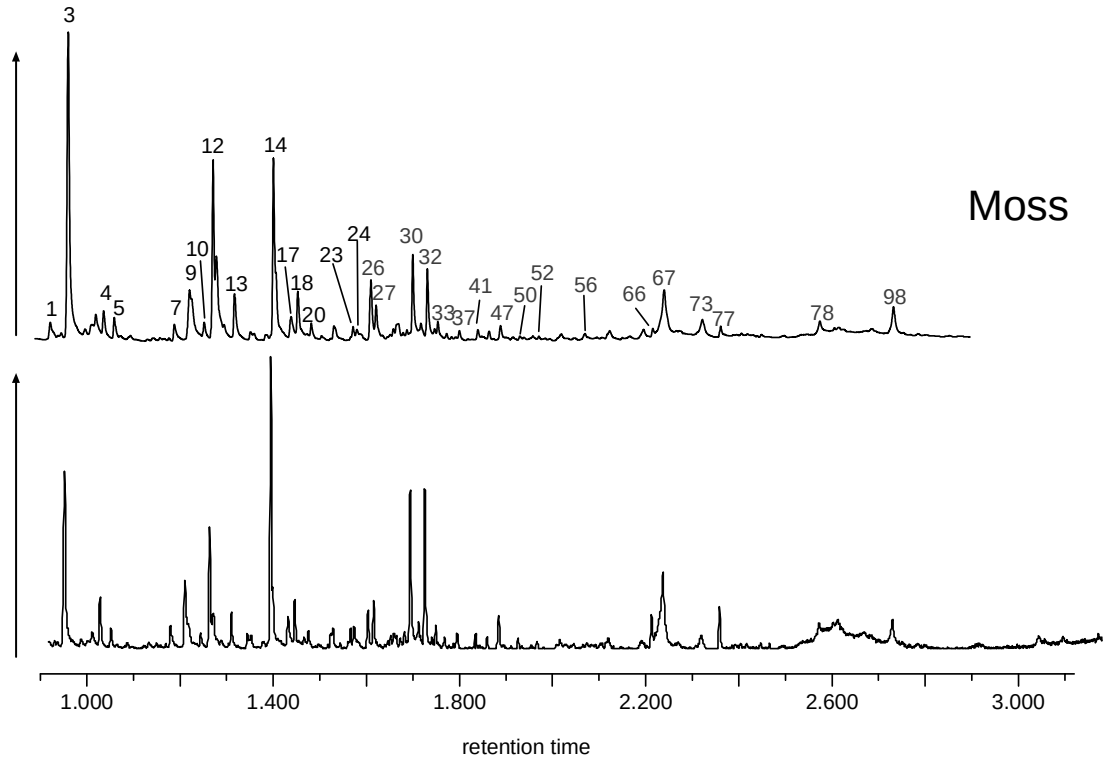
Moss
1
3
4
5
7
9
10
12
13
14
17
18
20
23
24
26
27
30
32
33
37
41
47
50
52
56
66
67
73
77
78
98
1.000
1.400
1.800
2.200
2.600
3.000
retention time

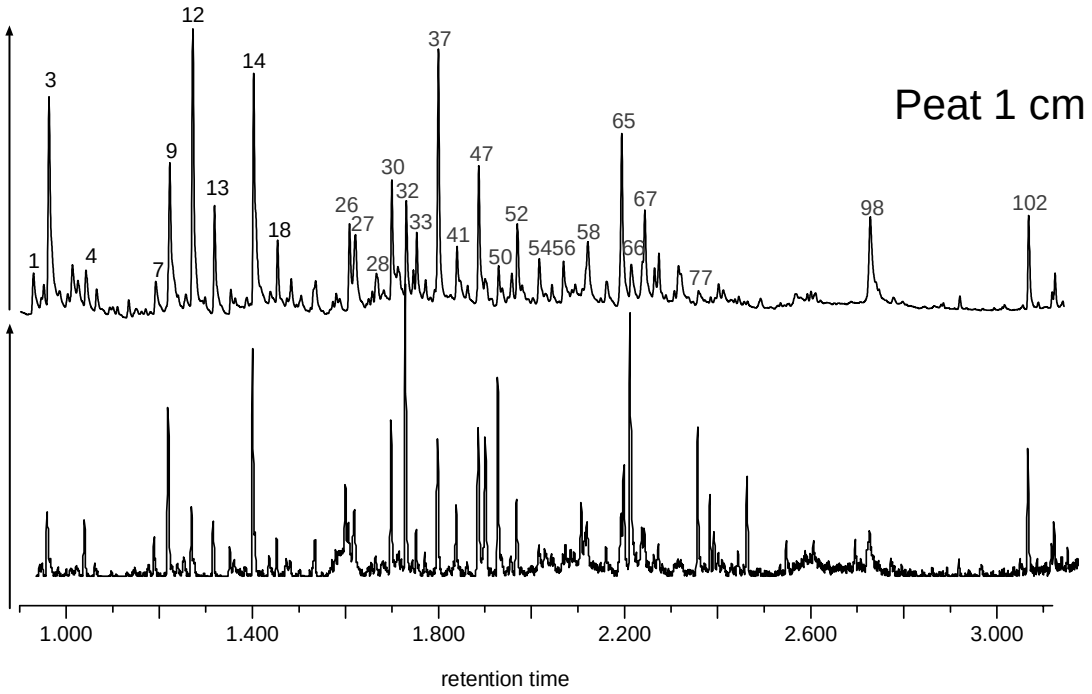
Peat 1 cm
1
3
4
7
9
12
13
14
18
26
27
28
30
32
33
37
41
47
50
52
54
56
58
65
66
67
77
98
102
1.000
1.400
1.800
2.200
2.600
3.000
retention time

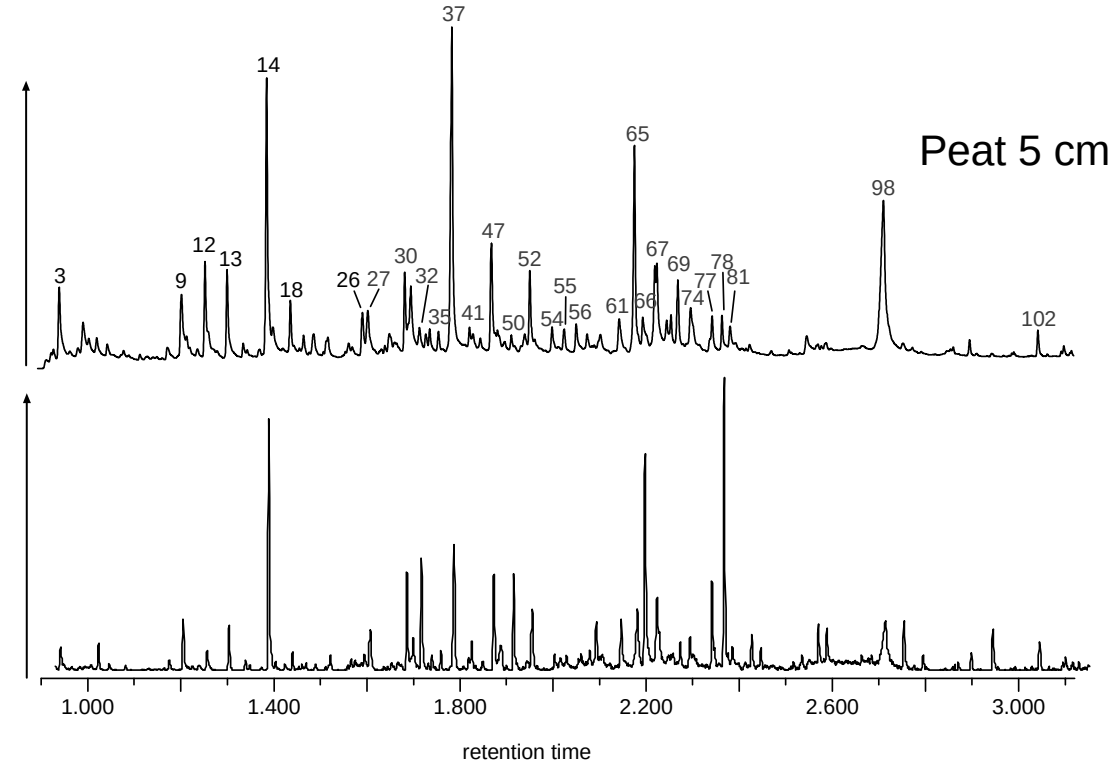
Peat 5 cm
3
9
12
13
14
18
26
27
30
32
35
37
41
47
50
52
54
55
56
61
65
66
67
69
74
77
78
81
98
102
1.000
1.400
1.800
2.200
2.600
3.000
retention time

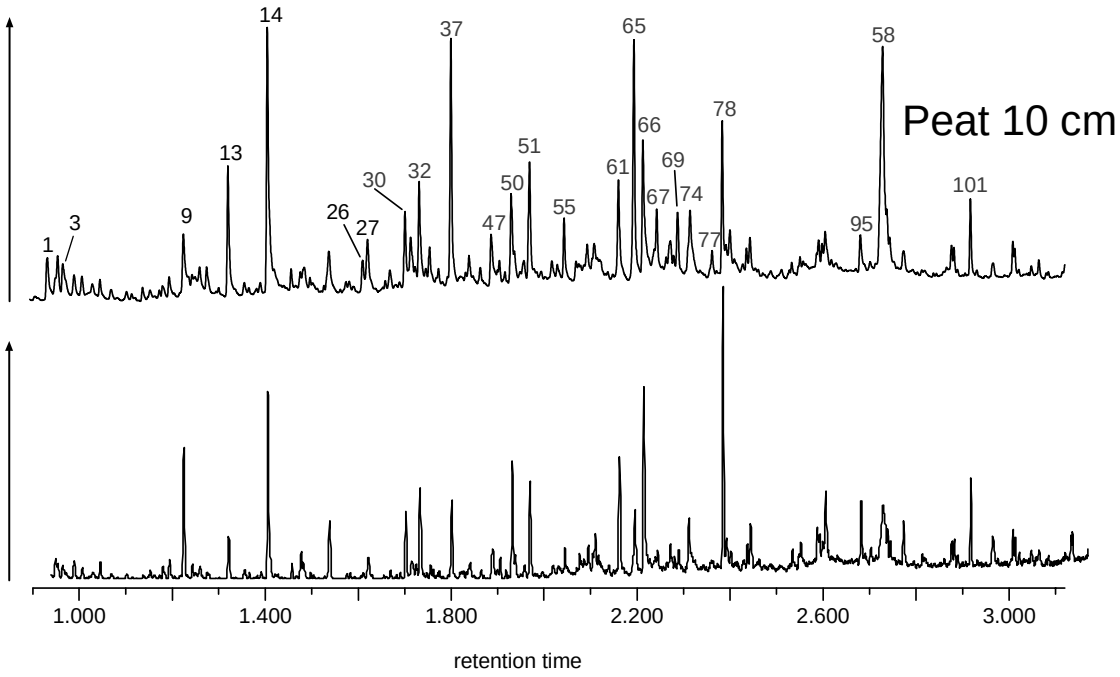
Peat 10 cm
1
3
9
13
14
26
27
30
32
37
47
50
51
55
61
65
66
67
69
74
77
78
95
58
101
1.000
1.400
1.800
2.200
2.600
3.000
retention time

Appendix V

The following is s a reprint of the paper by Kracht and Gleixner (2000), published in Organic Geochemistry 31(7-8), 645-654.

PERGAMON

Organic Geochemistry 31 (2000) 645–654

Organic Geochemistry

www.elsevier.nl/locate/orggeochem

Isotope analysis of pyrolysis products from *Sphagnum* peat and dissolved organic matter from bog water

Oliver Kracht, Gerd Gleixner *

Max-Planck-Institut für Biogeochemie, Postfach 100164, 07701 Jena, Germany

Abstract

Elemental analyses (H, N, C, O, S), bulk isotope analyses (^{13}C, ^{15}N) and ^{13}C content of pyrolysis products from *Sphagnum* moss, underlying peat from a bog and the bog water (Hohlohsee, Black Forest, Germany) were performed to identify humification processes in the early diagenesis of peat formation and to determine the origin of dissolved organic matter (DOM) in the bog lake. Atomic ratios of bulk elemental analysis suggest a compositional shift from carbohydrate dominated structures to phenolic polymers. Observed variations of bulk $\delta^{15}N$ and total nitrogen are likely due to microbial production. Combining isotopic and structural information using a coupled Py-GC/MS-IRMS system provides further information on the peat formation, e.g. biogeochemical processes of (1) biological degradation of source material, (2) selective preservation of individual compounds, and (3) formation of microbial biomass (e.g. trophic level effect). In particular, the stable isotope data helped to identify microbial processes as a source for carbohydrate pyrolysis products in deeper horizons. The comparison of pyrolysis products from peat and DOM from the bog lake indicates different sources. From the isotope ratios of pyrolysates it is suggested that DOM is formed in situ by microbial production and not simply dissolved from the peat profile. The uptake of ^{13}C depleted carbon, e.g. respired CO_2, CO_2 from the oxidation of methane or acetic acid is proposed as an important factor in the formation of dissolved organic matter.

Keywords: Humification; DOM; C-13; Hohlohsee; Py-GC/MS; Isotope ratio-mass spectrometry

1. Introduction

Soil organic matter (SOM) in peat plays a major role in the global CO_2 dynamics and consequently in the global climatic change (Öquist and Svensson, 1996; Charman et al., 1999). Neither the processes controlling the accumulation, stabilization and degradation of organic matter in peatlands and boreal regions, nor their behavior after climatic change are well understood. Of particular interest is the formation of dissolved organic matter (DOM) from peatland soils because the export of DOM from these ecosystems may constitute a major sink for carbon.

Measurements of stable isotope composition of OM have become an important tool to investigate the biogeochemical processes occurring in peat, soil and sediments (Nadelhoffer and Fry, 1988; Balesdent et al., 1993; Hedges and Oades, 1997; Ficken et al., 1998; Gleixner et al., 1999). Biogeochemical transformations are accompanied by isotope fractionations which are indicative of the processes involved. The isotopic signal of plant material, the initial substrate for humification, is determined primarily by fractionation processes occurring during photosynthesis. Additionally, due to varying (bio-)chemical compositions, carbon isotope ratios vary between different plant tissues. Leaves are commonly enriched in ^{13}C relative to the bulk material, whereas roots can be relatively enriched or depleted in ^{13}C (Nadelhoffer and Fry, 1988; Balesdent et al., 1993; Lichtfouse et al., 1995; Wedin et al., 1995). Lignins and other woody tissues are generally depleted in ^{13}C relative

* Corresponding author. Tel.: +49-3641-643707; fax +49-3641-643710.

E-mail address: gerd.gleixner@bgc-jena.mpg.de (G. Gleixner).

0146-6380/00/$ - see front matter
PII: S0146-6380(00)00041-3

to carbohydrates by 3 to 6‰ (Leavitt and Long, 1986; Benner et al., 1987; Gleixner et al., 1993). A net fractionation effect is also introduced by different decomposition rates of these organic molecules (Ågren et al., 1996; Miyajima et al., 1997). Therefore the use of bulk isotope measurements to understand soil carbon biogeochemistry is limited as observed changes of the isotope signal can reflect differing molecular compositions. However, detailed information can be revealed from the examination of compound specific isotope ratios (Hayes et al., 1990; Macko et al., 1990; Rieley et al., 1991; Schmidt et al., 1993; Lichtfouse et al., 1998). The change in the isotopic signal of individual compounds reflects biochemical conversion of corresponding source molecules (Macko et al., 1991; Balzer et al., 1997). In contrast, constant values indicate "preservation" of source molecules (Lichtfouse et al., 1998). For the most abundant biochemical compounds, e.g. cellulose and lignin, no selective solvents are available. Therefore time consuming chemical degradation, laborious sample clean up and additional derivatization steps have to be applied. All of these steps may cause isotope fractionation (Silfer et al., 1991; Demmelmair and Schmidt, 1993; Rieley, 1994).

To overcome these problems we used thermal degradation (flash pyrolysis, Py) to extract volatile products from solid, whole peat samples (freeze-dried and milled) and separated the pyrolysis products in a gas chromatograph (GC). The eluting substances were subsequently analyzed using ion-trap MS and simultaneously using IRMS (Gleixner et al., 1999). The applicability, reliability and limitations of pyrolysis for isotope measurements on pyrolysis products of organic compounds have already been demonstrated (Goñi and Eglinton, 1994; Gleixner and Schmidt, 1998; Pulchan et al., 1997). Here we apply this technique to samples of *Sphagnum* moss, peat and DOM from a peat profile in southern Germany, in order to demonstrate that the combination of molecular and isotope information can identify different humification processes and the origin of DOM in bog water.

2. Materials and methods

2.1. Materials

Samples were taken in June 1998 at the Hohlohsee, a bog lake in the Black Forest, Germany. The Hohlohsee is recharged only by precipitation and the water table is kept to a maximum level by a natural overflow. Consequently, peat at 5 cm depth is affected by minor water level fluctuations whereas peat at 10 cm is permanently below the water table. Peat was sampled at 1, 5, and 10 cm depth below the *Sphagnum* moss vegetation. These three depths were associated with distinct layers, distinguishable on the basis of color; samples becoming darker with depth. All samples, including the overlying moss, were freeze-dried and milled. DOM was isolated from unfiltered bog water sampled at a depth of 50 cm below water surface and freeze-dried.

2.2. Elemental analyses and ash content

Elemental analysis of H, C, N, O, and S was performed in a Vario EL (Elementar Analysensysteme GmbH, 63452 Hanau, Germany). For H, C, N, S measurements about 20 mg of sample material was combusted (temperature setting 1050°C). The oxidation products were reduced at 850°C to obtain N_2, SO_2, CO_2 and H_2O. After GC separation the gases were quantified by thermal conductivity. For the determination of the oxygen content about 1.5 mg of sample material was pyrolyzed (temperature setting at 1180°C) and all oxygen was converted to CO. After separation the amount of oxygen was quantified using a thermal conductivity detector.

The ash content of sample material was determined gravimetrically (TGA, Mettler-Toledo GmbH, 35396 Gießen, Germany) at a furnace temperature setting of 1000°C under pure oxygen.

2.3. Bulk isotope analysis

About 2 mg of sample material was combusted in an EA 1110 Elemental Analyzer (ThermoQuest, 20090 Rodano, Italy) using tin capsules (oxidation furnace setting 1020°C; reduction furnace setting 650°C). CO_2 and N_2 were separated by gas chromatography and analyzed for ^{13}C and ^{15}N in a Delta^{Plus}XL isotope ratio mass spectrometer (Finnigan MAT, 28127 Bremen, Germany). $\delta^{13}C$ and $\delta^{15}N$ values are expressed relatively to international standards V-PDB and atmospheric air, respectively.

2.4. Pyrolysis-gas chromatography–mass spectrometry-isotope ratio-mass spectrometry (Py-GC/MS-IRMS)

About 0.2–1 mg of solid sample was pyrolyzed in a Curie-point pyrolyzer (type 0316, Fischer, 53340 Meckenheim, Germany) using a ferro-magnetic sample tube. The pyrolysis products were transferred online to the GC. Pyrolysis temperature was 500°C; pyrolysis time 9.9 s; interface temperature was set to 250°C. Following split injection (split ratio approx. 10:1, flow rate 1.6 ml/min) the pyrolysis products were separated on a BPX 5 column (60 m×0.32 mm, film thickness 1.0 μm, Scientific Glass Engineering, 64331 Weiterstadt, Germany) in a HP 5890 (76337 Waldbronn, Germany) using a temperature program of 36°C for 5 min, then 5°C/min to 270°C followed by a jump (30°C/min) to a final temperature of 300°C. The injector temperature was set to 250°C. The column outlet was coupled to a fixed splitter (split ratio approx. 1:9). The major proportion was

transferred to a combustion furnace converting the pyrolysis products to CO_2, N_2 and H_2O (CuO, NiO and PtO, set at 960°C) and the $\delta^{13}C$ values were determined using an isotope ratio-mass spectrometer (Delta^{Plus}XL, Finnigan MAT, 28127 Bremen, Germany); dynamic background correction by ISODAT 7.0 software was applied (Finnigan MAT, 28127 Bremen, Germany). The threshold intensity for peak detection at the IRMS was set to 200 mV. This value was found to optimize the amount of peaks used for isotope determination and ion-source linearity, to minimize background effects and to reduce the isotopic influence of not entirely base-line separated peaks.

The minor proportion of the GC-eluates after the fixed splitter was transferred to an ion-trap mass spectrometer (GCQ, ThermoQuest, 63329 Egelsbach, Germany). The transfer line was heated to 270°C and source temperature was held at 180°C. Pyrolysis products were ionized by electron impact (EI) with 70 eV ionization energy and identified by comparison with reference spectra using GCQ identification software 2.2 and Wiley 6.0 mass spectra library based on the mass range m/z 25 to 450. Additionally, external standards and reference spectra from the literature were used (Van Smeerdijk and Boon, 1987; Stout et al., 1988; Durig et al., 1991; Ralph and Hatfield, 1991).

2.5. Calculations and data interpretation

Relative amounts of single pyrolysates were calculated by using the m/z 44 trace of the IRMS chromatogram used for $\delta^{13}C$ analyses. The amount of CO_2 produced by combustion of a single substance was normalized to the total amount of CO_2 in the analytical window (expressed in percentage of peak area to total area integrated over a fixed time interval). This method avoids the sometimes inaccurate results obtained by simple peak-to-peak relations and gives reasonable indication for the peak patterns obvious from the chromatograms.

3. Results and discussion

3.1. Bulk elemental analyses

The carbon content of the moss and peat samples increased with depth of the profile from 44.5% in the *Sphagnum* layer to 47.9% at 10 cm, while the amount of oxygen and hydrogen decreased from 45.6 to 30.1% and from 6.3 to 5.3%, respectively (Table 1). Major differences in composition are indicated between peat 10 cm and the overlying layers. In an O/C and H/C diagram (Fig. 1) these differences represent a dehydration process affecting the sample at 10 cm depth (Van Krevelen, 1993), i.e. a primary loss of hydroxyl groups. Alternatively, the observed shift can be explained by different decomposition rates of biomolecules. Moss and peat of 1 and 5 cm depth show H/C ratios close to cellulose (H/C: 1.67) whereas peat at 10 cm depth plots close to a region representative for phenylpropanes. Cellulose is known to be readily degraded (Deines, 1980; Benner et al., 1987) and this shift may also imply that the upper 5 cm are in an early stage of degradation. Alternatively, the permanent water saturation of peat in 10 cm depth might have inhibited particularly oxidative degradation of phenolic substances (Haider, 1996) and consequently accumulated these substances. However, the high ash content in peat 10 cm compared with the other samples indicates the progress of mineralization with depth.

The nitrogen content in the peat profile varies from 1.1% in the moss to 1.9% in 10 cm depth with a notable enrichment of 2.5% in 1 cm depth (Table 1). These variations of total N are assumed to reflect the different microbial activities in the profile. This would be in line with findings that peat samples are enriched in amino acids at the surface (Macko et al., 1990). However, the varying N contents of the samples from the Hohlohsee could be additionally influenced by the changing conditions, e.g. the change from oxygenated to reduced conditions as can be expected by water level fluctuations up to peat 5 cm. Products from nitrification and denitrification processes can account for the total N decrease from peat 10 cm to peat 5 cm. Nitrous oxide (N_2O), for example, has been found to be mainly produced at the water/air boundary (Schmidt et al., 1992) and subsequently released to the atmosphere. We can only speculate on the processes behind the N variations but microbial activity is most likely to be the cause of N variations. This is also discussed below in combination with $\delta^{15}N$ values.

The elemental composition of the water sample differs from that of the peat samples (Table 1, Fig. 1). Slightly lower amounts of H may be indicative of less aliphatic structures in DOM. Sulfur in the bog water is enriched by one order of magnitude compared to nearly constant values over the peat profile. This enrichment can be attributed to atmospheric input of sulfuric acid since acid rain is a known problem in the Black Forest for the last 20 years. Isotopic evidence for predominant atmospheric input of S in two forested catchments in the Black Forest has been reported (Mayer et al., 1995).

3.2. Bulk isotopic analyses

$\delta^{13}C$ values of the bulk samples were consistently around −26‰ (Table 1). In contrast to the atomic ratios the constancy in ^{13}C over the peat profile indicates that structural changes play only a minor role. An accumulation of lignins, as has been reported previously in low oxygenated, water saturated soils based on ^{13}C depletions (Deines, 1980; Benner et al., 1987), does not occur. This would be consistent with findings that lignins are absent from *Sphagnum* (Lewis et al., 1999) and, hence, from

Table 1
Elemental composition (C, N, S, H, and O) in wt.% and bulk isotope analyses (^{13}C and ^{15}N) of *Sphagnum* moss, different layers of peat and dissolved organic matter (DOM) from bog lake water with standard deviations (S.D.)

	%C	%N	%S	%H	%O	%ash	sum	$\delta^{15}N$	s.d.	$\delta^{13}C$	s.d.
Moss	44.5	1.1	0.1	6.3	45.6	1.7	99.2	0.1	0.4	−26.3	0.8
Peat 1 cm	44.4	2.5	0.4	6.2	41.6	5.6	100.7	0.1	0.5	−26.5	0.7
Peat 5 cm	45.6	1.1	0.3	6.5	42.9	2.2	98.6	−0.7	0.3	−26.1	0.4
Peat 10 cm	47.9	1.9	0.3	5.3	30.1	13.3	98.8	0.4	0.1	−26.9	0.2
DOM	44.1	1.2	1.4	4.6	43.1	7.9	102.3	−2.1	0.2	−26.3	0.3

Sphagnum derived peat. The $\delta^{15}N$ values in the peat profile were about 0‰, a value expected for a low nitrogen ecosystem having only atmospheric deposition of nitrogen (Schmidt et al., 1992). The slight shift of ^{15}N in peat 5 cm may be at least partly due to an occurrence of isotopically depleted amino acids in bacteria and fungi. It is possible that the nitrogen content, particularly above the water level, varies with the production of amino acids by bacterial and fungal growth and that isotope variations are caused by interaction of several biochemical reactions (Macko and Estep, 1984). Further analyses using N-isotope signatures of pyrolysis products from amino acids will help to identify these processes.

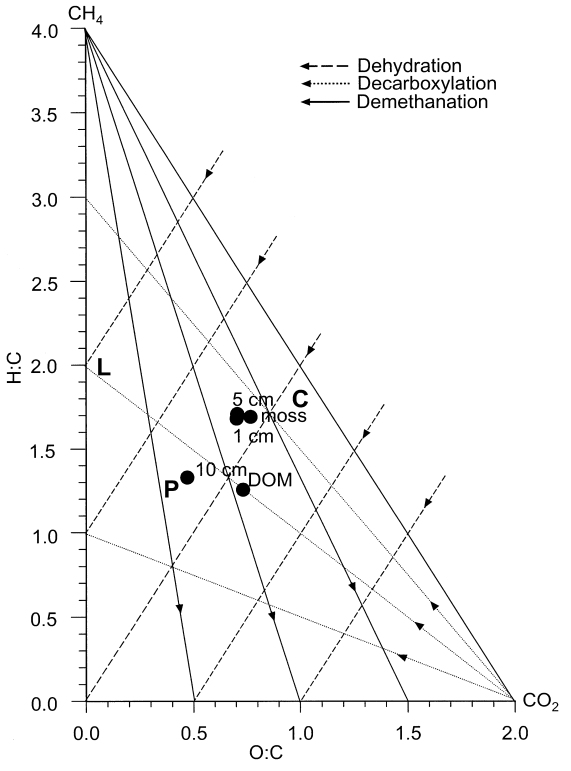

Fig. 1. Molar ratios of O/C versus H/C of bulk samples from *Sphagnum* moss, peat of given depth and dissolved organic matter (DOM) from bog lake water. Positions of important biological compounds such as carbohydrates (C), lignins (P, phenylpropanes) and lipids (L) are indicated. See text for discussion. The lines represent different condensation reactions in the formation of coal (after van Krevelen, 1993).

The $\delta^{13}C$ value of the DOM (bog water) matches exactly the value for the soil organic matter (SOM) fraction and therefore suggests that it could be directly released from the SOM pool. In contrast, the $\delta^{15}N$ value of DOM is notably depleted by 2‰ relative to the SOM pool. This strongly contradicts a simple solving mechanism from the peat. As partly discussed above and reported by Claus et al. (1999) and Macko and Estep (1984), this can be an effect of microbial interaction. Alternatively, an uptake of isotopically "light" N from atmospheric nitrogen fixed by azotrophic microorganisms or the consumption of isotopically depleted N_2O is also conceivable. More detailed investigations are needed.

3.3. Pyrolysis products of moss, peat and DOM

Only major peaks in the IRMS-chromatograms were identified using the ion-trap MS, since only these were suitable for simultaneous isotope ratio determinations. The relative amounts of pyrolysis products from the peat and DOM samples are given in Table 2. More than 60% of the major pyrolysis products investigated for this study are derivatives of furan and phenol. Additionally, some derivatives of benzene, pyran and cycloalkenones could be identified. Furan and furaldehyde derivatives are mainly pyrolysis products of polysaccharides (Irwin, 1982; Van Smeerdijk and Boon, 1987; Stout et al., 1988; Pouwels et al., 1989; Durig et al., 1991). The other group of important pyrolysis products are derivatives of phenol which are generated from various compounds of the shikimic acid pathway. Lignin as a common precursor of phenol derivatives is assumed not to be present in *Sphagnum*. Of the substances found in the fresh moss, the pyrolysis products such as phenol, vinylphenol and isopropenylphenol can be attributed to sphagnum acid (Van Smeerdijk and Boon, 1987; Stankiewicz et al., 1997; Van der Heijden et al., 1997). 4-Ethyl-2-methoxyphenol as a pyrolysis product of the coniferyl unit is also present in the pure fresh moss. Since the contamination of the *Sphagnum* sample by lignin containing plants is highly unlikely a potential occurrence of lignin-like

Table 2
Retention time (t_R), relative amount (area) and $\delta^{13}C$-values of pyrolysis products from *Sphagnum* moss, peat and dissolved organic matter (DOM) from bog lake water[a]

t_R	Moss					Peat 1 cm					Peat 5 cm					Peat 10 cm					DOM					
(s)	Area	S.D.	$\delta^{13}C$	S.D.	*n*	Area	S.D.	$\delta^{13}C$	S.D.	*n*	Area	S.D.	$\delta^{13}C$	S.D.	*n*	Area	S.D.	$\delta^{13}C$	S.D.	*n*	Area	S.D.	$\delta^{13}C$	S.D.	*n*	
1038	1.8	–	−25.8	–	1	0.9	–	−24.1	–	2																Furan, 2,5-dimethyl
1212	4.5	2.0	−21.7	0.6	3	2.9	0.1	−29.5	0.9	3	1.7	0.2	−23.8	1.1	5	2.3	1.1	−28.1	0.9	7	4.3	2.4	−31.3	1.5	7	Toluene
1309	2.3	0.4	−20.4	1.0	4	2.4	0.5	−22.0	1.7	7	2.7	0.7	−21.7	1.0	7	2.6	0.6	−22.3	1.4	7	*	*	*	*	*	2(5H)-Furanone
1393	8.0	1.2	−23.6	0.5	5	4.4	0.9	−23.6	0.7	7	5.2	0.7	−22.6	0.7	8	5.3	1.8	−23.2	0.3	7	8.2	4.0	−23.7	1.2	8	2-Furaldehyde
1688	4.0	0.3	−23.1	0.8	4	2.1	0.5	−22.5	1.1	6	1.9	0.5	−20.1	1.2	6	1.4	0.7	−23.6	1.0	7	3.9	2.1	−24.3	1.3	8	2-Furaldehyde, 5-methyl
1719	4.9	1.1	−28.3	0.9	7	3.3	1.1	−29.9	1.1	6	2.0	0.7	−28.3	1.2	8	1.7	0.1	−29.2	1.7	4	3.0	4.1	−30.4	0.6	8	Phenol
1744	1.0	0.1	−27.9	0.4	3	1.2	0.1	−26.1	0.8	3																2-Cyclohexen-1-one, 3-methyl
1788	1.6	0.3	−21.7	2.0	3	4.0	0.4	−23.6	1.8	6	5.4	0.9	−24.1	0.9	8	3.3	0.6	−23.7	0.9	7						2H-Pyran-2-one, 4-hydroxy-5,6-dihydro
1828	1.2	0.1	−21.2	1.8	3	1.3	0.3	−20.6	7.8	4	0.8	-	−25.2	-	1											2-Cyclopenten-1-one, 2-hydroxy-3-methyl
2028											0.8	0.3	−23.0	0.7	6	1.5	1.1	−22.2	0.9	6	0.9	–	−17.9	-	*2*	Levoglucosenone (T)
2056	1.3	–	−23.3	–	1	0.6	0.2	−21.1	1.2	3	0.6	-	−23.9	-	1											Phenol, dimethyl
2146											1.6	0.4	−19.0	1.2	6	2.9	0.9	−21.4	2.6	3						Phenol, 2-methoxy-4-methyl
2178						2.6	0.5	−27.1	1.2	6	3.2	0.5	−27.1	1.1	8	4.3	0.8	−27.4	0.6	7	1.5	0.4	−28.0	1.5	*3*	1-Dodecene
2199	1.8	–	−28.4	–	1	2.1	0.5	−29.4	0.5	4	1.9	0.5	−29.7	0.8	6	2.2	0.6	−30.3	0.5	5						Phenol, 4-vinyl
2298	1.8	–	−25.8	-	*2*	2.2	-	−21.3	-	*2*	2.2	0.8	−20.8	1.7	8	5.1	2.0	−22.6	1.1	5						Phenol, 4-ethyl-2-methoxy
2344	0.9	–	−29.0	-	*2*	0.9	-	−28.1	-	2	1.2	0.1	−26.3	1.4	4											Isopropenylphenol
2367											1.6	0.4	−30.9	1.4	8	1.8	0.4	−30.5	1.0	5						Phenol, 4-vinyl-2-methoxy
2709	2.4	0.7	−24.3	0.5	*3*	4.4	1.4	−24.1	0.7	6	5.7	1.6	−23.6	0.4	8	6.1	1.2	−22.4	1.1	7						Anhydropyranose

[a] Standard deviations (S.D.) for the relative amounts and $\delta^{13}C$ values as well as number of replicates (*n*) are given. (T) stands for tentative identification. See text for determinations of relative amounts. The number of replicates can vary with analytical conditions due to detection thresholds. Missing data indicates peaks below detection threshold in all runs.

*Means peak detectable but no reliable isotope signal because of coelution.

polyphenolic structures in *Sphagnum* is thus indicated. Similar results were reported earlier and are still under debate (Van Smeerdijk and Boon, 1987; Lewis et al., 1999).

Substances with low retention times in the chromatogram, e.g. furan derivatives, become less dominant, whereas peaks in the "phenol region", e.g. retention time between 1800 and 2500 s, increase with depth down the profile (Fig. 2). This shift of the molecular composition is consistent with the data from the bulk elemental measurements (Table 1 and Fig. 1), as discussed above. It suggests that phenols — mainly the methoxylated lignin derivatives — are preserved in the humification process of *Sphagnum* (Benner et al., 1987; Spiker and Hatcher, 1987; Stout et al., 1988). In contrast, the relative loss of carbohydrate pyrolysis products and the relative accumulation of pyrolysis products from phenolic compounds in the profile is not in line with bulk ^{13}C ratios as these structural changes would result in ^{13}C depletion over the peat profile (Benner et al., 1987; Gleixner and Schmidt, 1998). This may suggest that pyrolysis products from deeper horizons have different precursors, e.g. carbohydrates from *Sphagnum* in the upper horizons and from microorganisms in the deeper horizons. Further isotopic evidence is needed to understand the biogeochemical processes.

The chromatogram of the DOM consists mainly of substances identifiable at the beginning of the chromatogram, e.g. toluene, furaldehyde, furaldehyde-5-methyl and phenol (Fig. 2, Table 2). Compounds with high retention time and higher molecular weight, e.g. pyrolysis products of phenolic compounds and higher lipids are less abundant. The question arose if these products are related to the peat and therefore isotope information on pyrolysis products was employed to approach the process of DOM formation.

3.4. Combined information of structure and isotopic content: Py-GC/MS-IRMS

The main objective of this research was to combine structural information from Py-GC/MS with the isotope content of the pyrolysis products. This combination provides the unique possibility to indicate different biogeochemical processes at the molecular level. $\delta^{13}C$ values and standard deviations for 18 main pyrolysis products are given in Table 2. Mean standard deviation for all measurements was 1.2‰. Using the combination of structural and isotopic information we distinguished several processes of humification (Table 3). In order to demonstrate the corresponding processes we selected five pyrolysis products from the depth profile, e.g. 2-furaldehyde, phenol, 4-hydroxy-5,6-dihydro-2H-pyran-2-one, 1-dodecene and anhydropyranose. Their relative amounts and $\delta^{13}C$ values are given in Fig. 3. The relative amounts of 1-dodecene and anhydropyranose increase with profile depth. This is most distinct for the anhydropyranose (see also Fig. 2). Simultaneously, the isotopic content of the anhydropyranose tends to increase with profile depth. This suggests that this compound is formed as an anabolic product of microorganisms in the profile. The slight increase of ^{13}C is thought to be due to the trophic level effect. The isotopic content of 1-dodecene is rather constant with depth. For the fresh moss sample no isotope value could be determined as this compound was below the detection limit. Obviously, the precursor of 1-dodecene is not favored by microbial degradation and hence selectively preserved in the humification process. The $\delta^{13}C$ values of 4-hydroxy-5,6-dihydro-2H-pyran-2-one decrease from −21.7‰ in the moss to relatively constant values around −24‰ and there is also a decrease in relative amount indicated in peat 10 cm. This pyrolysis product is most likely derived from a pentose. Since the source of this carbohydrate could be plants as well as microorganisms it is here suggested that the isotope effect is caused by an introduction and/or replacement of carbohydrates from bacteria and fungi. A similar fractionation effect has been described for individual carbohydrates in peat by Macko et al. (1991) and must be related to a formation of microbial carbohydrates (biosynthesis) with a contrary isotope effect compared to the trophic level effect. The decrease in relative amount in peat 10 cm must then be attributed to a higher rate of utilization (Table 3).

The amounts of 2-furaldehyde and phenol clearly show a decrease from *Sphagnum* moss to peat, but only the δ-value of 2-furaldehyde remains constant. This is conceivable for substances which are gradually degraded. The ^{13}C values of phenol do not show a distinct tendency with depth. This pyrolysis product has obviously several precursors (Tsuge and Marsubara, 1985; Stout et al., 1988; Pouwels et al., 1989).

These results demonstrate that additional isotope information is needed to verify the structural results. Most precursors of the pyrolysis products must have been subject to (bio-)chemical conversion in the humification process. For example, pyrolysis products of carbohydrates at different depths of the profile have different sources, e.g. remaining carbohydrates from plants and accumulating ones from microorganisms. The only component in this study that indicates selective preservation is 1-dodecene, a potential product of lipids.

In contrast to the ^{13}C bulk isotope analyses a significant difference between the DOM and the peat samples could be found by Py-GC/MS-IRMS. Most pyrolysis products of DOM are depleted in ^{13}C relative to the moss (Table 2). Of the compounds examined only levoglucosenone (tentative identification) was clearly enriched in ^{13}C in DOM. It is obvious from the isotope ratios that the substances in the water must have been formed by different processes compared with those occurring in the peat. It is suggested here that the OM in DOM is

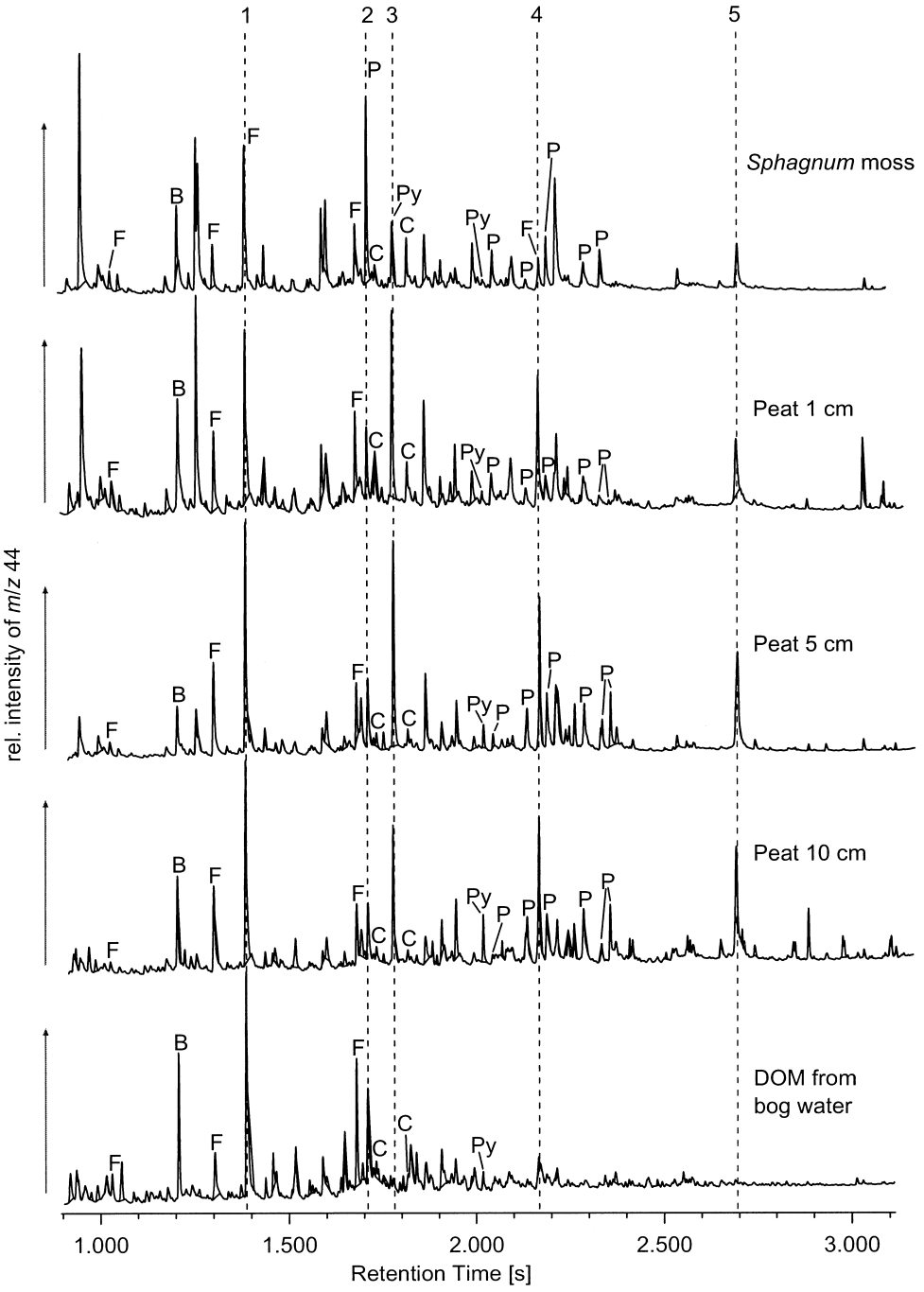

Fig. 2. Representative CO_2 trace (m/z 44) of pyrolysis products from *Sphagnum* moss, peat and dissolved organic matter (DOM) obtained from IRMS. Numbers correspond to (1) 2-furaldehyde, (2) phenol, (3) 4-hydroxy-5,6-dihydro-2H-pyran-2-one, (4) 1-dodecene and (5) anhydropyranose. All other peaks mentioned in the text and in Table 2 are indicated: F, furan derivative; P, phenol derivative; B, benzene derivative; C, cycloalkenone; Py, pyran derivative. It should be noted that peaks can appear larger due to magnification.

Table 3
Processes occurring during humification of *Sphagnum* moss as indicated by Py-GC/MS-IRMS analyses[a]

Relative amount	$\delta^{13}C$ of individual products	Process assumed
+	+(Δ +1.9‰)	Formation of microbial biomass (trophic level effect), e.g. anhydropyranose
+	−(Δ−2.0‰)	Biosynthesis of microbial carbohydrates, e.g. 4-hydroxy-5,6-dihydro-2H-pyran-2-one
+	Const.	Selective preservation, e.g. 1-dodecene
−	Not distinct	Mixed sources, e.g. phenol
−	Const.	Slow degradation, e.g. 2-furaldehyde

[a] +: increasing (i.e. enrichment of ^{13}C), −: decreasing (i.e. depletion of ^{13}C), const.: constant, i.e. within standard deviation of 1‰. Δ‰ values indicate the shift of $\delta^{13}C$ from *Sphagnum* to peat

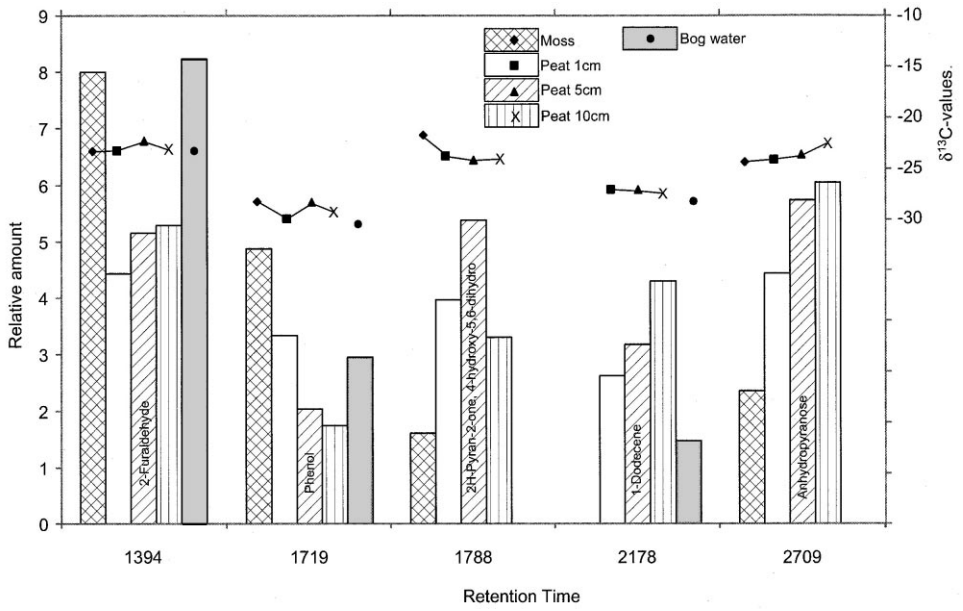

Fig. 3. Relative peak area (bars) and δ ^{13}C values (symbols) of selected pyrolysis products, e.g. 2-furaldehyde, phenol, 4-hydroxy-5,6-dihydro-2H-pyran-2-one, 1-dodecene and anhydropyranose from *Sphagnum* moss, peat and DOM from bog water.

formed in situ by the action of microorganisms in the water. The potential of microorganisms to alter the isotopic composition of organic matter, an enrichment as well as depletion, has been reported earlier (Macko and Estep, 1984; Macko et al., 1991; Claus et al., 1999). Most probably a depletion is associated with the uptake of isotopically light compounds such as respired CO_2, CO_2 from oxidation of CH_4, or acetic acid as has been proposed recently (Van der Meer et al., 1998; Schulten and Gleixner, 1999).

4. Conclusion

The combination of isotopic and structural information (Py-GC/MS-IRMS) has enabled us to distinguish different biogeochemical processes of humification, e.g. (1) biological degradation, (2) selective preservation of individual compounds, (3) formation of microbial biomass (trophic level effect), (4) introduction of microbially produced carbohydrates, and (5) a mixing of original and reworked material. In addition, we suggest this combined method is suitable to identify different sources of precursors, e.g. carbohydrates from plant or microorganisms.

A comparison of the peat samples with bog lake water indicates that the composition of DOM is not simply derived by solution of organic substances in the peat. This was particularly indicated by bulk $\delta^{15}N$ values whereas bulk $\delta^{13}C$ values were similar in peat and DOM. Only the combination of structural and $\delta^{13}C$ information of individual organic compounds demonstrated

that a majority of pyrolysis products of DOM are depleted in ^{13}C relative to the same products in peat. Thus, the DOM in water is suggested to be principally derived from microbial processes different to those occurring in the peat. An uptake of "light" carbon, e.g. respired $^{12}CO_2$, CO_2 from oxidation of $^{12}CH_4$, or acetic acid by microorganisms could possibly explain this effect.

Acknowledgements

We would like to thank S. Rühlow for technical assistance and J. Lloyd as well as D. Schimel for helpful comments on the manuscript. We also like to thank an anonymous reviewer and particularly Pim v. Bergen for critical and very constructive comments on the paper. This research was funded by the special research program "Refraktäre Organische Säuren in Gewässer (ROSIG)" (Gl 626/1-5) of the Deutsche Forschungsgemeinschaft (DFG), Bonn-Bad Godesberg, Germany.

References

Ågren, G.I., Bosatta, E., Balesdent, J., 1996. Isotope discrimination during decomposition of organic matter: a theoretical analysis. Soil Science Society of America Journal 60, 1121–1126.

Balesdent, J., Girardin, C., Mariotti, A., 1993. Site-related $\delta^{13}C$ of tree leaves and soil organic matter in a temperate forest. Ecology 74, 1713–1721.

Balzer, A., Gleixner, G., Grupe, G., Schmidt, H.L., Schramm, S., Turbanjust, S., 1997. In vitro decomposition of bone collagen by soil bacteria — the implications for stable isotope analysis in archaeometry. Archaeometry 39, 415–429.

Benner, R., Fogel, M.L., Sprague, E.K., Hodson, R.E., 1987. Depletion of ^{13}C in lignin and its implication for stable isotope studies. Nature 329, 708–710.

Charman, D.J., Aravena, R., Bryant, C.L., Harkness, D.D., 1999. Carbon isotopes in peat, DOC, CO_2, and CH_4 in a Holocene peatland on Dartmoor, southwest England. Geology 27, 539–542.

Claus, H., Gleixner, G., Filip, Z., 1999. Formation of humic-like substances in mixed and pure cultures of aquatic microorganisms. Acta Hydrochimica et Hydrobiologica 27, 200–207.

Deines, P., 1980. The isotopic composition of reduced organic carbon. In: Fritz, P., Fontes, J.C. (Eds.), Handbook of Environmental Isotope Geochemistry, Vol. 1 — The Terrestrial Environment, A. Elsevier, Amsterdam, pp. 329–406.

Demmelmair, H., Schmidt, H.L., 1993. Precise delta-C-13-determination in the range of natural-abundance on amino-acids from protein hydrolysates by gas-chromatography–isotope ratio mass-spectrometry. Isotopenpraxis 29, 237–250.

Durig, J.R., Calvert, G.D., Esterle, J.S., 1991. Particle size fraction and downhole depositional trends of a tropical domed peat deposit as determined by pyrolysis GC/FT-IR/FID and pyrolysis GC/MS. Journal of Analytical and Applied Pyrolysis 18, 293–324.

Ficken, K.J., Barber, K.E., Eglinton, G., 1998. Lipid biomarker, delta-C-13 and plant macrofossil stratigraphy of a Scottish montane peat bog over the last two millennia. Organic Geochemistry 28, 217–237.

Gleixner, G., Schmidt, H.L., 1998. On-line determination of group-specific isotope ratios in model compounds and aquatic humic substances by coupling pyrolysis to GC-C-IRMS. In: Stankiewicz, A.B., van Bergen, P.F. (Eds.), Nitrogen-Containing Macromolecules in the Bio- and Geosphere. ACS Symposium Series 707. American Chemical Society, Washington, pp. 34–46.

Gleixner, G., Danier, H.J., Werner, R.A., Schmidt, H.-L., 1993. Correlations between the ^{13}C content of primary and secondary plant products in different cell compartments and that in decomposing basidomycetes. Plant Physiology 102, 1287–1290.

Gleixner, G., Bol, R., Balesdent, J., 1999. Molecular insight into soil carbon turnover. Rapid Communications in Mass Spectrometry 13, 1278–1283.

Goñi, M.A., Eglinton, T.I., 1994. Analysis of kerogens and kerogen precursors by flash pyrolysis in combination with isotope-ratio-monitoring gas-chromatography mass-spectrometry (irm-GC–MS). HRC Journal of High Resolution Chromatography 17, 476–488.

Haider, K., 1996. Biochemie des Bodens, 1st Edition. Enke Verlag, Stuttgart.

Hayes, J.M., Freeman, K.H., Popp, B.N., Hoham, C.H., 1990. Compound-specific isotopic analyses — a novel tool for reconstruction of ancient biogeochemical processes. Organic Geochemistry 16, 1115–1128.

Hedges, J.I., Oades, J.M., 1997. Comparative organic geochemistries of soils and marine sediments. Organic Geochemistry 27, 319–361.

Irwin, W.I., 1982. Analytical Pyrolysis, 1st Edition. Marcel Dekker, Inc, New York.

Leavitt, S.W., Long, A., 1986. Stable-carbon isotope variability in tree foliage and wood. Ecology 67, 1002–1010.

Lewis, N.G., Davin, L.B., Sarkanen, S., 1999. The nature and function of lignins. In: Pinto, M.B. (Ed.), Carbohydrates and Their Derivatives Including Tannins, Cellulose, and Related Lignins, Vol. 3. Elsevier, Amsterdam, pp. 618–745.

Lichtfouse, E., Dou, S., Girardin, C., Grably, M., Balesdent, J., Behar, F., Vandenbroucke, M., 1995. Unexpected ^{13}C-enrichment of organic components from wheat crop soils: evidence for the in situ origin of soil organic matter. Organic Geochemistry 23, 865–868.

Lichtfouse, E., Chenu, C., Baudin, F., Leblond, C., Da Silva, M., Behar, F., Derenne, S., Largeau, C., Wehrung, P., Albrecht, P., 1998. A novel pathway of soil organic matter formation by selective preservation of resistant straight-chain biopolymers- chemical and isotope evidence. Organic Geochemistry 28, 411–415.

Macko, S.A., Estep, M.L.F., 1984. Microbial alteration of stable nitrogen and carbon isotopic composition of organic matter. Organic Geochemistry 6, 787–790.

Macko, S.A., Helleur, R., Hartley, G., Jackman, P., 1990. Diagenesis of organic matter- a study using stable isotopes of individual carbohydrates. Organic Geochemistry 16, 1129–1137.

Macko, S.A., Engel, M.H., Hartley, G., Hatcher, P., Helleur, R., Jackman, P., Silfer, J., 1991. Isotopic compositions of individual carbohydrates as indicators of early diagenesis of organic matter. Chemical Geology 93, 147–161.

Mayer, B., Feger, K.H., Giesemann, A., Jäger, H.J., 1995. Interpretation of sulfur cycling in 2 catchments in the Black Forest (Germany) using stable sulfur and oxygen-isotope data. Biogeochemistry 30, 31–58.

Miyajima, T., Wada, E., Hanba, Y.T., Vijarnsorn, P., 1997. Anaerobic mineralization of indigenous organic matters and methanogenesis in tropical wetland soils. Geochimica et Cosmochimica Acta 61, 3739–3751.

Nadelhoffer, K.J., Fry, B., 1988. Controls on natural nitrogen-15 and carbon-13 abundances in forest soil organic matter. Soil Science Society of America Journal 52, 1633–1640.

Öquist, M.G., Svensson, B.H., 1996. Non-tidal wetlands. In: Watson, R.T., Zinyowera, M.C., Moss, R.H., Dokken, D.J. (Eds.), Climate Change 1995 — Impacts, Adaptions and Mitigation of Climate Change: Scientific-Technical Analyses. Cambridge University Press, Cambridge, pp. 215–239.

Pouwels, A.D., Eijkel, G.B., Boon, J.J., 1989. Curie-point pyrolysis capillary gas-chromatography high-resolution mass-spectrometry of microcrystalline cellulose. Journal of Analytical and Applied Pyrolysis 14, 237–280.

Pulchan, J., Abrajano, T.A., Helleur, R., 1997. Characterization of tetramethylammonium hydroxide thermochemolysis products of near-shore marine sediments using gas chromatography mass spectrometry and gas chromatography combustion/isotope ratio mass spectrometry. Journal of Analytical and Applied Pyrolysis 42, 135–150.

Ralph, J., Hatfield, R.D., 1991. Pyrolysis-GC–MS characterization of forage materials. Journal of Agricultural and Food Chemistry 39, 1426–1437.

Rieley, G., 1994. Derivatization of organic-compounds prior to gas-chromatographic combustion-isotope ratio mass-spectrometric analysis — identification of isotope fractionation processes. Analyst 119, 915–919.

Rieley, G., Collier, R.J., Jones, D.M., Eglinton, G., Eakin, P.A., Fallick, A.E., 1991. Sources of sedimentary lipids deduced from stable carbon isotope analyses of individual compounds. Nature 352, 425–427.

Schmidt, H.-L., Voerkelius, S., Amberger, A., 1992. Nitrogen and oxygen isotopes as indicators for nitrification and denitrification. In: Matthess, G., Frimmel, F.H., Hirsch, P., Schulz, H.D., Usdowski, E. (Eds.), Progress in Hydrogeochemistry. Springer-Verlag, Berlin, pp. 212–219.

Schmidt, H.-L., Butzenlechner, M., Rossmann, A., Schwarz, S., Kexel, H., Kempe, K., 1993. Inter- and intramolecular isotope correlations in organic compounds as criterion for authenticity identification and origin assignment. Zeitschrift für Lebensmittel Untersuchung und Forschung 196, 105–110.

Schulten, H.-R., Gleixner, G., 1999. Analytical pyrolysis of humic substances and dissolved organic matter in aquatic systems: Structure and origin. Water Research 33, 2489–2498.

Silfer, J.A., Engel, M.H., Macko, S.A., Jumeau, E.J., 1991. Stable carbon isotope analysis of amino-acid enantiomers by conventional isotope ratio mass-spectrometry and combined gas-chromatography isotope ratio mass-spectrometry. Analytical Chemistry 63, 370–374.

Spiker, E.C., Hatcher, P.G., 1987. The effects of early diagenesis on the chemical and stable carbon isotopic composition of wood. Geochimica et Cosmochimica Acta 51, 1385–1391.

Stankiewicz, B.A., Hutchins, J.C., Thomson, R., Briggs, D.E.G., Evershed, R.P., 1997. Assessment of bog-body tissue preservation by pyrolysis-gas chromatography/mass spectrometry. Rapid Communications in Mass Spectrometry 11, 1884–1890.

Stout, S.A., Boon, J.J., Spackman, W., 1988. Molecular aspects of the peatification and early coalification of angiosperm and gymnosperm woods. Geochimica et Cosmochimica Acta 52, 405–414.

Tsuge, S., Marsubara, H., 1985. High-resolution pyrolysis-gas chromatography of proteins and related materials. Journal of Analytical and Applied Pyrolysis 8, 49–64.

Van der Heijden, E., Boon, J.J., Rasmussen, S., Rudolph, H., 1997. *Sphagnum* acid and its decarboxylation product isopropenylphenol as biomarkers for fossilised Sphagnum in peats. Ancient Biomolecules 1, 93–107.

Van der Meer, M.T.J., Schouten, S., Sinninghe Damsté, J.S., 1998. The effect of the reversed tricarboxylic acid cycle on the ^{13}C contents of bacterial lipids. Organic Geochemistry 28, 527–533.

Van Krevelen, D.W., 1993. Coal — Typology, Physics, Chemistry, Constitution, 3rd Edition. Elsevier, Amsterdam.

Van Smeerdijk, D.G., Boon, J.J., 1987. Characterisation of subfossil Sphagnum leaves, rootlets of Ericaceae and their peat by pyrolysis-high-resolution gas chromatography-mass spectrometry. Journal of Analytical and Applied Pyrolysis 11, 377–402.

Wedin, D.A., Tieszen, L.L., Dewey, B., Pastor, J., 1995. Carbon isotope dynamics during grass decomposition and soil organic matter formation. Ecology 76, 1383–1392.